R. BARAUSKAS

DYNAMIC ANALYSIS AND SYNTHESIS OF ELASTIC STRUCTURES WITH UNILATERAL CONSTRAINTS

COMPUTER METHODS AND APPLICATION TO CONTROLLED VIBRATIONAL SYSTEMS

CONTENTS

INTRODUCTION.....5
CONSTRUCTION DIAGRAMS AND MATHEMATICAL MODELS OF VIBRODRIVES...10

P.1 TECHNIQUES.....23

1.DYNAMIC MODELS AND THEIR REDUCTION.....26
1.1 Reduction of linear structural equations.....26
1.2 Reduction of nonlinear structural equations.....30
1.3 Reduction of structural equations with unilateral constraints.....32
2.DYNAMIC ANALYSIS OF LINEAR ELASTIC STRUCTURES.....40
2.1 Direct and indirect methods.....40
2.2 Criteria for selecting a direct integration numerical scheme.....44
2.3 Single-step numerical schemes.....52
2.3.1 Weighted residual approach.....52
2.3.2 Generalization of the Newmark's scheme.....56
2.3.3 Reduction to the first order system. Finite elements in time 58
3.TRANSIENT ANALYSIS OF NONLINEAR ELASTIC STRUCTURES.....63
3.1 Direct integration: solution of nonlinear equations at each time step.....63
3.2 Time domain approach.....69
3.3 Analysis of structures with local nonlinearities.....70
3.4 Direct integration of structural equations with unilateral constraints.....72
3.5 Application to systems with normal-impact interaction.....81
3.6 Application to the systems with oblique impact and sliding friction interaction 84
4.STATIONARY DYNAMIC ANALYSIS OF NONLINEAR ELASTIC STRUCTURES..91
4.1 Direct methods for obtaining forced and free vibration laws. Boundary value problem in time domain.....92
4.2 Weighted residual approach for obtaining forced vibration laws.....97
4.3 Transient and stationary analysis of nonlinear vibration with slow-varying amplitudes.....105
4.4 Stability analysis of vibration laws.....108

5.MOTION CONTROL OF ELASTIC STRUCTURES.....116
5.1 Fixed and varying time optimal control.....116
5.2 Inverse dynamic problem approach for control synthesis....123
5.2.1 Programmed control synthesis.....123
5.2.2 Linear closed-loop control synthesis.....125
5.3 Speed-up control synthesis.....129
5.4 Forced resonant vibration control.....133
P.2 APPLICATIONS.....139
6.MODEL EQUATIONS OF VIBRODRIVES.....141
6.1 Finite element models of piezoelectric vibroconverters....141
6.1.1 Variational formulation of the thermopiezoelectricity.141
6.1.2 Finite elements of piezoelectric continua.....146
6.2 Mechanical contact interaction models.....154
6.2.1 Vibrodrives with point-contact interaction.....154
6.2.2 Vibrodrives with continuous contact area.....157
6.3.3 Travelling wave vibrodrives.....162
6.3 Rigid body motion models of vibroconverters.....165
6.4 Dynamic characteristics of vibrodrives.....168
7. ANALYSIS AND SYNTHESIS OF VIBRODRIVES.....172
7.1 Free and forced vibration of systems with normal interaction 174
7.2 Forced motion of systems with normal and tangential interaction 193
7.2.1 Kinematic pair motion control by the tangential vibration.....193
7.2.2 Directive motion of a unidirectional vibration vibroconverter with internal impact pair.....207
7.2.3 Free and forced motion of a vibrodrive.....214
7.3 Synthesis of active links of vibrodrives.....224
7.3.1 Optimal shape synthesis problems.....224
7.3.2 Synthesis of asymmetric cycle vibroconverters.....230
7.3.3 Synthesis of concentrators and pulse-transformers.....233
7.4 Optimal control laws of output links.....241
7.4.1 Aperiodic motion control of a piezoelectric vibroconverter.....241
7.4.2 Kinematic pair motion control by varying normal force.250
CONCLUSION.....255
REFERENCES.....259
APPENDICES.....269

INTRODUCTION

The natural way of comprehension of the behavior of complex systems leads through their decomposition into components or units the governing laws of behavior of which are already known, followed by a subsequent reconstruction of the initial system by rejoining these components. In many cases the adequate mathematical model can be obtained by employing the finite number of components. From the mathematician's point of view, the discretization of a continuous system can be carried out in several alternative ways, e.g., employing the finite difference techniques, the weighted residuals, employing the stationarity conditions of certain functionals etc., considering as a source object the differential equations representing the system's behavior. Nevertheless, from an engineer's point of view an approach containing a greater amount of engineering intuition is often preferable, based upon an analogy between the discrete elements and the corresponding parts of a considered domain. For the time being a common way to solve engineering problems of various nature has been established and called by O.Zienkiewitcz a standard discrete problem solution method. With application to mechanical systems this method assumes establishing the force-displacement relations for each structure element, and assembling structure from the elements employing force equilibrium conditions at the nodes of jointing .

The way to obtain discrete mathematical models has found its perfect representation as the finite element method. Computer analysis of a continuous dynamic mechanical system, as a rule, deals with the discretization in space as well as in time. However, in order to preserve the idea of the standard discrete problem, usually it appears preferable to make an explicit distinction between space and time discretization stages.

The matrix equation of motion of a finite element structure appears as a result of the space discretization stage. In the dynamic system analysis such a presentation has its old tradition. In the pre-computer time as well as nowadays a lot of effort has been devoted to the analysis of the discrete one-mass or several-mass models taking on account the mutual stiffness,

dissipative and other linear or nonlinear elements. The large variety of dynamic mechanical systems can be represented in such a way, involving a great deal of engineering intuition and a proper comprehension of essence of the physical phenomena when obtaining a model. The advent of computers and the finite element techniques has presented a formal way for obtaining complex models of large dimension and for carrying out their analysis. On the other hand, treating traditional and finite element models from a common point of view enables to acquire a more profound comprehension about the dynamic features of a mechanical system.

For obtaining the time laws of motion of a mechanical system numerical and analytical techniques can be employed. Since the very formation of approximation techniques the minimum of manual calculations producing sufficient accuracy was regarded as the main efficiency feature of a method. Availability of computers nowadays has transferred the accent to the minimization of computer resource during the approximation techniques applications. This is especially actual when solving optimization and synthesis problems requiring to obtain the motion laws repeatedly as well as in everyday engineering computations employing small computers.

A computational effort can be reduced by developing techniques in two ways. First, the models of small dimension and at the same time preserving the adequateness of a model to the real system should be employed. On the contrary to the direct construction of several degree of freedom model, it appears preferable to consider as a source the finite element model and to develop the formal techniques for reducing the number of its dynamic degrees of freedom. On this account the substructuring techniques and other decomposition approaches, applicable in most cases to the linear systems, should be mentioned. Nevertheless, more research in this field should be done regarding the systematization and the development of new approaches applicable to certain classes of nonlinear systems. The second way for computational effort reduction is to develop efficient time integration schemes for obtaining the motion laws. A tremendous contribution to the development and systematic presentation of numerical integration techniques of equations of motion of finite element structures has been made by the scientists at the

well-known research centers guided by J.H.Argyris, K.J.Bathe, O.Zienkiewitcz.

The approximate analytical approaches to the structural dynamic analysis have not yet reached the same degree of perfection, though the approximate techniques of a nonlinear vibration theory have been developed and systematically presented by Н.Н.Боголюбов, Ю.А.Митропольский, Е.П.Попов, В.А.Якубович, В.М.Старжинский, В.В.Болотин, Е.Н.Розенвассер and oth. A development should be made applying existing approximate analytical techniques taking on account specific features of equations of motion of large dimension and obtaining the mixed analytical-numerical algorithms. The similar is to be pointed out considering the structure motion control problems. The case oriented algorithms can be obtained on the base of fundamental research carried out by Н.Н.Красовский, Л.С.Понтрягин, Н.В.Баничук, Ф.Л.Черноусько, Л.Д.Акуленко, Б.Н.Соколов, В.И.Уткин, В.А.Троицкий, Е.П.Попов, П.Д.Крутько, А.С.Галлиулин, М.З.Коловский.

This book carries out the message of unification of main ideas of finite element dynamic analysis of elastic mechanical systems and the theories of nonlinear vibration and control. The developed techniques can be applied to the range of problems encountered in the fields of mechanical system design taking on account the elastic vibration, e.g., when considering the problems of employing the controlled elastic vibration of rigid bodies and active vibrating systems. The significance of such problems has increased in connection with the development of precise vibromechanics systems founded by K.Ragulskis, J.Bansevičius, А.А.Ерофеев, В.В.Лавриненко and oth.

The book consists of an introduction an two parts. The introduction presents the construction diagrams of several traditional and original vibrodrives, the main features of their mathematical models are discussed. In the first part a systematic approach to the dynamic degree of freedom reduction, obtaining the transient and stationary motion laws and motion control synthesis of elastic structures with nonlinear interaction. The second part presents applications of the developed techniques to the analysis and synthesis of vibrodrives. Finite element models of piezoelectric vibroconverters and of vibrodrives are obtained,

taking on account the rigid body motion of the deformable links. The computed results of the real systems are presented.

The first chapter presents the techniques for the dynamic reduction of structural models with large number of d.o.f. to the simpler models with only several dynamic d.o.f. Such a transform is always more or less related with the loss of information about the dynamic features of the structure. The equations of motion are presented in the modal coordinates of the linear part of the structure. If the vibration frequency Fourier components lie in the lower range of the eigenfrequency spectrum, truncation of dynamic contributions of higher modes doesn't cause significant errors. The techniques are applicable to linear structures and to the structures with nonlinear interaction points.

The second chapter presents the techniques for obtaining the time laws of the linear structure motion or the Fourier components of the dynamic response. As the main techniques the direct numerical integration in time is considered. Several methods for obtaining the numerical schemes and the criteria evaluating their asymptotic features are presented.

In the third chapter the linear structure numerical integration techniques are extended in order to match the nonlinear problems by means of the linearization of nonlinearities or by iterating at each integration step. In the case of essentially nonlinear structures with kinematic pairs interacting by the normal, oblique impact and sliding friction forces the numerical integration scheme is developed enabling to take account of various normal contact and sliding friction force characteristics as well as the impact model represented by the coefficient of restitution. The scheme is presented as an extension of the generalized Newmark's scheme.

The fourth chapter presents the techniques for obtaining periodic stationary vibration laws and transient vibration laws with slow varying amplitudes of the high resonant quality structures with nonlinear interaction points. In this case direct numerical integration is hardly possible because of the large number of oscillations until a stationary motion is obtained. The presented semi-analytical techniques enable to obtain stable as well as unstable motion laws, therefore it is necessary to check their stability employing the stability criteria.

In the fifth chapter the techniques for obtaining the programmed and closed-loop control laws of the elastic structural deformation. The programmed control laws are obtained employing the optimum system control techniques, and the feedback control is synthesized by solving the inverse dynamic problems. In both cases the dynamic reduction techniques presented in the first chapter are employed. The problem of exciting a prescribed resonant structural vibration law is considered.

The sixth chapter presents the finite element models of piezoelectric vibroconverters and vibrodrives. The relations between the mechanical, electrical and thermal phenomena are considered together with the mechanical contact interaction models. The presented dynamic equations take on account a rigid body motion of an elastic structure. The dynamic criteria of a vibrodrive are formulated.

In the seventh chapter the techniques presented above are employed for the dynamic analysis of vibrodrives and their components, vibration-controlled kinematic pairs, impact-friction vibrations of vibroconverters. Optimal control laws of deformation motions of elastic structures are obtained and optimal shape synthesis of vibroconverters and vibration concentrators of complex vibrational motion laws is carried out.

In 1960-1970 a drive of a new type was created. It was based upon the conversion of high frequency mechanical vibrations into directive motion. Following the analogy with electric, pneumatic and hydraulic drives the new drive was named a vibrational drive, or a vibrodrive (VD).

The operation principle of a VD is close to that of a common class of mechanisms converting vibrations into directive motion. This class includes, e.g., ratchet-and -pawl gears, idle stroke mechanisms etc., operating at a frequency below 1kHz. Vibrodrives operate at a frequency from 20kHz and more. The operating frequency range is the main distinguishing feature between vibrodrives and the traditional mechanisms converting vibrations into rotative or linear motion. The high frequency causes qualitative differences in operation parameters as well as new phenomena that have not been observed in mechanisms before [56].

Maiden constructions of VD employed principles of low-frequency vibroconveyers. A diagram of one of the first and most simple constructions is presented in Fig.1 [119]. It is an unreversal VD with an active input link consisting of four piezoelectric plates the electrodes of which are fed by the high frequency voltage. The springs are employed for improving the contact interaction between the input and output links. In order to minimize energy dissipation the center points of the plates are employed for fixings because they coincide with the nodal points of odd vibrational modes.

The reverse motion of VD can be obtained by employing bimorfic plates and exciting their longitudinal and flexural vibration. A construction diagram of such a VD is presented in Fig.2 [119]. In the bimorfic plate with partitioned eleqtrodes the flexural and longitudinal vibrations are excited simultaneously, a phase shift between them being varied by adjusting the input voltage. If the phase shift is made equal to 180° by means of a switch, the reverse motion of the output link is obtained.

Improved operation characteristics exhibits the VD in Fig.3 [148]. It has a rotor 2 consisting of two truncated cones, piezoelectric plates 4 and 5 with the correspondingly truncated

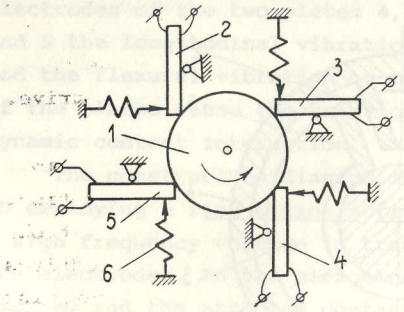

Fig.1 Vibrodrive: 1 - rotor; 2,3,4,5 - piezoelectric plates; 6 - springs

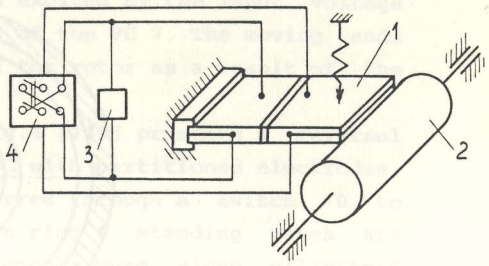

Fig.2 Reversal vibrodrive:
1 - piezoelectric plate;
2 - rotor;
3 - voltage converter;
4 - switches

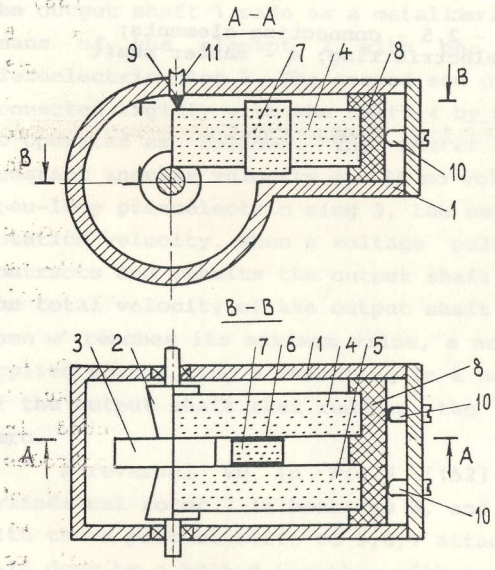

Fig.3 Vibromotor:
1 - frame; 2 - rotor;
3 - disc;
4,5-piezoelectric plates;
6 - dielectric spacers;
7 - additional vibro-converter; 8 - mount;
9-support; 10,11-screws

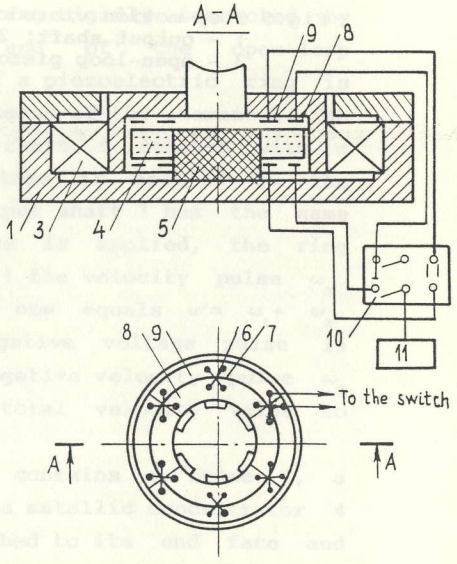

Fig.4 Piezoelectric vibrodrive with the ring vibroconverter:
1 - frame; 2 - rotor;
3-bearing; 4-piezoelectric ring; 5 - mount;6,7-straps;
8,9-eletrodes connected into separate electric circuits;
10-switch; 11-high voltage source; 12 - contact elements

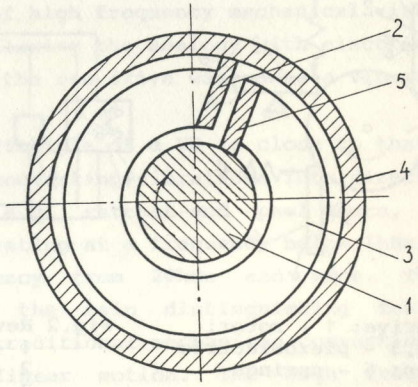

Fig.5 Step-motion vibrodrive:
1 - output shaft; 2 - 2,5 - connecting elements;
3 - open-loop piezoelectric ring; 4 - master shaft

ends and an auxiliary piezoelectric vibroconverter(VC) 7. A high frequency input voltage is applied simultaneously to the electrodes of the two plates 4,5 and the VC 7. In the plates 4 and 5 the longitudinal vibration is excited by the input voltage and the flexural vibration by means of the VC 7. The moving ends of the plates cause the rotation of the rotor as a result of the dynamic contact interaction.

The construction diagram in Fig.4 [149] presents a reversal VD employing a ring piezoelectric VC with partitioned electrodes. A high frequency voltage is transferred through a switch 10 to the electrodes. In the piezoelectric ring 4 standing waves are excited and the attached contact elements move along elliptical paths. The interaction between the contact elements and the rotor results in its rotational movement. The motion is reversed by means of switching into the position 11.

A step-motion VD is presented in Fig.5 [147]. It consists of the output shaft 1 made as a metallic ring rigidly connected by means of the element 2 with one end of the open-loop piezoelectric ring 3. The second end of a piezoelectric ring is connected rigidly with the shaft 4 by means of the element 5. The VD operates as follows. The master shaft 4 rotates with a constant angular velocity ω_1. If no voltage is applied to the open-loop piezoelectric ring 3, the output shaft 1 has the same rotation velocity. When a voltage pulse is applied, the ring contracts and submits the output shaft 1 the velocity pulse ω_2. The total velocity of the output shaft now equals $\omega' = \omega_1 + \omega_2$. When ω' reaches its maximum value, a negative voltage pulse is applied to the ring 3 resulting in a negative velocity pulse ω_3 of the output shaft that reduces the total velocity value to zero.

A reversal VD in Fig.6 [152] contains a frame 1, a cylindrical rotor 2 in bearings 3, and a metallic concentrator 4 with three piezoelectric VC 5,6,7 attached to its end face and held down by a bolt 9 together with a passive strap 8. The VC 5,6,7 are fed from the voltage block 11 through the phase-shift circuit 10. The moving end of the concentrator 4 contacts with the inner surface of the rotor 2, the other end being attached to frame 1 by means of the elastic plate 12 by the bolts 13. The voltage is applied to each VC 5,6,7 with the phase shift 60°, and

flexural vibrations are submitted to the concentrator 4. Its moving end follows a circular path and causes a rotation of the rotor 2. The rotation direction is reversed by reversing the voltage phase shift.

The VD in Fig.7 [150] consists of a rigid rotor 1, elastic element 2 made as a steel ring coaxial with the rotor 1. The bearing axes with the piezoelectric ring vibroconverters 5 free arranged in a gap between the rotor 1 and the ring 2 are mounted on the immobile support 3. The VC are fed by a high frequency voltage through a phase-shift circuit. Within the ring 2 the bearing element 6 is arranged.

The vibrodrive operates as follows. A high frequency voltage is supplied consequently through the phase shift circuit to the VC 5 exciting the radial as well as the tangential vibration. In the elastic rotor 2 a travelling wave is excited causing the rotation of the VC on their axes 4 and in their turn causing a rotation of the rotor 1. This construction enables to obtain an increased torque value in comparison with VD employing beam and plate VC, owing to the larger deformation forces of the cylindrical VC and their combined participation when transferring a torque from the elastic element 2 to the rotor 1.

The distinguishing feature of the above presented constructions appears to be the employment of resonant vibrations of an input link, because only in the vicinity of resonance the sufficiently large values of amplitudes are obtained. As a shortcoming of such VD appears the narrow range of operating frequencies because of a large value of the mechanical Q-factor of a VC. In order to obtain the sufficiently large values of amplitudes employing a nonresonant vibration the packages of vibroconverters are employed. In Fig.8 the construction diagram of such a vibrodrive is presented [151].

The VD consists of a VC package 1, where the polarization vectors of neighboring VC have the opposite directions. One end face of a package is attached to the basis 2, and the other one to the bar 3 that in its turn at one end is connected by a clamp with the basis 2, and at the other end with the rod 5. The rod 5 is fixed in cantilever on the basis 2, and its free end is attached with the moving link 6. The integrating circuit consists of two high-voltage gates 7 and 8 and two resistances 9 and 10.

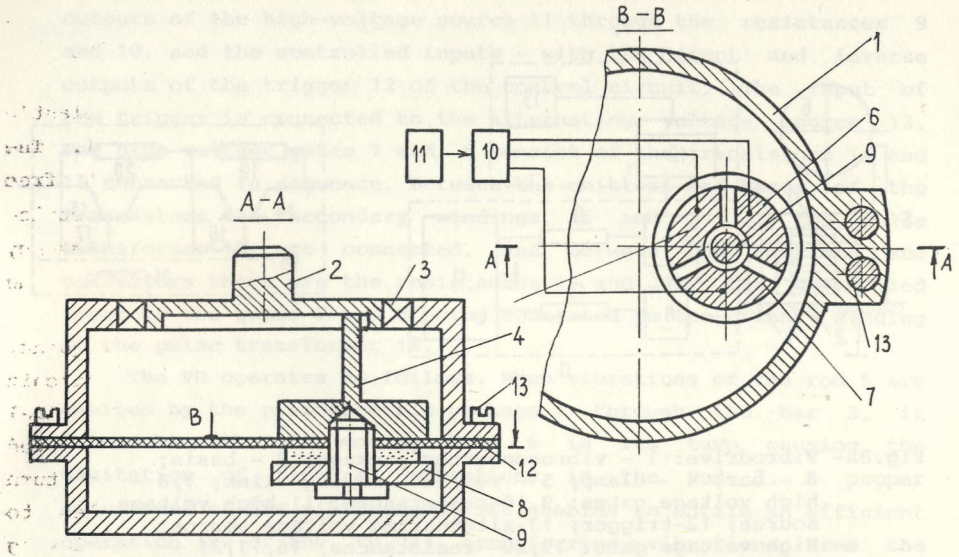

Fig.6 Reversal vibrodrive: 1 - frame; 2 - rotor; 3 - bearings; 4 - concentrator; 5-7 - piezoelectric vibroconverters; 8 - passive strap; 9 - tightening screw; 10 - phase-shift circuit; 11-voltage source; 12-elastic plate; 13 - screws

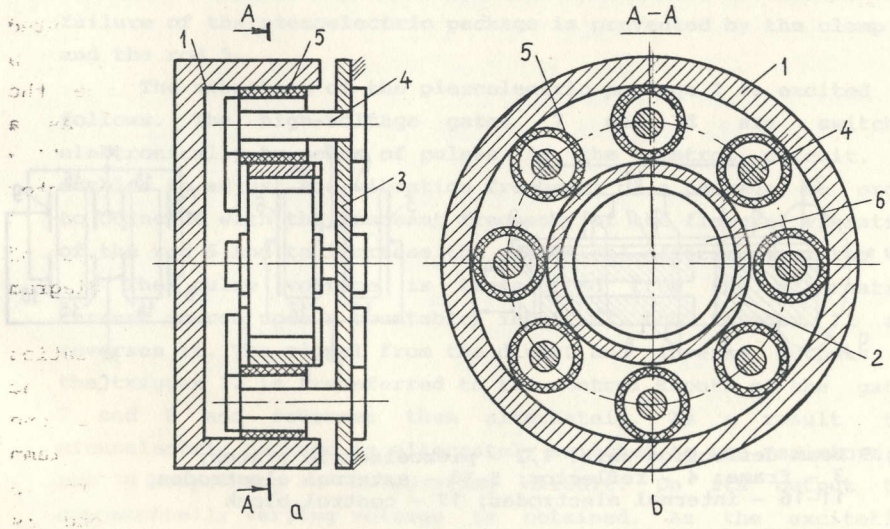

Fig.7 Vibrodrive: 1 - rotor; 2 - elastic element; 3 - immobile support; 4 - bearing axes; 5 - piezoceramic ring vibroconverters; 6 - bearing element

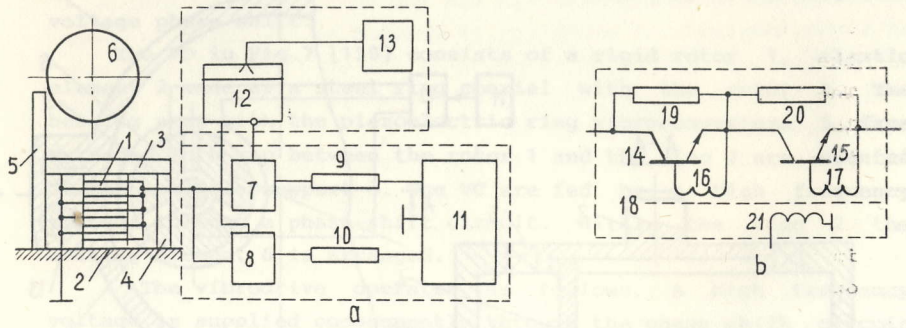

Fig.8a- Vibrodrive: 1 - vibroconverter package; 2 - basis; 3 - bar; 4 - clamp; 5 - rod; 6 - moving link; 7,8 - high voltage gates; 9,10-resistances; 11-high voltage source; 12-trigger; 13-alternating voltage source;
b- High voltage gate: 19,20- resistances; 16,17,21 - windings of the pulse transformer 18; 14,15-transistors

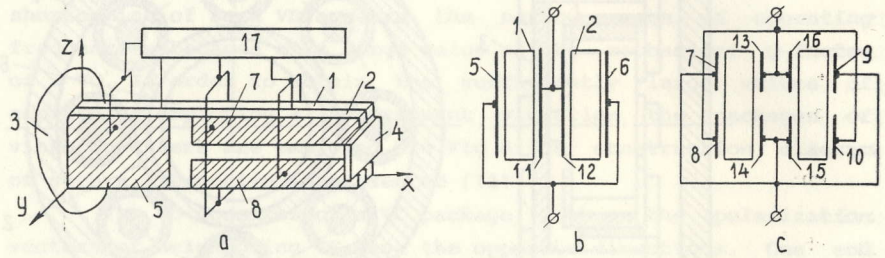

Fig.9 Beam deflection unit: 1,2 - piezoelectric plates; 3 - frame; 4 - reflector; 5-10 - external electrodes; 11-16 - internal electrodes; 17 - control block

The piezoelectric package 1 is connected electrically with the high-voltage gates 7 and 8 whose outputs are connected with the outputs of the high-voltage source 11 through the resistances 9 and 10, and the controlled inputs - with the direct and inverse outputs of the trigger 12 of the control circuit. The input of the trigger is connected to the alternating voltage source 13. The high voltage gates 7 and 8 consist of the transistors 14 and 15 connected in sequence. Between the emitters and bases of the transistors the secondary windings 16 and 17 of the pulse transformer 18 are connected, and between the emitters and collectors there are the resistances 19 and 20, the controlled input of the gates 7 and 8 being connected to the primary winding of the pulse transformer 18.

The VD operates as follows. When vibrations of the rod 5 are excited by the piezoelectric package 1 through the bar 3, it interacts with the moving link 6 in its turn causing the excitation of flexural vibrations in the rod 5. A proper adjustment of the vibration phases enables to obtain an efficient operation law of the VD by transferring vibrations from the piezoelectric package 1 to the rod 3 with the minimum loss of energy. The applied voltage is of the order of hundreds of volts, and the vibration amplitude reaches the value of 100μ. The failure of the piezoelectric package is prevented by the clamp 4 and the rod 5.

The vibration of the piezoelectric package 1 is excited as follows. The high-voltage gates 7 and 8 are switched electronically by means of pulses in the control circuit. It enables to adjust the vibration frequency of a package in order to coincide with the resonant frequency of the flexural vibration of the rod 5 and to increase the mechanical efficiency of the VD.

The pulse voltage is transferred from the alternating current source upon a countable input of the trigger 12 and reverses it. The signal from the direct and inverse outputs of the trigger 12 is transferred to the control inputs of the gates 7 and 8 and reverses them alternately. As a result the piezoelectric package is alternately switched to the resistors 9 and 10 comprising an integrating circuit. On its output the exponentially varying voltage is obtained. As the excitation frequency is considerably lower the the first resonant frequency

of the package 1, static electrical capacity prevails. The package is charged and uncharged from the high voltage source 11 through the keys 7(8) and the resistor 9(10) of the integrating circuit.

The above mentioned construction examples are presented in order to indicate at a wide variety of possible constructional solutions and to point out at typical features of VD rather than to make a a comprehensive overview. There are a lot of other mechanisms employing the controlled elastic deformation and vibration. A beam deflection unit, Fig.9 [119], employes the possibility of the flexural deformation control in bimorfic piezoelectric elements. This unit enables to increase an operation speed and precision of the scanning and simultaneously to simplify the construction and to reduce its weight in comparison with the conventional ones. Fig.11 shows the construction diagram of the unit and the sectional views. The piezoelectric plates 1 and 2 are rigidly connected into the bimorfic element and fixed into the frame 3 by one of its ends. At the other end the reflector 4 is attached. The external 5-10 and the internal 11-19 electrodes are connected electrically with the control block 17.

The unit operates as follows. If the control voltage is applied at the electrodes 5,6,11 and 12 , one of the plates elongates and the other shortens causing the bending of the bimorfic element in the plane XOY. If the control voltage is applied at the electrodes 7-10 and 13-16, the bending of the bimorfic element in the plane XOZ is obtained. These flexural motions cause the angular motions of the reflector 4 proportional to the magnitudes of the applied voltages.

Mathematical models of VD. Many of VD are obtained by modifying the traditional vibroconveyers by increasing their operation frequency several hundred times. However, at ultrasonic operating frequencies the elastic resonant vibration and elastic wave phenomena take place. The amplitudes and phases of the points of a VC differ from each other depending upon the form of standing or travelling waves.

The measuring and experimental investigation of the vibrations in the active links of VD is complicated because of very small amplitudes and high vibration frequencies. The

experimental investigation can be carried out by means of an interferometric holography. Fig.10a presents a resonant vibration hologram of the piezoelectric cylinder employed as an input link of a VD (vibration frequency ≈ 24000Hz). The vibration mode has three standing elastic waves along a circumference and one half of the wave along the height of the cylinder. Fig.10b presents the computed wave form. During contact interaction the elasticity of the contacting pairs is of great importance, too. The duration of the contact-impact interaction comprises a greater part of the vibration period, and in some cases contacting points don't separate at all. Consequently, deformations of the contacting surface and sliding friction forces are to be taken into account. Vibrodrives are separated into point-contact and surface-contact classes according to the way how the contact surface is deformed. In point-contact VD a contact interaction takes place only in discrete points by means of contact elements attached to an input link, local contact phenomena being assumed independent at each contact point. In the surface-contact VD their links contact along continuous parts of their surface.

The above mentioned considerations suggest the insufficiency of employing lumped parameter mathematical models for presenting the dynamic equations of VD. The adequate mathematical models of VD can be obtained employing the finite element techniques enabling to present a dynamic behavior of elastic links of a great variety of VD configurations (Fig.11) by means of structural dynamic equations. The dynamic behavior of a VD as of a whole is obtained by adding nonlinear terms and unilateral constraints upon displacements and velocities of nodal points of a model. In general, the dynamics of VD is governed by the system

$$
\begin{cases}
M\ddot{U} + C\dot{U} + KU = W(U,\dot{U}) + R(t) - P_N^T\lambda_N - P_T^T\lambda_T , & \text{(a)}\\
P_N U \le d , & \text{(b)}\\
a\dot{\psi} + P_T\dot{U} = 0 , \text{ in the case of active constraints (b),(c)} & \\
J\ddot{\psi} + b\dot{\psi} = a\lambda^T + M_{ext} , & \text{(d)}\\
|\lambda_T| \le k_f\lambda_N , & \text{(e)}\\
\lambda_N > 0 , & \text{(f)}
\end{cases}
$$

where M,C,K - mass, damping and stiffness matrices of the model,

U - nodal displacement vector,

R(t) - exciting force vector,

P_N - constraint matrix defining the constraints in the direction normal to the contacting surfaces,

d - vector defining initial clearances between the contact points of an input link and the surface of an output link,

a,P_T - matrices, in a no-sliding case defining the constraints upon the velocities in the direction tangential to the contacting surfaces,

λ_N,λ_T - normal and tangential components of the contact forces,

ψ - angular or linear displacement of an output link (in the case of several d.o.f. of an output link - displacement vector),

J - mass or moment of inertia of an output link,

b - fluid friction coefficient,

M_{ext} - external force moment or external force applied to an output link,

k_f - Coulomb friction coefficient,

W(U,$\dot{U}$) - term accounting for other nonlinear interaction forces and the nonlinear features of a structure.

The main difficulties of the computer analysis of the above mentioned model are due to its essential nonlinearity, large dimension and a necessity to compute during time intervals consisting of a large number of vibration periods. A thorough and comprehensive analysis of the dynamic equations is possible only if corresponding effective techniques and software is available. The techniques based upon the direct integration of the equations of motion and the time-averaging approach together with the structural displacement control synthesis algorithms are presented in the first part of this work. The second part concentrates upon the finite element models of VD and the analysis of computed results obtained employing the techniques presented in the first part.

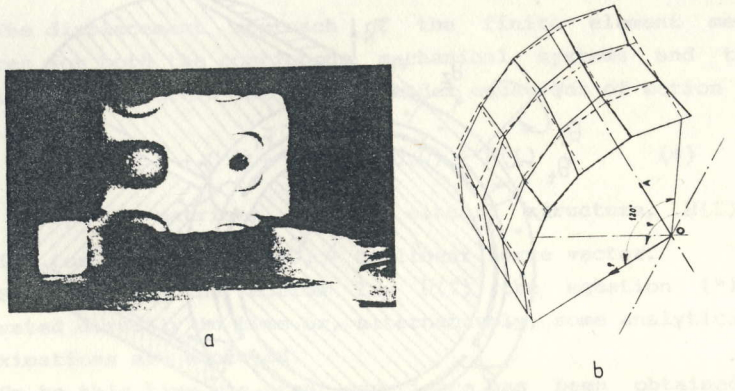

a b

Fig.10a- Resonant vibration hologram of a piezoelectric cylinder vibroconverter (vibration frequency ≈ 24000Hz)
b- computed standing wave shape of the 1/6 part of the cylinder

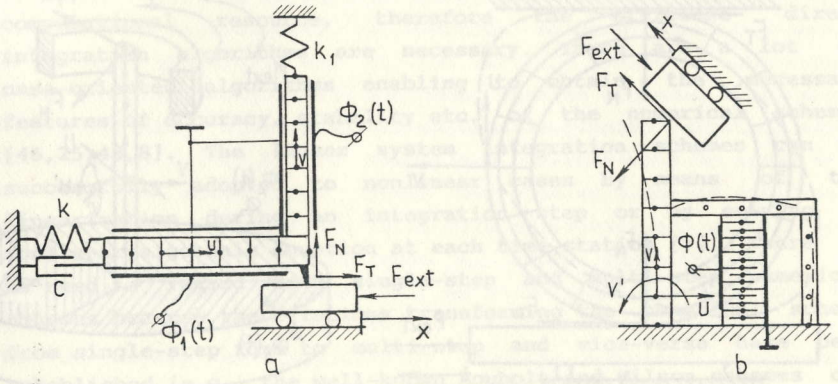

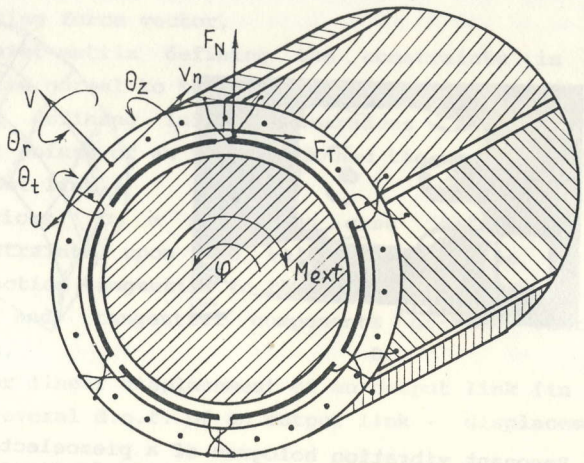

c

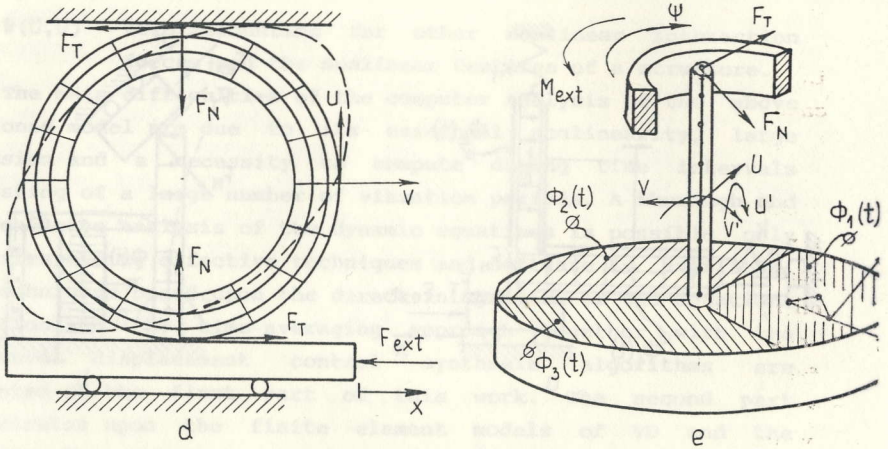

d e

Fig.11 Finite element models of vibrodrives:
a,b - with piezoelectric rod vibroconverters (VC);
c - with cylindrical VC; d - with ring VC;
e - with disk VC and rod concentrator

PART 1. TECHNIQUES

The displacement approach of the finite element method produces for both the continuous mechanical systems and those with lumped parameters the uniform model equations of motion

$$M\ddot{U} + C\dot{U} + KU = W(U,\dot{U}) + R(t) \quad , \qquad (*)$$

where M,C,K - matrices of the elastic structure, R(t) - exciting force vector, $W(U,\dot{U})$ - nonlinear force vector.

For obtaining the motion law U(t) the equation (*) is integrated directly in time or, alternatively, some analytical approximations are employed.

Up to this time the great experience has been obtained in the field of the linear and nonlinear mechanical vibration analysis [88,89]. As a rule, exact or approximate analytical approaches had been adopted successfully to the systems with only several degrees of freedom (d.o.f.), in remaining cases employing numerical or semianalytical techniques.

Obtaining the transient response of the structures with a large number of d.o.f. is expensive and requires great amounts of computational resource, therefore the efficient direct integration algorithms are necessary. There are a lot of case-oriented algorithms enabling to obtain the necessary features of accuracy, stability etc. of the numerical schemes [46,25,43,8]. The linear system integration schemes can be successfully adopted to nonlinear cases by means of the linearization during an integration step or by solving a nonlinear algebraic equation at each time station [1]. There is no need to regard both single-step and multi-step numerical schemes because the relations transforming the numerical scheme from single-step form to multi-step and vice-versa have been established (e.g., the well-known Houbolt and Wilson schemes can be derived from the generalized Newmark's method [46,25]).

The stationary motion laws of elastic structures as well as the transient ones can be obtained by the direct integration of the equations of motion. If the damping forces are present, the transient motions taking place after an external force

application upon a structure cease after a certain time interval t^* . The motion law after the time point t^* can be reasonably regarded as stationary. Unfortunately, for the structures with high values of the mechanical Q-factor (high-quality resonant structures) such an approach is very inefficient and can even produce incorrect results because of a very large number of integration steps until the stationary motion law is obtained. In some cases even the existence of a periodic motion at a given excitation law remains unclear. As a principal source of the rounding-off errors appears the essential difference between the magnitudes of conservative and dissipative members in the equations of motion. The inertia force $M\ddot{U}$ and elastic force KU predominate the dissipative force $C\dot{U}$, $|M\ddot{U}|>>|C\dot{U}|$, $|KU|>>|C\dot{U}|$, but the dynamic equilibrium requirement implies the relation $|M\ddot{U}+KU|\approx|C\dot{U}|$, resulting in poor accuracy of the computer arithmetics.

There are several approaches enabling to avoid or to reduce the difficulties mentioned above [49,51,30,131,142,145]. As a rule, they can be adopted directly to the structures with only several degrees of freedom. Regarding the large structures, some development is necessary. The analysis of stationary motion laws in time domain can be carried out by finding the zero values of some algebraic function obtained by integrating directly the equations of motion [137,101,28]. In the frequency domain the nonlinear harmonic balance equations are obtained, and the use of the averaging techniques enables to investigate transient motions in terms of slow-varying amplitudes [63,30,121]. In [63] the combined harmonic balance and direct integration approach was applied to the structures with local nonlinearities.

An important class is comprised by the systems with kinematic pairs interacting by the normal, oblique impact or sliding friction forces [133,107,108,50,51,122]. Considering the numerical analysis oriented formulation, in place of the nonlinear force term $W(U,\dot{U})$ the constraints $PU \le d_o$, $P^{(i)}U=d_i$, $i=1,2,\ldots$ are employed and the case oriented numerical integration and time-averaging techniques are to be developed [60-63] .

Obtaining a system with the prescribed dynamic features

comprises the essence of the synthesis problem. On one hand, it can be approached as the optimal shape design problem [52,14,139,124,127] or the materials with the necessary mechanical properties can be employed in order to obtain the desirable dynamic response [31]. On the other hand, active control methods can be adopted [95,109,110,112]. The prescribed motions of the mechanical structures can be obtained by employing the general optimal control techniques [39,114,143,141,118].

In [65,78] the transient structural vibration programmed control synthesis algorithm is presented. A general approach to the closed loop control synthesis is presented by the dynamic programming method, the use of which is restrained with the systems with several d.o.f. [9]. The most common way to obtain the closed loop control system is to employ the automatic control techniques [87,102,109]. The techniques based upon the inverse dynamic problem solution are applicable, too [93,115,129,80]. In this case the synthesis is carried out on base of the general statements defined by symmetry considerations. It has been shown that the properties of the obtained control laws are fully identical to those obtained by employing classical methods of the control theory based on the minimization of quadratic functional [115].

1. DYNAMIC MODELS AND THEIR REDUCTION

This chapter presents the techniques for reducing the number of dynamic degrees of freedom of elastic structures with nonlinearities. For the linear structures, the mass condensation and the higher mode dynamic contribution truncation approaches are possible. In nonlinear structural analysis the model equations are represented in modal coordinates of the linear part of the structure or in modal coordinates of the structure linearized at the solution point, with subsequent truncation of dynamic contributions of higher modes. The alternative approaches are based on identification techniques for obtaining a reduced set of dynamic equations.

The original results presented in this chapter consist of the development of the dynamic contribution truncation method applied to the elastic structures with unilateral constraints upon their displacements and velocities. The model equations are represented in modal coordinates of the linear structure, and as a result, a low-dimension equation system with the nonlinear term is obtained. This approach is directly applied to the structures with the impact and sliding friction interaction points. If simultaneously the dynamic and dissipative contributions of higher modes are truncated, the nonlinear term represents a force created by an elastic spring of unidirectional action. If the dissipative contributions are retained, a unidirectional dissipative element and a spring are represented by this nonlinear term.

1.1 REDUCTION OF LINEAR STRUCTURAL EQUATIONS

The mass condensation approach. The consideration is restricted within the range of elastic structures with proportional damping presented by the matrix equation of motion

$$M\ddot{U} + C\dot{U} + K U = R(t) \quad , \qquad (1.1)$$

where M, K, $C = \alpha M + \beta K$ - mass, stiffness and damping structural matrices U, R - nodal displacement and external force vectors. The early approaches to the reduction of the number of dynamic degrees of freedom (d.o.f.) of the equation (1.1) treated some of

them as the master d.o.f. and eliminated the remaining ones from (1.1) [13,19,27]. Such a reduction, called dynamic condensation, was obtained by presenting the equation (1.1) as

$$\begin{bmatrix} M_{11} M_{12} \\ M_{21} M_{22} \end{bmatrix} \begin{bmatrix} \ddot{U}_1 \\ \ddot{U}_2 \end{bmatrix} + \begin{bmatrix} C_{11} C_{12} \\ C_{21} C_{22} \end{bmatrix} \begin{bmatrix} \dot{U}_1 \\ \dot{U}_2 \end{bmatrix} + \begin{bmatrix} K_{11} & K_{12} \\ K_{21} & K_{22} \end{bmatrix} \begin{bmatrix} U_1 \\ U_2 \end{bmatrix} = \begin{bmatrix} 0 \\ R_2 \end{bmatrix} , \qquad (1.2)$$

where "2" indicates the master d.o.f.

External forces are assumed to be applied only to the master d.o.f., i.e., $R_1 = 0$. In the case of harmonic external excitation $R_2 e^{i\omega t}$, we cast the problem into frequency domain and represent the resulting motion law as $U e^{i\omega t}$. With no damping (C=0), the algebraic equation for obtaining the amplitudes appears as

$$\begin{bmatrix} D_{11} & D_{12} \\ D_{21} & D_{22} \end{bmatrix} \begin{bmatrix} U_1 \\ U_2 \end{bmatrix} = \begin{bmatrix} 0 \\ R_2 \end{bmatrix} , \qquad (1.3)$$

where $D = K - \omega^2 M$ is the dynamic stiffness matrix.

The effective dimension of the system is reduced by rearranging it to the form

$$D^* U_2 = R_2 \quad , \qquad (1.4)$$

where $D^* = D_{22} - D_{21} D_{11}^{-1} D_{12}$. (1.5)

The matrix M^* corresponding to the dynamic matrix D^* is obtained by the relation [27]

$$M^* = -\frac{\partial}{\partial(\omega^2)} D^* = M_{22} - D_{21} D_{11}^{-1} M_{12} - M_{21} D_{11}^{-1} D_{12} + D_{21} D_{11}^{-1} M_{11} D_{11}^{-1} D_{12} , \qquad (1.6)$$

and the matrix K^* - by the relation

$$K^* = D^* + \omega^2 M \quad . \qquad (1.7)$$

Finally, the reduced equation appears as

$$(K - \omega^2 M)\, U_2 = 0 \quad . \qquad (1.8)$$

It isn't a simple task to solve (1.8) , because the matrices K^*, M^* depend upon the frequency ω . In order to find the value of the lowest eigenfrequency, the equation (1.8) is solved

iteratively. At the i-th iteration the matrices $K^*(\omega)$, $M^*(\omega)$ are obtained by substituting the value $\omega^{(i-1)}$ obtained at the (i-1)-th iteration, [27]. As an initial estimate the value $\omega^{(0)}=0$ is regarded. The simplified approach to the mass condensation considers the approximate values of the matrices $K^*= K^*(0)$, $M^*=M^*(0)$. In this case the relation (1.6) in place of D employs K, and the reduced equation is obtained as

$$M^*\ddot{U}_2+ C^*\dot{U}_2+ K^*U_2= R_2(t) \quad , \qquad (1.9)$$

where $M^* = T^TM\,T$, $C^* = T^TC\,T$, $K^* = T^TK\,T$ with the transformation matrix $T = \begin{bmatrix} -K_{11}^{-1}K_{12} \\ I \end{bmatrix}$.

The value U_1 is obtained from the relation

$$U_1 = - K_{11}^{-1}K_{12}U_2. \qquad (1.10)$$

The shortcoming of the simplified approach is that the obtained results can significantly depend upon the proper selection of master d.o.f. thus requiring a great deal of engineering intuition.

Representing in the subspace of modal coordinates. It seems more natural to reduce the effective number of d.o.f. by presenting the equation of motion in modal coordinates and truncating the dynamic contributions of higher modes, eigenfrequencies of which are remote to the expected vibration frequency (e.g., substructure synthesis method [38]). Simultaneously an account of the remaining quasistatic structural compliance of the dynamically truncated modes is to be taken.

Consider the structural equation of motion (1.1) with the proportional damping, i.e., $C = \alpha M + \beta K$. As a result of solving the eigenproblem

$$(K - \omega^2M)\,U = 0 \quad , \qquad (1.11)$$

the eigenfrequencies ω_i, $i=\overline{1,n}$ and the eigenvectors, ordered as columns of the matrix Δ, are obtained. The transfer to modal coordinates is carried out employing the substitution [44]

$$U = \Delta\, z \quad . \qquad (1.12)$$

We present the vector of squares of eigenfrequencies as $\begin{bmatrix} \omega_1^2 \\ \omega_2^2 \end{bmatrix}$, and the matrix of eigenvectors as $\Delta = [\Delta_1,\Delta_2]$, where the submatrix Δ_2 and the subvector ω_2^2 correspond to the truncated modes. After the truncation, the equation (1.1) in modal coordinates takes the form

$$\begin{cases} I\,\ddot{z}_1 + \mathrm{diag}(\mu_1)\,\dot{z}_1 + \mathrm{diag}(\omega_1^2)\,z_1 = \Delta_1^T R, \\ \mathrm{diag}(\omega_2^2)\,z_2 = \Delta_2^T R, \end{cases} \qquad (1.13)$$

where $\mathrm{diag}(\mu_1)$, $\mathrm{diag}(\omega_1^2)$, $\mathrm{diag}(\omega_2^2)$ denotes the diagonal matrices containing the vectors μ_1, ω_1^2 and ω_2^2 on their main diagonals, and the equalities $\mathrm{diag}(\mu_1)=\Delta_1^TC\Delta_1$, $\mathrm{diag}(\omega_1^2)=\Delta_1^TK\,\Delta_1$, $\mathrm{diag}(\omega_2^2)=\Delta_2^TK\Delta_2$ are held.

The system (1.13) is the reduced one with regard to the original equation (1.1). The dimension of the first equation of (1.13) is the same as the length of the vector z_1. From the second equation of (1.13) the quasistatic correction caused by the remaining structural compliance of the truncated modes is obtained.

It should be noticed, that formally (1.13) can be obtained in place of (1.12) employing the substitution

$$U = \Delta_1z_1 + \Delta_2z_2 = \Delta_1z_1 + \tilde{U} \quad , \quad \dot{U} = \Delta_1\dot{z}_1 \quad , \quad \ddot{U} = \Delta_1\ddot{z}_1 \quad . \qquad (1.14)$$

Up to now it was assumed, that all the structural modes are obtained. In fact, it isn't necessary to determine the higher modes ω_2^2, Δ_2 explicitly. By multiplying the first relation of (1.14) by Δ_2^TK and by Δ_1^TK on the left, z_1 and z_2 are expressed from the obtained relations as

$$z_1 = \mathrm{diag}(\,{}^1\!/_{\omega_1^2}\,)\,\Delta_1^TK\,U \quad , \qquad (1.15)$$

$$z_2 = \mathrm{diag}(\,{}^1\!/_{\omega_2^2}\,)\,\Delta_2^TK\,U \quad . \qquad (1.16)$$

By multiplying (1.15) by Δ_1, and (1.16) – by Δ_2 on the right

hand side and expressing Z_1 and Z_2 , we obtain

$$U = [\, \Delta_1 \mathrm{diag}(\, {}^1/_{\omega_1^2}\,)\, \Delta_1^T + \Delta_2 \mathrm{diag}(\, {}^1/_{\omega_2^2}\,)\, \Delta_2^T \,]\, K\, U \,. \qquad (1.17)$$

From (1.17) follows the relation

$$\Delta_2 \mathrm{diag}(\, {}^1/_{\omega_2^2}\,)\, \Delta_2^T = K^{-1} - \Delta_1 \mathrm{diag}(\, {}^1/_{\omega_1^2}\,)\, \Delta_1^T \,. \qquad (1.18)$$

Denoting in (1.18) the right-hand side compliance matrix as

$$S_k = K^{-1} - \Delta_1 \mathrm{diag}(\, {}^1/_{\omega_1^2}\,)\, \Delta_1^T \,, \qquad (1.19)$$

the quasistatic correction of displacements $\tilde{U}$ is expressed as

$$\tilde{U} = S_k\, R(t) \,. \qquad (1.20)$$

In the case of singular stiffness matrix the relation (1.19) can't be applied directly. In order to determine S_k without obtaining higher structural modes, the approach proposed in [38] can be applied (see appendix 2).

1.2 REDUCTION OF NONLINEAR STRUCTURAL EQUATIONS

Representing in the subspace of modal coordinates of a linear part. Consider the structural equation of motion

$$M\, \ddot{U} + C\, \dot{U} + K\, U = W(\, U, \dot{U}\,) + R(t) \,, \qquad (1.21)$$

the only difference of which from (1.1) consists in the presence of a nonlinear function of displacements and velocities on the right hand side. The equation (1.34) is represented in a subspace of modal coordinates similar to the equations (1.13) :

$$\begin{cases} I\ddot{z}_1 + \mathrm{diag}(\,\mu_1)\dot{z}_1 + \mathrm{diag}(\omega_1^2) z_1 = \Delta_1^T R(t) + \Delta_1^T W(\Delta_1 z_1 \tilde{U},\ \Delta_1 \dot{z}_1), \\ \tilde{U} = S_k\,(\, R(t) + W(\Delta_1 z_1 + \tilde{U},\ \Delta_1 \dot{z}_1). \end{cases} \qquad (1.22)$$

In general, the equations (1.22) aren't independent because of the nonlinear function W the a right-hand side, therefore the

system (1.22) hasn't essential computational advantages in comparison with the original equation (1.21). Only when the resonant structural vibration takes place in the range of the lowest eigenfrequencies, we can simplify the equation system by ignoring the function W in the second equation of (1.22). In this case $\tilde{U}$ is expressed from the second equation of (1.22), that is linear now, and the first equation of (1.22) represents the reduced dynamic equation of a nonlinear structure. The aforementioned reduction is based upon a supposition, that higher harmonic components of a nonlinear force $W(U(t),\dot{U}(t))$ in the range of eigenfrequencies of truncated modes are comparatively small, and the lower harmonic components don't influence significantly the generalized displacements Z_2 .

If the nonlinear function is continuous and depends only upon the displacements $W(U)$, the structural equations at each time point t can be presented in the subspace of the modal coordinates of a linearized system [32] obtained by solving the eigenproblem

$$\left[\left(K - \frac{\partial W}{\partial U}\bigg|_t \right) - \omega^2 M \right] = 0 \,. \qquad (1.23)$$

Obviously, the tangential correction of the stiffness matrix used in (1.23) presents a better approximation in comparison with the representation in the modal coordinates of the linear part only. From the other point of view, the correction of modal coordinates at each computation step is a time consuming operation. In [18] the subspace of modal coordinates is completed by the derivatives of the eigenvectors with respect to generalized displacements in order to reduce the truncation errors, and enabling to keep the same modal coordinate basis during several time steps.

Application of identification techniques. The equations of motion in the subspace of the modal coordinates of the linear part are presented as

$$I\ddot{z} + \mathrm{diag}(\mu)\, \dot{z} + \mathrm{diag}(\omega^2)\, z = \Delta^T R(t) + \Delta^T W(\Delta z,\ \Delta \dot{z}). \qquad (1.24)$$

Employing the identification techniques the function W is replaced by the function

$$\hat{W} = \sum_j c_j \, f(z_{j_1}, z_{j_2}) \quad , \; i = \overline{1,n} \quad , \qquad (1.25)$$

and the subset of master generalized displacements $z_{j_1}, z_{j_2}, \ldots$ is determined. The parameters of the functional dependence (1.25) can be obtained, e.g., employing the least squares approach, considering the values of the functions W and $\hat{W}$ at random values of their arguments [29].

1.3 REDUCTION OF STRUCTURAL EQUATIONS WITH UNILATERAL CONSTRAINTS

The structural equation of motion with unilateral constraints we consider in the form

$$\begin{cases} M\ddot{U} + C\dot{U} + K U = R(t) \quad , \\ P U \le d_o \quad . \end{cases} \qquad (1.26)$$

By representing the problem in the modal coordinates of the linear part, truncating the dynamic contributions of higher modes and employing the Lagrange multipliers (see chap.3.4 for details) we obtain the system

$$\begin{cases} I\ddot{z}_1 + \mathrm{diag}(\mu_1)\dot{z}_1 + \mathrm{diag}(\omega_1^2) z_1 = \Delta_1^T (R - P^T\lambda) \quad , (1.27.1) \\ \mathrm{diag}(\omega_2^2) z_2 = \Delta_2^T (R - P^T\lambda) \quad , (1.27.2) \\ P\Delta_1 z_1 + P\Delta_2 z_2 = d_o \quad . (1.27.3) \end{cases} \qquad (1.27)$$

The values of the Lagrange multipliers λ denote the magnitudes of the normal interaction forces produced by the constraints upon a structure. Only nonnegative values of these forces are possible. Expressing z_2 from the second equation of (1.27) and substituting into the third equation, we obtain the vector λ as

$$\lambda(z_1) = (P S_k P^T)^{-1} (P \Delta_1 z_1 + P S_k R - d_o) \quad , \qquad (1.28)$$

and each component of λ is replaced by

$$\lambda_i = \begin{cases} \lambda_i \quad , & \text{if} \quad \lambda_i > 0 \quad , \\ 0 \quad , & \text{otherwise} \quad . \end{cases}$$

Substituting (1.28) into the first equation of (1.27) we obtain the reduced equation of motion

$$I\ddot{z}_1 + \mathrm{diag}(\mu_1)\dot{z}_1 + [\mathrm{diag}(\omega_1^2) + \Delta_1^T \bar{P}^T A^{-1} \bar{P} \Delta_1] z_1 = \Delta_1^T (I - \bar{P}^T A^{-1} \bar{P} S_k) R(t) \quad , \qquad (1.29)$$

where $A = \bar{P} S_k \bar{P}^T$, and $\bar{P}$ denotes the matrix P, from which the rows corresponding to the zero values of λ_i are deleted. That means, the matrix $\bar{P}$ represents only the constraints active at the time point t. The dimension of the reduced equation (1.29) is equal to the length of the vector z_1. The generalized displacements z_2 at each time point are obtained from the second equation (1.27).

The equation (1.27) was obtained by truncating not only dynamic, but also dissipative contributions of the higher modes. In order to take account of the dissipative forces caused by the inertialess motion of the higher modal components, the equations of the system (1.27), beginning with the second equation, are presented as

$$\begin{cases} \mathrm{diag}(\mu_2)\dot{z}_2 + \mathrm{diag}(\omega_2^2) z_2 = \Delta_2^T (R - P^T\lambda) \quad , & (1.27.2)' \\ P\Delta_1 z_1 + P\Delta_2 z_2 = d_o \quad , & (1.27.3)' \\ P\Delta_1 z_1^{(i)} + P\Delta_2 z_2^{(i)} = 0 \quad , \; i=1,2,\ldots \quad . & (1.27.4)' \end{cases}$$

Considering the numerical integration scheme it is reasonable to suppose that the values of the higher derivatives $z_2^{(i)}$ are equal to zero during one time step. Assume the zero values of all derivatives of the second and higher orders, i.e., $\ddot{z}_2 = z_2^{(3)} = \ldots = 0$. After differentiating the second equation of (1.27), we eliminate z_2, $\dot{z}_2$ from the obtained system. Derivatives

of the external force R is assumed to be $\dot{R} = \ddot{R} = 0$. After some manipulation we obtain

$$\lambda(z_1, \dot{z}_1) = A^{-1}(P\,\Delta_1 z_1 + B_1 A^{-1} P\,\Delta_1 \dot{z}_1 - d_o + P\,S_k R)\,, \qquad (1.30)$$

where $B_1 = P\,S_{D1}P^T$, $S_{D1} = \Delta_2 \mathrm{diag}(\mu_2/\omega_2^2)\,\Delta_2^T$, and the values of the components of the vector λ obtained by the relation (1.30) are replaced by

$$\lambda_i = \begin{cases} \lambda_i\,, & \text{if the value } \lambda_i > 0 \text{ was obtained from (1.30) and from (1.28)}\,, \\ 0\,, & \text{otherwise}\,. \end{cases}$$

If we assume the zero values of the derivatives $z_2^{(l)}$ beginning with $l=3$, i.e., $z_2^{(3)} = z_2^{(4)} = \ldots = 0$, the relation for obtaining λ takes the form

$$\lambda(z_1, \dot{z}_1, \ddot{z}_1) = A^{-1}(P\,\Delta_1 z_1 + B_1 A^{-1} P\,\Delta_1 \dot{z}_1 + B_1 A^{-1} B_1 A^{-1} P\,\Delta_1 \ddot{z}_1 - B_2 A^{-1} P\,\Delta_1 \ddot{z}_1 - d_o + P\,S_k R)\,, \qquad (1.31)$$

where $B_2 = P\,S_{D2}P^T$ and $S_{D2} = \Delta_2 \mathrm{diag}(\mu_2^2/\omega_2^6)\,\Delta_2^T$.

The matrix $\Delta_1^T \bar{P}^T A^{-1} \bar{P}\,\Delta_1$ appearing on the right hand side of the equation (1.29) can be regarded as a complementary stiffness matrix. Its presence explains the elastic behavior of the structure interacting with the constraint, regardless of the local contact conditions. Similarly, substituting the relations (1.30) and (1.31) into the first equation of (1.27), we obtain a complementary damping matrix $\Delta_1^T P^T A^{-1} B_1 A^{-1} P\,\Delta_1$ and a complementary mass matrix $\Delta_1^T P^T A^{-1}(B_1 A^{-1} B_1 + B_2) A^{-1} P \Delta_1$.

Structures with viscoelastic rheological models of the normal impact are presented by the following equation of motion with the constraints:

$$\begin{cases} M\ddot{U} + C\dot{U} + K U = R(t)\,, \\ c\dot{x} + k x = 0\,, \\ P U + Q x \le d_o\,, \\ P U^{(l)} + Q x^{(l)} = d_l\,, \quad l = 1, 2, \ldots\,. \end{cases} \qquad (1.32)$$

where c, k - damping and stiffness matrices or scalar coefficients, X - displacement vector or a displacement of the rheological model, Q - constraint matrix or coefficient.

The system (1.32) is represented in the truncated modal coordinates of the linear part as

$$\begin{cases} I\ddot{z}_1 + \mathrm{diag}(\mu_1)\dot{z}_1 + \mathrm{diag}(\omega_1^2) z_1 = \Delta_1^T (R - P^T \lambda)\,, \\ \mathrm{diag}(\omega_2^2) z_2 = \Delta_2^T (R - P^T \lambda)\,, \\ c\dot{x} + k x = -Q^T \lambda\,, \\ P\,\Delta_1 z_1 + P\,\Delta_2 z_2 + Q x = d_o\,, \\ P\,\Delta_1 z_1^{(l)} + P\,\Delta_2 z_2^{(l)} + Q x^{(l)} = 0\,, \quad l = 1, 2, \ldots \end{cases} \qquad (1.33)$$

Eliminating $z_2, \dot{z}_2, X, \dot{X}$ from (1.33), we obtain the relations similar to (1.28), (1.30), (1.31) for determining λ, where the matrices A, B_1, B_2 denote

$$\begin{aligned} A &= P\,S_k\,P^T + Q\,k^{-1}Q^T\,, \\ B_1 &= P\,S_{D1}P^T + Q\,k^{-1}c\,k^{-1}Q^T\,, \\ B_2 &= P\,S_{D2}P^T + Q\,k^{-1}c\,k^{-1}c\,k^{-1}Q^T\,. \end{aligned} \qquad (1.34)$$

In the case of the absolutely rigid local contact condition ($k \to \infty$), the relations (1.34) coincide with those presented by A, B_1, B_2.

Structures with the oblique impact and sliding friction interaction points. The dynamic behavior of such systems is presented by the structural equation of motion with the constraints

$$\begin{cases} M\ddot{U} + C\dot{U} + KU = R(t) \\ P_N U \le d_o \\ P_T \dot{U} = 0 \end{cases} , \qquad (1.35)$$

Each element of the matrix product $P_N U$ denotes the relative displacement of contacting points in the normal direction to the contact surface, where each element of the vector d_o represents the initial clearance between these points in the static equilibrium state (the negative value denotes the preload). The corresponding elements of the matrix product $P_T \dot{U}$ denote the tangential relative velocities of contacting points. They must have zero values until the tangential interaction force doesn't exceed its critical value.

Presenting the equations in the truncated modal coordinates and employing the Lagrange multipliers, we obtain

$$\begin{cases} I\ddot{z}_1 + \mathrm{diag}(\mu_1)\dot{z}_1 + \mathrm{diag}(\omega_1^2) z_1 = \Delta_1^T (R - P_N^T \lambda_N - P_T^T \lambda_T) , \\ \mathrm{diag}(\omega_2^2) z_2 = \Delta_2^T (R - P_N^T \lambda_N - P_T^T \lambda_T) , \\ P_N \Delta_1 z_1 + P_N \Delta_2 z_2 = d_o , \\ P_T \Delta_1 z_1 + P_N \Delta_2 z_2 = \begin{pmatrix} \vdots \\ P_{Tj}(\Delta_1 z_{1oj} + \Delta_2 z_{2oj}) \\ \vdots \end{pmatrix} . \end{cases} \qquad (1.36)$$

The values of the Lagrange multipliers λ_N, λ_T denote the magnitudes of the normal and tangential interaction forces produced by constraints upon a structure. The normal forces are allowed to acquire only nonnegative values $\lambda_{Nj} \ge 0$, and the absolute values of the tangential forces don't to exceed their

critical values, i.e., $|\lambda_{Tj}| \le k_f \lambda_{Nj}$, where k_f - the Coulomb friction coefficient. At the time point when the sliding in the j-th contact pair ceases, the values of the generalized displacements z_{1j}, z_{2j} are denoted through z_{1oj} , z_{2oj} . If in the j-th contact pair sliding takes place, the values z_{1oj}, z_{2oj} are updated at each time point. On this account we make the following definitions. Assume that the matrix P_N contains only the rows P_{Nj}, corresponding to the active constraints (i.e., having positive normal interaction forces $\lambda_{Nj} > 0$). The matrix $\hat{P}_N$ denotes the matrix formed from the rows of the matrix P_N as follows: each row P_{Nj} corresponding to the sliding contact pair (i.e., $|\lambda_{Tj}| \le k_f \lambda_{Nj}$), is replaced by the row $P_{Nj} + P_{Tj} k_f \operatorname{sign} \lambda_{Tj}$, otherwise, it remains unchanged. The matrix $\hat{P}_T$ denotes the matrix P_T, from which the rows corresponding to the inactive constraints and sliding contact pairs are deleted. In a compact form it is presented as

$$P_{Nj} = \begin{cases} P_{Nj}, & \text{if } \lambda_{Nj} > 0 , \\ 0 , & \text{otherwise ;} \end{cases}$$

$$\hat{P}_{Nj} = \begin{cases} P_{Nj}, & \text{if } |\lambda_{Tj}| < k_f \lambda_{Nj} , \\ P_{Nj} + P_{Tj} k_f \operatorname{sign} \lambda_{Tj} , & \text{otherwise ;} \end{cases}$$

$$\hat{P}_{Tj} = \begin{cases} P_{Tj}, & \text{if } \lambda_{Nj} > 0 \text{ and } |\lambda_{Tj}| < k_f \lambda_{Nj}, \\ 0 , & \text{otherwise ;} \end{cases}$$

$$\bar{P} = \begin{pmatrix} P_N \\ \hat{P}_T \end{pmatrix} , \quad \bar{\bar{P}} = \begin{pmatrix} \hat{P}_N \\ \hat{P}_T \end{pmatrix} , \quad \lambda = \begin{pmatrix} \lambda_N \\ \lambda_T \end{pmatrix} , \quad d = \begin{pmatrix} d_o \\ \hline \vdots \\ P_{Tj}(\Delta_1 z_{1oj} + \Delta_2 z_{2oj}) \\ \vdots \end{pmatrix} .$$

Taking account on the notation introduced above, the relation for determining λ is obtained as

$$\lambda = (\bar{P} S_k \bar{\bar{P}}^T)^{-1} (\bar{P} \Delta_1 z_1 + \bar{P} S_k R - d_o) . \qquad (1.37)$$

The actual impact and friction interaction points aren't known in advance, therefore it is necessary to iterate at each time integration step. The λ value from the relation (1.37) is obtained in by the following algorithm.

Algorithm 1.1

1. Include all the constraints into P_N, P_T. Assume
$$\bar{P} = \bar{\bar{P}} = \begin{bmatrix} P_N \\ P_T \end{bmatrix} .$$

2. Substitute the values of λ_N, λ_T, obtained from the relation (1.37), into the first two equations of (1.36), and obtain the value $Z_{t+\Delta t}$ by numerical integration.

3. Determine the values λ_N, λ_T at the time point $t+\Delta t$, substituting the value $Z_{i,\,t+\Delta t}$ into the relation (1.37).

4. If among the obtained values of elements of the vector λ_N there are any $\lambda_{Nj} < 0$, delete the corresponding rows from the matrices P_N, P_T.
If among the constraints there are any violating the constraint $P_{Nj}(\Delta_1 z_1 + \Delta_2 z_2) > 0$, place again the corresponding rows into the matrices P_N, P_T.
Redetermine the matrices $\bar{P} = \bar{\bar{P}}$.

5. If there are any changes made upon the matrices during the step 4., go to step 2.
Otherwise go to step 6.

6. If among the obtained values of the elements of the vector λ_T there are any satisfying the inequality $|\lambda_{Tj}| \geq k_f \lambda_{Nj}$, replace the corresponding row of the matrix P_{Nj} by $(P_{Nj} + P_{Tj} k_f \operatorname{sign} \lambda_{Tj})$ and delete the row P_{Tj} from the matrix P_T.
If among the contact pairs assumed to be in a sliding condition during the previous iteration there are any satisfying the inequality $\lambda_{Tj} P_{Tj} \Delta(Z_{t+\Delta t} - Z_t) > 0$ (i.e., the obtained friction force vector points out at the

direction of sliding), replace the corresponding rows P_{Nj}, P_{Tj} by their original values.
Make the corresponding changes upon the matrices $\bar{P}$, $\bar{\bar{P}}$.

7. If there are any changes made upon the matrices P_N, P_T during the step 6., go to step 2.
Otherwise case go to step 8.

8. For the tangential forces absent in the vector $\hat{\lambda}_T$ assign the values $\lambda_{Tl} = \pm k_f \lambda_{Nl}$.

9. Update the values $\dot{Z}_{1oj} = \dot{Z}_{1,\,t+\Delta t}$, $\dot{Z}_{2oj} = \dot{Z}_{2,\,t+\Delta t}$ for all the contact pairs where sliding takes place.

10. Go to the next time step $t+\Delta t$.

---

2. DYNAMIC ANALYSIS OF LINEAR ELASTIC STRUCTURES

Structural motion laws are obtained by integrating directly the equations of motion or employing the techniques based on integral transforms. The latter way leads to the presentation in time domain (Green's functions approach) or in frequency domain (Fourier series approach).

A direct numerical integration of equations of motion are the main techniques for obtaining structural motion laws. Various criteria are employed when selecting a time integration scheme for a given problem. For obtaining motion laws in the low-frequency range of an eigenfrequency spectrum implicit numerical schemes are preferable. Together with the often employed accuracy, stability, period elongation and numerical damping criteria, convergence of the matrix algebraic equation solution at each time step and overshooting at an initial stage of integration are considered. There are several approaches for obtaining numerical integration schemes, of which a truncation of Taylor series with the last retained term correction, weighted residuals, finite elements in time are considered below. Each approach produces a family of time integration schemes, among which many of the commonly employed numerical schemes can be found.

This chapter contains the systematic presentation of linear system numerical integration schemes and can be regarded as an overview. However, linear system time integration principles presented in this chapter further are employed for obtaining the nonlinear system integration schemes.

2.1 DIRECT AND INDIRECT METHODS

The equation of motion of an elastic structure is considered as

$$M\ddot{U} + C\dot{U} + K U = R(t) \quad , \qquad (2.1)$$

where M, C, K - mass, damping and stiffness matrices each of the dimension nxn , R(t) - external force vector, U, $\dot{U}$, $\ddot{U}$ - nodal displacement, velocity and acceleration vectors each of the

dimension nx1, where n - number of d.o.f. of the structure. It is necessary to obtain a motion law of the structure, i.e., the solution U(t) of the equation (2.1) , with prescribed initial conditions U(0), $\dot{U}(0)$ and excitation law R(t) . This problem can be approached directly or indirectly. The direct approach implies numerical integration of the equation of motion, and the indirect one is carried out by presenting the problem in time domain (Green's functions method) or in frequency domain (Fourier series method).

The direct integration method employs directly the equation of motion (2.1). It is discretized in time and the values of the vector U at time stations $t, t+\Delta t, \ldots$ are obtained by interpolating the values U(t) during the intervals $[t+(i-1)\Delta t, t+i\Delta t\ ]$, $i=1,2,\ldots$.

The time domain approach, or the Green's functions method, presents the dynamic response of the structure as a superposition of responses to the unity pulse excitations $\hat{\delta}(t^*,t)$, Fig.2.1, where the values $\hat{\delta}$ at time points $(t+i\Delta t)$ are defined as

$$\hat{\delta}(j\Delta t,t) = \begin{cases} -j+1+\dfrac{t}{\Delta t}, & \text{if} \quad (j-1)\Delta t \le t < j\Delta t \ , \\ j+1-\dfrac{t}{\Delta t}, & \text{if} \quad j\Delta t \le t < (j+1)\Delta t \ , \\ 0, \text{ otherwise.} \end{cases} \qquad (2.2)$$

The transient dynamic compliance matricx S(t) of the dimension nxn is obtained by integrating an equation of motion with n right-hand side vectors:

$$M\ddot{S} + C\dot{S} + K S = \hat{\delta}(0,t)\, I \qquad (2.3)$$

with the initial values $S_o = 0$, $\dot{S}_o = 0$, where I - the unity matrix of the dimension nxn . The matrices S^{uo}, $\dot{S}^{uo}$ containing in their columns the solutions of the homogeneous equation with unity initial values, are obtained by solving the equation

$$M\ddot{S}^{uo} + C\dot{S}^{uo} + K S^{uo} = 0 \qquad (2.4)$$

with the initial values $S_o^{uo} = I$, $\dot{S}_o^{uo} = 0$, and the equation

$$M \ddot{S}^{uo} + C \dot{S}^{uo} + K S^{uo} = 0 \qquad (2.5)$$

with the initial values $S_o^{uo} = 0$, $\dot{S}_o^{uo} = I$.

The matrices S, S^{uo}, $\dot{S}^{uo}$ define completely the dynamic behavior of the structure. If they are available, the dynamic response of the system to an arbitrary excitation can be obtained without employing the equation (2.1). The displacement vector $U_{k\Delta t}$ at an arbitrary time point $k\Delta t$ is obtained employing the relation

$$U_{k\Delta t} = S^{uo}_{k\Delta t} U_o + \dot{S}^{uo}_{k\Delta t} \dot{U}_o + \sum_{j=1}^{k} S_{(k-j)\Delta t} R_{j\Delta t} \qquad (2.6)$$

The matrices S, S^{uo}, $\dot{S}^{uo}$ can be obtained by integrating the equations (2.3), (2.4), (2.5) directly. However, the elements of these matrices can be obtained experimentally, too. The element S_{ij} can be considered as a response of i-th d.o.f. of a structure due to an excitation of j-th d.o.f. at the time point $t = 0$ by the pulse of the square Δt, where Δt - the time discretization step.

The time domain approach reduces the computational effort in the following cases:

1) when it is necessary to obtain a dynamic response of the same structure to a number of different excitation laws;

2) when it is necessary to obtain a dynamic response of a few specified d.o.f. due to a given excitation at a few specified d.o.f. In such case it is necessary to know only those dynamic compliances S_{ij}, the numbers of columns j of which correspond to the nonzero excitations, and the numbers of rows i correspond to the d.o.f. under consideration.

The frequency domain approach assumes the presentation of an excitation force as well as of a structural response as Fourier integrals

$$R(t) = \int_0^\infty [\, R_c(\omega) - iR_s(\omega) \,]\, e^{i\omega t} d\omega \ , \qquad (2.7)$$

$$U(t) = \int_0^\infty [\, U_c(\omega) - iU_s(\omega) \,]\, e^{i\omega t} d\omega \ . \qquad (2.8)$$

Substituting (2.7), (2.8) into the equation (2.1), we obtain

$$\int_0^\infty (-M\omega^2 + i\omega C + K)(U_c - iU_s)\, e^{i\omega t} d\omega = \int_0^\infty (R_c - iR_s)\, e^{i\omega t} d\omega \ . \qquad (2.9)$$

Equating the real and imaginary parts on the right- and left-hand sides of (2.9), we obtain an algebraic equation system in terms of the amplitudes U_s, U_c as

$$\tilde{K} \begin{bmatrix} U_c \\ U_s \end{bmatrix} = \begin{bmatrix} R_c \\ R_s \end{bmatrix} , \qquad (2.10)$$

for all the values of $\omega \in [0,\infty]$,where $\tilde{K} = \begin{bmatrix} K - \omega^2 M & \omega C \\ -\omega C & K - \omega^2 M \end{bmatrix}$.

Having obtained the amplitudes $U_c(\omega)$, $U_s(\omega)$ from the equation (2.10) an substituting them into the relation (2.8), a time law of a structural response is obtained.

The matrix $\tilde{K}$ is the dynamic stiffness matrix at the harmonic excitation of the frequency ω . The matrix $\tilde{K}^{-1}$ is the dynamic compliance matrix, each element $(\tilde{K}^{-1})_{ij}$ of which can be obtained experimentally, too. Its value equals to the harmonic vibration amplitude at i-th d.o.f, due to the unity harmonic excitation of the frequency ω at the j-th d.o.f.

The frequency domain approach reduces the computational effort in the following cases:

1) if it is necessary to obtain a spectrum of a structural response;

2) if the spectrum of R , and consequently the spectrum of U are discrete and finite, i.e., the integrals (2.7), (2.8) can be presented as truncated Fourier series

$$R(t) = \sum_{j=1}^{N} (R_{ck} - iR_{sk}) e^{ik\omega t} , \qquad (2.11)$$

$$U(t) = \sum_{j=1}^{N} (U_{ck} - iU_{sk}) e^{ik\omega t} , \qquad (2.12)$$

where the number N isn't very large. Only periodic functions possess such a spectrum, therefore the frequency domain approach is preferable for obtaining a periodic response to a periodic excitation.

2.2 CRITERIA FOR SELECTING DIRECT INTEGRATION SCHEME

Let's consider the matrix equation of motion (2.1). A direct numerical integration of this equation means obtaining the values of the vector U at the time points $t, t+\Delta t, t+2\Delta t, \ldots$ by appropriately interpolating the values U(t) during the intervals $[(i-1)\Delta t, i\Delta t]$, $i=1,2,\ldots$. Further we denote $U(i\Delta t) \equiv U_{i\Delta t}$. Let's consider the single-step schemes, defining the values $U_{t+\Delta t}$, $\dot{U}_{t+\Delta t}$, $\ddot{U}_{t+\Delta t}$, ... at the time point $t+\Delta t$ employing only the values U_t, $\dot{U}_t$, $\ddot{U}_t$, ... at the time point t and the equation of motion (2.1). The multi-step schemes employing the values at several previous time points t, $t-\Delta t$, $t-2\Delta t$, ... for obtaining the values at the time point $t+\Delta t$ at present aren't very popular for integration of structural equations of a large dimension because of greater amounts of computer storage in comparison with the single-step schemes and the necessity to obtain the start values $U_{-\Delta t}, U_{-2\Delta t}, \cdots$. Moreover, for the majority of multi-step schemes equivalent single-step schemes can be obtained.

There are explicit and implicit direct integration schemes. Assume the matrices M and C of the equation (2.1) being diagonal. An explicit scheme presents the relations for obtaining the values $U_{t+\Delta t}$ and its derivatives from the values U_t and its derivatives in an explicit form, i.e., without solving an algebraic equation system or employing a matrix inverse. The 1schemes that don't match this requirement are considered as implicit. However, explicit algorithms don't possess the

unconditional stability property and are therefore of a limited use.

The structural dynamics problems should be partitioned depending on the relation between the spectrum of excitation and the spectrum of eigenfrequencies:

1) obtaining stationary motion laws, when the dynamic behavior is determined basically by several lower modal components;

2) obtaining transient motion laws and solving wave propagation problems, when the dynamic behavior is heavily influenced by higher modal components;

The explicit schemes are best suited for the second group of problems, defining the time integration step sufficiently small to approximate the highest modal response and preserving the dynamic contributions of all the modal components. For the first group the implicit numerical schemes are preferable. Employing the unconditionally stable schemes it appears sufficient to define a time integration step sufficiently small to approximate the highest Fourier component of an excitation law. In some cases, e.g. [17], the implicit-explicit approaches are employed in order to cope with the dynamic problems of the coupled structures possessing subsets of eigenfrequencies severely differing from each other.

The numerous explicit and implicit schemes had been developed up to this time. In order to select a numerical scheme for a given structural dynamics problem, accuracy, stability and other asymptotic features of the scheme are to be considered. An analysis of such features is carried out by investigating the behavior of the scheme when approximating a free motion of a structure, i.e., by integrating the equation (2.1) with the zero right-hand side. Presenting equations in modal coordinates as n independent equations, the main asymptotic features of the numerical scheme are investigated by applying the scheme to the equation of motion of an undamped oscillator as

$$\ddot{u} + \omega_0^2 u = 0 , \qquad (2.13)$$

or of a damped oscillator as

$$\ddot{u} + 2h\dot{u} + \omega_o^2 u = 0 \quad . \qquad (2.14)$$

An arbitrary single-step scheme applied to the equation (2.13) or (2.14) can be presented as

$$r_{t+\Delta t} = E\, r_t \quad , \qquad (2.15)$$

where E - the amplification matrix , and $r = u$, or $r = \begin{Bmatrix} u \\ \dot{u} \end{Bmatrix}$, or $r = \begin{Bmatrix} u \\ \dot{u} \\ \ddot{u} \end{Bmatrix}$ etc., depending upon the numerical scheme under consideration. It follows, that asymptotic features of a numerical scheme applied to the equations (2.13) or (2.14) depend only upon the features of the matrix E , because after N steps the equality

$$r_{t+N\Delta t} = E^N r_t \quad . \qquad (2.16)$$

takes place.

It is known that

$$E^N \delta_i = \lambda_i^N \delta_i \quad , \qquad (2.17)$$

where λ_i , δ_i - the i-th eigenvalue and the i-th eigenvector of the matrix E [26].

An arbitrary vector r_t can be presented as a superposition of eigenvectors of the matrix E ,i.e., as

$$r_t = \sum_{i=1}^{l} \beta_i \delta_i , \qquad (2.18)$$

where l - dimension of the matrix E , and β_i - weight coefficients.

By substituting (2.18), (2.18) into (2.16), we obtain

$$r_{t+N\Delta t} = \sum_{i=1}^{l} \lambda_i^N \beta_i \delta_i \quad . \qquad (2.19)$$

It follows, that for long time intervals [t, t+NΔt] the asymptotic behavior of a numerical scheme is defined by the magnitude of a spectral radius of the matrix E .

Stability. A numerical integration scheme is stable, if the obtained solution of the homogeneous equation (2.13) or (2.14) is limited at arbitrary initial values. It follows from the relations (2.16), (2.18), that the stability is ensured if for the spectral radius of the matrix E the inequality

$$\rho \le 1 \quad , \qquad (2.20)$$

is held, and the multiple eigenvalues satisfy the inequality

$$|\lambda| < 1 \quad . \qquad (2.21)$$

A direct numerical integration scheme is unconditionally stable, if the solution of the equation (2.13) is limited at arbitrary initial values and at an arbitrary value of an integration step Δt . If stability is obtained only by defining the certain values of a time integration step, an algorithm is conditionally stable. The stability of the numerical scheme means, that the numerical round-off errors aren't accumulated. The unconditional stability means, that the solution remains limited at an arbitrary time integration step, even exceeding the free vibration period $T = \frac{2\pi}{\omega_o}$. In this case a magnitude of an integration step is defined in order to obtain a satisfactory approximation of the highest Fourier component taking an appreciable part in the response of the structure to a given excitation. The contributions of the higher modal components are filtered because of the unconditional stability of an algorithm.

Amplitude decrement and period elongation caused by a numerical scheme applied upon the equation (2.14) can be regarded as a measure of a non-coincidence of the amplitude and phase of a motion law produced by the scheme with those of the exact (analytic) solution during a sufficiently long time interval [t, t+NΔt] .

Assume $\lambda = a \pm ib$ as a pair of conjugate eigenvalues of the matrix E , and present the solution of (2.14) in the complex plane, Fig.2.1. The two complex magnitudes U_t and $U_{t+\Delta t}$ represent the amplitude and the phase of the vibration at the time points t and t+Δt. Without loss of generality they can be regarded as subvectors of an eigenvector δ_i of the matrix E, and, analogous to the relation (2.16), we obtain

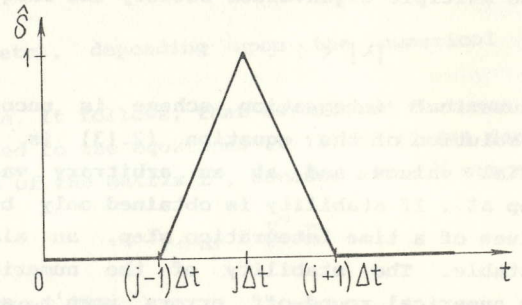

Fig.2.1 Unit pulse

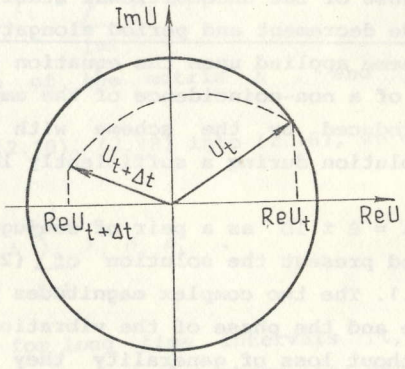

Fig.2.2 Displacement vectors on the complex plane at the time points t and t+Δt

$$U_{t+\Delta t} = \lambda\, U_t \quad , \tag{2.22}$$

where $\lambda = e^{\left(\frac{1}{2}\ln(a^2+b^2) \pm i\,\mathrm{arctg}\frac{b}{a}\right)}$.

At the same time the analytical solution of the equation (2.14) is presented by the relation

$$U_{t+\Delta t} = U_t\, e^{(-h \pm i\omega)\Delta t} \quad , \tag{2.23}$$

where $\omega = \sqrt{\omega_0^2 - h^2}$.

From the relations (2.22), (2.23) we obtain, that during the time interval of the length Δt the relative error caused by a numerical scheme equals

$$1-e^{\left(\frac{1}{2}\ln(a^2+b^2)+h\Delta t+i(\Phi-\omega t)\right)} = 1-e^{\nu\Delta t+i\varepsilon\Delta t} \cong O(\nu)+iO(\varepsilon) \quad , \tag{2.24}$$

where $\Phi = \mathrm{arctg}\,\frac{b}{a}$.

The order of the relative error (2.24) can be obtained by employing analytical expressions for ν and ε, and $O(\nu)$ and $O(\varepsilon)$ represent the amplitude and phase errors.

The value Φ can be expressed through the distorted (i.e., numerically obtained) vibration period as

$$\Phi = 2\pi\Delta t / \bar{T} \quad , \tag{2.25}$$

or

$$\bar{T} = \frac{2\pi\Delta t}{\Phi} \quad . \tag{2.26}$$

The vibration period, in accordance with the analytical solution, equals

$$T = \frac{2\pi}{\omega} \quad . \tag{2.27}$$

Expressing as a percentage, a period elongation produced by a numerical scheme is obtained as

$$100\,\frac{\bar{T}-T}{T} = 100\left(\frac{\omega\Delta t}{\Phi} - 1\right) , \tag{2.28}$$

and an amplitude decrement - as

$$100\left(1-e^{\left(\frac{1}{2}\ln(a^2+b^2)+h\Delta t\right)}\right) = 100\left(1 - |\lambda|e^{h\Delta t}\right) . \tag{2.29}$$

According to the stability requirement $|\lambda| \leq 1$, the relation (2.29) enables to evaluate the numerical damping feature of a time integration scheme. In the case of an undamped oscillator (h=0) the relation (2.29) defines in percentage the decrement of free vibration amplitude during one period caused by the numerical damping feature of a scheme. If the numerical damping is considerable at the values $\frac{\Delta t}{T} >> 1$, the contributions of higher Fourier components to the system's response are suppressed algorithmically.

The accuracy order of a numerical scheme for an undamped oscillator equation (2.13) is obtained by comparing an analytical solution with the numerical one during the time interval $[t,t+\Delta t]$. The relation (2.15) is presented as

$$\begin{bmatrix} u_{t+\Delta t} \\ \dot{u}_{t+\Delta t} \end{bmatrix} = E \begin{bmatrix} u_t \\ \dot{u}_t \end{bmatrix} \cong (E_o + E_t) \begin{bmatrix} u_t \\ \dot{u}_t \end{bmatrix} . \qquad (2.30)$$

The matrix E_o in (2.30) is obtained by solving the equation (2.13) during the time interval $[t, t+\Delta t]$ as

$$E_o = \begin{bmatrix} \frac{\sin\omega\Delta t}{\omega} & \cos\omega\Delta t \\ \cos\omega\Delta t & -\omega\sin\omega\Delta t \end{bmatrix} . \qquad (2.31)$$

The matrix E_t contains the first expansion members of an error caused by a numerical scheme. It is obtained by expanding the elements of the matrix E_o into the Taylor series and subtracting the corresponding elements from the elements of the matrix E. In general, the matrix E_t is presented as

$$E_t = O(\Delta t^{p+1}) \begin{bmatrix} a & b\Delta t \\ c\Delta t & d \end{bmatrix} , \qquad (2.32)$$

where the values of the coefficients a, b, c, d depend upon a given numerical scheme. The matrix E is called compatible with the matrix E_o, if $p \geq 1$ in the expression (2.32). The number p is an accuracy order of a numerical scheme defined by the matrix E.

"Overshoot" feature of a numerical scheme denotes its capability to produce excessively large values of a response during the very first stage of time integration. When applying the relation (2.15) at the time points $t+\Delta t$, $t+2\Delta t,\ldots,t+N\Delta t$, we

obtain

$$r_{t+N\Delta t} = E^N r_t . \qquad (2.33)$$

Considering the norms of vectors and matrices, it can be stated that

$$\| r_{t+N\Delta t} \| \leq \| E^N \| \, \| r_t \| . \qquad (2.34)$$

From the inequality (2.34) it appears that the value of the norm of the matrix E presents a more severe restriction, than the spectral radius (see the inequality (2.20). If $\rho < 1$, it is ensured that $\lim_{N\to\infty} \|E^N r\| = 0$. But when N isn't large, this norm can be large, and excessive values of $\|r_{t+N\Delta t}\|$ may be obtained. Therefore, irrespectively of a circumstance that the asymptotic behavior of a numerical scheme is governed by the spectral radius of the matrix E, the values $\|r_{t+N\Delta t}\|$ for small values of N depend upon the value of the norm of the matrix E. The matrix E satisfying the stability criteria (2.20) can possess an arbitrary large value of the norm.

Convergence. In order to obtain the matrix E for implicit schemes, it is necessary to invert one or several times the matrix of the dimension equal to that of the equation (2.1). From a computational point of view, it appears reasonable to present the relation (2.15) as

$$E_1 \, r_{t+\Delta t} = E_o \, r_t . \qquad (2.35)$$

where no matrix inversions by obtaining the matrices E_1 and E_o are employed. For obtaining $r_{t+\Delta t}$ from the equation (2.35) the iterative linear algebraic equation solution algorithms may be adopted as follows:

$$r^{k+1}_{t+N\Delta t} = E_o r_t + (I - E_1) \, r^k_{t+N\Delta t} , \qquad (2.36)$$

where k - the iteration number. The convergence of the iterative scheme (2.36) is ensured, if the spectral radius

$$\rho (I - E_1) \leq 1 . \qquad (2.37)$$

The inequality (2.38) is regarded as the convergence condition of a numerical scheme.

2.3 SINGLE-STEP NUMERICAL SCHEMES

2.3.1 Weighted residual approach

Let's consider the equation of motion (2.1). During the time interval $[t,t+\Delta t]$ the time function U is approximated by a p-th order polynomial as

$$U = \sum_{q=0}^{p-1} \overset{q}{U}_t \frac{t^q}{q!} + \alpha_t^{(p)} \frac{t^p}{p!} \quad , \qquad (2.38)$$

where $\overset{q}{U} = \dfrac{d^q U}{dt^q}$.

The relation (2.38) contains the p first terms of the Taylor series expansion of the function U , and the term $\alpha_t^{(p)} \dfrac{t^p}{q!}$ approximates the residual term of the expansion. Assume the values U_t , $\dot{U}_t$,..., $\overset{p-1}{U}_t$ at the time point t known. Employing the relation (2.38), we express the unknown values of $U_{t+\Delta t}$, $\dot{U}_{t+\Delta t}$,..., $\overset{p-1}{U}_{t+\Delta t}$ at the time point $t+\Delta t$ in terms of the unknown values of $\alpha_t^{(p)}$ as

$$\overset{k}{U}_{t+\Delta t} = \sum_{q=k}^{p-1} \overset{q}{U}_t \frac{\Delta t^{q-k}}{(q-k)!} + \alpha_t^{(p)} \frac{\Delta t^{p-k}}{(p-k)!} = \overset{\wedge k}{U}_{t+\Delta t} + \alpha_t^{(p)} \frac{\Delta t^{p-k}}{(p-k)!} \quad , \qquad (2.39)$$

for all $k = \overline{0,p-1}$.

The value of $\alpha_t^{(p)}$ is obtained employing the weighted residual approach. Substituting the relation (2.38) into the equation (2.1) we obtain

$$\int_0^{\Delta t} W \left(M\ddot{U} + C\dot{U} + KU - R \right) dt = 0 \quad , \qquad (2.40)$$

where W - the weight function.

Defining

$$\frac{\int_0^{\Delta t} Wt^q dt}{\int_0^{\Delta t} Wdt} = \theta_q \Delta t^q \quad , \; q = \overline{1,p} \quad , (2.41) \; ; \qquad \frac{\int_0^{\Delta t} WR dt}{\int_0^{\Delta t} Wdt} = \bar{R}, \qquad (2.42)$$

where $\theta_o = 1$, $0 \le \theta_q \le 1$, we obtain

$$\frac{\int_0^{\Delta t} WU dt}{\int_0^{\Delta t} Wdt} = \sum_{q=k}^{p-1} \overset{q}{U}_t \frac{\Delta t^{q-k}}{(q-k)!} \theta_{q-k} + \alpha_t^{(p)} \frac{\Delta t^{p-k}}{(p-k)!} \theta_{p-k} \quad , \; k=\overline{0,(p-1)}. \qquad (2.43)$$

Dividing the equation (2.40) by $\int_0^{\Delta t} Wdt$, we obtain

$$M \left[\sum_{q=2}^{p-1} \overset{q}{U}_t \frac{\Delta t^{q-2}}{(q-2)!} \theta_{q-2} + \alpha_t^{(p)} \frac{\Delta t^{p-2}}{(p-2)!} \theta_{p-2} \right] +$$

$$+ C \left[\sum_{q=1}^{p-1} \overset{q}{U}_t \frac{\Delta t^{q-1}}{(q-1)!} \theta_{q-1} + \alpha_t^{(p)} \frac{\Delta t^{p-1}}{(p-1)!} \theta_{p-1} \right] +$$

$$+ K \left[\sum_{q=0}^{p-1} \overset{q}{U}_t \frac{\Delta t^{q}}{q!} \theta_{q} + \alpha_t^{(p)} \frac{\Delta t^{p}}{p!} \theta_{p} \right] - \bar{R} = 0 \quad . \qquad (2.44)$$

From the equation (2.44) the vector $\alpha_t^{(p)}$ is obtained as

$$\alpha_t^{(p)} = \left(\frac{\Delta t^{p-2}}{(p-2)!} \theta_{p-2} M + \frac{\Delta t^{p-1}}{(p-1)!} \theta_{p-1} C + \frac{\Delta t^{p}}{p!} \theta_{p} K \right)^{-1} \cdot$$

$$\cdot \left(\bar{R} - M\ddot{\tilde{U}}_{t+\Delta t} - C\dot{\tilde{U}}_{t+\Delta t} - K\tilde{U}_{t+\Delta t} \right) \quad , \qquad (2.45)$$

where $\tilde{U}_{t+\Delta t} = \sum_{q=0}^{p-1} \overset{q}{U}_t \frac{\Delta t^q}{q!} \theta_q$, $\dot{\tilde{U}}_{t+\Delta t} = \sum_{q=1}^{p-1} \overset{q}{U}_t \frac{\Delta t^{q-1}}{(q-1)!} \theta_{q-1}$,

$$\ddot{\tilde{U}}_{t+\Delta t} = \sum_{q=2}^{p-1} \overset{q}{U}_t \frac{\Delta t^{q-2}}{(q-2)!} \theta_{q-2} \quad . \qquad (2.46)$$

The p-th order algorithm SSpj is completely defined by the relations (2.39), (2.45), (2.46) [46]. The number j denotes the equation order, and for the equation of the second order (2.1) we have j=2. The values θ_k, $k=\overline{0,p-1}$ are defined by a selection of a weight function W , and their values are defined in order to submit the desired features to the numerical scheme. The p-th order numerical scheme starts with the prescribed values of the vector U and its (p-1) derivatives at the time point t=0, i.e., with the values $\overset{k}{U}_0$, $k=\overline{0,p-1}$.

Algorithm 2.1

1. Obtain $\overset{q}{\tilde{U}}_{t+\Delta t}$ from the relation (2.46) employing the already known values $\overset{q}{U}_t$, $q = \overline{0,p-1}$.
2. Obtain $\alpha_t^{(p)}$ from the relation (2.45).
3. Obtain $\overset{q}{U}_{t+\Delta t}$ from the relation (2.39), $q = \overline{0,p-1}$.
4. Repeat steps 1,2,3 of this algorithm for the next time step.

In order to obtain the load vector $\bar{R}$ from (2.43), it is necessary to obtain the value of an integral in (2.43). However, often the the load vector is prescribed only by its values at the time points 0, Δt, $2\Delta t$,... . It appears reasonable to assume the linear variation law of R during the time interval [t, t+Δt], and to replace the relation (2.42) by

$$\bar{R} = \theta_1 R_{t+\Delta t} + (1-\theta_1) R_t \ . \qquad (2.42)'$$

Employing the Taylor series expansion of (2.45) and the equation (2.1), we obtain

$$\alpha_t^{(p)} = \overset{p}{U}_t + O(\Delta t) \ , \qquad (2.47)$$

where the values at the time point t are supposed to be accurate. Therefore the SSpj numerical scheme obtains the values $U_{t+\Delta t}$, $\Delta t\dot{U}_{t+\Delta t}$,..., $\Delta t^{p-1}\overset{(p-1)}{U}_{t+\Delta t}$ with an error $O(\Delta t^{p+1})$, and its accuracy order equals p+1 .

The relation (2.15) for the SSpj takes the form

$$\begin{Bmatrix} U_{t+\Delta t} \\ \dot{U}_{t+\Delta t}\Delta t \\ \vdots \\ \overset{(p-1)}{U}_{t+\Delta t}\Delta t^{p-1} \\ \hline 0 \end{Bmatrix} = E \begin{Bmatrix} U_t \\ \dot{U}_t \Delta t \\ \vdots \\ \overset{(p-1)}{U}_t \Delta t^{p-1} \\ \hline \alpha_t^p \Delta t^p \end{Bmatrix} \ , \qquad (2.48)$$

where

$$E^{(p)} = \left[\begin{array}{ccccc} 1 & 1 & 1/2! & \dots & 1/p! \\ 0 & 1 & 1 & \dots & 1/(p-1)! \\ 0 & 0 & 1 & \dots & 1/(p-2)! \\ \hline 0 & 0 & 0 & \dots 1 & 1 \\ \hline b_0 & b_1 & b_2 & \dots & b_{p-1} \ b_p \end{array}\right] \ , \qquad (2.49)$$

and $b_0 = \omega_0^2\Delta t^2\theta_0$, $b_1 = 2h\,\Delta t\,\theta_0 + \omega_0^2\Delta t^2\theta_1$,

$$b_k = \frac{\theta_{k-2}}{(k-2)!} + \frac{2h\Delta t\theta_{k-1}}{(k-1)!} + \frac{\omega_0^2\Delta t^2\theta_k}{k!} \ , \quad k=\overline{2,p} \ .$$

Defining $r^{(p)} = \begin{bmatrix} U \\ \dot{U}\Delta t \\ \vdots \\ \overset{(p-1)}{U}\Delta t^{p-1} \end{bmatrix}$, the relation (2.48) can be presented as

$$\begin{Bmatrix} r_{t+\Delta t}^{(p)} \\ \hline 0 \end{Bmatrix} = \left[\begin{array}{c|c} E_{rr}^{(p)} & E_{r\alpha}^{(p)} \\ \hline E_{\alpha r}^{(p)} & E_{\alpha\alpha}^{(p)} \end{array}\right] \begin{Bmatrix} r_t^{(p)} \\ \hline \alpha_t^{(p)} \end{Bmatrix} \ , \qquad (2.50)$$

where the matrix blocks E_{rr}, $E_{r\alpha}$, $E_{\alpha r}$, $E_{\alpha\alpha}$ are of the dimension pxp, px1, 1xp, 1x1 , as it follows from the definition (2.49). The relation (2.50) transforms into the relation

$$\left\{r_{t+\Delta t}^{(p)}\right\} = \left[E_{rr}^{(p)} - E_{r\alpha}^{(p)}\left(E_{\alpha\alpha}^{(p)}\right)^{-1}E_{\alpha r}^{(p)}\right]\left\{r_t^{(p)}\right\} \ . \qquad (2.51)$$

The stability, numerical damping and period elongation features are defined by analyzing the spectral radius values of

the matrix in the relation (2.51).

The analysis of the numerical schemes of the first and second order for the equation (2.1) is presented in detail in the Appendix 1.

2.3.2 Generalization of the Newmark's scheme

Consider the equation of motion (2.1) and approximate the values of the vectors $U_{t+\Delta t}$, $\dot{U}_{t+\Delta t}$, ..., $\overset{m}{U}_{t+\Delta t}$ at the time point $t+\Delta t$ as

$$\overset{k}{U}_{t+\Delta t} = \sum_{j=k}^{m} U_t \frac{\Delta t^{j-k}}{(j-k)!} + \beta_k \frac{\Delta t^{m-k}}{(m-k)!} \overset{m}{\Delta U} = q_k + b_k \overset{m}{\Delta U} \quad , \quad k=\overline{0,m} \quad , \qquad (2.52)$$

where $\overset{m}{\Delta U} = \overset{m}{U}_{t+\Delta t} - \overset{m}{U}_t$ and $\beta_m = 1$ is assumed.

The relation (2.52) can be regarded as Taylor series expansion up to the term containing $\overset{m}{U}$, and the remaining terms

$$\beta_k \frac{\Delta t^{m-k}}{(m-k)!} (\overset{m}{U}_{t+\Delta t} - \overset{m}{U}_t) = \beta_k \frac{\Delta t^{m-k+1}}{(m-k)!} \overset{m+1}{U} \quad , \quad k=\overline{0,m} \quad , \qquad (2.53)$$

can be regarded as approximations of the residual terms.

If $\beta_k = \frac{1}{m-k+1}$, $k=\overline{0,m}$, the residual terms (2.53) are the Taylor series terms containing $\overset{m+1}{U}$. However, in general arbitrary values β_t can be selected in order to obtain necessary features of a numerical scheme (e.g., to achieve a compromise between accuracy and stability). Substituting the relation (2.52) into the equation (2.1) at a time point $t+\Delta t$, we obtain

$$M \ddot{U}_{t+\Delta t} + C \dot{U}_{t+\Delta t} + K U_{t+\Delta t} = R_{t+\Delta t} \quad . \qquad (2.54)$$

After some manipulation the basic relation for an m-th order numerical scheme is obtained as

$$(b_2 M + b_1 C + b_0 K) \overset{m}{\Delta U} = R_{t+\Delta t} - (M q_2 + C q_1 + K q_0) \quad . \qquad (2.55)$$

The m-th order numerical scheme starts with the prescribed values of the vector U and its m derivatives at the time point

t=0. If at the time point t = 0 only the values U_o, $\dot{U}_o$ are prescribed, it is necessary to obtain the values $\overset{k}{U}_o$ from the equations

$$M \overset{k}{U}_o = C \overset{k-1}{U}_o + K \overset{k-2}{U}_o - \overset{k-2}{R}_o \quad , \quad k=\overline{2,m} \quad . \qquad (2.56)$$

Algorithm 2.2

1. Obtain the right-hand side vector of the equation (2.55)
$$R_{t+\Delta t} - (M q_2 - C q_1 - K q_0) \quad ,$$
and simultaneously assign
$$\overset{k}{U}_{t+\Delta t} = q_k \quad , \quad k = \overline{0,m} \quad .$$
2. Obtain $\overset{m}{\Delta U}$ from the equation (2.55).
3. Obtain the values of the vectors $\overset{k}{U}_{t+\Delta t}$, employing the relations
$$\overset{k}{U}_{t+\Delta t} = \overset{k}{U}_{t+\Delta t} + b_k \overset{m}{\Delta U} \quad , \quad k = \overline{0,m} \quad .$$
4. Repeat the steps 1-3 for the next time point.

Sometimes it may be preferable in place of the unknown vector $\overset{m}{\Delta U}$ in the equation (2.55) to consider the vector $\overset{s}{\Delta U}$ (if $s = 0$, the displacement vector is regarded as an unknown). In order to substitute the variables, the relation (2.52) is cast to the form

$$\overset{m}{\Delta U} = (\overset{s}{U} - q_s) / b_s \quad . \qquad (2.57)$$

The equation (2.55) preserves its form, if in place of b_k, q_k we consider b_k^*, q_k^*, $k = \overline{1,m}$ defined as

$$b_k^* = b_k / b_s \quad , \quad q_k^* = q_k - b_k^* q_s \quad , \quad k=\overline{1,m} \quad . \qquad (2.58)$$

The relations for obtaining $\overset{k}{U}_{t+\Delta t}$ at the steps 1. and 3. of the algorithm 2.2 take the form

$$\overset{k}{U}_{t+\Delta t} = q_k^* + b_k^* \overset{s}{\Delta U} \quad , \quad k = \overline{0,m} \quad . \qquad (2.59)$$

(for $k = s$ an identity takes place).

The relation (2.15) for the generalized Newmark's scheme

is considered as

$$\begin{Bmatrix} U_{t+\Delta t} \\ \dot{U}_{t+\Delta t} \\ \vdots \\ \overset{m}{U}_{t+\Delta t} \\ \hline 0 \end{Bmatrix} = E^{(m)} \begin{Bmatrix} U_t \\ \dot{U}_t \\ \vdots \\ \overset{m}{U}_t \\ \hline \overset{m}{\Delta U} \end{Bmatrix} , \qquad (2.60)$$

$$E^{(m)} = \begin{bmatrix} 1 & 1 & 1/2! & \dots & 1/m! & \beta_0/m! \\ 0 & 1 & 1 & \dots & 1/(m-1)! & \beta_1/(m-1)! \\ 0 & 0 & 1 & \dots & 1/(m-2)! & \beta_2/(m-2)! \\ \hline 0 & 0 & 0 & \dots & 1 & \beta_m \\ \hline d_0 & d_1 & d_2 & \dots & d_m & d_{m+1} \end{bmatrix} , \qquad (2.61)$$

where

$$d_0 = \omega_0^2,\ d_1 = 2h/\Delta t + \omega_0^2,\ d_j = \frac{1}{\Delta t^2 (j-2)!} + \frac{2h}{\Delta t (j-1)!} + \frac{\omega_0^2}{j!},\ k=\overline{2,m} ,$$

$$d_{m+1} = \frac{\beta_2}{\Delta t^2 (m-2)!} + \frac{2h\beta_1}{\Delta t (m-1)!} + \frac{\omega_0^2 \beta_0}{m!} .$$

In the Appendix 1.2 an influence of the values of β_i upon the accuracy and stability of the numerical scheme is investigated, and the relation of the presented scheme with other well known numerical integration schemes is shown.

2.3.3 Reduction to the first order system. Finite elements in time

The equation (2.1) can be presented as a first order differential equation

$$\dot{X} = AX + P , \qquad (2.62)$$

where $A = \begin{bmatrix} -M^{-1}C & -M^{-1}K \\ I & 0 \end{bmatrix}$, $P = \begin{Bmatrix} M^{-1}R \\ 0 \end{Bmatrix}$, $X = \begin{Bmatrix} \dot{U} \\ U \end{Bmatrix}$.

Consider the values of the vector X and it s derivatives up

to the p-th order at the time points t and t+Δt , denoting them as $X_0, \dot{X}_0, \dots, \overset{p}{X}_0$ (at the time point t) and as $X_1, \dot{X}_1, \dots, \overset{p}{X}_1$ (at the time point t+Δt). The value X_τ at an arbitrary time point within the interval $\tau \in [\, t, t+\Delta t\,]$ can be expressed through the values of the vector and its derivatives at the begin an end points of the interval, employing a set of orthogonal functions defined within this time interval. Let's employ the p-th order (p=0,1,...) Hermitian polynomial family denoting them as ϑ^p_{kj}, $k = \overline{0,p}$, $j = 0,1$, containing the (2p+1)-th order polynomials. Denoting $\xi = \frac{\tau}{\Delta t}$, they are presented explicitly in the Appendix 1.3.

The value of X at an arbitrary time point within the interval $\tau \in [t, t+\Delta t]$ is interpolated as

$$X_\tau = \sum_{k=0}^{p} \overset{k}{X}_0 \vartheta^p_{k0}(\tau) + \overset{k}{X}_1 \vartheta^p_{k1}(\tau) . \qquad (2.63)$$

In fact, the time interval[t, t+Δt] can be regarded as a finite element in time with the nodes at the ends points of the interval. The values $\overset{i}{X}_0, \overset{i}{X}_1$, $i = \overline{1,p}$ should be regarded as nodal values, and the Hermitian polynomials ϑ^p_{kj} , $k=\overline{0,p}$, $j=0,1$ - as form functions. Substituting the relation (2.63) into the equation (2.62), we obtain

$$\sum_{k=0}^{p} \left[\overset{k}{X}_0 \dot{\vartheta}^p_{k0}(\tau) + \overset{k}{X}_1 \dot{\vartheta}^p_{k1}(\tau) \right] = A \sum_{k=0}^{p} \left[\overset{k}{X}_0 \vartheta^p_{k0}(\tau) + \overset{k}{X}_1 \vartheta^p_{k1}(\tau) \right] + P(\tau),\ \tau \in [t, t+\Delta t\,] \qquad (2.64)$$

Employing the weighted residual approach, we require the zero value of an integral multiplied by a certain weight function :

$$\int_0^{\Delta t} W(\bar{\tau}) \rho(\bar{\tau}) d\bar{\tau} = 0 ,$$

where $W(\tau)$ is a weight function. Let's employ the δ-function $W(\bar{\tau}) = \delta(\bar{\tau} - (t+\tau))$ as a weight function. Such weighting is called collocation at the point t+τ, and the equality

$\int_0^{\Delta t} \delta(\bar{\tau}-\tau-t)\rho(\bar{\tau})d\bar{\tau}=\rho(\tau+t)$ takes place. The zero value of the weighted residual $\rho(\tau+t)$ is obtained by selecting the values X_i, $i=\overline{0,p}$ in the (2.64). Differentiating k times the equation (2.62) and expressing the derivatives $X^{(k)}$ through X, we obtain the relation

$$X^{(k)} = A^k X + \sum_{k=0}^{p} A^{k-i} P^{(i)} , \quad k=\overline{0,p} . \qquad (2.65)$$

Substituting (2.65) into (2.64) and considering the obtained equation at the collocation point $\tau = \xi\Delta t$, we obtain

$$\sum_{k=0}^{p}\left(\dot{\vartheta}^p_{ko} - A\,\vartheta^p_{ko}\right)\left(A^k X_o + \sum_{i=1}^{k} A^{k-i} P^{(i)}\right) +$$

$$\sum_{k=0}^{p}\left(\dot{\vartheta}^p_{k1} - A\,\vartheta^p_{k1}\right)\left(A^k X_1 + \sum_{i=1}^{k} A^{k-i} P^{(i)}\right) = P . \qquad (2.66)$$

From the equation (2.66) the vector X_1 is obtained employing the known values of X_o and the load vector Q. The vector X_1 is obtained from the relation

$$_{2p+1}B_1 X_1 = {}_{2p+1}B_o X_o + P_{2p+1} , \qquad (2.68)$$

where

$$_{2p+1}B_1 = \sum_{k=0}^{p}\left(\dot{\vartheta}^p_{k1} - A\,\vartheta^p_{k1}\right) A^k ,$$

$$_{2p+1}B_o = -\sum_{k=0}^{p}\left(\dot{\vartheta}^p_{ko} - A\,\vartheta^p_{ko}\right) A^k , \qquad (2.68)$$

$$P_{2p+1} = P - \sum_{k=0}^{p}\left[\left(\dot{\vartheta}^p_{k1} - A\,\vartheta^p_{k1}\right)\sum_{i=1}^{k} A^{k-i} P^{(i)}\right] .$$

Usually the excitation values are interpolated linearly during the interval [t, t+Δt], and in the relations (2.68) in

place of the term $\sum_{i=1}^{k} A^{k-i} P^{(i)}$ the term $(1-\xi)P_o + \xi P_1$ (if k=1) and the term $A^{k-1}\left[(1-\xi)P_o + \xi P_1\right] + A^{k-2}\frac{P_1 - P_2}{\Delta t}$ (if $k\geq 2$) can be employed. The amplification matrix E of this algorithm is obtained from by the relation

$$E = {}_{2p+1}B_1^{-1}\,{}_{2p+1}B_o . \qquad (2.69)$$

The formulae of the numerical schemes of the 1-th, 3-rd, 5-th order are presented explicitly in the Appendix 1.3.

Now we investigate asymptotic features of the numerical schemes presented in Chap. 2.3.1, 2.3.2, 2.3.3. The results presented below are taken from [1].

In Fig.2.3, 2.4 the numerical damping and period elongation characteristics obtained by the formulae (2.28), (2.29) are presented. The curves 8 in Fig.2.3, 2.4 correspond to a damped oscillator case at the value h = 0.5 . The negative values of the numerical damping signify the amplification of oscillations with regard to the analytical solution. In Fig.2.5 there are presented the values of the norm of the amplification matrix at the first time integration steps at $\omega\Delta t\to\infty$.

The large values of the norm of the Newmark's scheme amplification matrix are caused by the value $\rho = 1$ of its spectral radius. However, this circumstance doesn't imply overshooting of the displacement values due to a lower triangular form of the matrix at the values $\omega\Delta t \to \infty$ taking the form

$$A = \begin{bmatrix} 0 & 0 & 0 \\ -2 & -1 & 0 \\ -4 & -4 & -1 \end{bmatrix} .$$

Obviously, all the exponents A^n of the matrix A preserve the lower triangular form.

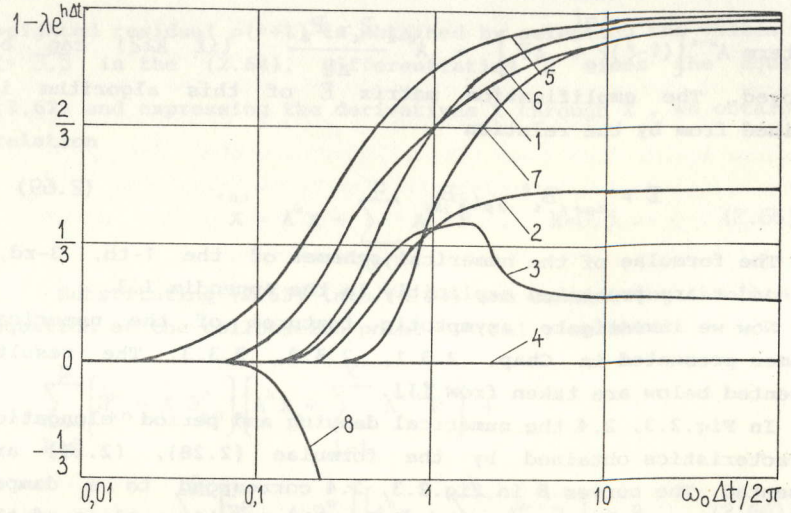

Fig.2.3 Damping characteristics of some numerical schemes: 1 - Houbolt, $\theta_1=2$, $\theta_2=11/3$, $\theta_3=6$; ($\beta_0=6$, $\beta_1=11/2$, $\beta_2=2$); 2 - cubic, $\xi=2/3$; 3 - Wilson, $\theta_1=1.4$, $\theta_2=1.4^2$, $\theta_3=1.4^3$, ($\beta_0=1.4^3$, $\beta_1=1.4^2$, $\beta_2=1.4$); 4 - Newmark, $\beta_0=\beta_1=1/2$; 5 - linear, $\xi=1$, p=0; 6 - cubic, $\xi=1$; p=1; 7 - fifth order scheme, $\xi=1$; p=2; 8-SS21, $\theta_1=\theta_2=1/2$ for the damped oscillator;

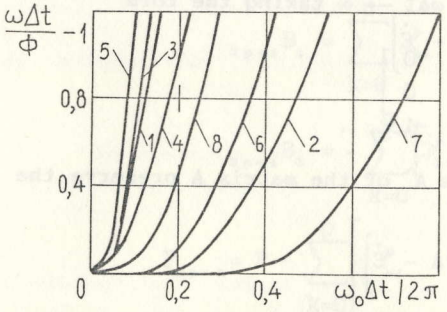

Fig.2.4 Period elongation of some numerical schemes, notations as in Fig.2.3

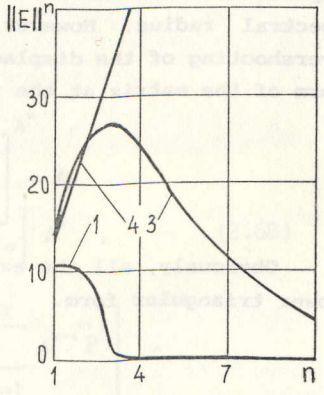

Fig.2.5 Norms of amplification matrices of some numerical schemes, notations as in Fig.2.3

3. TRANSIENT ANALYSIS OF NONLINEAR ELASTIC STRUCTURES

In this chapter the numerical integration schemes of linear dynamic equations are extended in order to deal with nonlinear ones. For the dynamic equations with a nonlinear term only explicit schemes can be immediately adopted. Employing the implicit schemes, the values of a nonlinear term are approximated by means of extrapolation, or it is necessary to solve a nonlinear algebraic equation system at each time integration step. In time domain the dynamic response is represented by a superimposing the transient dynamic compliances of the linear part, regarding the values of a nonlinear term as external force evaluated by means of extrapolation or by solving nonlinear algebraic equations.

For the direct numerical integration of equations of motion of the structures with unilateral constraints case oriented algorithms are developed employing the Lagrangian multiplier approach and supposing the minimum work of interaction forces for making corrections upon the velocities and accelerations when the structure meets the constraint. A numerical scheme is presented as an extension of the generalized Newmark's scheme. Equations of motion of the structures with kinematic pairs interacting by normal, oblique impact and sliding friction forces are presented employing the constraints upon nodal displacements, velocities and accelerations. Arbitrary values of the impact coefficient of restitution can be presented by selecting appropriate right-hand side terms of the constraint relations.

3.1 DIRECT INTEGRATION: SOLUTION OF NONLINEAR EQUATIONS AT EACH TIME STEP

Consider the following structural equation of motion:

$$M\ddot{U} + C\dot{U} + KU = W(U, \dot{U}) + R(t) \quad . \qquad (3.1)$$

The term $W(U,\dot{U})$ in the equation (3.1) represents a nonlinear part of the structure, signifying a vector of forces caused by an interaction of a linear structure with the surrounding or with other bodies.

Applying the m-th order generalized Newmark's scheme to the equation (3.1), we obtain the relations similar to (2.55), (2.57)-(2.59):

$$A\,\Delta U_{t+\Delta t} = G_{t+\Delta t} + W(U_{t+\Delta t}, \dot{U}_{t+\Delta t}) \,. \qquad (3.2)$$

$$\overset{k}{U}_{t+\Delta t} = q_k^* + b_k^*\,\Delta U_{t+\Delta t} \,, \quad k = \overline{0,m} \,. \qquad (3.3)$$

where $A = b_2^* M + b_1^* C + b_0^* K$, $G_{t+\Delta t} = R_{t+\Delta t} - (M^* q_2 - C^* q_1 - K^* q_0)$,

$$b_0^* = 1 \,, \quad q_0^* = 0 \,, \quad b_k^* = b_k / b_0 \,, \quad q_k^* = q_k - b_k^* q_0 \,, \quad k=1,2 \,,$$

$$q_k = \sum_{j=k}^{m} \overset{j}{U}_t \frac{\Delta t^{j-k}}{(j-k)!} \,, \quad b_k = \beta_k \frac{\Delta t^{m-k}}{(m-k)!} \,, \quad k=\overline{0,m} \,.$$

The value of the right-hand term $G_{t+\Delta t}$ at the time point $t+\Delta t$ depends upon the unknown values $U_{t+\Delta t}$, $\dot{U}_{t+\Delta t}$, therefore for obtaining the solution of the equation (3.2) it is necessary to approximate the value $W(U_{t+\Delta t}, \dot{U}_{t+\Delta t})$ employing the values U, $\dot{U}$ at the previous time points, or to solve the nonlinear matrix equation (3.2) at each time point. The following approaches for obtaining $\Delta U_{t+\Delta t}$ are possible.

Application of explicit numerical schemes enables to avoid the difficulties related with the solution of the nonlinear equation (3.2), if the nonlinear function W depends only upon the displacements U , i.e., if $W = W(U)$. Setting the value of the numerical scheme parameter $\beta_0=0$, we obtain $U_{t+\Delta t} = q_0$ from the relation (2.52), and in place of (3.2) the equation

$$(b_2 M + b_1 C)\,\overset{m}{\Delta U}_{t+\Delta t} = R_{t+\Delta t} - (M\,q_2 + C\,q_1 + K\,q_0 - W(q_0)) \qquad (3.4)$$

is to be considered.

From the linear equation (3.4) the value of the unknown vector $\overset{m}{\Delta U}_{t+\Delta t}$ is obtained. If the equation contains a nonlinear term $W = W(U,\dot{U})$, it is necessary to present the equation (3.1) in the form

$$\dot{X} = \begin{bmatrix} -M^{-1}C & -M^{-1}K \\ I & 0 \end{bmatrix} X + \begin{bmatrix} M^{-1}R + M^{-1}W \\ 0 \end{bmatrix} \,, \qquad (3.5)$$

considering the vector $X = \begin{bmatrix} \dot{U} \\ U \end{bmatrix}$ as the new unknown.

Applying the Runge-Kutta schemes or the explicit versions of the SSpj scheme (see Chap.2.3.1) to the equation (3.5) it isn't necessary to solve nonlinear equations. However, a shortcoming of such an approach is a conditional stability of a numerical scheme. To be exact, an unconditional stability of an algorithm applied to a linear structure doesn't guarantee the unconditional stability when applied to a nonlinear system. It can be shown, [1], that the numerical schemes unconditionally stable for linear structures become only conditionally stable when applied to nonlinear structures. Nevertheless, in many practical applications nonlinearities don't impose such severe limits upon the integration step, as an explicit scheme does. Therefore for integrating nonlinear structural equations implicit numerical schemes are preferable.

Pseudo-force approach. The vector $W = W(U,\dot{U})$ is considered as an external force vector acting upon a linear elastic structure, and its value at the time point $t+\Delta t$ is extrapolated linearly as

$$W_{t+\Delta t} = 2\,W_t - W_{t-\Delta t} \,. \qquad (3.6)$$

In this case there is no need to solve nonlinear equations. The obtained numerical scheme, based upon the relations (3.2), (3.3), (3.6), isn't cumbersome and can be easily programmed. However, the accuracy and stability of such a scheme depends significantly upon a nonlinear function. Therefore the pseudo-force approach is applicable only if the nonlinearities are not severe.

Tangential linearization. The nonlinear equation (3.2) is considered as

$$F\,(\Delta U_{t+\Delta t}) = 0 \quad , \tag{3.7}$$

where $F(\Delta U_{t+\Delta t}) = A\,\Delta U_{t+\Delta t} - G_{t+\Delta t} - W(\,U_t+\Delta U_{t+\Delta t}, \dot{U}_t+\Delta\dot{U}_{t+\Delta t})$.

During each time step the function F is replaced by a linear function of $\Delta U_{t+\Delta t}$, obtained by linearizing the function F at the value $\Delta U_{t+\Delta t} = 0$. This linearized function is presented as

$$\tilde{F} = F(0) + \left[\frac{\partial F}{\partial(\Delta U_{t+\Delta t})}\bigg|_{\Delta U_{t+\Delta t}=0}\right]\Delta U_{t+\Delta t} \quad . \tag{3.8}$$

It is necessary to obtain the value $\Delta U_{t+\Delta t}$ satisfying the equation

$$\tilde{F}\,(\,\Delta U_{t+\Delta t}) = 0 \quad . \tag{3.9}$$

Obtaining the corresponding derivatives

$$\frac{\partial F}{\partial(\Delta U_{t+\Delta t})} = A - \left[\frac{\partial F}{\partial(\Delta U_{t+\Delta t})}\frac{\partial U_{t+\Delta t}}{\partial(\Delta U_{t+\Delta t})} + \frac{\partial F}{\partial(\Delta\dot{U}_{t+\Delta t})}\frac{\partial \dot{U}_{t+\Delta t}}{\partial(\Delta U_{t+\Delta t})}\right] ,$$

$$\frac{\partial U_{t+\Delta t}}{\partial(\Delta U_{t+\Delta t})} = b_o \quad , \quad \frac{\partial \dot{U}_{t+\Delta t}}{\partial(\Delta U_{t+\Delta t})} = b_1 \quad ,$$

and having in mind, that

$$\frac{\partial W}{\partial(\Delta U_{t+\Delta t})}\bigg|_{\Delta U_{t+\Delta t}=0} = \frac{\partial W}{\partial U}\bigg|_{\substack{U=U\\ \dot{U}=\dot{U}_t}} , \qquad \frac{\partial W}{\partial(\Delta \dot{U}_{t+\Delta t})}\bigg|_{\Delta U_{t+\Delta t}=0} = \frac{\partial W}{\partial \dot{U}}\bigg|_{\substack{U=U\\ \dot{U}=\dot{U}_t}} ,$$

the linearized equation (3.9) is presented as

$$\tilde{A}_{t+\Delta t}\,\Delta U_{t+\Delta t} = G_{t+\Delta t} + W(\,U_t,\,\dot{U}_t) \quad . \tag{3.10}$$

where $\tilde{A}_{t+\Delta t} = b_2^* M + b_1^* C + b_o^* K$, $\tilde{C} = C - \frac{\partial W}{\partial \dot{U}}\Big|_{U_t,\dot{U}_t}$, $\tilde{K} = K - \frac{\partial W}{\partial U}\Big|_{U_t,\dot{U}_t}$.

The accuracy of the tangential linearization at evaluating $W_{t+\Delta t}$ is significantly better, than the accuracy of pseudo-force approach. However, in the case of severe nonlinearities the integration step value must be sufficiently small in order to obtain a satisfactory approximation of the nonlinear function variation by its differential during one time step.

In order to avoid very small integration steps and to enhance the approximation accuracy of a nonlinear function, at each time step the nonlinear equation (3.2) can be solved. It is carried out iteratively, obtaining successive approximations of the exact solution $\Delta U^i_{t+\Delta t}$, i=1,2,... . The additional computation time required at each time step for solving a nonlinear equation is compensated by an obtained possibility to employ significantly larger time steps. The following approaches are possible.

Simple iteration. The equation (3.2) is solved by obtaining successive approximations $\Delta U^{\,i}_{t+\Delta t}$ from the algebraic equation

$$A\,\Delta U^{i+1}_{t+\Delta t} = G_{t+\Delta t} + W(\,U^i_{t+\Delta t}, \dot{U}^i_{t+\Delta t}) \quad , \quad i=0,1,\ldots \tag{3.11}$$

where i - the iteration number.

For obtaining a first approximation $\Delta U^o_{t+\Delta t}$ it appears reasonable to apply the relation (3.6) as $W(U^o_{t+\Delta t}, \dot{U}^o_{t+\Delta t}) = 2W_t - W_{t-\Delta t}$.

The convergence rate of a simple iteration isn't high, and for certain nonlinear functions it may diverge. In some cases the "oscillating" iterative process can be damped, in place of $U^{i+1}_{t+\Delta t}$ as the next approximation employing $\alpha U^{i+1}_{t+\Delta t} + (1-\alpha)U^i_{t+\Delta t}$, where $0 \le \alpha \le 1$.

Newton-Raphson iteration for the equation (3.7) is defined as

$$\Delta U^{i+1}_{t+\Delta t} = \Delta U^{i}_{t+\Delta t} - \left[\frac{\partial F}{\partial (\Delta U_{t+\Delta t})} \Big|_{\Delta U^{i}_{t+\Delta t}} \right]^{-1} F(\Delta U^{i}_{t+\Delta t}) \quad , \qquad (3.12)$$

and can be presented as a relation

$$\tilde{A}^{i} \Delta U^{i+1}_{t+\Delta t} = G_{t+\Delta t} + W(U^{i}_{t+\Delta t}, \dot{U}^{i}_{t+\Delta t}) \quad , \quad i=0,1,... \qquad (3.13)$$

For the first approximation $\Delta U^{o}_{t+\Delta t} = 0$ is employed. Usually only few iterations are necessary. The less is the integration step, the better is the first approximation for solving a nonlinear equation. However, the additional computational time is necessary for obtaining the values of derivatives $\frac{\partial W}{\partial U}$, $\frac{\partial W}{\partial \dot{U}}$ at each time step.

Application of quasi-Newton methods for solving the nonlinear equation (3.7) is based upon a substitution of the dynamic equilibrium equation by a functional minimization problem $\min f = \frac{1}{2} F^{T} F$. It is solved employing the following iteration [12] :

$$\Delta U^{i+1}_{t+\Delta t} = \Delta U^{i}_{t+\Delta t} - s^{i} \bar{H}_{i}^{-1} F(\Delta U^{i}_{t+\Delta t}) \quad . \qquad (3.14)$$

The matrix $\bar{H}_{i}^{-1}$ is obtained recursively from the relation

$$\bar{H}_{i}^{-1} = (I + w_i v_i^{T}) \bar{H}_{i-1}^{-1} (I + v_i w_i^{T}) \quad , \qquad (3.15)$$

where $v_i = g_{i-1} \left[1 + s_{i-1} \left(\frac{d_{i-1}^{T} \gamma_i}{d_i^{T} g_{i-1}} \right)^{\frac{1}{2}} \right] - g_i$, $w_i = \frac{\delta_i}{\delta_i^{T} \gamma_i}$,

$\delta_i = \Delta U^{i}_{t+\Delta t} - \Delta U^{i-1}_{t+\Delta t}$, $\gamma_i = g_i - g_{i-1}$, $g_i = F(\Delta U^{i}_{t+\Delta t})$,

and s_i is obtained regarding the condition

$$g_i^{T} (\bar{H}_{i-1}^{-1})^{T} g_{i+1} = 0 \quad . \qquad (3.16)$$

The advantage of the quasi-Newton methods consists in reducing the computational effort by employing the recursively obtained matrix $\bar{H}_i$ in place of the derivative matrix $\frac{\partial F}{\partial (\Delta U)}$.

3.2 TIME DOMAIN APPROACH

The dynamic response of the structure is presented as a superposition of transient dynamic compliances of the linear part of the structure. Consider the dynamic compliance matrices S , S^{uo}, $\dot{S}^{uo}$ of the linear part, defined in Chap.2.1. At each time point $i\Delta t$ we define vector P_i as

$$P_i = \sum_{j=1}^{i} S_{i-j} R_j \quad , \qquad (3.17)$$

where the lower indices denote the time point number.

The nonlinear term $W(U, \dot{U})$ is presented as an external force depending upon the displacements and velocities, and a recursive relation for obtaining the displacements at the time point $n+1$ is

$$U_{n+1} = S^{uo}_{n+1} U_o + \dot{S}^{uo}_{n+1} \dot{U}_o + P_{n+1} + \sum_{j=1}^{k} S_{n+1-j} W_j + S_o W_{n+1} \quad , \qquad (3.18)$$

$$n = 0,1,2,... \quad ,$$

where the notation $W_i = W(U_i, \dot{U}_i)$ is employed.

For obtaining the value U_{n+1} it is necessary to solve the nonlinear equation (3.18) at the known values $U_i, \dot{U}_i, W_i$, $i=0,1,2,...,n$. If the value U_{n+1} is known already, the value $\dot{U}_{n+1}$ is obtained from the relation (3.3).

Denoting the terms of the equation (3.18) independent of U_{n+1}, $\dot{U}_{n+1}$ through Q_{n+1}, the equation (3.18) is presented as

$$U_{n+1} = Q_{n+1} + S_o W (U_{n+1}, \dot{U}_{n+1}) \quad . \qquad (3.19)$$

For solving the equation (3.19) the approaches presented in Chap.3.1 can be applied.

Pseudo-force approach results in the relation

$$U_{n+1} = Q_{n+1} + S_o (2 W_n - W_{n-1}) \quad . \qquad (3.20)$$

Tangential linearization of a nonlinear function results in the relation

$$\bar{A}_n\,(U_{n+1} - U_n) = U_n - Q_{n+1} - S_o W_n \quad , \qquad (3.21)$$

where $\bar{A}_n = I - S_o \left[\left. \frac{\partial W}{\partial U} \right|_{U_n,\dot{U}_n} + b_1 \left. \frac{\partial W}{\partial \dot{U}} \right|_{U_n,\dot{U}_n} \right]$.

Simple iteration for the equation (3.19) is presented as

$$U^{i+1}_{n+1} = Q_{n+1} + S_o W\,(U^i_{n+1},\ \dot{U}^i_{n+1}) \quad . \qquad (3.22)$$

Newton-Raphson iteration is presented as

$$\bar{A}^i_n\,(U^{i+1}_{n+1} - U_n) = U_n - Q_{n+1} - S_o W^i_n \quad . \qquad (3.23)$$

3.3 ANALYSIS OF STRUCTURES WITH LOCAL NONLINEARITIES

The dynamic analysis of a transient motion of large nonlinear structures requires large amounts of computational effort, e.g., the Newton-Raphson iteration for a nonlinear algebraic equation requires obtaining a derivative matrix at each time step. If only few d.o.f. of a structure are subjected to a nonlinear interaction, the computational effort can be reduced by applying substructuring techniques.

Let's consider the equation of motion in the form

$$\begin{bmatrix} M_{11} M_{12} \\ M_{21} M_{22} \end{bmatrix} \begin{bmatrix} \ddot{U}_1 \\ \ddot{U}_2 \end{bmatrix} + \begin{bmatrix} C_{11} C_{12} \\ C_{21} C_{22} \end{bmatrix} \begin{bmatrix} \dot{U}_1 \\ \dot{U}_2 \end{bmatrix} + \begin{bmatrix} K_{11} & K_{12} \\ K_{21} & K_{22} \end{bmatrix} \begin{bmatrix} U_1 \\ U_2 \end{bmatrix} = \begin{bmatrix} 0 \\ W_2(U_2,\dot{U}_2) \end{bmatrix} + \begin{bmatrix} R_1 \\ R_2 \end{bmatrix}, \qquad (3.24)$$

where two substructures denoted by the indices "1" and "2" are distinguished. The nonlinear interaction forces depend only upon the displacements and velocities of the substructure "2", and they are applied only upon the substructure "2" . The equation (3.2) defining the generalized Newmark's scheme for the equation (3.24) here acquires the form

$$\begin{bmatrix} A_{11} A_{12} \\ A_{21} A_{22} \end{bmatrix} \begin{bmatrix} \Delta U_1 \\ \Delta U_2 \end{bmatrix} = \begin{bmatrix} G_1 \\ G_2 \end{bmatrix} + \begin{bmatrix} 0 \\ W_2(U_2,\dot{U}_2) \end{bmatrix} , \qquad (3.25)$$

where the values of the vectors U and G correspond to the time point $t+\Delta t$.

From the first equation (3.25) the relation between ΔU_1 and ΔU_2 is obtained as

$$\Delta U_1 = -A_{11}^{-1} A_{12} \Delta U_2 + A_{11}^{-1} G_1 \quad . \qquad (3.26)$$

Substituting (3.26) into the second equation of (3.25), we obtain

$$(A_{22} - A_{21} A_{11}^{-1} A_{12})\ \Delta U_2 = G_2 - A_{21} A_{11}^{-1} G_1 + W_2(U_2, \dot{U}_2) \quad . \qquad (3.27)$$

If the number n_2 of nonlinearly interacted degrees of freedom (the length of U_2) is small in comparison with the total structure dimension ($n_2 << n_1+n_2$), the employment of the substructuring relations (3.27), (3.26) reduces considerably the computational effort in comparison with the relation (3.2), because the matrices $A_{22} - A_{21} A_{11}^{-1} A_{12}$ and A_{11}^{-1} can be obtained in advance during an initial operation. The algebraic equation (3.27) to be solved at each time step is of the dimension $n_2 \times n_2$ in place of $n \times n$. The displacement increment ΔU_2 can be obtained applying any approach from those presented in Chap.3.1. So, the Newton-Raphson iteration for the equation (3.27) is defined by the relation

$$\tilde{\hat{A}}^i_{22}\ \Delta U_2^{i+1} = \hat{G}_2 + W_2(U_2^i,\ \dot{U}_2^i) \quad , \quad i=0,1,\ldots \qquad (3.28)$$

where $\hat{A}_{22} = A_{22} - A_{21} A_{11}^{-1} A_{12}$, $\tilde{\hat{A}}_{22} = \hat{A}_{22} - b_0 \frac{\partial W_2}{\partial U_2} - b_1 \frac{\partial W_2}{\partial \dot{U}_2}$, $\hat{G}_2 = G_2 - A_{21} A_{11}^{-1} G_1$.

Having obtained the value ΔU_2^{i+1} , the value ΔU_1^{i+1} follows from the relation (3.26).

If the equation (3.24) in time domain is considered, the dynamic compliance matrices S, S^{UO}, $S^{\dot{U}O}$ and the matrices P, Q, defined in Chap.3.2 by the relations (3.17)-(3.19), are presented as

$$S = \begin{bmatrix} S_{11} S_{12} \\ S_{21} S_{22} \end{bmatrix},\ S^{uo} = \begin{bmatrix} S^{uo}_{11} & S^{uo}_{12} \\ S^{uo}_{21} & S^{uo}_{22} \end{bmatrix},\ S^{\dot{u}o} = \begin{bmatrix} S^{\dot{u}o}_{11} & S^{\dot{u}o}_{12} \\ S^{\dot{u}o}_{21} & S^{\dot{u}o}_{22} \end{bmatrix},\ P = \begin{bmatrix} P_1 \\ P_2 \end{bmatrix},\ Q = \begin{bmatrix} Q_1 \\ Q_2 \end{bmatrix}.$$

The equation (3.19) transforms to

$$U_1 = Q_1 + S_{12,o}\, W_2(U_2, \dot{U}_2) \quad , \tag{3.29}$$

$$U_2 = Q_2 + S_{22,o}\, W_2(U_2, \dot{U}_2) \quad . \tag{3.30}$$

The system (3.29), (3.30) allows to obtain U_2 from the nonlinear equation (3.30) of a comparatively small dimension $n_2 x n_2$, and, after that, to substitute the value U_2 into the equation (3.29), in order to define the value U_1. The value U_2 from the equation (3.30) can be obtained by applying any approach presented in Chap.3.2. The Newton-Raphson iteration for the equation (3.30) is defined by the relation

$$\bar{A}^{i}_{22}(U^{i+1}_2 - U_2) = U_{2,t} - Q_2 - S_{22,o} W^{i}_2 \quad , \tag{3.31}$$

where $$\bar{A}_{22} = I - S_{22,o}\left(\left.\frac{\partial W_2}{\partial U_2}\right|_{U_2,\dot{U}_2} + b_1 \left.\frac{\partial W_2}{\partial \dot{U}_2}\right|_{U_2,\dot{U}_2} \right) .$$

3.4 DIRECT INTEGRATION OF STRUCTURAL EQUATIONS WITH UNILATERAL CONSTRAINTS

Consider the structural equation of motion

$$M \ddot{U} + C \dot{U} + K U = R(t) \quad , \tag{3.32}$$

with the constraints upon the displacements

$$P U \le d_o \quad , \tag{3.33}$$

where M, C, K of dimension nxn and P of dimension pxn , $p \le n$, are constant or explicitly time-dependent matrices, and U, R of dimension nx1 - vectors of nodal displacements and external forces.

If the variable U wouldn't vary in time, a corresponding static problem would appear as the functional minimization problem

$$\begin{cases} \min \left(\frac{1}{2} U^T K U - U^T R \right), \\ \text{with the constraint (3.33).} \end{cases} \tag{3.34}$$

We introduce the penalty function $B = \sum_{i=1}^{p} B_i$, each component of which is defined as

$$B_i = \frac{1}{2} k (P_i U - d_{oi})^T (P_i U - d_{oi}) \quad , \tag{3.35}$$

where $B_i = \begin{cases} B_i \ , \text{ if } P_i U - d_{oi} > 0, \\ 0 \ , \text{ otherwise} \end{cases}$.

The minimum condition of the functional (3.34) is

$$K U = R - F \quad , \tag{3.36}$$

where $F = \frac{\partial B}{\partial U} = \sum_{i=1}^{p} \frac{\partial B_i}{\partial U}$,

$$\frac{\partial B_i}{\partial U} = \begin{cases} k P_i^T (P_i U - d_{oi}) \ , \text{ if } P_i U > 0 \ , \\ 0 \ , \text{ otherwise} \end{cases} .$$

Adding the dynamic terms to the equation (3.36), we obtain the equation

$$M \ddot{U} + C \dot{U} + K U = R - F \quad , \tag{3.37}$$

where F is the nodal force vector produced by constraints upon a structure.

If the value k in the expression (3.35) is sufficiently large, the solution of (3.37) will not violate the constraint (3.33) more than to infinitesimal value. However, (3.33) imposes constraints only upon the displacements, the velocities and accelerations of the structure depending upon the features of the

penalty function B_i (e.g., in the expression (3.35) the arbitrary value of k can be employed, and the penalty function itself can be defined in the form other than (3.35)) .

In order to define completely the motion of the system approaching the constraint, the auxiliary constraints should be employed. In general, the motion of the structure is defined by the initial values of its displacements and velocities and by an external forcing law. If the numerical scheme is applied, the status of the system at the next time integration point is defined by the values at the current time point of displacements, velocities, accelerations and, perhaps, higher time derivatives of displacements, depending upon the order of an integration scheme. It follows, that the auxiliary constraints upon the velocities, accelerations, etc. should be used together with those presented by (3.33)upon the displacements. They should be imposed upon a structure in the case when the constraints (3.33) are active, i.e., when they are satisfied as an equality.

Applying Lagrange multipliers. Let's consider the equation of motion (3.32) with the constraints (3.33), and, if they are satisfied as an equality $PU-d_o=0$, let's impose the auxiliary constraints upon m time derivatives of the displacements U :

$$P\overset{(k)}{U} = d_k \quad , \quad k = \overline{1,m} \quad . \tag{3.38}$$

If U would be time-independent, the Lagrange multipliers can be employed in order to obtain the values of displacements satisfying the minimum condition of the functional (3.34) from the equation system

$$\begin{cases} K\,U + P^T\lambda_o = R \quad , \\ P\,U = d_o \quad , \end{cases} \tag{3.39}$$

where λ_o is the Lagrange multiplier vector of dimension pX1. Each negative value λ_{oj} of some j-th component of the vector λ_o, obtained by solving the system (3.39) signifies that the corresponding j-th constraint is inactive. Really, only at $\lambda_{oj}>0$ the unsatisfied constraint $P_iU-d_{oi}\le 0$ increases the value of the functional (3.34) by the magnitude $\lambda_{oj}(P_iU-d_{oi})$, and requires the expression P_iU-d_{oi} to be zero. If $\lambda_{oj}<0$, the value of the

functional is increased in the case of satisfied constraint $P_iU-d_{oi}\le 0$, therefore this constraint shouldn't be regarded. The value of the j-th component of the vector λ_o must be redefined as follows:

$$\lambda_{oj} = \begin{cases} \lambda_{oj} \quad , \text{ if } \lambda_{oj} \ge 0 \quad , \\ 0 \quad , \text{ otherwise} \quad . \end{cases} \tag{3.40}$$

To be accurate, the decision of regarding or not the j-th constraint $P_iU-d_{oi}=0$ of the system (3.39) must be carried out iteratively, solving the system (3.40) several times. The j-th row of the matrix P is deleted, if at the current iteration the value $\lambda_{oj}<0$ is obtained. It is reincluded into the matrix P , if at some other iteration the constraint upon the displacements $P_iU-d_{oi}\le 0$ is violated. The iteration is over, when all the λ_{oj}, obtained by solving the system (3.39), satisfy the condition $\lambda_{oj}\ge 0$, and at the same time no constraints $P_iU-d_{oi}\le 0$ are violated. A physical sense of the term $-P_i^T\lambda_o$ is a force, produced upon a structure by constraints.

Supplying dynamic terms to the system (3.39) and the auxiliary constraints (3.38), we obtain the equation system

$$\begin{cases} M\ddot{U} + C\dot{U} + K\,U + P^T\lambda_o = R \quad , \\ P\,U \le d_o \quad , \\ P\overset{(k)}{U} = d_k \quad , \quad k = \overline{1,m} \quad . \end{cases} \tag{3.41}$$

Let's integrate (3.41) numerically. If at the time point $t+\Delta t$ the second relation of (3.41) is satisfied as an equality, and the third isn't satisfied for some values of k , the corrections upon the values of velocities, accelerations and higher time derivatives $\overset{(k)}{U}$ must be made. The time interval for these corrections is reasonable to assume very short, as it is usually supposed by considering a dynamic contact of rigid bodies.

Assume that the corrections of the velocities are carried out during the time interval Δt_e that is very short in comparison with the integration step. The velocities at the beginning and end are represented by $\dot{U}^-$ and $\dot{U} = \dot{U}^- + \Delta\dot{U}$. Accordingly to the

Carnot's theorem, the change of the kinetic energy of a structure because of introducing a new constraint equals to the kinetic energy of lost velocities $\frac{1}{2}\,\Delta\dot{U}^T M\,\Delta\dot{U}$. The loss of energy is caused by the work done by contact forces during the time interval Δt_e . It appears natural to require, that the motion of the system would correspond to the minimum value of this work, or, what is the same, to the minimum change of the kinetic energy of the structure. At the end of the time interval $(t,t+\Delta t_e)$ the constraints upon velocities must be satisfied, i.e., it is necessary to solve the problem

$$\begin{cases} \min \frac{1}{2}\,\Delta\dot{U}^T M\,\Delta\dot{U} \ , \\ \text{with the constraint} \quad P\,\Delta\dot{U} = -\,P\,\dot{U}^- + d_1 \ . \end{cases} \tag{3.42}$$

The same presentation of the problem in the form (3.42) can be obtained by employing the momentum conservation theorem as

$$M\,\Delta\dot{U} = \int_t^{t+\Delta t_e} (\,R - K\,U - C\,\dot{U}\,)\,dt \ . \tag{3.43}$$

The right-hand side of the equality (3.43) presents the impetus of the internal and external forces, that is assumed to be zero because of very short duration of the time interval Δt_e and the finite values of velocities and displacements. In this way the equation $M\Delta\dot{U}=0$ is obtained, that can be presented as functional minimization problem $\min \frac{1}{2}\Delta\dot{U}^T M\Delta\dot{U}$ with the constraints. As a result, the same system (3.42) is obtained..

The functional minimum condition appears as

$$\begin{cases} M\,\Delta\dot{U} + P^T\lambda_1 = 0 \ , \\ P\,\Delta\dot{U} = -\,P\,\dot{U}^- + d_1 \ . \end{cases} \tag{3.45}$$

Solving the system (3.45), we obtain

$$\lambda_1 = (P\,M^{-1}P^T)^{-1}(\,P\,\dot{U}^- - d_1\,) \ , \tag{3.46}$$

$$\Delta\dot{U} = -\,M^{-1}P^T(P\,M^{-1}P^T)^{-1}(\,P\,\dot{U}^- - d_1\,) \ . \tag{3.47}$$

After differentiating in time the first equation of (3.41) and writing the relations for accelerations similar to (3.42)-(3.47) for velocities, we obtain the Lagrange multipliers λ_2 and the acceleration increments $\Delta\ddot{U}$ as

$$\lambda_2 = (P\,M^{-1}P^T)^{-1}(\,P\,\ddot{U}^- - d_2\,) \ , \tag{3.48}$$

$$\Delta\ddot{U} = -\,M^{-1}P^T(P\,M^{-1}P^T)^{-1}(\,P\,\ddot{U}^- - d_2\,) \ . \tag{3.49}$$

In the same way we obtain all λ_k and $\Delta\overset{(k)}{U}$, $k \le m$ for an arbitrary order m of a derivative. The physical sense of the Lagrange multipliers λ_1, λ_2, λ_3,... is the normal impetus, normal forces, derivatives of normal forces, etc., representing the action of constraints upon a structure during the time interval $(t,t+\Delta t_e)$.

It follows from the relation (3.47), that the impetus of constraint forces in global coordinates during the time interval $(t,\ t+\Delta t_e)$ is obtained as

$$S_1 = -\,P^T S_N = -\,P^T(P\,M^{-1}P^T)^{-1}(\,P\,\dot{U}^- - d_1\,) \ . \tag{3.50}$$

The forces of constraints enabling the acceleration change (3.49) during the time interval $(t,\ t+\Delta t_e)$ is defined as

$$F_1 = -\,P^T F_N = -\,P^T(P\,M^{-1}P^T)^{-1}(\,P\,\ddot{U}^- - d_2\,) \ . \tag{3.51}$$

<u>Numerical integration scheme</u> is obtained by expressing the values of displacements and their derivatives at successive discrete time points employing the relations of the m-th order generalized Newmark's scheme. The sequence of steps for obtaining the values $U_{t+\Delta t}$, $\dot{U}_{t+\Delta t}$, $\ddot{U}_{t+\Delta t}$,... at the time point $t+\Delta t$ employing the values U_t, $\dot{U}_t$, $\ddot{U}_t$,... at the time point t are defined by the Algorithm 2.2 . Expressing λ_o from the first equation of the system (3.41) and regarding the relations (3.47), (3.49), the equation (2.55) and the formulae of the step 3 of the Algorithm 2.2 are presented as

$$A\,\Delta U = G - P^T\lambda_o \ , \tag{2.55)'}$$

where $A = b_2 M + b_1 C + b_0 K$, $G = R_{t+\Delta t} - (M q_2 + C q_1 + K q_0)$,

$$U = q_0^* + b_0^* \Delta U \quad , \tag{3.52}$$

$$\overset{(k)}{U}{}^- = q_k^* + b_k^* \Delta U \quad , \quad \overset{(k)}{U} = \overset{(k)}{U}{}^- - M^{-1} P^T \lambda_k \quad , \; k = \overline{1,m} \quad , \tag{3.53}$$

where the Lagrange multiplier vectors are obtained from the relations

$$\begin{aligned} \lambda_0 &= (P A^{-1} P^T)^{-1} (P A^{-1} G - d_0) \quad , \\ \lambda_k &= (P M^{-1} P^T)^{-1} (P \overset{(k)}{U}{}^- - d_k) \quad , \; k = \overline{1,m} \quad . \end{aligned} \tag{3.54}$$

It's worth to mention, that the Lagrange multipliers λ_0 evaluate the impetus of normal interaction forces rather than their values that go to infinity when the finite mass points are interacting. The impetus of the normal interaction forces S_N during the time interval equal the integration step Δt are approximately obtained as

$$S_N^{t+\Delta t} = \frac{F_N^t + \lambda_0^{t+\Delta t}}{2} \Delta t + \lambda_1^{t+\Delta t} \quad . \tag{3.55}$$

The normal forces F_N ensuring the dynamic equilibrium at the time point $t+\Delta t$ are obtained as

$$F_N^{t+\Delta t} = \lambda_0^{t+\Delta t} + \lambda_2^{t+\Delta t} \quad . \tag{3.56}$$

The meaning of the relations (3.55), (3.56) is explained in Fig.3.1 assuming that the velocity and acceleration corrections are carried out during the time interval significantly shorter than the integration step.

In general, if the number of constraints exceeds unity, (i.e., number of rows of the matrix P is more than one), at each time point an iteration defined by the following algorithm is necessary.

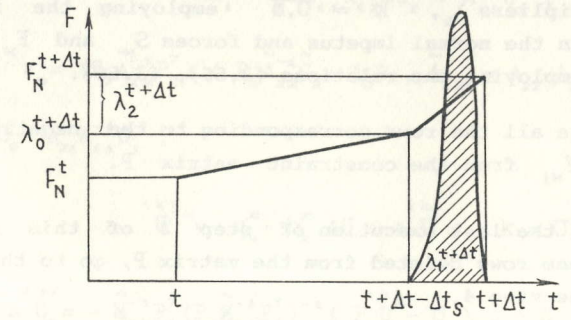

Fig.3.1 Time-laws of the contact force and impetus during one integration step

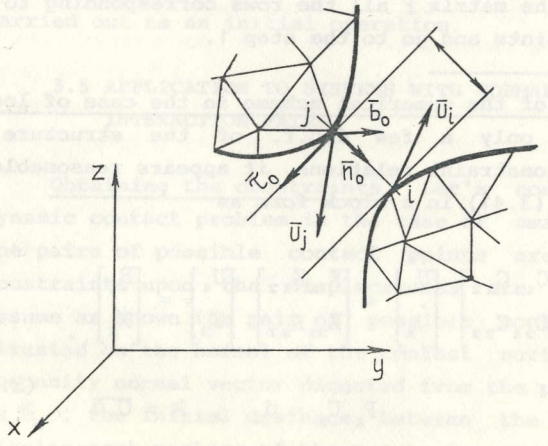

Fig.3.2 Vicinity of the contact points i and j

Algorithm 3.1

1. At the current time step obtain the values of the Lagrange multipliers λ_k, $k = \overline{0,m}$ employing the relations (3.54). Obtain the normal impetus and forces S_N and F_N of the constraints employing the relations (3.55), (3.56).

2. Delete all the rows corresponding to the negative values of λ_{oj}, S_{Nj}, F_{Nj} from the constraint matrix P.

3. If at the last execution of step 2 of this algorithm there were some rows deleted from the matrix P, go to the step 1. Else go to the step 4.

4. Obtain the values $\overset{(k)}{U}$, $k = \overline{0,m}$ employing the relations (2.55)', (3.52), (3.53).

5. Check if the constraints (3.33) are satisfied, taking account upon the constraints deleted during the execution of the step 2. If all of them are satisfied by the vectors U obtained during the execution of the step 4., go to to the next time step. Else include into the matrix P all the rows corresponding to the unsatisfied constraints and go to the step 1.

The relations of the numerical scheme in the case of local nonlinearities. If only a few d.o.f. of the structure are involved into the constraint relations, it appears reasonable to present the system (3.41) in a block form as

$$\begin{cases} \begin{bmatrix} M_{11} M_{12} \\ M_{21} M_{22} \end{bmatrix} \begin{bmatrix} \ddot{U}_1 \\ \ddot{U}_2 \end{bmatrix} + \begin{bmatrix} C_{11} C_{12} \\ C_{21} C_{22} \end{bmatrix} \begin{bmatrix} \dot{U}_1 \\ \dot{U}_2 \end{bmatrix} + \begin{bmatrix} K_{11} K_{12} \\ K_{21} K_{22} \end{bmatrix} \begin{bmatrix} U_1 \\ U_2 \end{bmatrix} = \begin{bmatrix} R_1 \\ R_2 \end{bmatrix} , \\ P_2 \overset{(k)}{U}_2 = d_k \quad , \quad k = \overline{0,m} \quad , \end{cases} \tag{3.41}'$$

where the length of the total vector U exceeds considerably the length of the subvector U_2. In this case the relations (2.55)' and (3.53) can be presented as

$$\tilde{A}_{22} \Delta U_2 = \tilde{G}_2 - P_2^T \lambda_o \quad ,$$
$$\Delta U_1 = - A_{11}^{-1} A_{12} \Delta U_2 + A_{11}^{-1} G_1 \quad , \tag{2.55)''}$$

where $\lambda_o = (P_2 \tilde{A}_{22}^{-1} P_2^T)^- (P_2 \tilde{A}_{22}^{-1} \tilde{G}_2 - d_o)$, $\tilde{A}_{22} = A_{22} - A_{21} A_{11}^{-1} A_{12}$,

$\tilde{G}_2 = G_2 - A_{21} A_{11}^{-1} G_1$,

$$\overset{(k)}{U}{}^- = q_k^* + b_k^* \Delta U + \Delta \overset{(k)}{U} , \quad k = \overline{0,m} \quad , \tag{3.53)'}$$

where $\Delta \overset{(k)}{U}_2 = - \tilde{M}_{22}^{-1} P_2^T (P_2 \tilde{M}_{22}^{-1} P_2^T)^{-1} (P_2 \overset{(k)}{U}{}_2^- - d_k)$, $\Delta \overset{(k)}{U}_1 = - M_{11}^{-1} M_{12} \Delta \overset{(k)}{U}_2$,

$\tilde{M}_{22} = M_{22} - M_{21} M_{11}^{-1} M_{12}$.

Employing the formulae (2.55)'', (3.53)' enables to economize the computational effort, because the major part of computations is carried out upon the matrix blocks of small dimension. The inversion of blocks with the indices "11" is carried out as an initial operation.

3.5 APPLICATION TO SYSTEMS WITH NORMAL IMPACT INTERACTION PAIRS

Obtaining the constraints. Let's consider the structural dynamic contact problem in the case of small displacements. If the pairs of possible contact points are known apriori, the constraints upon the displacements are obtained as follows. Assume as known the pair of possible contact points i and j situated on the normal of the contact surface, Fig.3.2. Denote the unity normal vector directed from the point j to the point i as $\bar{n}_o$, the initial distance between the points as d_{ij}, the displacement vectors of the points i and j as $\bar{u}_i = (u_{ix}, u_{iy}, u_{iz})$, $\bar{u}_j = (u_{jx}, u_{jy}, u_{jz})$, where u_{ix}, u_{iy}, u_{iz} are the Cartesian components of the displacement of the point i. Taking on account, that the projections of the displacement vectors $\bar{u}_i$, $\bar{u}_j$ upon the normal are $pr_{\bar{n}_o} \bar{u}_i = \bar{n}_o \bar{u}_i$, $pr_{\bar{n}_o} \bar{u}_j = \bar{n}_o \bar{u}_j$, the constraint upon the

displacement components is presented as

$$\bar{n}_o \bar{u}_i \le \bar{n}_o \bar{u}_j + d_{ij} \quad . \qquad (3.57)$$

Using the matrix notation, the inequality (3.57) can be presented as

$$[\underbrace{000}_{i} \ldots \underbrace{n_{ox} n_{oy} n_{oz}}_{i} \ldots \underbrace{-n_{ox} -n_{oy} -n_{oz}}_{j} \ldots 000\ ]\ U \le d_{ij} \ , \qquad (3.58)$$

where $U = (000 \ldots u_{ix} u_{iy} u_{iz} \ldots u_{jx} u_{jy} u_{jz} \ldots 000)^T$ is the displacement vector of the whole structure. The entire constraint system is presented as

$$P\,U \le d_o \ ,$$

where each row of the matrix P is similar to (3.58), and the elements of the vector d_o contain the values of the initial clearances d_{ij} .

Employing rheological models of a contact surface. If a contact interaction takes place, i.e., if the constraints (3.58) are violated, the holding up contact forces occur hindering the penetration of the parts of the structure into each other. Supposing that these forces are caused by local deformations of the contact zone, the rheological models of the contact area are employed. They are usually represented by certain unions of stiffness and dissipative elements. The contact forces are represented by linear or nonlinear functions of displacements and velocities of the contacting points. The vector of the nodal contact forces is obtained as

$$W\,(\,U, \dot{U}\,) = -\,P^T F \quad . \qquad (3.59)$$

where F - the vector of normal contact forces, each element f(ij) of which represents the normal contact force between the points i and j . If the rheological model consists of the stiffness element k_{ij} and the dissipative one c_{ij} connected by parallel, the force f(ij) is obtained as

$$f(ij) = \begin{cases} k_{ij} P(ij) U + c_{ij} P(ij) \dot{U}, & \text{if } f(ij) > 0 \ , \\ 0 \ , & \text{otherwise} \ . \end{cases} \qquad (3.60)$$

where P(ij) denotes the row of the matrix P , corresponding to the contact pair ij .

Employing rheological models the structural dynamic contact problem is presented as a matrix equation of motion with the general nonlinear term (3.1). The summary of the generalized Newmark's scheme relations for the equation (3.1) is presented in the Appendix 1, Table A1.5. The computational effort can be reduced, taking on account local nonlinearities.

Applying the Lagrange multipliers enables to present the local phenomenological contact model in terms of the impact restitution coefficient. Consider the constraints as

$$P\,U \le d_o \ , \qquad (3.61)$$

and assume that during the time interval when (3.61) is satisfied to equality, the auxiliary constraints

$$P\,\overset{(k)}{U} = 0 \ , \quad k = \overline{1,m} \ , \qquad (3.62)$$

are to be taken on account, where m - the order of the generalized Newmark's scheme. The satisfaction of (3.61), (3.62) as an equality implies the plastic contact condition, because in this case coincide the post-impact positions of the contact points as well as their velocities, accelerations and higher time derivatives of displacements that are taken on account by the m-th order integration scheme, implying the perfectly plastic local impact condition. Employing the second order integration scheme m = 2 with the parameter values $\beta_o = \beta_1 = \frac{1}{2}$ (the constant acceleration algorithm), the constraints

$$\begin{cases} P\,U \le d_o \ , & (3.63) \\ P\,\dot{U} = 0 \ , & (3.64) \end{cases}$$

present the perfectly elastic local contact condition with the restitution coefficient R_f because of the constant acceleration value held by the integration scheme during an integration step. The intermediate values of the restitution coefficiemt $0 \le R_f \le 1$ are obtained employing the constraints (3.63), (3.64) and, simultaneously, the constraint

$$P\,\ddot{U} = -\frac{1}{\Delta t} R_f P\,\dot{U}_t \quad , \tag{3.65}$$

where Δt is the integration step.

The summary of the generalized Newmark's scheme relations is presented in the Appendix 1, Table A1.6.

3.6 APPLICATION TO SYSTEMS WITH OBLIQUE IMPACT AND SLIDING FRICTION INTERACTION

Obtaining the constraints. Considering an oblique impact, not only normal, but also tangential interaction forces are to be taken on account. If the tangential interaction is governed by the Coulomb friction law, there is no sliding until the magnitude of tangential interaction forces doesn't exceed the critical value $k_f F_N$, where F_N - normal interaction force, and k_f - Coulomb friction coefficient. The difference between the tangential components of the velocities of the points i and j equals $[(\dot{\bar{u}}_j - \dot{\bar{u}}_i)\bar{\tau}_o]\bar{\tau}_o + [(\dot{\bar{u}}_j - \dot{\bar{u}}_i)\bar{b}_o]\bar{b}_o$, where $\bar{n}_o$, $\bar{\tau}_o$, $\bar{b}_o$ - three mutually orthogonal unit vectors with $\bar{n}_o$ directed in the normal direction to the contact surface, Fig.3.2. If there is no sliding, the velocities and accelerations of contact points satisfy the constraint

$$\begin{bmatrix} 000 \ldots -\tau_x -\tau_y -\tau_z \ldots \tau_x\ \tau_y\ \tau_z \ldots 000 \\ 000 \ldots -b_x -b_y -b_z \ldots b_x\ b_y\ b_z \ldots 000 \end{bmatrix}^{(k)} U = 0 \ , \quad k=1,2 \ . \tag{3.66}$$

The full constraint system is

$$\begin{cases} P_N U \le d_o \ , \ P_N \dot{U} = 0 \ , \ P_N \ddot{U} = 0 \ , & (3.67.1) \\ P_T \dot{U} = 0 \ , \ P_T \ddot{U} = 0 \ , & (3.67.2) \end{cases}$$

where the relations (3.67.1) impose the constraints upon the normal, and the relation (3.67.2) - upon the tangential components of the displacements, velocities and accelerations of the contact points. In general, the submatrix P_T consists of two submatrices $P_T = \begin{bmatrix} P_{T\tau} \\ P_{Tb} \end{bmatrix}$, corresponding to the two perpendicular directions on the contact surface, but here we restrict ourselves with the consideration of two-dimensional problem, i.e., with $P_{Tb} = 0$.

If the second order generalized Newmark's scheme is employed (m=2), the zero right-hand parts of (3.67.1), (3.67.2) denote the plastic contact condition in both the normal and tangential direction. In (3.67.2) only the constraints should be regarded, tangential forces of which don't exceed their critical values $k_f F_N$, otherwise the magnitude of the tangential force is supposed to be equal to $k_f F_N$ and sliding takes place. Obviously, the rows of the matrix P_T corresponding to the sliding contact points are to be deleted.

Obtaining a system with single-valued nonlinearity. The tangential interaction force depends upon the tangential component of the mutual velocity as

$$F_T = - k_f F_N \ \mathrm{sign}\ (P_T \dot{U}) \ , \tag{3.68}$$

where F_N, F_T - the normal and tangential component of the tangential force. Employing the relation (3.68) for obtaining the tangential force, the equation of motion with the constraints is presented as

$$\begin{cases} M\,\ddot{U} + C\,\dot{U} + K\,U = - P_T^T F_T + R(t) \ , \\ P_N U \le d_o \ , \ P_N \dot{U} = 0 \ , \ P_N \ddot{U} = 0 \ . \end{cases} \tag{3.69}$$

The numerical integration of the system (3.69) is carried out employing the relations of the Appendix 1, Table A1.6, where at each time step the nonlinear algebraic equation is solved iteratively. Employing rheological models for representing the contact interaction forces, the normal forces F_N are expressed through the displacements and velocities of the contact points,

and the system (3.69) is presented as (3.1). However, if the equality $P_T\dot{U}=0$ is satisfied, the force F_T obtained from the relation (3.68) is non defined. It results in the oscillating behavior of the tangential force values, if the mutual tangential velocity of contact points is close to zero.

To avoid this, the function sign may be approximated by some single-valued function, e.g., $\frac{2}{\pi}\,\mathrm{arctg}\,[\alpha(\cdot)]$, where by increasing the value of α the better approximation is obtained. The relation (3.68) is presented as

$$F_T = - k_f F_N \frac{2}{\pi}\,\mathrm{arctg}\,(\alpha P_T\dot{U}) \quad . \qquad (3.68)'$$

Employing rheological models. If the magnitude of the tangential force doesn't exceed its critical value, in place of substituting the friction law (3.68) by the relation (3.68)' rheological models of the tangential contact interaction can be employed. Similar to the normal contact models, it is supposed that the values of the tangential force corresponding the multi-value segment of the friction law (3.68) (at $P_T\dot{U}=0$) are determined by local contact phenomena. The tangential forces F_T are represented by the linear or nonlinear functions of displacements and velocities of contact points. If a rheological model consists of the stiffness element k_{ij} and the dissipative one c_{ij} connected by parallel, the force f(ij) is obtained as

$$f_T(ij) = \begin{cases} k_{ij}P_T(ij)(U-U_o)+c_{ij}P_T(ij)\dot{U}, & \text{if } |f_T(ij)|>k_f f_N(ij) \\ k_f f_N(ij)\,\mathrm{sign}\left[k_{ij}P_T(ij)(U-U_o)+c_{ij}P_T(ij)\dot{U}\right], & \text{otherwise} \end{cases} , \qquad (3.70)$$

where $f_N(ij)$ - the normal interaction force of the contact pair ij , U_o - displacement vector of the structure at the time point of the beginning of the contact without sliding between the points ij.

To be accurate, after disconnecting of the contact points the displacements of the rheological model don't become zero instantaneously. In order to account for this circumstance it is necessary to consider the equations of motion of the rheological model simultaneously with those of the structure. However,

rheological models are introduced basically for representing the tangential interaction forces at the beginning of the interaction, and it looses its physical sense when the contacting points disconnect. Therefore the expression (3.70) is usually employed during the contact without sliding, and the displacements are assumed to be zero when sliding occurs or when the contact points disconnect. The rheological model equations are to be solved, if they consist of the sequentially connected elements, and in this case the total number of degrees of freedom of the structure increases.

As a shortcoming of rheological models the lack of simple and reliable methods for obtaining their parameters can be mentioned. Usually the parameters are obtained experimentally in order to obtain a possibly good approximation of the real system's motion.

Applying Lagrange multipliers. The equations of motion (3.41), (3.45) for the structure with unilateral constraints (3.67.1), (3.67.2) are presented as

$$\begin{cases} M\ddot{U} + C\dot{U} + KU + P_N^T\lambda_o = R(t) , \\ P_N U \le d_o , \end{cases} \qquad (3.71)$$

$$\begin{cases} M\,\Delta\overset{(k)}{\dot{U}} + P_N^T\lambda_k + P_T^T\mu_k = 0 , \\ P_N\Delta\overset{(k)}{U} = - P_N\Delta\overset{(k)}{U^-} , \\ P_T\Delta\overset{(k)}{U} = - P_T\Delta\overset{(k)}{U^-} , \quad k = 1,2 . \end{cases} \qquad (3.72)$$

A physical sense of the Lagrange multipliers is as follows:

λ_o - normal forces, ensuring the coincidence of the contacting points of the structure at the time point $t+\Delta t$,

λ_2 - normal forces ensuring the correction of the acceleration value,

λ_1 - impetus of the normal forces, ensuring the correction of the velocity value,

μ_2 - tangential forces ensuring the correction of the acceleration value,

μ_1 - impetus of normal forces, ensuring the correction of the velocity value,

If all the constraints in (3.71), (3.72) are satisfied as equalities, no sliding between the contact points occurs. If sliding takes place at the contact pair ij , we assume the magnitude of the corresponding tangential force to acquire its critical value:

$$|\mu_{kj}| = k_f \lambda_{kj} \quad , \quad k = 1,2 \; . \qquad (3.73)$$

In this case the system (3.72) is presented as

$$\begin{cases} M \overset{(k)}{\Delta U} + \hat{P}_N^T \lambda_k + \hat{P}_T^T \hat{\mu}_k = 0 \; , \\ P_N \overset{(k)}{\Delta U} = - P_N \overset{(k)}{\Delta U^-} \; , \\ \hat{P}_T \overset{(k)}{\Delta U} = - \hat{P}_T \overset{(k)}{\Delta U^-} \; , \quad k = 1,2 \; ,. \end{cases} \qquad (3.74)$$

where $\hat{P}_N$ denotes the matrix P_N with the row $P_N(ij)$, corresponding to the contact pair ij, replaced by the row $P_N(ij)+k_f P_T(ij)$; $\hat{P}_T$ denotes the matrix P_T with the row $P_T(ij)$ deleted ; $\hat{\mu}_k$ denotes the vector μ_k with the elements $\mu_k(ij)$ deleted. Denoting $\begin{bmatrix} \hat{P}_N \\ \hat{P}_T \end{bmatrix} = \overset{=}{P}$, $\begin{bmatrix} P_N \\ \hat{P}_T \end{bmatrix} = \bar{P}$, $\begin{bmatrix} \lambda_k \\ \hat{\mu}_k \end{bmatrix} = \overset{=}{\lambda}_k$, the system (3.74) is presented as

$$\begin{cases} M \overset{(k)}{\Delta U} + \overset{=}{P}^T \overset{=}{\lambda}_k = 0 \; , \\ \bar{P} \overset{(k)}{\Delta U} = - \bar{P} \overset{(k)}{U^-} \; , \quad k = 1,2 \; . \end{cases} \qquad (3.75)$$

Presenting the relations (2.55)', (3.52)-(3.54) for the system (3.71), we obtain numerical integration relations as

$$A \, \Delta U = G - P^T \lambda_o \; , \qquad (2.55)'$$

where $A = b_2 M + b_1 C + b_o K$, $G = R_{t+\Delta t} - (M q_2 + C q_1 + K q_o)$.

$$U = q_o^* + b_o^* \, \Delta U \; , \qquad (3.52)''$$

$$\overset{(k)}{U^-} = q_k^* + b_k^* \, \Delta U \; , \quad \overset{(k)}{U} = \overset{(k)}{U^-} - M^{-1} \overset{=}{P}^T \overset{=}{\lambda}_k \; , \; k = 1,2 \; , \qquad (3.53)''$$

$$\lambda_o = (P A^{-1} P^T)^{-1} (P A^{-1} G - d_o) \; ,$$

$$\overset{=}{\lambda}_k = (\bar{P} M^{-1} \overset{=}{P}^T)^{-1} (\bar{P} \overset{(k)}{U^-} - d_k) \; , \quad k = 1,2 \; . \qquad (3.54)''$$

As a rule, the sliding contact points aren't known apriori, therefore at each time point an iteration governed by the following algorithm is necessary.

Algorithm 3.2

1. Assume $\overset{=}{P} = \bar{P} = \begin{bmatrix} P_N \\ P_T \end{bmatrix}$.

2. From the relations (3.54)'' obtain the Lagrange multipliers λ_o, λ_k, μ_k, $k = 1,2$ at the time point $t+\Delta t$.

3. Obtain the vectors of normal and tangential impetus of constraint forces employing the relations

$$S_N^{t+\Delta t} = \frac{F_N^t + \lambda_c^{t+\Delta t}}{2} \Delta t + \lambda_1^{t+\Delta t} \; , \quad S_T^{t+\Delta t} = \hat{\mu}_1^{t+\Delta t} \; ,$$

and the vectors of the normal and tangential forces at the time point $t+\Delta t$ employing the relations

$$F_N^{t+\Delta t} = \lambda_o^{t+\Delta t} + \lambda_2^{t+\Delta t} \; , \quad F_N^{t+\Delta t} = \mu_2^{t+\Delta t} \; .$$

4. Delete all the rows of the constraint matrices $P_N(ij)$, $P_T(ij)$ corresponding to the negative values of $\lambda_o(ij) < 0$, $S_N(ij) < 0$, or $F_N(ij) < 0$ at the time point $t+\Delta t$.

5. If there are some rows deleted at the step 4, go to step 1, else go to step 6.

6. Mark all the rows corresponding to the pairs of the contact points ij, where the values of tangential impetus of the constraints exceeds their critical values, i.e., where the inequality $k_f |S_N(ij)| \le |S_T(ij)|$ is satisfied.

7. If there are no rows marked during the execution of step 6, go to the next time point , else go to step 8.

8. Transform the constraint matrices $\overset{=}{P}$, $\bar{P}$, taking on account the constraints, marked at the step 6. Go to the step 2.

The summary of the numerical integration relations is presented in the Appendix 1, Table A1.7. The computational effort can be reduced taking account for the local nonlinearities.

Employing complex friction laws. When the sliding friction law besides the Coulomb friction term includes also other terms, e.g., linear and cubic [113], it appears reasonable to take account for the Coulomb term employing the constraints (3.67.1),(3.67.2) and to present the other terms by a nonlinear continuous function of velocities. In this case the problem is presented as a nonlinear equation of motion

$$M\ddot{U} + C\dot{U} + KU = V(\dot{U}) + R(t) \quad , \qquad (3.76)$$

with the constraints (3.67.1),(3.67.2), where $V(\dot{U})$ presents the contribution of continuous terms of the sliding friction law.

The system mentioned above is integrated in time employing the Algorithm 3.2, supplemented by the formulae of the Table A1.5 of the Appendix 1.

4. STATIONARY DYNAMIC ANALYSIS OF NONLINEAR ELASTIC STRUCTURES

This chapter presents analysis techniques of the resonant elastic mechanical structures with nonlinear interactions vibrating with stationary or slow-varying amplitudes.

For the stationary motion law analysis two alternative techniques are employed: the solution of the boundary value problem in time and the weighted residual approach. In the first case the motion law is obtained by the numerical integration of the equations of motion, and the displacements and velocities at the beginning of the period are established in order to coincide with those at the end of the period. This approach can be employed for the free vibration analysis, too, considering the vibration period as an auxiliary unknown. In the second case the motion law is represented as a superposition of some set of orthogonal periodic functions, obtaining the weighting factors by minimizing the residual. The harmonic balance techniques are shown to be a special case of the weighted residual approach.

For obtaining the motion law analysis in terms of slow varying amplitudes the averaging techniques are employed. When integrating the averaged equations of motion numerically, at each time station harmonic components are obtained by means of the Fourier transform.

The above mentioned techniques enable to obtain both stable and unstable motion laws of the structure. The stability of the motion laws can be approximately evaluated employing transfer matrices, Hill's determinants, or approximate stability evaluations based upon the averaged equation analysis and upon the energy criterion can be carried out.

The original results of this chapter are the algorithms for obtaining the stationary and slow varying vibration amplitudes of the unilaterally constrained structures and the linearized equations for the motion law stability analysis of the structures with the impact and friction interaction points.

4.1 DIRECT METHODS FOR OBTAINING FORCED AND FREE VIBRATION LAWS. BOUNDARY VALUE PROBLEM IN TIME DOMAIN

Consider the matrix equation of motion of an elastic structure with nonlinear interaction as

$$M\ddot{U} + C\dot{U} + K\,U = W(U,\dot{U}) + R(t) \quad . \qquad (4.1)$$

The stationary structural response to the periodic excitation $R(t)=R(t+T)$ can be presented as a vibration with the period T or sT, where the values $s=2,3,\ldots$ correspond to the subharmonic, and the values $s=\frac{1}{2}, \frac{1}{3}, \ldots$ - to the hyperharmonic vibration. In certain cases there can be no periodic response irrespective to the periodic excitation. In this chapter we consider only the stationary motion laws with $s=1$, i.e., when the periods of excitation and structural response coincide. In this case the displacements and velocities of the structure satisfy the equation system

$$U_T = U_o \quad , \quad \dot{U}_T = \dot{U}_o \quad , \qquad (4.2)$$

where $U_T=U(T)$, $\dot{U}_T=\dot{U}(T)$, $U_o=U(0)$, $\dot{U}_o=\dot{U}(0)$.

It appears natural to regard the values of U_o, $\dot{U}_o$ as unknowns, and the values U_T, $\dot{U}_T$ as functions obtained from the equation (4.1), integrating it from the initial values U_o, $\dot{U}_o$.

The simple iteration for solving the equation (4.2) is applied as

$$U_o^{i+1} = U_T^i \quad , \quad \dot{U}_o^{i+1} = \dot{U}_T^i \quad , \qquad (4.3)$$

where the upper index "i" denotes an iteration number, and the values U_T^i, $\dot{U}_T^i$ are obtained by means of the numerical integration of the equation (4.1) during the period $[0, T]$ from the initial values U_o^i, $\dot{U}_o^i$. An iteration presented by the relations (4.3), is adequate to the numerical integration of the equation (4.1) during the m excitation periods, where m coincides with

the number of iterations. If the structural dissipation forces are significant, the stationary motion law is obtained after several iterations, i.e., the iteration scheme (4.3) converges. In the case of insignificant structural dissipation the convergence rate is very low, and prohibitive numerical errors can be accumulated during the large number of integration periods. However, the motion laws obtained by the simple iteration are always stable.

The Newton-Raphson iteration enables to obtain considerably higher convergence rates. The Newton-Raphson iteration scheme for of the equation (4.2) appears as

$$\begin{bmatrix} \frac{\partial U_T}{\partial U_o} - I & \frac{\partial U_T}{\partial \dot{U}_o} \\ \frac{\partial \dot{U}_T}{\partial U_o} & \frac{\partial \dot{U}_T}{\partial \dot{U}_o} - I \end{bmatrix} \begin{pmatrix} U_o^{i+1} - U_o^i \\ \dot{U}_o^{i+1} - \dot{U}_o^i \end{pmatrix} = \begin{pmatrix} U_o^i - U_T^i \\ \dot{U}_o^i - \dot{U}_T^i \end{pmatrix} \quad , \qquad (4.4)$$

where the derivative matrix on the left-hand side of (4.4) is of the dimension $2n\times 2n$, and $I_{n\times n}$ denotes the unity matrix. In order to determine the derivative matrix it is necessary to obtain a relation between the variations of the functions δU_T, $\delta \dot{U}_T$ and the variations of the unknowns δU_o, $\delta \dot{U}_o$. Considering a small perturbation δU of the motion law $U(t)$, the equation (4.1) appears as

$$M(\ddot{U}+\delta\ddot{U}) + C(\dot{U}+\delta\dot{U}) + K(U+\delta U) = W(U+\delta U,\dot{U}+\delta\dot{U}) + R(t) \quad . \qquad (4.5)$$

Expanding the nonlinear terms as the Taylor series, we restrict ourselves with the first order infinitesimal terms. Taking on account that the equation (4.1) remains valid for an unperturbed motion, too, we obtain

$$M\,\delta\ddot{U} + \tilde{C}\,\delta\dot{U} + \tilde{K}\,\delta U = 0 \quad , \qquad (4.6)$$

where $\tilde{K} = K - \frac{\partial W}{\partial U}$, $\tilde{C} = C - \frac{\partial W}{\partial \dot{U}}$. Multiplying (4.6) on the left side by the conjugate variable vectors $\lambda(t)$ and $\dot{\mu}(t)$

correspondingly and integrating it in time from 0 until T, we obtain

$$\begin{cases} \int_0^T \lambda\,(M\delta\ddot{U} + \tilde{C}\delta\dot{U} + \tilde{K}\delta U)\,dt = 0\,, \\ \int_0^T \mu\,(M\delta\ddot{U} + \tilde{C}\delta\dot{U} + \tilde{K}\delta U)\,dt = 0\,. \end{cases} \tag{4.7}$$

Integrating each equation of (4.7) by parts, after some manipulation we obtain

$$(\lambda_T^T+\dot{\mu}_T^T)M\delta\dot{U}_T+(\lambda_T^T\tilde{C}-\dot{\lambda}_T^TM+\mu_T^T\tilde{K})\delta U_T - (\lambda_o^T+\dot{\mu}_o^T)M\delta\dot{U}_o-(\lambda_o^T\tilde{C}-\dot{\lambda}_o^TM+\mu_o^T\tilde{K})\delta U_o +$$

$$+\int_0^T(\ddot{\lambda}^TM - \dot{\lambda}^T\tilde{C} + \lambda^T\tilde{K})\delta U\,dt - \int_0^T(\ddot{\mu}^TM - \dot{\mu}^T\tilde{C} + \mu^T\tilde{K})\delta\dot{U}\,dt = 0\,. \tag{4.8}$$

The equation (4.8) enables to establish the relation between the variations of the time-laws of displacements $\delta U(t)$, velocities $\delta\dot{U}(t)$ and their values at the beginning and the end of the period δU_o, $\delta\dot{U}_o$, δU_T, $\delta\dot{U}_T$. In order to express δU_T through the values δU_o, $\delta\dot{U}_o$, we require $\lambda(t)$ and $\mu(t)$ to satisfy the equations of motion

$$M\ddot{\lambda} - \tilde{C}^T\dot{\lambda} + \tilde{K}^T\lambda = 0\,, \quad M\ddot{\mu} - \tilde{C}^T\dot{\mu} + \tilde{K}^T\mu = 0\,, \tag{4.9}$$

with the end values at the time point T obtained from the equation system

$$M(\lambda_T + \dot{\mu}_T) = 0\,, \quad \tilde{C}^T\lambda_T - M\dot{\lambda}_T + \tilde{K}^T\mu_T = I\,. \tag{4.10}$$

Each of the equations (4.9), (4.10) have n right-hand side vectors, therefore their solutions $\lambda(t)$, $\mu(t)$ are matrices, each column of which is obtained by solving the linear matrix equation with the corresponding column of the right-hand side matrices as the right-hand side vector. The transpose signs at the matrix M are omitted because of its symmetry. The matrices $\tilde{K}$, $\tilde{C}$ here should be regarded as time functions obtained by substituting

into their expressions the time laws $U^i(t)$, $\dot{U}^i(t)$ obtained during the previous iteration. The system (4.10) has more unknowns as the equations, and the end values can be taken as, e.g.,

$$\lambda_T = 0\,, \quad \mu_T = 0\,, \quad \dot{\mu}_T = 0\,, \quad \dot{\lambda}_T = -M^{-1}\,. \tag{4.11}$$

Taking on account (4.8)-(4.10), we obtain the relations

$$\frac{\partial U_T}{\partial U_o} = \lambda_o^T\,\tilde{C} - \dot{\lambda}_o^T\,M + \mu_o^T\tilde{K}\,, \quad \frac{\partial U_T}{\partial \dot{U}_o} = (\,\lambda_o^T + \dot{\mu}_o^T\,)\,M\,. \tag{4.12}$$

In a similar way the derivatives $\frac{\partial \dot{U}_T}{\partial U_o}$, $\frac{\partial \dot{U}_T}{\partial \dot{U}_o}$ can be obtained.

Integrating the equations (4.9) with the end values

$$\lambda_T = 0\,, \quad \dot{\lambda}_T = 0\,, \quad \mu_T = 0\,, \quad \dot{\mu}_T = M^{-1}\,, \tag{4.13}$$

we obtain the relations

$$\frac{\partial \dot{U}_T}{\partial U_o} = \lambda_o^T\,\tilde{C} - \dot{\lambda}_o^T\,M + \mu_o^T\tilde{K}\,, \quad \frac{\partial \dot{U}_T}{\partial \dot{U}_o} = (\,\lambda_o^T + \dot{\mu}_o^T\,)\,M\,. \tag{4.14}$$

The two matrix equations of the system (4.9) are identical, and the end values (4.11) for λ and (4.13) for μ are of the equal magnitude and have opposite signs. Therefore there is no necessity to integrate each equation of (4.9). Moreover, the end values of (4.11) for μ and (4.13) for λ are zero, and the corresponding values $\mu_o = \dot{\mu}_o = 0$ and $\lambda_o = \dot{\lambda}_o = 0$. The system (4.9) can be transformed into the system with the positive damping term by means of the substitution $t^* = T - t$.

Summarizing the above consideration, it follows, that in order to obtain the derivative matrix of (4.4) the following steps are necessary.

1) Numerical integration during the period $t^* \in (0,T)$ of the matrix equation of motion

$$M\ddot{\lambda} + [\tilde{C}(T-t^*)]^T\dot{\lambda} + [\tilde{K}(T-t^*)]^T\lambda = 0 \tag{4.15}$$

with the initial values $\lambda_o = 0$, $\dot{\lambda}_o = -M^{-1}$, where $\tilde{C}(T-t^*)$ and $\tilde{K}(T-t^*)$ are obtained by substituting into their expressions the time laws $U^i(T-t^*)$, $\dot{U}^i(T-t^*)$. As a result the values λ_T, $\dot{\lambda}_T$ are obtained.

2) Obtaining the derivative matrix blocks from the relations

$$\frac{\partial U_T}{\partial U_o} = -\lambda_T^T\tilde{C} - \dot{\lambda}_T^T M \ , \quad \frac{\partial U_T}{\partial \dot{U}_o} = -\lambda_T^T M \ , \quad \frac{\partial \dot{U}_T}{\partial U_o} = \lambda_T^T\tilde{K}_o \ , \quad \frac{\partial \dot{U}_T}{\partial \dot{U}_o} = -\dot{\lambda}_T^T M \ . \quad (4.16)$$

The convergence rate of the Newton-Raphson iteration scheme is very high, if the initial approximation is good (e.g., for the linear system one iteration is necessary). In order to obtain the amplitude-frequency relation of a vibrating structure, the excitation frequency is varied in small steps, and the solution obtained at the current frequency value is employed as the initial approximation at the next frequency value.

As the drawback of the Newton-Raphson iteration the comparatively large computational costs for obtaining the derivative matrix at each iteration should be mentioned. However, in the case of local nonlinearities the computational scheme can be considerably economized. If the vector of nonlinear forces is presented as $W(U,\dot{U}) = \begin{bmatrix} 0 \\ W_2(U_2,\dot{U}_2) \end{bmatrix}$, at each numerical integration time point the relations of Chap.3.3 can be employed, where the matrix blocs A_{11}, A_{12}, A_{21} are independent of $U_2,\dot{U}_2$ and therefore are constant during all the integration time. The same values of the matrix blocs are valid for the equation (4.15), too, and the computation of $A_{11}^{-1}A_{12}$ and $A_{21}A_{11}^{-1}A_{12}$ can be carried out as an initial operation.

The computational resource reduction can be obtained, carrying out computations in time domain. So, after the substitution $t^*=T-t$ the vectors $\frac{\partial W_2}{\partial U_2}$ and $\frac{\partial W_2}{\partial \dot{U}_2}$ can be regarded as initial forces. The displacements U as well as the conjugate variables λ are obtained employing the same blocks of the dynamic compliance matrices S^{uo}, S^{uo}, S determined during an initial operation.

The case of unknown vibration period. Investigating the auto-oscillations and the free structural vibration, the period T is to be regarded as an unknown. In this case for carrying out

the Newton-Raphson iteration the derivatives $\frac{\partial U_T}{\partial T}$, $\frac{\partial \dot{U}_T}{\partial T}$ are necessary. Taking on account the relations

$$\delta U(T+\delta T) = \delta U_T + \dot{U}_T \delta T \ , \quad \delta \dot{U}(T+\delta T) = \delta \dot{U}_T + \ddot{U}_T \delta T \ , \quad (4.17)$$

the variational equation similar to (4.8) is obtained as

$$(\lambda_T^T+\mu_T^T)M\delta\dot{U}_T + (\lambda_T^T\tilde{C}-\dot{\lambda}_T^T M+\mu_T^T\tilde{K})\delta U_T - (\lambda_o^T+\mu_o^T)M\delta\dot{U}_o - (\lambda_o^T\tilde{C}-\dot{\lambda}_o^T M+\mu_o^T\tilde{K})\delta U_o +$$

$$+((\lambda_T^T+\mu_T^T)M\ddot{U}_T + (\lambda_T^T\tilde{C}-\dot{\lambda}_T^T M+\mu_T^T\tilde{K})\dot{U}_T)\delta T + \int_o^T (\ddot{\lambda}^T M - \dot{\lambda}^T\tilde{C} + \lambda^T\tilde{K})\delta U \, dt -$$

$$- \int_o^T (\ddot{\mu}^T M - \dot{\mu}^T\tilde{C} + \mu^T\tilde{K})\delta\dot{U} \, dt = 0 \ . \quad (4.18)$$

Substituting the end values (4.11) and (4.13), we obtain the relations

$$\frac{\partial U_T}{\partial T} = \dot{U}_T \ , \quad \frac{\partial \dot{U}_T}{\partial T} = \ddot{U}_T \ . \quad (4.19)$$

4.2 THE WEIGHTED RESIDUAL APPROACH FOR OBTAINING FORCED VIBRATION LAWS

Structural equations with the nonlinear terms. Consider the matrix equation of motion of an elastic structure with nonlinear interaction as (4.1) with the periodic excitation $R(t)=R(t+T)$. The motion law $U(t)$ of the structure during the vibration period is represented as a superposition of a set of some T-periodic time functions as

$$U(t) = N(t)\, U_A \ , \quad (4.20)$$

where $N(t)$ - the matrix containing the time functions, and U_A - the constant vector of the generalized amplitudes of the points of the structure. Substituting (4.20) into (4.1) and weighting

the residual during the period leads us to the nonlinear equation in terms of generalized amplitudes U_A :

$$A\,U_A = \int_0^T N^T W(NU_A, \dot{N}U_A)\,dt + \int_0^T N^T R(t)\,dt \quad , \qquad (4.21)$$

where $A = \int_0^T (N^T M\,\ddot{N} + N^T C\,\dot{N} + N^T K\,N)\,dt$.

The simple iteration scheme for the equation (4.21) is presented as

$$U_A^{i+1} = A^{-1}\left[\int_0^T N^T W(NU_A^i, \dot{N}U_A^i)\,dt + \int_0^T N^T R(t)\,dt\right] . \qquad (4.22)$$

The Newton-Raphson iteration is obtained by presenting the equation (4.21) in increments as

$$A(U_A+\delta U_A) = \int_0^T N^T\left[(W(NU_A, \dot{N}U_A) + \frac{\partial W}{\partial U}\,N\delta U_A + \frac{\partial W}{\partial \dot{U}}\,\dot{N}\delta U_A\,dt + R(t)\right]dt \ . \qquad (4.23)$$

From (4.21) follows the relation

$$U_A^{i+1} = U_A^i + A_T^{-1}(R_A - A\,U_A^i + R_N) \quad , \qquad (4.24)$$

where $A_T = A - \int_0^T N^T \frac{\partial W}{\partial U}\Big|_i N\,dt - \int_0^T N^T \frac{\partial W}{\partial \dot{U}}\Big|_i \dot{N}\,dt$, $R_N = \int_0^T N^T W(NU_A^i, \dot{N}U_A^i)\,dt$, $R_A = \int_0^T N^T R(t)\,dt$,

and the notation $\Big|_i$ means "obtained by substituting the values NU_A^i, $\dot{N}U_A^i$ ".

If the structural nonlinearities are localized in local zones, i.e., if $W(U,\dot{U}) = \begin{pmatrix} 0 \\ W_2(U_2,\dot{U}_2) \end{pmatrix}$, the equation (4.21) is presented as

$$\begin{bmatrix} A_{11} & A_{12} \\ A_{21} & A_{22} \end{bmatrix}\begin{pmatrix} U_{A1} \\ U_{A2} \end{pmatrix} = \begin{pmatrix} 0 \\ \int_0^T N_2^T W_2(N_2U_{A2}, \dot{N}_2U_{A2})\,dt \end{pmatrix} + \begin{pmatrix} \int_0^T N_1^T R(t)\,dt \\ \int_0^T N_2^T R(t)\,dt \end{pmatrix} . \qquad (4.21)'$$

After some manipulation the equation (4.24) has the dimension equal to the length of the nonlinear force vector W_2 and is presented as

$$U_{A2}^{i+1} = U_{A2}^i + \hat{A}_{T22}^{-1}(R_{A2} - A_{21}A_{11}^{-1}R_{A1} - \hat{A}_{22}U_{A2}^i + \hat{R}_{N2}) \quad , \qquad (4.24)'$$

where $\hat{A}_{22} = A_{22} - A_{21}A_{11}^{-1}A_{12}$, $\hat{A}_{T22} = \hat{A}_{22} - \int_0^T N_2^T \frac{\partial W_2}{\partial U_2}\Big|_i N_2\,dt - \int_0^T N_2^T \frac{\partial W_2}{\partial \dot{U}_2}\Big|_i \dot{N}_2\,dt$,

$\hat{R}_{N2} = \int_0^T N_2^T W_2(N_2U_{A2}^i, \dot{N}_2U_{A2}^i)\,dt$, $R_{A1} = \int_0^T N_1^T R(t)\,dt$, $R_{A2} = \int_0^T N_2^T R(t)\,dt$.

Unilaterally constrained structures. We consider the linear structural equation of motion with the constraints

$$\begin{cases} M\,\ddot{U} + C\,\dot{U} + K\,U = R(t) \quad , \\ P\,U \le d \quad . \end{cases} \qquad (4.25)$$

Substituting the relation (4.20) into (4.25) and weighting the residual, we obtain

$$\begin{cases} A\,U_A = R_A \quad , \\ P\,N\,U \le d \quad . \end{cases} \qquad (4.26)$$

The constraints of the system (4.26) must be satisfied at each time point during the vibration period. Introducing the Lagrange multiplier vector $\lambda(t) \ge 0$, we obtain the following equation system

$$\begin{cases} A\,U_A + \int_0^T N^T P^T \lambda\,dt = R_A \quad , \\ P\,N\,U_A = d \quad , \end{cases} \qquad (4.27)$$

where $\lambda(t) = \begin{cases} \lambda(t), & \text{at each time point } t, \text{ where } \lambda(t) \ge 0, \\ 0 \ , & \text{otherwise} \ . \end{cases}$

The physical sense of the conjugate variables $\lambda(t)$ is the normal force of constraints upon a structure. Similar to the

relation (4.20), the time-law $\lambda(t)$ is approximated by a sum of T-periodic functions in the time interval [0,T]:

$$\lambda \cong \hat{N}\,\Lambda \quad . \tag{4.28}$$

We replace the constraint $P\,N\,U_A = d$ at each time point of the interval [0,T] by the projections of this constraint upon a subspace of the same functions, by the superposition of which the time law λ has been approximated:

$$\int_0^T \hat{N}^T P\,N\,dt\,U_A = \int_0^T \hat{N}^T d\,dt \quad . \tag{4.29}$$

Taking account of (4.29), the system (4.27) is presented as

$$\begin{cases} A\,U_A + B^T\Lambda = R_A \quad , \\ B\,U_A = D \quad . \end{cases} \tag{4.30}$$

where $B = \int_0^T \hat{N}^T P\,N\,dt$, $D = \int_0^T \hat{N}^T d\,dt$.

Expressing Λ from the system (4.30), we obtain

$$\Lambda = (BA^{-1}B^T)^{-1}(BA^{-1}R_A - D) \quad .$$

The time law $\lambda(t)$ during the period is approximated by the relation (4.28), and at some time points it may occur that $\lambda<0$, causing the negative normal interaction forces. In order to exclude these negative values, the constraints shouldn't be considered at the negative values of λ . Therefore we regard the rows of the constraint matrix as the time functions $P = P(t)$, and prescribe them the zero values at the time points when the corresponding elements of the vector λ are obtained negative from the relation (4.28).

In general, the contact forces are obtained employing the following algorithm.

Algorithm 4.1

1. $P^0(t) = P = \text{const}$, $i = 0$.
2. $B^i = \int_0^T \hat{N}^T P^i N\,dt$,
3. $\Lambda^i = (B^i A^{-1} B^{iT})^{-1}(B^i A^{-1} R_A - D)$,
4. $\lambda^i = \hat{N}\,\Lambda^i$,
5. For each row P_j of the matrix P, $j=1,2,\ldots$, obtain

$$P_j^{i+1} = \begin{cases} P_j^i(t) \text{ for all time points } t, \text{ where } \lambda_j(t) \geq 0 \ , \\ 0 \ , \text{ otherwise} \quad . \end{cases}$$

6. If P^{i+1} coincides with P^i , end of the algorithm; Otherwise $i=i+1$ and go to step 2.

With the known values of $\lambda(t)$, the generalized amplitude vector is determined by the relation

$$U_A = A^{-1}(R_A - B^T\Lambda) \quad . \tag{4.31}$$

Structures with normal and tangential constraints. We consider a linear structural equation of motion with the constraints

$$\begin{cases} M\ddot{U} + C\dot{U} + K\,U = R(t) \ , \\ P_N U \leq d \ , \\ P_T \dot{U} = 0 \ , \end{cases} \tag{4.32}$$

where the pairs of the corresponding rows of the matrices P_N, P_T impose the normal and tangential constraints upon the displacements of the structure points. The tangential constraint is to be regarded only when the corresponding normal constraint is active, i.e., if it is satisfied as an equality. Moreover, the magnitude of a tangential force μ_j can't exceed its critical value $\mu_j \leq k_f\,\lambda_j$, determined by the magnitude of the corresponding normal force λ_j and the Coulomb friction coefficient k_f . The equation system similar to (4.27) appears as

$$\begin{cases} A\,U_A + \int_0^T N^T \hat{P}_N^T \lambda\, dt + \int_0^T \dot{N}^T \hat{P}_T^T \mu\, dt = R_A \ , \\ P_N N\, U_A = d \ , \\ \hat{P}_T \dot{N}\, U_A = 0 \ , \end{cases} \qquad (4.33)$$

where the normal force is determined as

$$\lambda(t) = \begin{cases} \lambda(t), \text{ at each time point } t, \text{ where } \lambda(t) \geq 0, \\ 0 \ , \text{ otherwise} \ , \end{cases}$$

and the tangential force is determined as

$$\dot{\mu}(t) = \begin{cases} \dot{\mu}(t), \text{ at each time point } t, \text{ where } |\dot{\mu}(t)| \leq k_f \lambda(t), \\ k_f \lambda(t) \operatorname{sign} \dot{\mu}(t), \text{ otherwise} \ . \end{cases}$$

The matrices $\hat{P}_N$, $\hat{P}_T$ are obtained from the matrices P_N, P_T as follows. The matrix $\hat{P}_N$ is the matrix P_N, each j-th row P_{Nj} of which is replaced by the row $(P_{Nj} + k_f P_{Tj} \operatorname{sign} \dot{\mu}_j)$ at the time points, when sliding in the j-th contact pair occurs. The matrix $\hat{P}_T$ is the matrix P_T, each j-th row of which is replaced by zero at the time points, when sliding in the j-th contact pair occurs. The time laws $\lambda(t)$, $\mu(t)$ are approximated by

$$\lambda = \hat{N}\,\Lambda \ , \qquad \mu = \hat{N}\,M \ . \qquad (4.34)$$

Assuming the notations

$$\bar{\bar{P}} = \begin{bmatrix} \hat{P}_N & 0 \\ 0 & \hat{P}_T \end{bmatrix}, \ \bar{P} = \begin{bmatrix} P_N & 0 \\ 0 & \hat{P}_T \end{bmatrix}, \ \bar{N} = \begin{bmatrix} N \\ \dot{N} \end{bmatrix}, \ \bar{\bar{N}} = \begin{bmatrix} \hat{N} \\ \dot{\hat{N}} \end{bmatrix}, \ \bar{\Lambda} = \begin{bmatrix} \Lambda \\ M \end{bmatrix}, \ \bar{D} = \begin{bmatrix} D \\ 0 \end{bmatrix},$$

the system (4.33) is presented as

$$\begin{cases} A\,U_A + \int_0^T \bar{N}^T \bar{\bar{P}}^T \bar{\bar{N}}\, \Lambda dt = R_A \ , \\ \bar{P}\,\bar{N}\,U_A = \bar{D} \ . \end{cases} \qquad (4.35)$$

In general, the values of the contact forces are obtained by the following algorithm.

Algorithm 4.2

1. $P_N^0(t) = P_N = \text{const}$, $P_T^0(t) = P_T = \text{const}$, $i = 0$.

2. $\bar{B}^i = \int_0^T \bar{N}^T \bar{P}^i \bar{N}\, dt$, $\bar{\bar{B}}^i = \int_0^T \bar{\bar{N}}^T \bar{\bar{P}}^i \bar{N}\, dt$,

3. $\bar{\Lambda}^i = (\bar{B}^i A^{-1} \bar{\bar{B}}^{iT})^{-1} (\bar{B}^i A^{-1} R_A - \bar{D})$,

4. $\lambda^i = \hat{N}\,\Lambda^i$, $\mu^i = \hat{N}\,M^i$,

5. For each row P_{Nj} of the matrix P_N, $j = 1, 2, \ldots$, obtain

$$P_{Nj}^{i+1} = \begin{cases} P_{Nj}^i(t) \text{ at all time points } t, \text{ where } \lambda_j(t) \geq 0 \ , \\ 0 \ , \text{ otherwise} \ . \end{cases}$$

6. If P_N^{i+1} coincides with P_N^i , go to step 7.
Otherwise assume $i = i+1$ and go to step 2.

7. Transform all the rows of the matrices P_N^i , P_T^i as follows:
$\hat{P}_{Nj}^{i+1}(t) = k_f P_{Tj}^i(t) + P_{Nj}^i(t)$, $\hat{P}_{Tj}^{i+1}(t) = 0$, at time points t , where $|\dot{\mu}_j(t)| \leq k_f\, \lambda_j(t)$. At the other time points don't change the rows P_{Nj}^i , P_{Tj}^i .

8. If there exists at least one pair of rows P_{Nj}^i , P_{Tj}^i transformed at step 7 , increment $i = i+1$ and go to step 2.
Otherwise - end of the algorithm.

Analysis in frequency domain employing the harmonic balance techniques is may be considered as a special case of the weighted residual approach. The harmonic functions are employed as weighting functions $N(t)$, $\hat{N}(t)$

$$N(t)= [\ I\ I\cos\omega t\ \ I\sin\omega t\ \ I\cos 2\omega t\ \ I\sin 2\omega t\ \dots\ ]\ ,$$

$$\hat{N}(t)= [\ \hat{I}\ \hat{I}\cos\omega t\ \ \hat{I}\sin\omega t\ \ \hat{I}\cos 2\omega t\ \ \hat{I}\sin 2\omega t\ \dots\ ]\ ,$$

where I - unity matrix of the dimension equal to the length of the vector U, $\hat{I}$ - unity matrix of the dimension equal to the number of constraints, i.e., to the number of rows of the matrix P, and $T=\frac{2\pi}{\omega}$. The generalized amplitude vector consists of the sine and cosine Fourier amplitudes $U_A=\left[U^0,U_c^1,U_s^1,U_c^2,U_s^2,\dots\right]^T$, the harmonic balance method relations being presented in the Appendix 3.1.

Finite element approach in time domain is obtained by dividing the interval $[0,T]$ into m finite elements each of the length $\frac{T}{m}$. When employing the second order elements with three nodes, the generalized amplitude vector on the i-th element is presented as

$$U = N\,U_A^i = \left[\ I\,N_0\ ,\ I\,N_1\ ,\ I\,N_2\ \right]\begin{bmatrix} U_{2i-1} \\ U_{2i} \\ U_{2i+1} \end{bmatrix}\ ,$$

where $N_0=\frac{\xi(\xi-1)}{2}$, $N_1=-(\xi-1)(\xi+1)$, $N_2=\frac{\xi(\xi+1)}{2}$, $\xi=\frac{t}{T}$.

During each iteration the matrices for the whole time interval $[0,T]$ are obtained according to the global finite element matrix assembling rules, imposing the periodic motion condition as $U_1=U_{2m+1}$. The global generalized amplitude vector is

$$U_A = \left[\ U_1,U_2,U_3,\dots,U_{2m}\right]^T\ .$$

4.3 TRANSIENT AND STATIONARY ANALYSIS OF NONLINEAR VIBRATION WITH SLOW VARYING AMPLITUDES

Employing the time-averaging techniques. Consider the matrix equation of motion of an elastic structure with the nonlinear interaction as (4.1) with the periodic excitation $R(t)=R(t+T)$. We present the displacements and forces as truncated Fourier series as

$$U(t) \cong \sum_{k=1}^{p} U_c^k\cos(k-1)\omega t + U_s^k\sin(k-1)\omega t\ ,$$

$$R(t) \cong \sum_{k=1}^{p} R_c^k\cos(k-1)\omega t + R_s^k\sin(k-1)\omega t\ , \qquad (4.36)$$

$$W(t) = \sum_{k=1}^{p} W_c^k\cos(k-1)\omega t + W_s^k\sin(k-1)\omega t\ ,$$

where according to the definition $U_s^1=R_s^1=W_s^1=0$, and $\omega=\frac{2\pi}{T}$. Employing the averaging in time techniques [98], we consider the amplitudes U_c^k, U_s^k, $k=\overline{1,p}$ as time functions. Moreover, we require that the expressions of the velocities should be presented in the same form as in the case of the stationary amplitudes:

$$\dot{U}(t) = \sum_{k=1}^{p} -U_c^k(k-1)\omega\,\sin(k-1)\omega t + U_s^k(k-1)\omega\,\cos(k-1)\omega t\ , \qquad (4.37)$$

In reality U_c^k, U_s^k are time functions, therefore it is necessary to take account upon this circumstance when differentiating in time. The form of the relation (4.37) assumes satisfying the relations

$$\dot{U}_c^k\cos(k-1)\omega t + \dot{U}_s^k\sin(k-1)\omega t = 0\ ,\ k=\overline{1,p}\ . \qquad (4.38)$$

Differentiating (4.37) in time, we obtain

$$\ddot{U}(t) = \sum_{k=1}^{p}\Big[\ -U_c^k(k-1^2)\omega^2\cos(k-1)\omega t - U_s^k(k-1)^2\omega^2\sin(k-1)\omega t -$$

$$-\dot{U}_c^k(k-1)\omega\,\sin(k-1)\omega t + \dot{U}_s^k(k-1)\omega\,\cos(k-1)\omega t\ \Big]\ . \qquad (4.39)$$

Substituting (4.36)-(4.39) into (4.1), and averaging during the time interval [0, T], after some manipulation we obtain the equation of motion in terms of slow varying amplitudes as

$$\begin{bmatrix} 0 & & & & \\ 2\omega M & 0 & & & \\ 0 & 2\omega M & & & \\ & \ddots & \ddots & & \\ & & 2(p-1)\omega M & 0 & \\ & & 0 & 2(p-1)\omega M & \end{bmatrix} \begin{Bmatrix} \dot{U}^0_c \\ \dot{U}^1_c \\ \dot{U}^1_s \\ \vdots \\ \dot{U}^p_c \\ \dot{U}^p_s \end{Bmatrix} =$$

$$= \begin{bmatrix} -K & & & & \\ -\omega C & K-\omega^2 M & & & \\ -K+\omega^2 M & -\omega C & & & \\ & \ddots & \ddots & & \\ & & -(p-1)\omega C & K-\omega^2(p-1)^2 M & \\ & & -K+\omega^2(p-1)^2 M & -(p-1)\omega C & \end{bmatrix} \begin{Bmatrix} U^0_c \\ U^1_c \\ U^1_s \\ \vdots \\ U^p_c \\ U^p_s \end{Bmatrix} + \begin{Bmatrix} W^0_c \\ -W^1_s \\ W^1_c \\ \vdots \\ -W^p_s \\ W^p_c \end{Bmatrix} = \begin{Bmatrix} R^0_c \\ -R^1_s \\ R^1_c \\ \vdots \\ -R^p_s \\ R^p_c \end{Bmatrix} . \qquad (4.40)$$

Matrices in the equation (4.40) are block-diagonal. With no nonlinearities present ($W \equiv 0$) , the equation (4.40) decomposes into k independent equations, each of which enables to obtain the corresponding Fourier amplitudes. If the nonlinearities are present, it is necessary to solve the equation (4.40) of the dimension $2(p-1)n \times 2(p-1)$.

If the nonlinear interaction forces are concentrated in the localized points or zones of the structure, the vectors and matrices can be represented in the block form, where blocks correspond to the linear and nonlinear parts of the structure. The matrix inverse and other block operations corresponding to the linear part of the structure are carried out during an initial operation. As a result, during each iteration the nonlinear matrix equation of dimension $2(p-1)n_2 \times 2(p-1)n_2$ is to be considered, where n_2 – the number of the nonlinear degrees of freedom.

If the simple iteration scheme for solving the nonlinear equation at each numerical integration step doesn't converge, the Newton-Raphson iteration is necessary. In this case at each

iteration the derivative matrix $\frac{\partial W_A}{\partial U_A}$ is to be determined employing the relations of the Appendix 3.2.

In the case of ill-conditioned stiffness matrix ,i.e., if rigid body motions of the structure are possible, the system (4.40) can't be solved, because at the very first iteration it is necessary to invert the matrix K . As a rescue from this situation the equivalent transformation of the matrix K and of the nonlinear term W can be accomplished by presenting the left upper block of the equation (4.40) as

$$0 = -\hat{K}\, U^0_c + \hat{W}^0_c + R^0_c \quad , \qquad (4.40)'$$

where $\hat{K} = K + \max_{i,j} |k_{ij}|\, I$, $\hat{W}^0_c = W^0_c + \max_{i,j} |k_{ij}|\, U^0_c$, with the nonsingular matrix $\hat{K}$.

The dynamics of rigid-body displacements of a structure can be taken into account by presenting the equation (4.40)' as

$$M\, \ddot{U}^0_c + C\, \dot{U}^0_c = -K\, U^0_c + W^0_c + R^0_c \quad , \qquad (4.40)''$$

that coincides with the initial equation (4.1). However, in this case the implicit unconditionally stable numerical integration scheme must be adopted, because otherwise the presence of the equation (4.40)" prohibits the time integration steps exceeding the shortest natural vibration period of the linear part of the structure (see Chap.2).

For obtaining stationary vibration laws the left-hand side of the equation (4.40) is assumed to be zero. The derivative matrix necessary for applying the Newton-Raphson iteration to the obtained nonlinear algebraic equation is presented by means of the same relations of the Appendix 3.2, as in the case of averaged equations of motion.

The case of unilaterally constrained structures. The dynamic reduction of an elastic structure with unilateral constraints is carried out by truncating the dynamic contributions of the higher modes of the linear part of the structure (see Chap.1). In

general, when the normal and tangential constraints are present, the Lagrange multiplier values λ_N , λ_T are obtained from the relation (1.50), Chap.1. In this case the equivalent nonlinear force

$$W(z_i) = -\Delta_i^T \bar{\bar{P}} \left(\bar{P} S_k \bar{\bar{P}}^T \right)^{-1} \left(\bar{P} \Delta_i z_i + \bar{P} S_k R - d_o \right) . \qquad (4.41)$$

is to be regarded.

If the time law $z_i(t)$ is known, the value $W(z_i)$ is to be determined according to the Algorithm 1.1 of Chap.1. As a result, the matrices $\bar{P}$, $\bar{\bar{P}}$ acquire the predetermined values at each time point, i.e., they can be regarded as time functions and employed in order to determine the derivative

$$\frac{\partial W}{\partial z_i} = -\Delta_i^T \bar{\bar{P}} \left(\bar{P} S_k \bar{\bar{P}}^T \right)^{-1} \bar{P} \Delta_i \qquad (4.42)$$

at each time point. Further the relation (4.42) is employed in place of $\frac{\partial W}{\partial U}$, that in its turn is employed when obtaining $\frac{\partial W}{\partial U_A}$ (see Appendix 3.2).

4.4 STABILITY ANALYSIS OF THE VIBRATION LAWS

Linearization of equations of motion at the solution point. The stationary motion laws obtained by integrating the equations of motion numerically until the end of transient vibrations, are always stable. However, among the motion laws obtained by solving a boundary value problem in time domain (Chap.4.1) and by employing the weighted residual approach (Chap.4.2) may appear unstable ones.

The stability of stationary motion laws of nonlinear mechanical systems is usually investigated considering the equations of motion linearized at the solution point. Assume, that the equation of motion is presented as (4.1) and a stationary solution $U^*(t) = U^*(t+T)$ is obtained, the period T of which coincides with the period of the exciting force $R(t)=R(t+T)$. In this case the linearized equation for investigating the stability of the solution $U^*(t)$ is obtained as

$$M \ddot{X} + \tilde{C}(t) \dot{X} + \tilde{K}(t) X = 0 , \qquad (4.43)$$

where $\tilde{K}(t) = K - \frac{\partial W}{\partial U}\Big|_{U^*(t)}$ and $\tilde{C}(t) = C - \frac{\partial W}{\partial \dot{U}}\Big|_{U^*(t)}$ are the time functions.

Consider the equation of motion with unilateral constraints

$$\begin{cases} M \ddot{U} + C \dot{U} + K U = R(t) , & (4.44a) \\ P U \le d_o , & (4.44b) \\ \text{and if the constraints (4.44b) are satisfied as equality (i.e., if they are active) there are considered the auxiliary constraints} & (4.44) \\ {}^{(k)}P \dot{U} = 0 , \; k = \overline{1,m} . & (4.44c) \end{cases}$$

Considering $U^*(t)$ as a T-periodic solution of this equation, the linearized equation for investigating the stability of the motion law $U^*(t)$ appears as

$$\begin{cases} M \ddot{X} + C \dot{X} + K X = 0 , & (4.45a) \\ \text{and at the time points when the equality} \\ P U^*(t) = d_o , \\ \text{is satisfied, consider the constraints} & (4.45) \\ P X = 0 , & (4.45b) \\ {}^{(k)}P \dot{X} = 0 , \; k = \overline{1,m} . & (4.45c) \end{cases}$$

The numerical integration of the system (4.45) is carried out by employing the approaches presented in Chap. 3.4 - 3.6 with the only difference that the activity or nonactivity of the constraints is predetermined at each time point by substitution of the solution $U^*(t)$ into (4.44b). Therefore the system (4.45) can be regarded as the system with periodic coefficients.

Applying the dynamic reduction techniques of the unilaterally constrained structures by truncating the higher mode dynamic contributions of the linear part, we obtain the relation (see Chap.1)

$$\lambda(z_i, \dot{z}_i) = A^{-1} (P \Delta_i z_i + B_i A^{-1} P \Delta_i \dot{z}_i) . \qquad (1.43)$$

Presenting the contact forces in the form of the nonlinear function $W(z_i, \dot{z}_i) = -\Delta_i^T P^T \lambda$, at all the time points where $\lambda > 0$ the following relations can be obtained

$$\frac{\partial W}{\partial z_i} = -\Delta_i^T P^T A^{-1} P \Delta_i \ , \qquad \frac{\partial W}{\partial \dot{z}_i} = -\Delta_i^T P^T A^{-1} B_i A^{-1} P \Delta_i \ , \qquad (4.46)$$

At the remaining time points (i.e., where $\lambda < 0$) , the relations $\frac{\partial W}{\partial z_i} = \frac{\partial W}{\partial \dot{z}_i} = 0$ are assumed. The time functions (4.46) are employed in order to obtain the time-dependent stiffness and damping matrices of the system (4.43).

The transfer matrices $Q_{2n \times 2n}$ are obtained by integrating numerically the linearized system (4.43) or (4.45) with T-periodic coefficients during the time interval [0, T] with the following initial values at the time point t=0 :

for $j \le n$, $x_j(0)=1$, $x_i(0)=0$, $i=\overline{1,n}$, $i \ne j$,

$$\dot{x}_i(0)=0, \quad i=\overline{1,n} \ ,$$

for $j > n$, $\dot{x}_{j-n}(0)=1$, $\dot{x}_i(0)=0$, $i=\overline{1,n}$, $i \ne j$,

$$x_i(0)=0, \quad i=\overline{1,n} \ .$$

The j-th column of the transfer matrix presents the solution $\begin{pmatrix} X \\ \dot{X} \end{pmatrix}$ of the system (4.43) or (4.45) at the time point t=T .

The characteristic equation of the system (4.43) or (4.45) of dimension 2nx2n is

$$\det \left[Q - \rho I \right] = 0 \ . \qquad (4.47)$$

After obtaining the roots of the characteristic equation (4.47), the stability or instability of the motion law of the initial nonlinear system is determined employing the well-known Liapunov's theorems :

1. If the absolute values of all the roots ρ of the characteristic equation (4.47) are less than unity, the motion

law is stable irrespectively of the higher order infinitesimal terms.

2. If among the roots of the characteristic equation (4.47) there is one exceeding unity by its absolute value, the motion law is unstable irrespectively of the higher order infinitesimal terms.

If among the roots of the characteristic equation (4.47) there are some equal to unity, the necessary condition for stability is that they should be simple or have simple elementary dividers.

The Hill's generalized determinant techniques present the solution of the linearized equation as

$$X(t) \cong e^{ht} \sum_{k=1}^{p} X_c^k \cos(k-1)\omega t + X_s^k \sin(k-1)\omega t \ . \qquad (4.48)$$

The time functions $\tilde{K}^*(t)$, $\tilde{C}^*(t)$ are obtained by substituting (4.48) into (4.43). Equating the coefficients at the sine and cosine functions correspondingly, the equation for determining the characteristic indices is obtained as [82]

$$\det \left[Y(\omega) - h I \right] = 0 \ , \qquad (4.49)$$

where $\omega = \frac{2\pi}{T}$.

The presence of at least one positive characteristic index h>0 indicates the instability of the solution of the original equation. The Hill's determinant method is preferable for investigating the stability of the systems with parametric excitation, because the equation

$$\det \left[Y(\omega) \right] = 0 \ , \qquad (4.50)$$

enables to obtain the borders of the stability region for the T-periodic solution. Having in mind that the values of the elements of the matrix Y depend upon the parameters of the system, the parameter values are obtained by solving the equation (4.50) for the different values of ω . For investigating the stability of stationary motion laws of a nonlinear system, the Hill's determinant techniques don't possess any advantages in

comparison with the transfer matrix approach, because the dimension of the equation (4.49) isn't lower than the dimension of the equation (4.47).

Investigation of stability by employing averaged equations. Having obtained the stationary motion laws by the weighted residual approach, it appears reasonable to employ the stability investigation methods, taking account for the assumptions employed by obtaining the motion laws.

Assume, that the small perturbations don't change the presentation form of the solution in the subspace of basic functions, but only influents slightly the values of the generalized amplitudes. Employing the harmonic functions as a basis and presenting the nonlinear term $W(U,\dot{U})$ as well as the motion law in the form of truncated Fourier series, the time-averaging approach produces the following differential equation (4.40) in terms of slow varying amplitudes

$$B\,\dot{U}_A = A\,U_A + W_A + R_A \quad . \qquad (4.40)'$$

Denoting the stationary solution as $U_A^*(t) = U_A^* = \text{const}$, the linearized equation for investigating the stability of this solution is obtained as

$$\dot{X}_A = B^{-1}\left(A + \frac{\partial W_A}{\partial U_A}\bigg|_{U_A^*} \right) X_A \quad . \qquad (4.51)$$

The derivative $\frac{\partial W_A}{\partial U_A}$ in (4.51) is defined using the relations of the Appendix 3.2. The inversion of the matrix B isn't a time-consuming operation because of its block-diagonal form, and in the case of a diagonal mass matrix it is trivial. The coefficients of the equation (4.51) are constant, and for the stability investigation it is enough to evaluate the signs of the roots of the characteristic equation employing the Routh-Hurwitz criterion.

It appears worth to mention, that in the case of the stationary motion law obtained by integrating the time-averaged equation (4.40)' in the "slow" time from some initial values $U_A(0)$ until the stationary value U_A^* , the stability of such

motion is ensured. However, the stability concept here has its approximate meaning, because the solution U_A^* itself is approximate.

Simplified stability test employing energy criterion. The nonlinear system stationary motion law investigation methods presented above require a considerable computational effort for obtaining the transfer matrices as well as for solving an eigenproblem of large dimension, or for obtaining the coefficients of a linearized equation and determinant values when employing the Routh-Hurwitz criterion. If the number of degrees of freedom is large, the time-consuming computations at the stability investigation stage may appear as prohibitive. However, the approximate stability investigation can be carried out by evaluating the change of the amounts of work done by external and internal forces during one oscillation period when the generalized amplitudes or the initial conditions are perturbed. Such an approach was employed in [91].

The difference between the amounts of work done by the external and internal forces during one vibration period equals

$$A = A_i - A_e \quad , \qquad (4.52)$$

where A_i - the work of internal forces, A_e - the work of external forces.

In the case of the stationary motion law $U^*(t)$, obviously, $A=0$, because the balance between the amounts of work done by the external and internal forces is the basic feature of the dynamic equilibrium of the mechanical system. A small perturbation of the motion law leads to an increase of the internal force work (i.e., the increase of dissipation), and $A>0$ is obtained.

Assume that the stationary motion law defined by the values $U(0)$, $\dot{U}(0)$ at the begin of each excitation period has been obtained by solving the boundary value problem in time domain. Integrating the equations of motion in time, the motion law satisfying the condition $U(T)=U(0)$, $\dot{U}(T)=\dot{U}(0)$ is obtained. The time law of the $U(t)$ being known, we consider the nonlinear function $W(U(t),\dot{U}(t))$ as the time function $W(t)$, and the equation (4.1) is considered as a linear one with the periodic excitation $R(t)+W(t)$. The difference between the amounts of work

(4.52) is presented as

$$A = \int_0^T \dot{U}^T(t)\left[M\ddot{U} + C\dot{U} + KU - W(t) - R(t) \right] . \quad (4.53)$$

In order to evaluate A for the perturbed initial values $\hat{U}(0)$, $\hat{\dot{U}}(0)$, it is necessary to integrate the equation (4.1) from these initial values during the vibration period $[0,T]$, and to substitute the obtained motion law $\hat{U}(t)$ into the relation (4.53). However, it remains unclear what kind of perturbation should be made upon the initial values. E.g., we can choose the perturbation

$$\hat{U}(0) = (1 + \varepsilon_1)\, U(0) \quad ,$$
$$\hat{\dot{U}}(0) = (1 + \varepsilon_2)\, \dot{U}(0) \quad . \quad (4.54)$$

If the value $A > 0$ is obtained, it doesn't guarantee the stability of the motion law. However, the value $A > 0$ obtained at several different perturbations, allows to expect the stability. The value $A<0$, obtained at any perturbation, shows the instability of the motion law.

Assume, that the stationary motion law has been obtained in terms of generalized amplitudes U_c^k, U_s^k, $k = \overline{1,p}$. Substituting the time laws $U(t) \cong \sum_{k=1}^{p} U_c^k \cos(k-1)\omega t + U_s^k \sin(k-1)\omega t$ into the expression $W(U, \dot{U})$ and expanding the obtained time law as a truncated Fourier series, we obtain the amplitudes W_c^k, W_s^k. Considering W_c^k, W_s^k, R_c^k, R_s^k as a polyharmonic excitation, substituting it into the equation (4.53) and obtaining the integral value, we express the difference between the amounts of work as

$$A = \sum_{k=1}^{p} \Big[\pi(k-1)^2\omega\, (U_c^{kT} C\, U_c^k + U_s^{kT} C\, U_s^k) -$$
$$-(k-1)\pi (U_s^{kT}(R_c^k + W_c^k) + U_c^{kT}(R_s^k + W_s^k)) \Big] . \quad (4.55)$$

The relation (4.55) is obtained, taking account for the

symmetry of the matrices K and M. It is employed for evaluating the difference between the amounts of work done by external and internal forces after a small perturbation of the amplitudes of single or several harmonic components as

$$\hat{U}_c^k = (1 + \varepsilon_1)\, U_c^k \quad ,$$
$$\hat{U}_s^k = (1 + \varepsilon_2)\, U_s^k \quad . \quad (4.56)$$

where U_c^k, U_s^k - amplitudes of a stationary motion law, ensuring $A=0$, and $\hat{U}_c^k$, $\hat{U}_s^k$ - amplitudes of the perturbed motion law.

5. MOTION CONTROL OF ELASTIC STRUCTURES

There are two alternative approaches for obtaining programmed control laws. The first one is based upon a target function minimization considering the excitation forces as parameters and solving an optimal control problem with the fixed or varying time. The other approach employs a presentation of structural dynamic equations in modal coordinates with truncated dynamic contributions of higher modes. The number of coordinates with retained dynamic contributions is selected in order to obtain a unique solution of the problem.

A linear closed-loop control with the displacement and velocity feedback is obtained by employing the inverse dynamic problem approach, the prescribed motion of a structure being expressed as a superposition of exponent functions. In most cases a solution isn't unique, and approximation errors are minimized employing the generalized matrix inverse or representing a problem in a subspace of modal coordinates.

A structural motion control synthesis employing logical elements in a feedback circuit is carried out by resolving the dynamic equations into modal components and employing a separate feedback for each of them.

The excitation laws ensuring the prescribed resonant vibration patterns of structural nodes are obtained by solving the inverse dynamic or optimization problems.

The original results presented in this chapter consist of the development of programmed and closed-loop control synthesis techniques based upon the inverse dynamic problem and dynamic contribution truncation approach. The method is applied to the motion control synthesis of structures with the logical feedback circuit.

5.1 FIXED AND VARYING TIME OPTIMAL CONTROL

Gradients of target function. We consider the equations of motion of an elastic structure as

$$M\ddot{U} + C\dot{U} + K U = W (U, \dot{U}, p) + R f , \qquad (5.1)$$

where M, C, K_{nxn} - structural matrices of an elastic structure, U_{nx1} - displacement vector, W_{nx1} - nonlinear function, p_{lx1} - parameter vector, R_{nxm} - constant transformation matrix of an input vector f_{mx1} into a nodal force vector. It is necessary to obtain an input law f and the values of parameters p minimizing the functional

$$\mathcal{J} = \varphi (U_T, \dot{U}_T) + \int_0^T \psi (U, \dot{U}, p) dt , \qquad (5.2)$$

defined upon the time interval $[0,T]$. The values at the end of the interval are denoted through U_T, $\dot{U}_T$. If the control time T is prescribed, the relations (5.1), (5.2) represent a fixed time optimal control problem, otherwise a varying time optimal control problem is obtained. The maximum speed problem is obtained by solving a varying time problem and assuming $\psi \equiv 1$.

The equation (5.1) may represent a programmed control system as well as a closed-loop one. In the last case a proper choice of parameters p enables to optimize a feedback circuit according to the criteria defined by the functional $\mathcal{J}$.

In order to obtain the optimality condition we employ the Pontriagin's maximum principle [130,115]. Assume the initial approximations of the values of $f(t)$, p, T and the corresponding motion laws $U(t)$, $\dot{U}(t)$ known. Assume δf, δp, δT being infinitesimal variations of the vectors of input laws, parameters and the control time correspondingly causing the variations $h(t)$, $\dot{h}(t)$ of the motion law. Substituting the values $f+\delta f$, $p+\delta p$, $T+\delta T$, $U+h$, $\dot{U}+\dot{h}$ into the relation (5.2), we express a variation of the functional as

$$\delta\mathcal{J} = \varphi_{U_T} \delta U_T + \varphi_{\dot{U}_T} \delta\dot{U}_T + \psi(U_T, \dot{U}_T, p)\delta T + \int_0^T (\psi_U h + \psi_{\dot{U}} \dot{h} + \psi_p \delta p) dt . \qquad (5.3)$$

Except the variations of the independent quantities δf, δp, δT the relation (5.3) contains variations h, $\dot{h}$ of the motion law that can be expressed through δf, δp, δT employing the equation (5.1). In order to obtain this relation the conjugate vectors $\lambda(t)$, $\mu(t)$ are introduced. Multiplying the equation (5.1) by λ^T

and by $\dot{\mu}^T$ from the left-hand side and integrating during the time interval [0,T] we obtain

$$\begin{cases} \int_0^T (\lambda^T M\ddot{U} + \lambda^T C\dot{U} + \lambda^T KU)dt = \int_0^T \lambda^T W(U,\dot{U},p)dt + \int_0^T \lambda^T R\, f\, dt\ , \\ \int_0^T (\dot{\mu}^T M\ddot{U} + \dot{\mu}^T C\dot{U} + \dot{\mu}^T KU)dt = \int_0^T \dot{\mu}^T W(U,\dot{U},p)dt + \int_0^T \dot{\mu}^T R\, f\, dt\ . \end{cases} \tag{5.4}$$

Replacing the right- and left-hand sides of the equation (5.4) by their first variations, we obtain

$$\begin{cases} \lambda_T^T(M\,\ddot{U}_T + C\,\dot{U}_T + K\,U_T - W(U_T,\dot{U}_T,p) - R\,f_T)\,\delta T + \\ \qquad \int_0^T \lambda^T(M\ddot{h} + \tilde{C}\dot{h} + \tilde{K}h)dt = \int_0^T \lambda^T\left(\frac{\partial W}{\partial p}\,\delta p + R\,\delta f\right)dt\ , \\ \dot{\mu}_T^T(M\,\ddot{U}_T + C\,\dot{U}_T + K\,U_T - W(U_T,\dot{U}_T,p) - R\,f_T)\,\delta T + \\ \qquad \int_0^T \dot{\mu}^T(M\ddot{h} + \tilde{C}\dot{h} + \tilde{K}h)dt = \int_0^T \dot{\mu}^T\left(\frac{\partial W}{\partial p}\,\delta p + R\,\delta f\right)dt\ , \end{cases} \tag{5.5}$$

where $\tilde{K} = K - \frac{\partial W}{\partial U}$, $\tilde{C} = C - \frac{\partial W}{\partial \dot{U}}$.

Integrating by parts the integrals in the equation (5.5), after some manipulation we express the values of h_T, $\dot{h}_T$ through δU_T, $\delta \dot{U}_T$ as

$$\delta U_T = h_T + \dot{U}_T \delta T\ ,\quad \delta \dot{U}_T = \dot{h}_T + \ddot{U}_T \delta T\ . \tag{5.6}$$

Substituting (5.6) into (5.5), we obtain

$$(\lambda_T^T + \dot{\mu}_T^T)(C\dot{U}_T + KU_T - W(U_T,\dot{U}_T,p) - Rf_T)\delta T + (\dot{\lambda}_T^T M - \lambda_T^T \tilde{C}_T - \mu_T^T \tilde{K}_T)\dot{U}_T \delta T +$$

$$+ (\lambda_T^T + \dot{\mu}_T^T)M\delta\dot{U}_T - (\dot{\lambda}_T^T M - \lambda_T^T \tilde{C}_T - \mu_T^T \tilde{K}_T)\delta U_T + \int_0^T (\ddot{\lambda}^T M - \dot{\lambda}^T \tilde{C} + \lambda^T \tilde{K})h dt -$$

$$- \int_0^T (\ddot{\mu}^T M - \dot{\mu}^T \tilde{C} + \mu^T \tilde{K})h dt - \int_0^T (\lambda^T + \dot{\mu}^T)\left(\frac{\partial W}{\partial p}\,\delta p + R\,\delta f\right)dt = 0\ . \tag{5.7}$$

The relation (5.7) doesn't contain the values of any quantities at the time point t=0, because the initial values are assumed to be prescribed and, consequently, $h(0)=\dot{h}(0)=\delta U_o=\delta \dot{U}_o=0$. Comparing the relations (5.3) and (5.7), we require the following conjugate equations to be satisfied :

$$\begin{cases} M\,\ddot{\lambda} - \tilde{C}^T\dot{\lambda} + \tilde{K}^T\lambda = \psi_U^T\ , \\ M\,\ddot{\mu} - \tilde{C}^T\dot{\mu} + \tilde{K}^T\mu = \psi_U^T\ , \end{cases} \tag{5.8}$$

their end values at the time point t=T being obtained from the algebraic equation system

$$\begin{cases} M\,\dot{\lambda}_T - \tilde{C}_T^T\lambda_T - \tilde{K}_T^T\mu_T = -\varphi_{U_T}^T\ , \\ M\,(\lambda_T + \dot{\mu}_T) = \varphi_{U_T}^T\ . \end{cases} \tag{5.9}$$

As the number of unknowns in the system (5.9) exceeds the number of equations, the end values of the system (5.8) can be determined as

$$\lambda_T = \mu_T = 0,\ \dot{\lambda}_T = M^{-1}\varphi_{U_T}^T\ ,\ \dot{\mu}_T = M^{-1}\varphi_{U_T}^T\ . \tag{5.9}'$$

Regarding the relations (5.8), (5.9)', we express the variation of the functional (5.3) as

$$\delta\mathcal{J} = \int_0^T \left(\frac{\partial \mathcal{J}}{\partial f}\,\delta f + \frac{\partial \mathcal{J}}{\partial p}\,\delta p\right)dt + \frac{\partial \mathcal{J}}{\partial T}\,\delta T\ , \tag{5.10}$$

where $\frac{\partial \mathcal{J}}{\partial f} = (\lambda^T + \dot{\mu}^T)R$, $\frac{\partial \mathcal{J}}{\partial p} = (\lambda^T + \dot{\mu}^T)\frac{\partial W}{\partial p} + \psi_p$, (5.11)

$$\frac{\partial \mathcal{J}}{\partial T} = \psi(U_T, \dot{U}_T, p) - (\lambda_T^T + \dot{\mu}_T^T)(C\dot{U}_T + KU_T - W(U_T, \dot{U}_T, p) - Rf_T) - (\dot{\lambda}_T^T M - \lambda_T^T \tilde{C}_T - \mu_T^T \tilde{K}_T)\dot{U}_T .$$

The relations (5.11) present the gradient vectors of the functional $\mathcal{J}$ through the parameters p, control time T and input functions f(t) at each time instant from the interval [0,T]. The optimality condition is expressed as the equation system

$$\frac{\partial \mathcal{J}}{\partial p} = 0 \quad , \quad \frac{\partial \mathcal{J}}{\partial f} = 0 \quad , \quad \frac{\partial \mathcal{J}}{\partial T} = 0 \quad , \qquad (5.12)$$

that is to be solved together with the conjugate equations (5.8) with the end values (5.9)'.

The solution of the system (5.12) in an explicit form can be found in very few cases, therefore practically the minimum point of the functional $\mathcal{J}$ is obtained by employing gradient optimization algorithms beginning from some initial approximation p, f, T, U, $\dot{U}$.

In the case of a fixed-time problem all the above presented relations remain valid assuming the value $\delta T = 0$ and ignoring the derivative $\frac{\partial \mathcal{J}}{\partial T}$.

The values of the function $\frac{\partial \mathcal{J}}{\partial f}$ at the time points from the interval $t \in [0,T]$ present the infinite-dimensional gradient vector of the functional $\mathcal{J}$. However, in practical cases it is reasonable to restrict ourselves with the finite-dimensional control functions.

Let's present each component of the vector f(t) as a superposition of a finite number of basic functions as follows

$$f(t) = [a]^T g(t) \quad . \qquad (5.13)$$

The components of the vector $g_{r\times 1}(t)$ are the functions $g_j(t)$, $j = \overline{1,r}$ composing a basic function system, and $[a]_{r\times m}$ is the coefficient matrix, in the i-th column a^i containing the coefficients of the expansion of the function f(t) in terms of

the functions $g_j(t)$. The components of the vector g(t) being prescribed, the variation $\delta f(t)$ is presented as

$$\delta f(t) = \delta[a]^T g(t) \quad , \qquad (5.14)$$

Substituting (5.14) into (5.10), we obtain

$$\delta \mathcal{J} = \int_0^T \left(\frac{\partial \mathcal{J}}{\partial f} \delta[a]^T g(t) + \frac{\partial \mathcal{J}}{\partial p} \delta p \right) dt + \frac{\partial \mathcal{J}}{\partial T} \delta T \quad . \qquad (5.15)$$

In order to obtain the gradient vector of the functional $\mathcal{J}$ in the space of the coefficients a_i^j , we transform (5.15) as follows:

$$\delta \mathcal{J} = \sum_{i=1}^{m} \int_0^T \frac{\partial \mathcal{J}}{\partial f_i} \delta(a^i)^T g(t) dt + \int_0^T \frac{\partial \mathcal{J}}{\partial p} \delta p \, dt + \frac{\partial \mathcal{J}}{\partial T} \delta T \quad , \qquad (5.16)$$

where $\frac{\partial \mathcal{J}}{\partial f_i}(t)$ is the i-th component of the vector $\frac{\partial \mathcal{J}}{\partial f}(t)$, and $\delta(a^i)$ - the i-th column of the matrix $\delta[a]$.

Taking the transpose in (5.16), we obtain

$$\delta \mathcal{J} = \sum_{i=1}^{m} \left(\int_0^T \frac{\partial \mathcal{J}}{\partial f_i} g^T(t) \, dt \right) \delta a^i + \int_0^T \frac{\partial \mathcal{J}}{\partial p} \delta p \, dt + \frac{\partial \mathcal{J}}{\partial T} \delta T \, . \qquad (5.17)$$

Denoting in (5.17) the first integral through G_i^T , the variation $\delta \mathcal{J}$ can be expressed as

$$\delta \mathcal{J} = \sum_{i=1}^{m} G_i^T \delta a^i + \int_0^T \frac{\partial \mathcal{J}}{\partial p} \delta p \, dt + \frac{\partial \mathcal{J}}{\partial T} \delta T \quad , \qquad (5.18)$$

where $G_i^T = \int_0^T \frac{\partial \mathcal{J}}{\partial f_i} g^T(t) \, dt$.

The gradient vector of the functional $\mathcal{J}$ in the finite-dimensional space of the elements of the matrix [a] is obtained by presenting the components of the vectors G_i^T in sequence as a row-matrix

$$\frac{\partial \mathcal{J}}{\partial [a]} = \langle\, G_1^T,\ G_2^T,\ \ldots,\ G_m^T \,\rangle\ , \qquad (5.19)$$

where $\dfrac{\partial \mathcal{J}}{\partial [a]}$ is time independent.

Truncation of dynamic contributions of higher modes at the optimization of feedback parameters. In place of the variational equation (5.5) the following system can be employed (see (1.13), (1.22)) :

$$\begin{cases} I\,\delta\ddot{z}_1 + \mathrm{diag}(\mu_1)\,\delta\dot{z}_1 + \mathrm{diag}(\omega_1^2)\,\delta z_1 = \\ \qquad = \Delta_1^T \dfrac{\partial W}{\partial U}\,(\Delta_1 \delta z_1 + \Delta_2 \delta z_2) + \Delta_1^T \dfrac{\partial W}{\partial \dot{U}}\,\Delta_1 \delta \dot{z}_1 + \Delta_1^T \dfrac{\partial W}{\partial p}\,\delta p\ , \\ \mathrm{diag}(\omega_2^2)\,\delta z_2 = \Delta_2^T \dfrac{\partial W}{\partial U}\,(\Delta_1 \delta z_1 + \Delta_2 \delta z_2) + \Delta_2^T \dfrac{\partial W}{\partial \dot{U}}\,\Delta_1 \delta \dot{z}_1 + \Delta_2^T \dfrac{\partial W}{\partial p}\,\delta p\ , \end{cases} \qquad (5.20)$$

where notations coincide with those of the Chap.1, assuming $R \equiv 0$. Representing each of the vectors λ, μ as two subvectors

$\lambda = \begin{bmatrix} \lambda_1 \\ \lambda_2 \end{bmatrix}$, $\mu = \begin{bmatrix} \mu_1 \\ \mu_2 \end{bmatrix}$, we obtain the conjugate equations

$$\begin{cases} I\,\ddot{\lambda}_1 - c_1^T \dot{\lambda}_1 + [k_1^T - k_{12}(k_2^T)^{-1} k_{12}^T]\,\lambda_1 = -[k_{12}(k_2^T)^{-1}\Delta_2^T + \Delta_1^T] \left[\dfrac{\partial \psi}{\partial U}\right]^T , \\ I\,\ddot{\mu}_1 - c_1^T \dot{\mu}_1 + [k_1^T - k_{12}(k_2^T)^{-1} k_{12}^T]\,\mu_1 = [-k_{12}(k_2^T)^{-1}\Delta_2^T + \Delta_1^T] \left[\dfrac{\partial \psi}{\partial \dot{U}}\right]^T , \end{cases} \qquad (5.21)$$

where $k_1 = \mathrm{diag}(\omega_1^2) - k_{11}^T$, $k_2 = \mathrm{diag}(\omega_2^2) - k_{12}^T$, $c_1 = \mathrm{diag}(\mu_1) - \Delta_1^T \dfrac{\partial W}{\partial \dot{U}}\,\Delta_1$,

$$k_{11} = \Delta_1^T \frac{\partial W}{\partial U}\,\Delta_1\ ,\quad k_{12} = \Delta_1^T \frac{\partial W}{\partial U}\,\Delta_2\ ,\quad k_{22} = \Delta_2^T \frac{\partial W}{\partial U}\,\Delta_2\ .$$

Considering the case $\varphi \equiv 0$ in the expression of the target functional (5.2), the equations (5.21) are to be integrated with zero end values, i.e., $\lambda_{1_T} = \dot{\lambda}_{1_T} = \mu_{1_T} = \dot{\mu}_{1_T} = 0$. The subvectors λ_2, μ_2 at each time point are obtained from the relations

$$\begin{cases} \lambda_2 = (k_2^T)^{-1} k_{12}^T \lambda_1 - (k_2^T)^{-1} \Delta_2^T \left[\dfrac{\partial \psi}{\partial U}\right]^T , \\ \dot{\mu}_2 = (k_2^T)^{-1} k_{12}^T \dot{\mu}_1 - (k_2^T)^{-1} \Delta_2^T \left[\dfrac{\partial \psi}{\partial \dot{U}}\right]^T . \end{cases} \qquad (5.22)$$

The gradient vector of the functional $\mathcal{J}$ in the space of parameters p is obtained from the relation

$$\frac{\partial \mathcal{J}}{\partial p} = \int_0^T \left[(\lambda_1^T + \dot{\mu}_1^T)\,\Delta_1^T + (\lambda_2^T + \dot{\mu}_2^T)\,\Delta_2^T \right] \frac{\partial W}{\partial p}\,dt\ . \qquad (5.23)$$

The advantage of such an approach is that the conjugate system (5.21) has a considerably lower dimension than the source equation (5.1).

5.2 INVERSE DYNAMIC PROBLEM APPROACH FOR CONTROL SYNTHESIS

5.2.1 Programmed control synthesis

Consider a linear mechanical structure governed by the equation of motion

$$M\,\ddot{U} + C\,\dot{U} + K\,U = R\,f\ . \qquad (5.24)$$

where $M_{n\times n}$, $C_{n\times n}$, $K_{n\times n}$ - structural mass, damping and stiffness matrices, $U_{n\times 1}$ - nodal displacement vector, $R_{n\times m}$ - the matrix transforming the input excitation $f_{m\times 1}$ into the equivalent nodal forces, where the relation $m<n$ is held.

To solve a programmed control synthesis problem means to obtain an input vector f ensuring a prescribed motion law U(t). Employing the inverse dynamic problem approach, the control law synthesis is based upon the symmetry of the structure of the mathematical model and upon the inverse of the operations presenting the essence of the controlled object [115,129]. In the case of the elastic structure (5.24) the problem is complicated by the circumstance that the range of the matrix R and the number of control functions f are significantly less than the total dimension of the structural equation. As a result, the matrix R

can't be inverted and f can't be immediately obtained from the equation (5.24).

The most simple alternative is to employ the least squares approach and the generalized inversion of the matrix R ([48,80]):

$$f(t) = R^{+}(M \ddot{U} + C \dot{U} + K U) \quad . \qquad (5.25)$$

Nevertheless, regarding the case of elastic structural vibrations in the lower range of eigenfrequency spectrum, a control in the subspace of modal coordinates is preferable. In order to obtain such a control law, the equation (5.24) is presented in truncated modal coordinates as

$$\begin{cases} I \ddot{z}_1 + \mathrm{diag}(\mu_1) \dot{z}_1 + \mathrm{diag}(\omega_1^2) z_1 = \Delta_1^T R f \ , \\ \mathrm{diag}(\omega_2^2) z_2 = \Delta_2^T R f \ . \end{cases} \qquad (5.26)$$

Relaxing the control quality requirement we restrict ourselves with ensuring the necessary motion law only for several components of the vector $U(t)$, and presenting them as $\tilde{U}(t)$. Forming the the matrices $\tilde{\Delta}_1$, $\tilde{\Delta}_2$ from the corresponding rows of Δ_1, Δ_2 , we obtain the relation

$$\tilde{U} = \tilde{\Delta}_1 z_1 + \tilde{\Delta}_2 z_2 \quad . \qquad (5.27)$$

After some manipulation, from (5.26),(5.27) we obtain an equation of motion

$$\tilde{\Delta}_1^{-1} \ddot{\tilde{U}}_1 + \mathrm{diag}(\mu_1) \tilde{\Delta}_1^{-1} \dot{\tilde{U}}_1 + \mathrm{diag}(\omega_1^2) \tilde{\Delta}_1^{-1} \tilde{U}_1 =$$

$$= [\mathrm{diag}(\omega_1^2) \tilde{\Delta}_2 \mathrm{diag}(1/\omega_2^2) \Delta_2^T + \Delta_1^T] R f \qquad (5.28)$$

If $\tilde{U}(t)$ is prescribed, the programmed control $f(t)$ is immediately obtained from (5.28) assuming that the number of displacements in $\tilde{U}$ is equal to the number of modes with preserved dynamic contributions (i.e., the matrix $\tilde{\Delta}_1$ is to be square and nonsingular). The nonsingularity of the right-hand side matrix in (5.28) is necessary, otherwise the problem is to be solved employing the least squares approach.

5.2.2 Linear closed-loop control synthesis

Approximate control synthesis. The practical use of the programmed control laws obtained in Chap.5.2.1 is that they can be employed as a basis for the closed-loop control synthesis. The closed-loop control can be obtained by prescribing the necessary motion laws linearly related to their time derivatives (e.g., a superposition of exponent functions [115,129,80]). Consider a linear system presented by the structural equation of motion (5.24). It is necessary to obtain the closed-loop control $f=f(U)$ such that the motion of the structure would match the prescribed motion law $U(t) = U^{*}(t)$. Consider only such aperiodic motion laws $U^{*}(t)$ that can be presented as

$$U^{*}(t) = \bar{U} \left(1 + \frac{\lambda}{\mu-\lambda} e^{\lambda t} + \frac{\mu}{\lambda-\mu} e^{\mu t} \right) \ , \qquad (5.29)$$

where $\bar{U}$ – the displacement vector defining the end state of a structure, and the exponents $\lambda<0$, $\mu<0$.

Obviously, the motion law (5.29) satisfies the relations $U^{*}(0)=\dot{U}^{*}(0)=0$, $U^{*}(\infty)=\bar{U}$, $\dot{U}^{*}(\infty)=0$,i.e., we consider an elastic transfer of a structure from one stationary state to another. Assume the results of measuring the displacements and velocities of the structure points at each time instant being presented as vectors

$$g_{k\times 1} = Q_{k\times n} U_{n\times 1} \ , \quad \dot{g}_{k\times 1} = Q_{k\times n} \dot{U}_{n\times 1} \ , \qquad (5.30)$$

where Q – the transformation matrix.

In order to obtain a completely observable system it necessary to match the condition $\mathrm{rank}(Q)=n$, that is impossible in most cases. Therefore the reconstruction of the values of the vector U employing the measurement results g isn't unique. Employing the generalized inverse of matrices, the vector U is presented as

$$U = Q^{+} g + (I - Q^{+}Q) y \ , \qquad (5.31)$$

where I denotes the unity matrix, and y is an arbitrary vector. Selecting the value of y as

$$y = G\,g \quad ,$$

where $G_{n\times k}$ - constant matrix (unknown for the present), we present the relation (5.31) as

$$U = [\,Q^{+} + (I - Q^{+}Q)\,G\,]\,g = \tilde{Q}\,g \quad . \qquad (5.32)$$

Denoting through F the equivalent nodal force vector

$$F = R\,f \quad ,$$

a nodal forcing law ensuring the prescribed motion law $U^{*}(t)$ is obtained as

$$F^{*} = M\,\ddot{U}^{*} + C\,\dot{U}^{*} + K\,U^{*} \quad . \qquad (5.33)$$

With regard to the equation (5.29), the accelerations $\ddot{U}^{*}$ are expressed through velocities and displacements as

$$\ddot{U}^{*} = \dot{U}^{*}(\lambda + \mu) - U^{*}\lambda\mu + \bar{U}\,\lambda\mu \quad . \qquad (5.34)$$

As only the values of g and $\dot{g}$ can be measured, employing the relation (5.32) we obtain

$$\ddot{U}^{*} = (\lambda + \mu)\,\tilde{R}\,\dot{g} - \lambda\mu\,\tilde{R}\,g + \lambda\mu\,\bar{U} \quad , \qquad (5.35)$$

where $\tilde{R} = [\,R^{+} + (I - R^{+}R)\,H\,]$, and $H_{m\times n}$ - the constant matrix unknown for the present.

Substituting (5.35) into (5.33), we obtain

$$F^{*} = V\,\tilde{R}\,\dot{g} + S\,\tilde{R}\,g + P\,\bar{U} \quad , \qquad (5.36)$$

where $V = M\,(\lambda + \mu) + C$, $S = K - \lambda\mu\,M$, $P = \lambda\mu\,M$.

Now the values of the input functions f are to be expressed through the measuring results g , $\dot{g}$. Employing the least squares approach it can be done as follows:

$$f^{*} = \tilde{R}\,F^{*} \quad . \qquad (5.37)$$

Finally, the obtained closed-loop control system can be presented as shown in Fig.5.1. According to the relations (5.36), (5.37) the input f^{*}_{in} is approximately obtained as

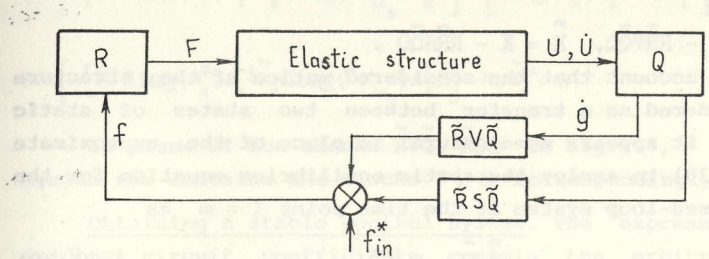

Fig.5.1 Linear control system obtained by means of the inverse dynamics problem solution

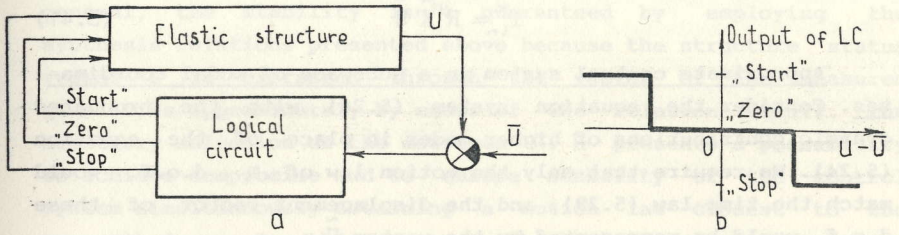

Fig.5.2 Control system with the logical feedback circuit

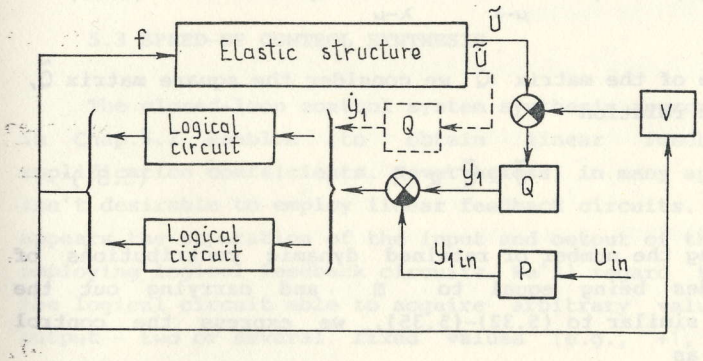

Fig.5.3 Control system with the logical feedback circuits for each modal coordinate

$$f^*_{in} = \tilde{R}\, P\, \bar{U}\,, \qquad (5.38)$$

and the resulting motion of a controlled structure is

$$M\,\ddot{U} + \bar{\bar{C}}\,\dot{U} + \bar{\bar{K}}\,U = R\, f^*_{in}\,, \qquad (5.39)$$

where $\bar{\bar{C}} = C - \tilde{R}\tilde{R}\tilde{V}\tilde{Q}\tilde{Q}$, $\bar{\bar{K}} = K - \tilde{R}\tilde{R}\tilde{S}\tilde{Q}\tilde{Q}$.

Taking account that the considered motion of the structure can be considered as a transfer between two states of static equilibrium, it appears more natural in place of the approximate relation (5.38) to employ the static equilibrium equation for the obtained closed-loop system at the time point $t = \infty$ as

$$\bar{\bar{K}}\,\bar{U} = R\, f^*_{in}\,. \qquad (5.40)$$

Consequently, the input vector f^*_{in} can be obtained from the relation

$$f^*_{in} = R^{+}\bar{\bar{K}}\,\bar{U} \qquad (5.41)$$

Approximate control system in a subspace of modal coordinates. Consider the equation system (5.26) with the truncated dynamic contributions of higher modes in place of the equation (5.24). We require that only the motion law of m d.o.f. would match the time law (5.29), and the displacement vector of these d.o.f. would be represented by the vector $\tilde{U}$:

$$\tilde{U}^*(t) = \tilde{\bar{U}}\,\left(1 + \frac{\lambda}{\mu-\lambda}e^{\lambda t} + \frac{\mu}{\lambda-\mu}e^{\mu t}\right)\,. \qquad (5.29)'$$

In place of the matrix Q we consider the square matrix $\tilde{Q}$, obtaining the relation

$$\tilde{U} = \tilde{Q}^{-1} g\,. \qquad (5.31)'$$

Selecting the number of retained dynamic contributions of the lower modes being equal to m and carrying out the manipulation similar to (5.32)-(5.35), we express the control force vector as

$$\ddot{F}^* = V'\,\dot{g} + S'\,g + P'\,\tilde{\bar{U}}\,, \qquad (5.36)'$$

where

$$V' = \left[\Delta_1^T R + \mathrm{diag}(\omega_1^2)\tilde{\Delta}_1^{-1}\tilde{\Delta}_2\,\mathrm{diag}(1/\omega_2^2)\Delta_2^T R\right]^{-1}\left[\mathrm{diag}(\mu_1)\tilde{\Delta}_1^{-1} + (\lambda+\mu)\tilde{\Delta}_1^{-1}\right]\tilde{Q}^{-1},$$

$$S' = \left[\Delta_1^T R + \mathrm{diag}(\omega_1^2)\tilde{\Delta}_1^{-1}\tilde{\Delta}_2\,\mathrm{diag}(1/\omega_2^2)\Delta_2^T R\right]^{-1}\left[\mathrm{diag}(\omega_1^2)\tilde{\Delta}_1^{-1} - \lambda\mu\tilde{\Delta}_1^{-1}\right]\tilde{Q}^{-1},$$

$$P' = \left[\Delta_1^T R + \mathrm{diag}(\omega_1^2)\tilde{\Delta}_1^{-1}\tilde{\Delta}_2\,\mathrm{diag}(1/\omega_2^2)\Delta_2^T R\right]^{-1}\lambda\mu\tilde{\Delta}_1^{-1}\,.$$

In place of the blocks $\tilde{R}\tilde{V}\tilde{Q}$, $\tilde{R}\tilde{S}\tilde{Q}$ in Fig.5.1, the control system now contains the blocks V', S' correspondingly.

Obtaining a stable control system. The expressions of the feedback circuit coefficients contain the arbitrary constant matrices G and H (see the relations (5.32), (5.37). It follows, that the values of these matrices can be selected in order to ensure the stability of the control system. Obviously, in general, the stability isn't guaranteed by employing the synthesis relations presented above because the structure status vector U is expressed through the vector of the measured quantities approximately by means of the relation (5.31). The arbitrary selection of the matrices G, H presents a possibility to achieve compromise and to ensure stability of the control system simultaneously obtaining a motion law closest to the prescribed one. For this purpose the Appendix 4 presents an algorithm based upon a gradient procedure of minimizing the real parts of the eigenvalues of a closed-loop system [58].

5.3 SPEED-UP CONTROL SYNTHESIS

The closed-loop control system synthesis approach presented in Chap.5.2 enables to obtain linear feedback circuit amplification coefficients. Nevertheless, in many applications it isn't desirable to employ linear feedback circuits. As preferable appears the separation of the input and output of the system by employing logical feedback circuits. We'll regard the input of the logical circuit able to acquire arbitrary values, and the output - two or several fixed values (e.g., +1, 0, -1). In general, such a system can be classified under speed-up control systems [39]. A formal logical feedback circuit synthesis is a

complicated task, therefore it is usually obtained from general engineering considerations employing available logical elements. A very simple tracking control system with one input and one output signal is presented in Fig.5.2. Such a control is often insufficient for elastic structures with many d.o.f. because it doesn't damp the residual elastic vibration due to higher modal components.

We'll show, that the control system synthesis regarding several modal coordinates is possible employing the equations of motion with truncated dynamic contributions of higher modes. In such a case a separate logical circuit is employed for ensuring control of each modal coordinate. As a start point for the synthesis we employ the equation system (5.26), selecting a subset of modal coordinates in order to obtain a square and nonsingular matrix $\Delta_1^T R$ of the dimension $m \times m$. In the equation (5.26) we make the substitution $y_1 = (\Delta_1^T R)^{-1} Z_1$. Denote the vector of measured quantities of the length m through $\tilde{U}$, and from the corresponding rows of the matrices Δ_1, Δ_2 the matrices $\tilde{\Delta}_1$, $\tilde{\Delta}_2$. are obtained. Prescribed displacement values are presented by the vector $\tilde{U}_{in}$. From the definition of modal displacements follows the relation

$$Z_{in} = \Delta^T M U_{in} ,$$

and the following equality takes place:

$$\tilde{U} - \tilde{U}_{in} = \tilde{\Delta}_1^T (Z_1 - Z_{1_{in}}) + \tilde{\Delta}_2^T (Z_2 - Z_{2_{in}}) . \qquad (5.42)$$

From (5.42) it follows

$$Z_1 = \tilde{\Delta}_1^{-1} [\, \tilde{U} - \tilde{\Delta}_2 \mathrm{diag}(1/\omega_2^2) \Delta_2^T R f \,] , \qquad (5.43)$$

and, consequently,

$$y_1 = (\Delta_1^T R)^{-1} \tilde{\Delta}_1^{-1} [\, \tilde{U} - \tilde{\Delta}_2 \mathrm{diag}(1/\omega_2^2) \Delta_2^T R f \,] . \qquad (5.44)$$

Then, denoting

$$V = \tilde{\Delta}_2 \mathrm{diag}(1/\omega_2^2) \Delta_2^T R , \quad S = (\Delta_1^T R)^{-1} \tilde{\Delta}_1^{-1} , \quad Q = (\Delta_1^T R)^{-1} \tilde{\Delta}_1^{-1} , \qquad (5.45)$$

$$P = (\Delta_1^T R)^{-1} \Delta^T M ,$$

the control system can be presented as shown in Fig.5.3. Inputs of logical circuits can be supplied with the generalized velocity vector $y_1 = Q\dot{\tilde{U}}$, if it appears necessary for the operation of the control algorithm and if the measured values of the velocities are available.

As it can be seen from Fig.5.3, in addition to the main feedback we have obtained an additional feedback in the control circuit. It can operate asynchronously assuming infinitesimal delays in the electrical control circuit, as well as synchronously employing the clock frequency significantly higher than the frequency of the highest mode with the retained dynamic contribution in the equations (5.26).

The obtained control system can appear non-optimal because of neglecting the higher mode dynamic contributions as well as because of an heuristic approach defining the basic logical circuit. Therefore the control system can be optimized employing the optimum system control techniques for obtaining the values of some parameters (e.g., time points for voltage reverse, the magnitudes of voltage pulses, the width of insensitivity range, etc.). The techniques for solving such problems are presented in Chap.5.1. If logical circuits are employed, the expression of the function $W(U,\dot{U},p)$ contains the discontinuous functions

$$h(x-a) = \begin{cases} 0, & x<a , \\ 1, & x>a , \end{cases} \qquad \mathrm{sign}(x-a) = \begin{cases} -1, & x<a , \\ 0, & x=a , \\ 1, & x>a . \end{cases}$$

The derivatives of such functions with respect to the variable X as well as with respect to the parameter a contain the δ-functions. During the computation we employ the numerical equivalents of these functions presented in Fig.5.4. For example, the logical function presented in Fig.5.2 results in a block-diagram in Fig.5.5. Its mathematical expression is

$$W(U,p) = h(|U-U_{in}| - p) \left[h(U-U_{in})\, W^- + (1 - h(U-U_{in}))\, W^+ \right] .$$

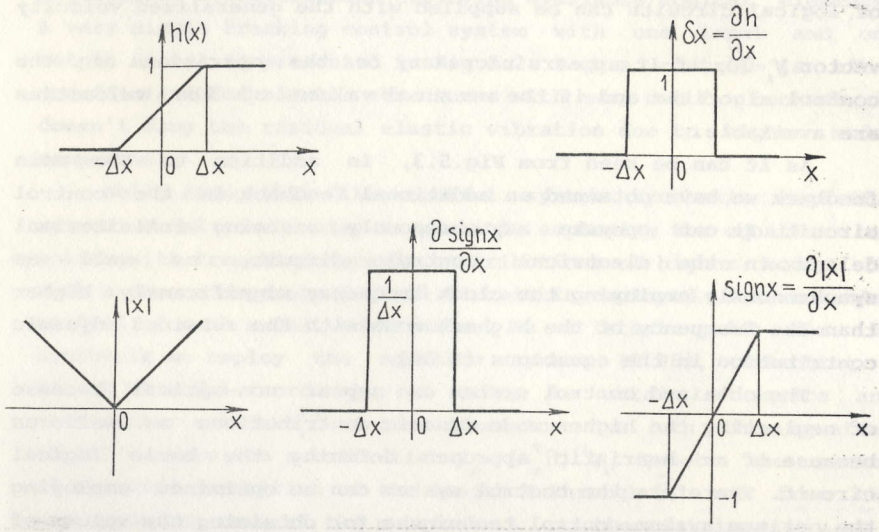

Fig.5.4 Numerical equivalents of discontinuous functions

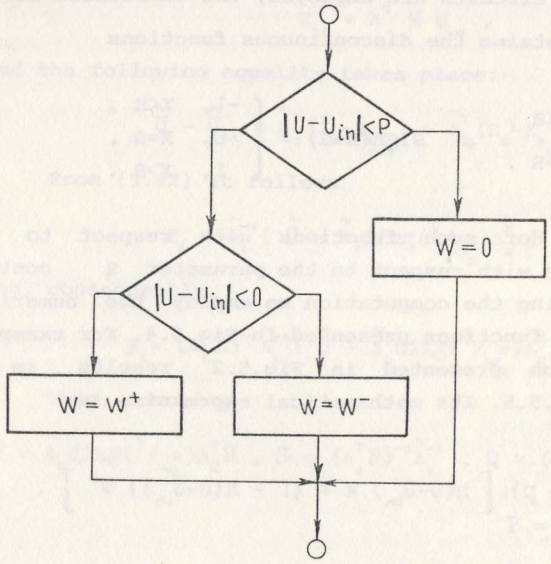

Fig.5.5 Block-diagram of the feedback algorithm presented in Fig.5.2

The following derivatives with respect to U and p can be employed for obtaining the gradient vector of the target function:[1]

$$\frac{\partial W}{\partial U} = 2\delta(|U-U_{in}|- p)\ \mathrm{sign}(U-U_{in})\Big[\ h(U-U_{in})W^{-}+ (1 -h(U-U_{in}))W^{+}\ \Big]+$$

$$+ h(|U-U_{in}| - p)\Big[\ \mathrm{sign}(U-U_{in})\ W^{-} - \mathrm{sign}(U-U_{in})\ W^{+}\ \Big],$$

$$\frac{\partial W}{\partial p} = -2\delta(|U-U_{in}|- p)\ \Big[\ h(U-U_{in})W^{-}+ (1 -h(U-U_{in}))W^{+}\ \Big]\ ,$$

5.4 FORCED RESONANT VIBRATION CONTROL

Problem formulation. If piezoelectric vibroconverters (VC) are employed as input links of vibrodrives, it is necessary to excite their vibration ensuring the prescribed motion laws and paths of some of their d.o.f. Although in reality VC operate in a nonlinear interaction with other links, here we restrict ourselves with the linear vibration law synthesis problem. Such an approach appears as reasonable from the engineer's point of view, because at the first approximation many mechanical systems containing VC are designed considering the ability of free VC to produce prescribed vibration paths.

We consider the structural dynamic equation (5.24) as a mathematical model of a VC, the excitation frequency being close to one of the resonant frequencies (only in the vicinity of the resonance it is possible to obtain sufficiently large values of the vibration amplitudes). Presenting the problem in modal coordinates, we obtain

$$\ddot{z}_i + \mu_i \dot{z}_i + \omega_i^2 z_i = \delta_i^T R f\ , \quad i=\overline{1,n} \qquad (5.46)$$

and the motion law is approximately obtained by superimposing the contributions of the modes possessing the eigenfrequency values in the vicinity of the excitation frequency, and neglecting the contributions of the remaining modal components.

Three problems of different complexity can be distinguished:

a) exciting vibrations of the prescribed mode, b) obtaining prescribed planar or spatial vibration paths in symmetric structures by means of multi-phase excitation, c) obtaining prescribed planar vibration paths by means of a single phase harmonic excitation in the vibroconverters possessing several modes with approximately equal eigenfrequency values.

Exciting vibrations of the prescribed mode is the simplest synthesis problem. Assume that it is necessary to excite the vibration of the i-th mode. If the excitation frequency $\omega = \omega_i$, in place of the system (5.46) we consider only the i-th equation, presenting the equivalent excitation force of the i-th mode by the right-hand term $\delta_i^T R f$. The most effective excitation of the modal vibration is obtained the equivalent force being of the maximal magnitude. Assume the elements of the vector f being harmonic functions, i.e., $f = f^A \sin\omega t$ with prescribed amplitudes $f^A = \pm f^*$. In this case the maximal amplitude of the equivalent excitation force of the i-th mode is ensured obtaining the forcing amplitudes from the relation

$$f_i^A = \text{sign}\,(\delta_i^T R)_j \,, \qquad (5.47)$$

where $(\delta_i^T R)_j$ denotes the j-th element of the row-vector $\delta_i^T R$.

Prescribed planar or spatial vibration paths in symmetric structures by means of multi-phase excitation are obtained, if vibrations of several modes are excited simultaneously. The vibrations of each mode are to be excited with the prescribed phase shift $\Delta\varphi$. Assume the eigenfrequencies of several modes being coincident, as it is the case in the symmetrical VC, such as rings, circular and square plates, cylinders etc. Exciting simultaneously the vibration of i-th and j-th modes with the eigenfrequencies $\omega_i = \omega_j = \tilde{\omega}$, the equation system in modal coordinates appears as

$$\begin{cases} \ddot{z}_i + \mu_i \dot{z}_i + \tilde{\omega}^2 z_i = \delta_i^T R f^{Ai} \sin\omega t \,, \\ \ddot{z}_j + \mu_j \dot{z}_j + \tilde{\omega}^2 z_j = \delta_j^T R f^{Aj} \sin(\omega t + \Delta\varphi). \end{cases} \qquad (5.48)$$

Nonzero values of f_k^{Ai}, f_k^{Aj} in (5.48) are not allowed to be coincident, i.e., $f_k^{Ai} f_k^{Aj} = 0$, $k = \overline{1,m}$. It means that the same

input excitation can't present two harmonic signals with different phase shifts, otherwise summers of input signals are necessary. Taking on account that the left-hand sides of the equations (5.48) are identical, the relation between the vibration amplitudes and phases of z_i, z_j are determined by the relation between the amplitudes and phases of the excitation signal. If $\Delta\varphi$ is a prescribed quantity, the amplitude values of the elements of the vector f^A satisfying the relation

$$\frac{\delta_i^T R f^{Ai}}{\delta_j^T R f^{Aj}} = \alpha \qquad (5.49)$$

are to be obtained, where α - prescribed ratio between the vibration amplitudes corresponding to the modes i and j.

If there is no possibility to satisfy accurately the relation (5.49), an approximation is to be found by solving the optimization problem

$$\begin{cases} \max\limits_{f^{Ai}} | \delta_i^T R f^{Ai} | \,, \\ f_k^{Ai} f_k^{Aj} = 0, \; k = \overline{1,m} \,, \\ f_k^{Ai}, f_k^{Aj} \in \{ f^*, -f^* \} . \end{cases} \qquad (5.50)$$

Such a problem can be solved, e.g., by means of an exhaustive search procedure or employing other discrete optimization techniques. If other values of the amplitudes are allowed besides $f^*, -f^*$, only the constraint $f_k^{Ai}, f_k^{Aj} \in \{ f^*, -f^* \}$ of the optimization problem (5.50) is to be changed.

Obtaining prescribed planar vibration paths by means of single phase harmonic excitation is possible if the eigenfrequencies ω_i, ω_j of two modes are close but not coinciding. The excitation frequency ω is selected in the vicinity of the two eigenfrequencies $\omega_i \cong \omega_j \cong \omega$. The formation of the phase shift between the two modal responses is presented by the amplitude-frequency and phase-frequency characteristics (AFCH and PFCH) in Fig.5.6. The vibration phase shift $\Delta\varphi(\omega)$ depends upon the difference between the eigenfrequencies ω_i and ω_j and upon the Q-factor of a vibrating system, i.e., upon the peak shapes of the amplitude-frequency curve. In general, peak values depends upon the selected excitation law and aren't known in

advance. The algorithm for obtaining the excitation law reads as follows:

Algorithm 5.1

1. Consider the equation system

$$\begin{cases} \ddot{z}_i + \mu_i \dot{z}_i + \omega_i^2 z_i = \delta_i^T R f^{Ai} \sin \omega t , \\ \ddot{z}_j + \mu_j \dot{z}_j + \omega_j^2 z_j = \delta_j^T R f^{Aj} \sin \omega t . \end{cases} \qquad (5.51)$$

For z_i and z_j the PFCH are obtained. The AFCH are obtained for unity excitations, i.e., assuming the right-hand sides of the equations of the system (5.51) being equal to $\sin\omega t$.

2. According with the PFCH (independent of the excitation amplitude) the ω value is obtained ensuring the prescribed phase shift $\Delta\varphi$. The amplitude values of the two AFCH corresponding to this ω value are marked (a_i and a_j in Fig.5.6).

3. The prescribed ratio of the generalized displacement amplitudes being equal to $\frac{z_i}{z_j} = \alpha$, the excitation vector f^A is obtained satisfying the relation

$$\frac{\delta_i^T R f^{Ai} a_i}{\delta_i^T R f^{Aj} a_j} = \alpha . \qquad (5.52)$$

During the step 3 of the Algorithm 5.1 the following optimization problem is to be solved:

$$\begin{cases} \max\limits_{f^{Ai}} | \delta_i^T R f^{Ai} | \\ \text{with the constraint (5.52),} \\ f^{Ai}, f^{Aj} \in \{ f^*, -f^* \} . \end{cases} \qquad (5.53)$$

The constraint $f_k^{Ai} f_k^{Aj} = 0$, $k=\overline{1,m}$, isn't included into (5.53), because the phases of input excitations are coincident. As a rule, the value of ω ensuring the phase shift $\Delta\varphi$ between the two modal responses isn't unique, therefore the algorithm should be applied at several excitation frequency values in order to obtain the optimal solution.

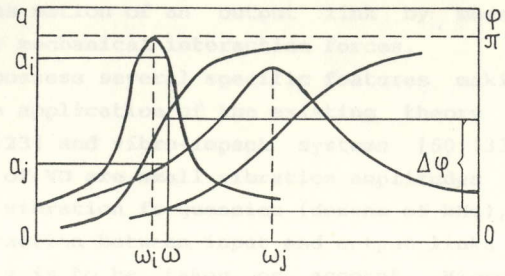

Fig.5.6 Obtaining a vibration phase difference between two response components at a single-phase excitation

PART 2. APPLICATIONS

Vibrodrives (VD) are the mechanisms converting high-frequency vibrations of an input link into the directed stepwise or continuous motion of an output link by means of essentially nonlinear mechanical interaction forces.

VD possess several specific features making difficult the immediate application of the existing theory of vibroconveyers [79,122,123] and vibro-impact systems [50,133]. Distinquishing features of VD are small vibration amplitudes (several microns) and high vibration frequencies (dozens of kHz), therefore during the interaction between input and output links a contact surface elasticity is to be taken on account. Microimpacts can't be assumed instantaneous, as an impact time takes a significant part of a vibration period. Consequently, a stereomechanical model characterized by a velocity restitution ratio in general is insufficient for presenting the contact phenomena in VD. Moreover, a resonant modal vibration of the input links usually is employed in VD, therefore the distributed parameter or finite element models are necessary.

An overview of numerous theoretical and experimental investigations of VD is presented in [37]. The main results of research have been presented in [56,116,47,119,94]. For obtaining adequate mathematical models of VD a correct representation of the contact interaction is of primary importance. Together with the stereomechanical impact models, the combined local and wave contact interaction models have been taken into account, the viscoelastic surface rheology approach being commonly employed. The finite element models enable to present the complex geometry of the links of VD and the inverse piezoeffect in piezoceramic input links [71,133]. Finite element formulations based upon the updated Lagrangian approach enable to take account for large strains taking place in the contact zone [117,10]. Nevertheless, the contact zone investigation problem appears to be of similar complexity, and often even more complex than the global problem of obtaining the motion law of a VD with a prescribed contact interaction characteristic. Therefore usually compromise formulations are preferable, restricting with small displacement finite element models and the viscoelastic rheology of the

contact interaction [15,36,97,71]. The surface rheology approach can be regarded as an extension of the oblique impact phenomenological models with lumped parameters [133]. As promising appears an approach taking account for rigid body motions of finite element models of vibrodrive links, a full finite element formulation of free and restricted rigid body motions of deformable bodies being presented in [40].

An effect of sliding between the links of a VD under the sliding friction forces is to be regarded simultaneously with the deformation of an interface layer. Usually local contact effects are assumed independent at each separate contact zone. The more complex models are to be employed for the VD with the continuous contact zone [71].

A vibroconverter(VC) should be regarded as the main part of a VD. VC produce mechanical vibrations under the high-frequency alternating voltage applied to their electric terminals. Their operation can be based upon different effects, such as electrostrictive, piezoelectric, magnetostrictive etc. [140].

As a rule, the operation of piezoelectric vibroconverters is based upon the excitation of their modal vibration employing an inverse piezoelectric effect. In general it presents a complex set of phenomena in polarized dielectrics and connects elastic, electric and thermal properties of piezoelectric materials. The constitutive relations of electro- and magnetothermoelasticity are obtained in [11,33,20]. The investigations of electromechanical vibrations in piezoelectric rectangular plates and axisymmetric shells have been carried out in [83,84,96,99]. In [102] the behavior of piezoelectric vibroconverters in an electrical circuit has been presented by means of equivalent four-terminal networks, the reference [100] being an overview of various engineering applications.

The finite element techniques for the piezoelectric structure analysis have been developed in [21-24] by Y.Kagawa et al. In [104] the techniques have been applied for the transient vibration analysis in two-dimensional piezoelectric VC, and in [3,71] - for the dynamic analysis of input links of VD.

6. MODEL EQUATIONS OF VIBRODRIVES

In this chapter finite element models of piezoelectric vibroconverters (VC) and vibrodrives (VD) are obtained and the dynamic characteristics of VD are formulated.

Employing the variational formulation of thermopiezoelectricity, the relations for obtaining matrices of piezoelectric continua finite elements and the relations for presenting the properties of VC as electric circuit elements are obtained. Several energy dissipation models during the vibration of a VC are considered. The contact interaction models for point-interaction and travelling wave VD are obtained employing a small displacement finite element model and phenomenological models of an interface between contacting links. A full model of a VD is presented taking account for rigid body motions of the vibrating links, the finite element models of each link being presented in truncated modal coordinates.

6.1 FINITE ELEMENT MODELS OF PIEZOELECTRIC VIBROCONVERTERS

6.1.1 Variational formulation of thermopiezoelectricity

Consider a piezoelectric body occupying a volume V and bounded by a surface S. The surface S is divided into parts $S_u \cup S_\sigma = S_\varphi \cup S_D = S_\theta \cup S_h = S$ such that $S_u \cap S_\sigma = S_\varphi \cap S_D = S_\theta \cap S_h = 0$, n being an outward normal vector to the surface. Assume a vector of body forces $f = (X,Y,Z)^T$ acting inside the volume, where X,Y,Z - components of the body force vector in the directions of the Cartesian axes. Upon the surface part S_σ acts a prescribed surface force vector $g_s = (X_n, Y_n, Z_n)^T$, and a displacement vector $u_s = (u_{1s}, u_{2s}, u_{3s})^T$ is prescribed upon S_u. Similarly, upon S_D, S_φ a charge q_s and an electric potential φ_s, and upon S_h, S_θ a heat flux v_s and a temperature θ_s are prescribed. In the volume V displacements $u=(u_1,u_2,u_3)$, strains $\varepsilon^T=(\varepsilon_1,\varepsilon_2,\varepsilon_3,\gamma_{23},\gamma_{13},\gamma_{12})$, stresses $\sigma^T = (\sigma_1,\sigma_2,\sigma_3,\tau_{23},\tau_{13},\tau_{12})$, an electric field vector $E^T=(E_1,E_2,E_3)$, an electric displacement vector $D^T = (D_1,D_2,D_3)$, thermal flux vector $h^T = (h_1,h_2,h_3)$ as well as an electric potential φ, a temperature deviation θ from a certain positive reference temperature θ_0 and an entropy density η will be

considered. In the following we employ matrix differential operators

$$\mathbf{A} = \begin{bmatrix} \frac{\partial}{\partial x} & 0 & 0 \\ 0 & \frac{\partial}{\partial y} & 0 \\ 0 & 0 & \frac{\partial}{\partial z} \\ \frac{\partial}{\partial y} & \frac{\partial}{\partial x} & 0 \\ 0 & \frac{\partial}{\partial z} & \frac{\partial}{\partial y} \\ \frac{\partial}{\partial z} & 0 & \frac{\partial}{\partial x} \end{bmatrix}, \quad \mathbf{a} = \begin{bmatrix} \frac{\partial}{\partial x} \\ \frac{\partial}{\partial y} \\ \frac{\partial}{\partial z} \end{bmatrix},$$

and an outward normal vector n direction cosine matrices

$$\mathbf{A} = \begin{bmatrix} \cos(n,x) & 0 & 0 \\ 0 & \cos(n,y) & 0 \\ 0 & 0 & \cos(n,z) \\ \cos(n,y) & \cos(n,x) & 0 \\ 0 & \cos(n,z) & \cos(n,y) \\ \cos(n,z) & 0 & \cos(n,x) \end{bmatrix}, \quad \mathbf{a}_s = \begin{bmatrix} \cos(n,x) \\ \cos(n,y) \\ \cos(n,z) \end{bmatrix}.$$

Employing the matrix notation, we present the equations of thermopiezoelectricity for the volume $\bar{V}$ as [11]

$$\begin{cases} \mathbf{A}^T\sigma + \mathbf{f} = \rho\ddot{\mathbf{u}} & , \in \bar{V}; \\ \mathbf{a}^T\mathbf{D} = 0 & , \in \bar{V}; \\ \mathbf{a}^T\mathbf{h} = -\theta_o\dot{\eta} & , \in \bar{V}; \end{cases} \tag{6.1}$$

$$\begin{cases} \varepsilon = \mathbf{A}\,\mathbf{u} & , \in \bar{V}; \\ \mathbf{E} = -\mathbf{a}\,\varphi & , \in \bar{V}; \\ \mathbf{h} = -\mathbf{k}\,\mathbf{a}\,\theta & , \in \bar{V}; \end{cases} \tag{6.2}$$

$$\begin{cases} \sigma = \mathbf{c}^E(\varepsilon - \varepsilon_o) - \mathbf{e}\,\mathbf{E} - \lambda\,\theta + \sigma_o & , \in \bar{V}; \\ \mathbf{D} = \mathbf{e}^T(\varepsilon - \varepsilon_o) + \mathfrak{E}^S\mathbf{E} + \mathbf{l}\,\theta & , \in \bar{V}; \\ \eta = \lambda^T(\varepsilon - \varepsilon_o) + \mathbf{l}^T\mathbf{E} + \alpha\,\theta & , \in \bar{V}; \end{cases} \tag{6.3}$$

where k - thermal conductivity tensor, $\mathbf{c}^E$ - stiffness tensor under constant electric field, $\mathfrak{E}^S$ - dielectric permittivity tensor under constant strain, e - piezoelectric stress tensor, λ - thermal stress tensor, l - pyroelectric tensor, α - material constant ($\alpha = \rho\, c_v\, \theta_o^{-1}$, where c_v - specific heat under constant volume), ρ - material density, ε_o, σ_o - initial strains and stresses.

The boundary values defined by surface forces, displacements, charges, potentials, temperatures and thermal flux upon the surface parts S_u, S_σ, S_φ, S_D, S_θ, $S_h \in S$ are presented as

$$\begin{cases} \mathbf{A}_S^T\sigma = \mathbf{g}_S & , \in S_\sigma; \\ \mathbf{u} = \mathbf{u}_S & , \in S_u; \end{cases} \tag{6.4}$$

$$\begin{cases} \mathbf{a}_S^T\mathbf{D} = q_S & , \in S_D; \\ \varphi = \varphi_S & , \in S_\varphi; \end{cases} \tag{6.5}$$

$$\begin{cases} \mathbf{a}_S^T\mathbf{h} = V_S & , \in S_h; \\ \theta = \theta_S & , \in S_\theta; \end{cases} \tag{6.6}$$

Integrating by parts and applying the Green's theorem, it can be shown that for the differential operators A and a presented above, arbitrary vectors $\xi^T = (\xi_1, \xi_2, \xi_3)$, $\varkappa^T = (\varkappa_1, \varkappa_2, \varkappa_3, \varkappa_4, \varkappa_5, \varkappa_6)$ and a scalar function ζ defined in $\bar{V}$ and upon the boundary S the following relations take place:

$$\int_V (\mathbf{A}\,\xi)^T\varkappa\, dV = \int_S \xi^T\mathbf{A}_S^T\,\varkappa\, dS - \int_V \xi^T\mathbf{A}^T\varkappa\, dV,$$

$$\int_V (\mathbf{a}\,\zeta)^T\varkappa\, dV = \int_S \zeta\,\mathbf{a}_S^T\,\varkappa\, dS - \int_V \zeta\,\mathbf{a}^T\varkappa\, dV. \tag{6.7}$$

Employing (6.7), we'll present the equations (6.1)-(6.6) as integral identities.

The true values σ, ε, u, D, E, φ, η, h, θ, i.e., satisfying the equations (6.1)-(6.3) and the boundary values (6.4)-(6.6), have unique values because of the uniqueness theorem of the solution of the system (6.1)-(6.6). Consider the class of virtual

quantities $\bar{\sigma}$, $\bar{D}$, $\bar{h}$, $\bar{\eta}$, satisfying the equations (6.1) and the boundary conditions, and the class of virtual quantities $\bar{\varepsilon}^*$, $\bar{u}^*$, $\bar{E}^*$, $\bar{\varphi}^*$, $\bar{\theta}^*$, satisfying the equations (6.2) and the boundary conditions. Though the relations (6.1),(6.2),(6.4)- (6.6) don't define the virtual quantities uniquely, the true values belong to the classes defined above.

Employing the identities (6.7), the equations (6.1)-(6.2) and the boundary conditions (6.4)-(6.6) it can be shown that the virtual quantities satisfy the following integral identities:

$$\begin{cases} \int_V \bar{\varepsilon}^{*T}\bar{\sigma}\,dV = \int_{S_\sigma} \bar{u}^{*T} g_s\,dS + \int_{S_u} u_s^T A_s^T \bar{\sigma}\,dS + \int_V \bar{u}^{*T}(f - \rho\ddot{\bar{u}})\,dV , \\ \int_V \bar{E}^{*T}\bar{D}\,dV = -\int_{S_D} \bar{\varphi}^* q_s\,dS - \int_{S_\varphi} \varphi_s a_s^T \bar{D}\,dS , \\ \int_V (a\bar{\theta}^*)^T \bar{h}\,dV = \int_{S_h} \bar{\theta}^* v_s\,dS + \int_V \theta(\theta_o\dot{\bar{\eta}})\,dV . \end{cases} \tag{6.8}$$

Assume

$$\bar{\sigma} = \sigma , \ \bar{D} = D , \ \bar{\eta} = \eta , \ \bar{\varepsilon}^* = \varepsilon + \delta\varepsilon , \ \bar{E}^* = E + \delta E ,$$
$$\bar{h} = h , \ \bar{u}^* = u + \delta u , \ \bar{\varphi}^* = \varphi + \delta\varphi , \ \bar{\theta}^* = \theta + \delta\theta , \ \ddot{\bar{u}}^* = \ddot{u} ,$$

where σ, ε, u, D, E, φ, η, h, θ - the true values, satisfying all the equations of thermopiezoelectricity (6.1)-(6.3) and the boundary conditions (6.4)-(6.6), δ - variations of the true values, $\delta\varepsilon = A\,\delta u$, $\delta E = a\,\delta\varphi$.

Substituting into (6.8) and taking on account that $\delta u=0$ upon S_u, $\delta\varphi=0$ upon S_φ, $\delta\theta=0$ upon S_θ, and that the true values satisfy the equations (6.8), we obtain the variational identities

$$\begin{cases} \int_V \delta\varepsilon^T\sigma\,dV = \int_{S_\sigma} \delta u^T g_s\,dS + \int_V \delta u^T(f - \rho\ddot{u})\,dV , \\ \int_V \delta E^T D\,dV = -\int_{S_D} \delta\varphi\, q_s\,dS , \\ \int_V (a\delta\theta)^T h\,dV = \int_{S_h} \delta\theta\, v_s\,dS - \theta_o\int_V \delta\theta\,\dot{\eta})\,dV . \end{cases} \tag{6.9}$$

Now we refuse of the assumption that σ, D, h, η, $\ddot{u}$ are the true values, supposing that they only satisfy the identities (6.9). Employing the relations (6.7) immediately for the left-hand sides of (6.9) and uniting the obtained identities with (6.9), we obtain

$$\begin{cases} \int_{S_\sigma} \delta u^T(A_s^T\sigma_s - g_s)dS - \int_V \delta u^T(A^T\sigma + f - \rho\ddot{u})dV = 0 , \\ \int_{S_D} \delta\varphi\,(a_s^T D - q_s)dS - \int_V \delta\varphi^T a^T D\,dV = 0 , \\ \int_{S_h} \delta\theta\,(a_s^T h - v_s)dS - \int_V \delta\theta\,(a^T h + \theta_o\dot{\eta})dV = 0 . \end{cases}$$

The values of δu, $\delta\varphi$, $\delta\theta$ being arbitrary, the last relations impose upon σ, D, h, η the requirement to satisfy the equations (6.1) and the boundary conditions upon S_σ,S_D,S_h. Thus the system (6.9) contains the equations (6.1) and the boundary conditions upon S_σ,S_D,S_h. Adding to this system the equations (6.3) and the boundary conditions (6.4)-(6.6) upon S_u,S_φ,S_θ, we obtain a thermopiezoelectricity problem formulation in terms of displacements, potentials and temperatures. As a result, if u, φ, θ satisfy the boundary conditions (6.4)-(6.6) upon S_u,S_φ,S_θ and the integral identities

$$
\begin{cases}
\int_V (\mathbf{A}\,\delta u)^T (c^E \mathbf{A}\, u + e\, a\, \varphi - \lambda\, \theta) dV + \int_V \delta u^T \rho\, \ddot{u}\, dV = \\
\quad = \int_{S_\sigma} \delta u^T g_S\, dS + \int_V \delta u^T f\, dV + \int_V (\mathbf{A}\,\delta u)^T c^E \varepsilon_o\, dV - \int_V (\mathbf{A}\,\delta u)^T \sigma_o\, dV\,, \\
\int_V (a\,\delta\varphi)^T (e^T \mathbf{A}\, u - \vartheta^S a\, \varphi + 1\, \theta) dV = \int_{S_q} \delta\varphi\, q_S\, dS + \int_V (a\,\delta\varphi)^T e^T \varepsilon_o\, dV\,, \\
\int_V (a\,\delta\theta)^T k\, a\, \theta\, dV + \theta_o \int_V \delta\theta\, (\alpha\, \dot{\theta} - 1^T a\, \dot{\varphi})\, dV = - \int_{S_h} \delta\theta\, v_S\, dS\,,
\end{cases}
\tag{6.10}
$$

they satisfy all the equations of thermopiezoelectricity and the boundary conditions, i.e., they are the true values of displacements, potentials and temperatures. The obtained integral identities can be employed for obtaining the finite element method relations for piezoelectric VC analysis.

6.1.2 Finite elements of piezoelectric continua

Assume the volume occupied by a piezoelectric body being divided into finite elements. Consider the volume V^e occupied by a finite element (FE) with the nodes i, j, m,..., bounded by the surface S^e. The status of each point of the FE is completely defined by the displacements u, potential φ and temperature θ. According to the general scheme of the displacement formulation of the finite element method, the values of u, φ, θ at each point of a FE are expressed through the nodal values of these quantities as

$$
\begin{cases}
u(x,y,z) = N\, U^e = [\, N_i,\, N_j,\, N_k, \dots \,] \begin{bmatrix} U_i \\ U_j \\ U_k \\ \vdots \end{bmatrix}, \\
\varphi(x,y,z) = L\, \Phi^e = [\, L_i,\, L_j,\, L_k, \dots \,] \begin{bmatrix} \Phi_i \\ \Phi_j \\ \Phi_k \\ \vdots \end{bmatrix}, \\
\theta(x,y,z) = P\, \Theta^e = [\, P_i,\, P_j,\, P_k, \dots \,] \begin{bmatrix} \Theta_i \\ \Theta_j \\ \Theta_k \\ \vdots \end{bmatrix},
\end{cases}
\tag{6.11}
$$

where N, L, P - form functions, $U_i = \begin{bmatrix} U_{1i} \\ U_{2i} \\ U_{3i} \end{bmatrix}$ - nodal displacements, Φ_i - nodal potentials, Θ_i - nodal temperatures.

Denote $B = \mathbf{A}\, N$, $B_E = a\, L$, $B_T = a\, P$. Substituting (6.11) into the integral identities(6.10) and regarding that $\delta u = N\, \delta U^e$, $\delta\varphi = L\, \delta\Phi^e$, $\delta\theta = P\, \delta\Theta^e$ and that the identities (6.10) are valid for arbitrary values δu, $\delta\varphi$, $\delta\theta$, we obtain the equation system

$$
\begin{cases}
M^e \ddot{U}^e + K^e U^e + T^e \Phi^e - V^e \Theta^e = F^e\,, \\
\qquad\quad T^{eT} U^e - S^e \Phi^e + W^e \Theta^e = Q^e\,, \\
H^e \dot{\Theta} + \theta_o V^{eT} \dot{U}^e - \theta_o W^{eT} \dot{\Phi}^e + G^e \Theta^e = Z_T^e\,,
\end{cases}
$$

where the FE matrices are defined correspondingly as mass, stiffness, electromechanical, capacity, thermoelastic, thermoelectric, heat conductivity and heat capacity matrices:

$$
M^e = \int_{V^e} N^T \rho\, N\, dV\,, \qquad K^e = \int_{V^e} B^T c^E B\, dV\,, \qquad T^e = \int_{V^e} B^T e\, B_E\, dV\,,
$$

$$
S^e = \int_{V^e} B_E^T \vartheta^S B_E\, dV\,, \qquad V^e = \int_{V^e} B^T \lambda\, P\, dV\,, \qquad W^e = \int_{V^e} B_E^T 1\, P\, dV\,,
$$

$$G^e = \int_{V^e} B_T^T \, k \, B_T \, dV , \qquad H^e = \alpha\theta_o \int_{V^e} P^T P \, dV .$$

The vectors F^e, Q^e, Z_T^e are defined as follows:

$$F^e = \int_{S_\sigma^e} N^T g_S dS + \int_{V^e} N^T f \, dV + \int_{V^e} B^T c^E \varepsilon_o dV - \int_{V^e} B^T \sigma_o dV ,$$

$$Q^e = \int_{S_D^e} L^T q_S dS + \int_{V^e} B_E^T e^T \varepsilon_o dV , \qquad Z_T^e = - \int_{S_h^e} P^T v_S dS .$$

Surface integrals in the latter relations can be nonzero only if a FE is situated at the boundary of a piezoelectric body. After assembling the structural matrices, the equation system can be presented as

$$\begin{bmatrix} M & 0 & 0 \\ 0 & 0 & 0 \\ 0 & 0 & 0 \end{bmatrix} \begin{bmatrix} \ddot{U} \\ \ddot{\Phi} \\ \ddot{\Theta} \end{bmatrix} + \begin{bmatrix} 0 & 0 & 0 \\ 0 & 0 & 0 \\ \theta_o V^T & -\theta_o W^T & H \end{bmatrix} \begin{bmatrix} \dot{U} \\ \dot{\Phi} \\ \dot{\Theta} \end{bmatrix} + \begin{bmatrix} K & T & -V \\ T^T & -S & W \\ 0 & 0 & G \end{bmatrix} \begin{bmatrix} U \\ \Phi \\ \Theta \end{bmatrix} = \begin{bmatrix} F \\ Q \\ Z_T \end{bmatrix} \tag{6.12}$$

If at the nodes of the structure additional forces are applied, they are to be added to the corresponding components of the vector F .

Consider the thermal flux boundary condition in the form

$$v_S = p \, (\theta - \theta_\infty + \theta_o) ,$$

where p - heat exchange coefficient with the environment, θ_∞ - temperature of the environment, θ_o - reference temperature.

In such a case it is easy to show, that the heat conductivity matrix G^e and the vector Z_T^e can be presented as

$$G^e = \int_{V^e} B_T^T \, k \, B_T \, dV + p \int_{S_h^e} P^T P \, dS , \qquad Z_T^e = - \int_{S_h^e} P^T (\theta_o - \theta_\infty) dS .$$

If the reference temperature coincides with the environment temperature θ_∞ , the equality $Z_T^e = 0$ takes place.

In a high-frequency mechanical vibration analysis of VC the coupling terms $\theta_o V^T \dot{U}$, $-\theta_o W^T \dot{\Phi}$ and the heat conductivity term $H\dot{\Theta}$ can be omitted in (6.12) without causing significant errors. In such an uncoupled formulation the analysis procedure is decomposed into thermal analysis and piezoelectric vibration analysis problems.

A VC employed as an input link of a VD always is to be regarded as an element of an alternating current circuit, therefore its electrical characteristics present a considerable interest. Let's omit thermomechanical and thermoelectric terms in (6.12), assume zero mechanical boundary conditions upon S_U as $u_S = 0$ and $F = 0$ and regroup the components of the vectors Φ and Q presenting them as $\Phi = \begin{bmatrix} \Phi_1 \\ \Phi_2 \end{bmatrix}$, $Q = \begin{bmatrix} Q_1 \\ Q_2 \end{bmatrix}$, where the index "1" corresponds to the nodal points on the electric terminals of a VC, and the index "2" - to the remaining nodal points, inclusively the nodal points of the surface S_D. The charges Q_2 of the part of a VC without electric terminals can be assumed being equal to zero, if only the electric field lines don't leave the volume occupied by a VC, what is practically always the case. Regrouping correspondingly the rows and columns of the structural matrices and assuming a harmonic vibration law $U = U\cos\omega t$, we obtain

$$\begin{bmatrix} K-\omega^2 M & T_1 & T_2 \\ T_1^T & -S_{11} & -S_{12} \\ T_2^T & -S_{12}^T & -S_{22} \end{bmatrix} \begin{bmatrix} U \\ \Phi_1 \\ \Phi_2 \end{bmatrix} = \begin{bmatrix} 0 \\ Q_1 \\ 0 \end{bmatrix} . \tag{6.13}$$

In general, the charge Q_1 in the left-hand side of (6.13) isn't known. Nevertheless, if the potentials Φ_1 are known, the number of unknowns is equal to the number of equations. In the case when Φ_1 isn't known, for the harmonic time law of the input potential the charge Q_1 is related with Φ_1 as

$$I = j \omega Q_1 = Y_E \Phi_1 , \tag{6.14}$$

where $Y_E = [y_{ij}]$ - input electrical admittance matrix, each component y_{ij} presenting an admittance between the nodes i and j, and I -vector of nodal currents. An explicit expression for Y_E is obtained by solving simultaneously the equations (6.13), (6.14):

$$Y_E = j\omega \left\{ S_{11} + \left[T_1^T \,\middle|\, -S_{12} \right] \left[\begin{array}{cc} K - \omega^2 M & T_2 \\ T_2^T & -S_{22} \end{array} \right]^{-1} \left[\begin{array}{c} T_1 \\ \cdots\cdots \\ -S_{12}^T \end{array} \right] \right\} , \qquad (6.15)$$

An important characteristic of a VC is presented by its eigenfrequencies and eigenforms at short-circuited ($\Phi_1=0$) and open ($Q_1=0$) electric terminals (resonances and antiresonances correspondingly). The characteristic equations for obtaining the eigenfrequencies and eigenforms are obtained from (6.13) as

a) short-circuited electric terminals ($\Phi_1=0$):

$$\det \left\{ K + T_2 S_{22}^{-1} T_2^T - \omega^2 M \right\} = 0 \ ; \qquad (6.16.1)$$

b) open electric terminals ($Q_1=0$):

$$\det \left\{ K + T S^{-1} T^T - \omega^2 M \right\} = 0 \ . \qquad (6.16.2)$$

At the resonant eigenfrequencies the dynamic admittance of a VC is infinite (see the second term in the relation (6.15)). At the antiresonant frequencies the dynamic admittance is equal to zero, i.e., the minimum electric current flows through a VC.

Energy dissipation in VC . The phenomena causing energy dissipation in VC are extremely complex. Energy looses depend upon a number of factors, such as vibration amplitude and frequency, temperature, operating point, electrical and magnetic fields etc. As a rule, account for the above mentioned factors is taken approximately by introducing corresponding terms into equations of motion.

Energy looses during a vibration of a VC are assumed to be caused by mechanic, piezoelectric and dielectric phenomena [146,100,140]. Each kind of the looses is supposed to be due to a hysteresis loop in the relations $\sigma(\varepsilon)$, $\sigma(E)$, $D(E)$. In order to take account for them, the stiffness c^E, piezoelectric e and dielectric ϑ^S tensors are presented as complex quantities

$$c^E = c^{E'} + jc^{E''} \ , \quad e = e' + je'' \ , \quad \vartheta^S = \vartheta^{S'} + j\vartheta^{S''} \ . \qquad (6.17)$$

Consider longitudinal vibrations of a rod-type VC with the short-circuited electric terminals ($E_3=0$). Assuming the harmonic time law for the longitudinal strain $\varepsilon_1 = \varepsilon_{10}\sin\omega t$, the relation $\sigma_1(\varepsilon_1)$ can be presented as [31]

$$\sigma_1 = c_{11}^{E'}\varepsilon_1 + \omega^{-1} c_{11}^{E''} \dot{\varepsilon}_1 \ , \qquad (6.18)$$

because of the relation $\dot{\varepsilon}_1 = j\omega\varepsilon_1$. Substituting $\varepsilon_1 = \varepsilon_{10}\sin\omega t$ into the relation (6.18), we obtain

$$\sigma_1 = c_{11}^{E''}\varepsilon_{10}\sin(\omega t+\xi) \left(1+\eta_M^2\right)^{\frac{1}{2}} \ , \qquad (6.19)$$

where $tg\xi = \eta_M = \dfrac{c_{11}^{E''}}{c_{11}^{E'}}$ is called the mechanical dissipation factor and ξ denotes the phase shift between the stress and strain harmonic vibration laws. The relation (6.19) can be presented as

$$\sigma_1 = c_{11}^{E'}\varepsilon_1 \pm c_{11}^{E''} \left(\varepsilon_{10}^2 - \varepsilon_1^2\right)^{\frac{1}{2}} \ . \qquad (6.20)$$

The equation (6.20) presents an elliptical path on the plane (ε_1,σ_1) approximating the real hysteresis loop. Considering the relations $\sigma_1 = (e'_{31} + je''_{31})E_3$, $D_3 = (\vartheta_{33}^{S'} + j\vartheta_{33}^{S''})E_3$ for the same VC with fixed ends ($\varepsilon_1=0$), a piezoelectric and dielectric dissipation factors $\eta_P = \dfrac{e''_{31}}{e'_{31}}$ and $\eta_D = \dfrac{\vartheta_{33}^{S''}}{\vartheta_{33}^{S'}}$ are introduced. Similarly the physical sense of the remaining complex components of the stiffness, piezoelectric and dielectric tensors can be explained.

To measure the dissipation factors for all the tensor components is a very complicated task. However, usually it isn't necessary to know all the tensor components when carrying out an analysis of a specified VC. From the other point of view, approximately the same dissipation factor value can be employed for all the components of a tensor. In the latter case the relations (6.17) are presented as

$$c^E = c^E(1+j\eta_M) \ , \quad e = e(1+j\eta_P) \ , \quad \vartheta^S = \vartheta^S(1+j\eta_D) \ . \qquad (6.21)$$

The dissipation factors can be assumed to be dependent upon a vibration frequency value as $\eta_M(\omega)$, $\eta_P(\omega)$, $\eta_D(\omega)$.

By employing the complex values of c^E, e, ϑ^S we assume that dynamic analysis is carried out in a frequency domain. In order to carry out the transient analysis it appears preferable to consider structural equations of motion (6.12) of a VC, and to employ the explicit expressions of the relations $\sigma(\varepsilon)$, $\sigma(E)$, $D(E)$ in the form (6.20) instead of the complex tensors (6.21). However, in such a case we obtain a nonlinear problem requiring considerably greater amounts of a computational resource. Naturally, a compromise between accuracy and computational efficiency is preferable. In order to obtain a linear equation of motion, we present dissipation as viscous friction force and electrical voltage drop across a resistance, and at a harmonic excitation obtain the following equation system in terms of complex quantities:

$$\begin{cases} -\omega^2 M\,U + K(1+j\eta_M)\,U + T(1+j\eta_P)\,\Phi = F \ , \\ T^T(1+j\eta_P)U - S(1+j\eta_D)\,\Phi = Q \ , \end{cases}$$

Taking account for a symmetry of the matrix S, the equation system can be transformed to the real form

$$\begin{cases} -\omega^2 M\,U + \tilde{K}\left(1+\dfrac{1+2\eta_P\eta_D-\eta_P^2}{1+\eta_D^2}\right)U + j\tilde{K}\left(\eta_M+\dfrac{2\eta_P-\eta_D+\eta_D\eta_P^2}{1+\eta_D^2}\right)U - \\ \qquad -\tilde{T}\,\dfrac{1+\eta_P\eta_D}{1+\eta_D^2}\,Q - j\tilde{T}\,\dfrac{\eta_P-\eta_D}{1+\eta_D^2}\,Q = F \ , \qquad (6.22) \\ \tilde{T}^T\,\dfrac{1+\eta_P\eta_D}{1+\eta_D^2}\,U + j\tilde{T}^T\,\dfrac{\eta_P-\eta_D}{1+\eta_D^2}\,U - S^{-1}\,\dfrac{1}{1+\eta_D^2}\,Q + S^{-1}\,\dfrac{\eta_D}{1+\eta_D^2}\,Q = \Phi \ , \end{cases}$$

where $\tilde{K} = K + T\,S^{-1}T^T$, $\tilde{T} = T\,S^{-1}$.

At the excitation frequency value ω a periodic response of (6.22) coincides with the solution of the system

$$\begin{cases} M\ddot{U} + C\dot{U} - R\dot{Q} + \hat{K}U - \hat{T}Q = F \ , \\ R^T\dot{U} + P\dot{Q} + \hat{T}^TU - S^{-1}\dfrac{1}{1+\eta_D^2}\,Q = \Phi \ , \end{cases} \qquad (6.23)$$

where $R = \omega^{-1}\tilde{T}\,\dfrac{\eta_P-\eta_D}{1+\eta_D^2}$, $C = \omega^{-1}\tilde{K}\left(\eta_M+\dfrac{2\eta_P-\eta_D+\eta_D\eta_P^2}{1+\eta_D^2}\right)$,

$P = \omega^{-1}S^{-1}\dfrac{\eta_D}{1+\eta_D^2}$, $\hat{K} = \omega^{-1}\tilde{K}\left(1+\dfrac{1+2\eta_P\eta_D-\eta_P^2}{1+\eta_D^2}\right)$, $\hat{T} = \omega^{-1}\tilde{T}\,\dfrac{1+\eta_P\eta_D}{1+\eta_D^2}$.

The matrix R in the system (6.23) presents equivalent resistances connected in sequence with the electric terminals of a VC, and the vector $\dot{Q}$ - the amplitudes of alternating electrical currents flowing through a VC.

The difference between the systems (6.22) and (6.23) is that in (6.22) the dissipation forces don't depend explicitly upon a vibration frequency. Such a dependence can be introduced only by employing frequency-dependent dissipation factors $\eta_M(\omega)$, $\eta_P(\omega)$, $\eta_D(\omega)$. At the same time in the system (6.23) the forces are direct proportional to a frequency value, because the factor ω is obtained as a result of differentiating in time the time laws U and Q. Moreover, the values of resonant frequencies of the system (6.22) coincide with the resonant frequencies of the corresponding conservative system (without dissipation). The magnitudes of the resonant frequencies of the system (6.23) are obtained less than of a corresponding conservative system, since they depend upon the dissipation level.

One more possibility of a simplified presentation of dissipation forces can be obtained by introducing a modal damping and assuming that damping phenomena are due to only to the mechanical viscous friction forces.

The modes of a VC are obtained by solving an eigenvalue problem for a VC with open electric terminals (6.16.2). We denote the obtained angular eigenfrequencies through ω_i, $i=\overline{1,n}$, representing the corresponding eigenvectors as columns of the matrix $\Delta=\left[\delta_1,\delta_2,\ldots,\delta_n\right]$. A transfer to modal coordinates is

carried out by substituting $U = \Delta Z$, the dynamic equation in modal coordinates being obtained as

$$I\ddot{z} + \mathrm{diag}(\omega_i^2)\, z = \Delta^T \tilde{T}\, Q + \Delta^T F \quad , \qquad (6.24)$$

Assuming that the dissipation forces caused by different modal vibration components are independent, we introduce a diagonal matrix of modal damping coefficients $\mathrm{diag}(\mu_i)$, and add the term $\mathrm{diag}(\mu_i)\dot{z}$ to the left-hand side of the equation (6.24). If the Q-factor Q_i of a vibrating system at the frequency value ω_i is known, the values of μ_i can be obtained from the relation

$$\mu_i = \frac{\omega_i}{Q_i} \ .$$

The damping matrix in modal coordinates is diagonal, if it can be expressed as $C=\alpha_1 M+\alpha_2 K$, where α_1 and α_2 are the coefficients obtained at the known values of two Q-factors Q_i and Q_j of a VC at two different vibration frequency values ω_i and ω_j from the relations

$$\alpha_1 = \frac{\omega_i \omega_j (\omega_j Q_j - \omega_i Q_i)}{(\omega_j^2 - \omega_i^2) Q_i Q_j} \ , \quad \alpha_2 = \frac{\omega_i Q_j - \omega_j Q_i}{(\omega_j^2 - \omega_i^2) Q_i Q_j} \ .$$

6.2 MECHANICAL CONTACT INTERACTION MODELS

6.2.1 Vibrodrives with point-contact interaction

The simplest model of a VD is presented in Fig.6.1a. If an elastic vibration is excited in a rod-type VC 1, it begins to move directively as a rigid body. An average directive tangential interaction force is obtained as a result of a certain time-law of the normal interaction force. An oscillating value of the magnitude of the normal force can be obtained,e.g., by pressing with tension the VC 1 to the horizontal plane by means of VC 2.

The varying tension force is obtained creating an inverse piezoeffect in VC 2, i.e., by means of an alternating high frequency voltage applied to its electric terminals, Fig.6.1b. In order to obtain the sufficient normal force magnitude, high-frequency alternating voltage source ensuring voltage

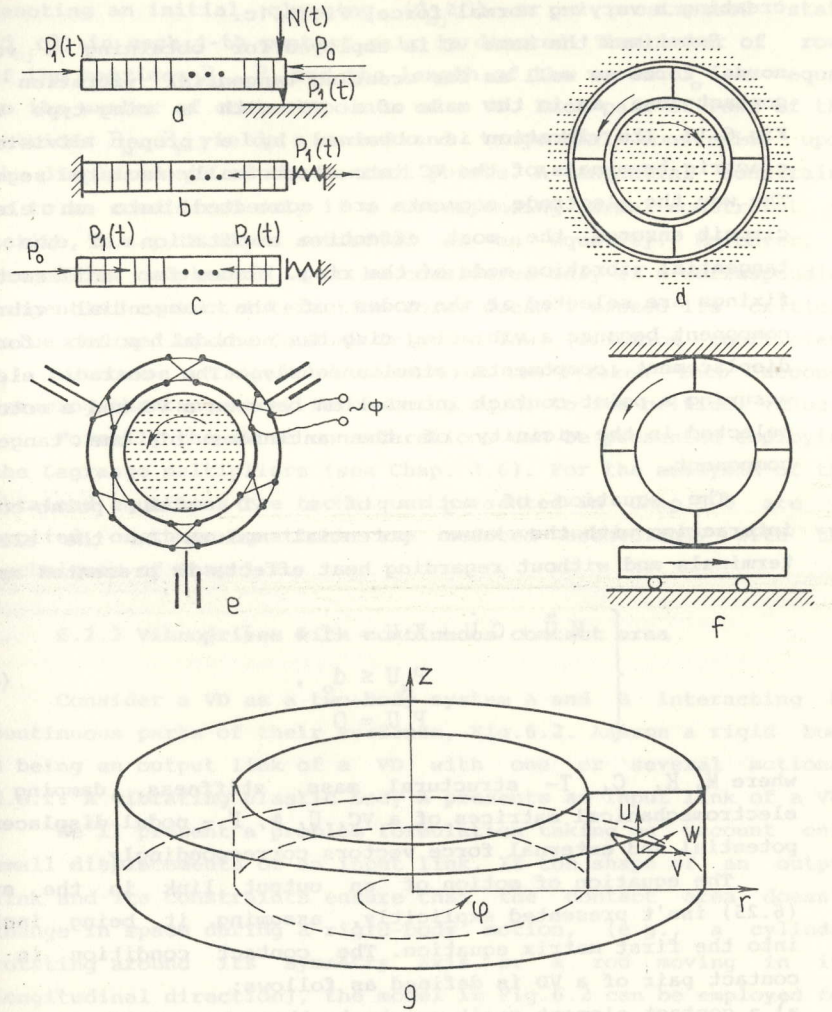

Fig.6.1 Construction diagrams of vibrodrives:
a,b,c - links of the simplest model;
d - vibrodrive with the ring VC;
e,f - traveling wave vibrodrives;
g - finite element of a traveling wave vibrodrive

amplitudes of hundreds of volts are often necessary. Therefore resonant vibroimpact motion laws of VC 2 are employed for creating a varying normal force, Fig.6.1c.

Sometimes the same VC is employed for obtaining a varying normal force as well as for creating tangential vibration of a contact zone, as in the case of a VD with a ring-type VC in Fig.6.1d. Its vibration is obtained by a proper division of electric terminals of the VC into electrically isolated segments. The way the electrode segments are connected into an electric circuit ensures the most effective excitation of the third tangential vibration mode of the ring. Places for unidirectional fixings are selected at the nodes of the tangential vibration component because a vibrating ring has no nodal points for two displacement components simultaneously. The contact elements ensuring a point-contact interaction between a VC and a rotor are selected in the vicinity of the antinodes of the tangential component.

The equation of motion of a VD with point-contact interaction with the known potential values on the electric terminals and without regarding heat effects is presented as

$$\begin{cases} M\ddot{U} + C\dot{U} + KU = -T\Phi + F \ , \\ P_N U \le d_o \ , \\ P_T \dot{U} = 0 \ , \end{cases} \qquad (6.25)$$

where M, K, C, T- structural mass, stiffness, damping and electromechanical matrices of a VC, U, Φ, F - nodal displacement, potential and external force vectors correspondingly.

The equation of motion of an output link in the system (6.25) isn't presented explicitly, assuming it being included into the first matrix equation. The contact condition in each contact pair of a VD is defined as follows:

a) a contact element can't penetrate through a rigid surface of an output link,

b) if a tangential interaction force doesn't exceed its critical value, a contact element of a VC and the corresponding point of an output link move together without sliding.

The constant matrices P_N, P_T contain the direction cosines

of a contact surface. Multiplying the matrices by a nodal displacement vector, normal and tangential displacements of the contact points are obtained. Through d_o a constant vector denoting an initial clearing ($d_{oj} \ge 0$) or a prestressed state ($d_{oj} < 0$) in each j-th contact pair is denoted. The number of rows of the matrices P_N, P_T and the length of the vector d_o is equal to the number of contact points of a VD. Each pair of rows of the matrices P_N, P_T yields a normal and tangential constraint upon the displacements of the contact points. A tangential constraint is to be considered only if a corresponding normal constraint is active, i.e., if it is satisfied as an equality. Moreover, a tangential constraint is to be considered only if a corresponding tangential contact interaction force doesn't exceed its critical value defined by the Coulomb friction law (friction coefficient k_f). Otherwise a tangential constraint isn't taken into account assuming the tangential force being equal to its critical value.

Formally the above considerations can be presented employing the Lagrange multipliers (see Chap. 3.6). For the analysis of the obtained equations the techniques presented in Chap.3.6 are applied, or these equations are reduced accordingly with the techniques of Chap.1.2.

6.2.2 Vibrodrives with continuous contact area

Consider a VD as a two-body system A and B interacting by continuous parts of their surfaces, Fig.6.2. Assume a rigid body B being an output link of a VD with one or several motional d.o.f. A vibrating elastic body A presents an input link of a VD.

We'll present a problem formulation taking on account only small displacements of an input link. If the shape of an output link and its constraints ensure that the contact area doesn't change in space during a rigid-body motion, (e.g., a cylinder rotating around its symmetry axis or a rod moving in its longitudinal direction), the model in Fig.6.2 can be employed for finite displacements of an output link, too.

Denote a contact surface through S and assume it being continuous. If S consists of a finite number of continuous parts, the following considerations are valid for each part separately.

The contact interaction is not necessary in all points of S

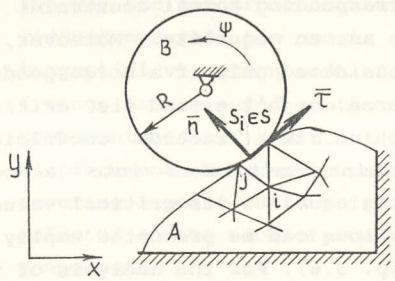

Fig.6.2 Surface contact vibrodrive

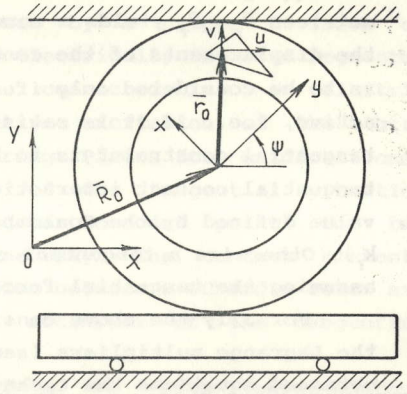

Fig.6.3 Displacements of an internal point of a finite element of a vibrodrive link moving as a rigid body

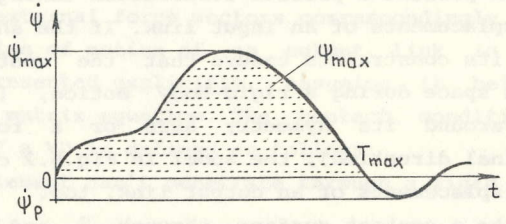

Fig.6.4 Time-law of the velocity of an output link in the step-motion mode

at an arbitrary time instant. Nevertheless, a contact interaction is possible at these points as a result of small displacements of the points of an input link. Assume a function $d(x,y)$ defining an initial distance between the contact surface points when no vibration is present. The values of $|d(x,y)|$ are of the same magnitude order as displacements, i.e., significantly less than the size of a finite element (FE). The negative values of $d(x,y)$ denote a prestressed condition.

Consider a mechanical contact interaction between the links of a VD. Electromechanical forces exciting a vibration of an input link are presented by a nodal force vector $-T\Phi$, and the equations of motion of a VD are presented as

$$\begin{cases} M\ddot{U} + C\dot{U} + KU = -T\Phi + F + \begin{bmatrix} \vdots \\ F_k \\ \vdots \end{bmatrix}, \\ J\ddot{\psi} + c(\dot{\psi}) = -M_e - M_k(F_k), \end{cases} \qquad (6.26)$$

where F_k – nodal force vector, J – centroidal moment of inertia of an output link, $c(\dot{\psi})$ – fluid friction force momentum, M_e – external force momentum applied to an output link, $M_k(F_k)$ – momentum produced by contact interaction forces.

The third term on the right-hand side of the system (6.26) signifies that the components of F_k are distributed through its entire length, according to the numbering of nodes. The second equation of (6.26) is presented assuming that an output link has only one motional d.o.f. In the case of several d.o.f. this equation is replaced by the system of equations of motion of a rigid body subjected to contact interaction and other external forces.

Consider the part S_i of the contact surface corresponding to the side of the i-th FE. The constraints imposed upon the displacements of each surface point of a FE are

$$\begin{cases} n^T(s)\,u(s) \le d(s), \\ \dot{\tau}^T(s)\,\dot{u}(s) - R\dot{\psi} = 0, \end{cases} \qquad (6.27)$$

where $u(s)=\begin{pmatrix}u\\v\end{pmatrix}$ - displacement vector of the surface point $s(x,y)$ in the directions of the global reference system Oxy , and the unity vectors of the local reference system at the considered point are $n_{2\times 1}$, $\tau_{2\times 1}$, where n is normal to S_i . Denoting through N_i the form function matrix corresponding to the element side S_i, the dynamic equation of the i-th FE with the constraints is presented as

$$\begin{cases} M^i\ddot{U}^i + C^i\dot{U}^i + K^iU^i = -T^i\Phi^i + F^i - \int_{S_i} N_i^T\, n\, \lambda_N^i\, ds - \int_{S_i} N_i^T\, \tau\, \lambda_T^i\, ds , \\ J\ddot{\psi} + c(\dot{\psi}) = -M_c + R\sum_i\left[\int_{S_i}\tau\,\lambda_T^i\,ds\right] , \qquad (6.28) \\ n^T(s)\,N_iU^i = d(s) , \qquad (6.28.3) \\ \tau^T(s)\,N_iU^i - R\,\psi = \tau^T(s)\,N_i(s)U_o^i - R\,\psi_o(s) , \qquad (6.28.4) \end{cases}$$

where the index i signifies that the matrices and vectors are related to the i-th FE, the constraints (third and fourth relation of (6.28)) are to be satisfied at each point s of the side S_i . The nodal displacement vector $U_o^i(s)$ defining the displacement values at an instant when the contacting points begin to move together without sliding is in general different for each surface point s , because the sliding conditions are not the same at each point of the element side.

If instead of requiring to satisfy the constraints at each point of an element side we require only to satisfy the projections of these constraints to upon the subspace of the functions N_i , the constraints of (6.28) are presented as

$$\int_{S_i} N_i^T\, n^T(s)\, N_i\, ds\, U^i = \int_{S_i} N_i^T ds , \qquad (6.28.3)'$$

$$\int_{S_i} N_i^T\tau^T(s)N_i\,ds\,U^i - R\psi\int_{S_i} N_i^T ds = \int_{S_i} N_i^T\tau^T(s)N_iU_c^i(s)ds - R\int_{S_i} N_i^T\psi_o\,ds , \qquad (6.28.4)'$$

The values of the normal and tangential forces λ_N^i , λ_T^i at

each point s of the side S_i are approximated through the nodal values of these forces by employing the functions N_i as

$$\lambda_N^i = N_i\,\Lambda_N^i , \quad \lambda_T^i = N_i\,\Lambda_T^i .$$

Taking on account that the normal interaction force $\lambda_N^i(s)$ can't be negative, and the magnitude of the tangential force $\lambda_T^i(s)$ can't exceed its critical value $k_f\lambda_N^i(s)$, denote

$$n(s) = \begin{cases} n(s), \text{ for all } s \text{ , where } \lambda_N^i(s) > 0, \\ 0 \quad \text{, otherwise ;} \end{cases}$$

$$\hat{\tau}(s) = \begin{cases} \tau(s), \text{for all } s, \text{ where } \lambda_N^i(s)>0 \text{ and } |\lambda_T^i(s)|<k_f\lambda_N^i(s) , \\ 0 \quad \text{, otherwise ;} \end{cases}$$

$$\hat{n}(s) = \begin{cases} n(s) \text{ for all } s, \text{ where } \lambda_N^i(s)>0 \text{ and} |\lambda_T^i(s)|<k_f\lambda_N^i(s) , \\ \qquad\qquad\qquad\qquad\qquad\qquad \text{(no sliding)} , \\ n(s)+k_f\tau(s)\,\mathrm{sign}\lambda_T^i(s) \text{ for all } s, \text{where } \lambda_N^i(s)>0 \text{ и} \\ \qquad\qquad\qquad |\lambda_T^i(s)|\ge k_f\lambda_N^i(s) \text{ , (sliding)} , \\ 0 \quad \text{, otherwise ;} \end{cases}$$

$$P_N^i = \int_{S_i} N_i^T n^T(s) N_i\,ds ; \quad \hat{P}_N^i = \int_{S_i} N_i^T\hat{n}^T(s)N_i\,ds ; \quad P_T^i = \int_{S_i} N_i^T\hat{\tau}^T(s)N_i\,ds .$$

Taking on account the above notations, the system (6.28) for a single FE is presented as

$$\begin{cases} M^i\ddot{U}^i + C^i\dot{U}^i + K^iU^i = -T^i\Phi^i + F^i - \hat{P}_N^{iT}\Lambda_N^i - \hat{P}_T^{iT}\Lambda_T^i , \\ J\ddot{\psi} + c(\dot{\psi}) = -M_c + R\sum_i\left[\int_{S_i}\tau N_i ds\,\Lambda_T^i\right] , \\ P_N^iU^i = \int_{S_i} N_i d(s)ds , \\ \hat{P}_T^iU^i = \hat{P}_T^i\int_{S_i} N_i^T\hat{\tau}^T(s)N_iU_o^ids - R\int_{S_i} N_i^T\psi_o(s)ds , \end{cases} \quad (6.29)$$

similar to the point-contact interaction case.

Having obtained such equation systems as (6.29) for all the FE of the contact surface, a global matrices should be assembled following the common procedure of the finite element method. The obtained structural equation system is solved iteratively at each numerical integration time point, until the actual contact interaction and sliding zones are obtained.

6.2.3 Travelling wave vibrodrives

In continuous contact area VD ring-type VC are usually employed. By means of a multi-phase excitation law a high-frequency vibration imitating an elastic displacement wave travelling along a circumference of a ring can be obtained. As a result of an interaction with an output link and with an external constraint a rigid-body motion and (or) a motion of an output link is obtained, Fig.6.1f. The division of the electric terminals shown in Fig.6.1e,f enables to excite two modal vibrations of a ring simultaneously, the axes of two elliptical shapes of a standing wave being perpendicular to each other [116]. If the phase shift between the two vibration components is equal to $\frac{\pi}{2}$, a rotating elliptical shape is obtained, the rotation angular frequency being half of the vibration angular frequency.

A mathematical model of a travelling wave VD can be presented employing the system (6.28), considering each point on the ring circumference as a contact point. However, the dimensions of the matrices P_N and P_T increase significantly.

Employing semianalytic FEM procedures [44], models of lower dimension can be obtained. In this case only a two-dimensional area of the radial section of a ring is discretized into FE, Fig.6.1g. The displacements $\begin{pmatrix} u \\ v \\ w \end{pmatrix}$ of each FE point of this section in radial, axial and circumferential directions are presented as

$$\begin{pmatrix} u \\ v \\ w \end{pmatrix} = G(\varphi)\begin{pmatrix} u \\ v \\ w \end{pmatrix}_A , \quad (6.30)$$

where a functional relation of the displacements from the polar angle φ is expressed as a superposition of some basic functions $G(\varphi)$. Employing harmonic functions, $G(\varphi)$ appears as

$$G_a(\varphi) = \left[I_a, I_a\cos\varphi, I_a\sin\varphi, \ldots, I_a\cos(h-1)\varphi, I_a\sin(h-1)\varphi\right] \quad (6.31)$$

where I_a - the unity matrix of the dimension 3x3.

The generalized displacement vector $\begin{pmatrix} u \\ v \\ w \end{pmatrix}_A$ at each point of a FE consists from triplets of coefficients at each basic function and is presented as $\begin{pmatrix} u \\ v \\ w \end{pmatrix}_A^T = \left[\begin{pmatrix} u \\ v \\ w \end{pmatrix}_1^T, \begin{pmatrix} u \\ v \\ w \end{pmatrix}_2^T, \ldots, \begin{pmatrix} u \\ v \\ w \end{pmatrix}_{2h-1}^T\right]$. It is expressed through generalized nodal displacements as

$$\begin{pmatrix} u \\ v \\ w \end{pmatrix}_i^T = N(r,z)\,U_i ,$$

where $N(r,z)$ - a usual form function matrix of a FE.

In general, the relation between the displacements at each point of a FE and its generalized nodal displacements appears as

$$\begin{pmatrix} u \\ v \\ w \end{pmatrix}_A = G_a(\varphi)\begin{bmatrix} N & & \\ & N & \\ & & \ddots \\ & & & N \end{bmatrix} U_A = G_a(\varphi)\,\mathrm{diag}N\,U_A . \quad (6.32)$$

The structural equations of motion are assembled employing a common procedure of the finite element method and can be presented as

$$\begin{cases} M_A\ddot{U}_A + C_A\dot{U}_A + K_A U_A = -T_A\Phi_A + F_A \,, \\ G_m(\varphi)\ \mathrm{diag}P_N\ U_A \le d \,, \\ G_m(\varphi)\ \mathrm{diag}P_T\ \dot{U}_A = 0 \,, \end{cases} \tag{6.33}$$

where $\mathrm{diag}\ P = \begin{bmatrix} P & & & \\ & P & & \\ & & \ddots & \\ & & & P \end{bmatrix}$, $G_m(\varphi) = \underbrace{[I_m, I_m\cos\varphi,\ I_m\sin\varphi, \ldots]}_{2m-1}$,

m - the number of rows of the matrix P_N.

Replacing the requirement of satisfying the constraints in (6.33) for each value of φ by the requirement of satisfying only the projections of these constraints upon the basic function subspace $G_m(\varphi)$, the following constraints are obtained:

$$\begin{cases} \int_0^{2\pi} G_m^T G_m\,\mathrm{diag}P_N\ r\,d\varphi\ U_A \le \int_0^{2\pi} G_m^T\ r\,d\varphi \\ \int_0^{2\pi} G_m^T G_m\,\mathrm{diag}P_T\ r\,d\varphi\ \dot{U}_A = 0 \,. \end{cases} \tag{7.33}'$$

The expressions of the normal and tangential contact forces are approximated as

$$\lambda_N(\varphi) = G_m(\varphi)\ \Lambda_{NA} \,, \quad \lambda_T(\varphi) = G_m(\varphi)\ \Lambda_{TA} \,. \tag{6.34}$$

In order to obtain time laws of a VD motion, numerical integration techniques for the unilaterally constrained structures are to be employed (see Chap.3.6). Employing the dynamic reduction (see Chap. 1.2), the contact forces Λ_N, Λ_T, Λ_{NA}, Λ_{TA} can be expressed as nonlinear functions of the displacements. The obtained dynamic structural equation with a nonlinear term can be approached employing the numerical integration techniques of Chap.3.1, 3.2, 3.3, 4.1 and averaging techniques of Chap.4.2, 4.3 .

In general, each link of a VD not only performs elastic vibrations, but also moves as a rigid body. Therefore sometimes the presentation of a VC dynamics by the matrices M, C and K of a small displacement model appears as insufficient, because of disregarding of finite rotations. A full dynamic model is obtained by deriving the FEM relations in a moving reference system, Fig.6.3 [40].

Consider a fixed reference system of axes OXY and a moving reference system oxy connected with an elastic body. A position of each point of FE in space is determined by the position vector

$$R = R_o + r_o + u, \tag{6.35}$$

where R_o - position vector of the origin of the moving reference system , r_o - position vector of a FE point of an undeformed structure in the moving reference system , u - displacement vector of this point due to structural deformation.

The directions of the axes of the moving reference system oxy aren't constant and at each time instant they are determined by the rotation angle ψ. According to the Coriolis theorem, a full acceleration of a FE point is expressed as

$$\frac{d^2R}{dt^2} = \ddot{R}_o + \ddot{u} + \dot{\Omega}xr_o + \dot{\Omega}xu + 2\Omega xu + \Omega x(\Omega xr_o) + \Omega x(\Omega xu) \tag{6.36}$$

where $\ddot{u}$ - relative acceleration (measured in the moving reference system), and $\Omega = \dot{\psi}$ - angular rotation velocity of the body and of the moving system.

The equilibrium equations of a moving elastic body are

$$\begin{cases} \int_V \rho\,\dfrac{d^2R}{dt^2}\,dV = F_{ext} \,, \\ \dfrac{d}{dt}\int_V \rho\left[R x \dfrac{dR}{dt}\right] dV = M_{ext} \,, \\ \int_V \delta\varepsilon^T \sigma\,dV + \int_V \rho\,\delta u^T \dfrac{d^2R}{dt^2}\,dV + \int_V \delta u^T f_b\,dV = 0 \,, \end{cases} \tag{6.37}$$

where ε - strain, σ - stress, f_b - volume force, F_{ext} - principal

vector of external forces acting upon an elastic body, M_{ext} - principal external force momentum with respect to the origin of the system oxy.

The first equation of (6.37) expresses D'Alembert's principle for a system of material points, the second - angular momentum theorem, and the third - virtual work principle for internal, external and inertia forces acting upon an elastically deformed body. In each equation volume integrals are obtained by integrating through the body volume V that is assumed to be constant because of small displacements and strains.

The displacements u of an arbitrary point of a FE can be expressed through the nodal displacements U as $u = NU$ employing a form function matrix N, the strains ε - through the nodal displacements as $\varepsilon = BU$, and the stresses σ - through the strains as $\sigma = c^E \varepsilon$ and substituting into (6.37), we obtain an equation of motion for a single FE as

$$\begin{bmatrix} M^e_{rr} & M^e_{r\psi} & M^e_{re} \\ M^{eT}_{r\psi} & M^e_{\psi\psi} & M^e_{\psi e} \\ M^{eT}_{re} & M^{eT}_{\psi e} & M^e_{ee} \end{bmatrix} \begin{pmatrix} \ddot{U}^e \\ \ddot{\psi} \\ \ddot{U}^e_e \end{pmatrix} + \begin{bmatrix} 0 & 0 & 0 \\ 0 & 0 & 0 \\ 0 & 0 & K^e_{ee} \end{bmatrix} \begin{pmatrix} U^e \\ \psi \\ U^e_e \end{pmatrix} = \begin{pmatrix} W^e_r(\dot{\psi}, \dot{U}^e_e, U^e_e) \\ W^e_\psi(\dot{\psi}, \dot{U}^e_e, U^e_e) \\ W^e_e(\dot{\psi}, \dot{U}^e_e, U^e_e) \end{pmatrix} + \begin{pmatrix} \Sigma F^e_{ext} \\ \Sigma M^e_{ext} \\ F^e_{ext} \end{pmatrix}, \quad (6.38)$$

where $M^e_{rr} = \begin{bmatrix} m & 0 \\ 0 & m \end{bmatrix}$, $m = \int_V \rho dV$ - mass of FE;

$M^e_{r\psi} = \begin{bmatrix} 0 & -1 \\ 1 & 0 \end{bmatrix} (r + \tilde{m}U^e)$, $r = \int_V \rho \begin{pmatrix} X_o \\ y_o \end{pmatrix} dV = \tilde{m}X$, $\tilde{m} = \int_V \rho N dV$, X^e - vector containing the nodal point coordinates of a FE, where $\begin{pmatrix} X_o \\ y_o \end{pmatrix} = NX^e$;

$M^e_{re} = \tilde{m}$;

$M^e_{\psi\psi} = J + 2\tilde{r}^T U^e + U^{eT} M^e_{ee} U^e$, $\tilde{r} = \int_V \rho N^T \begin{pmatrix} X_o \\ y_o \end{pmatrix} dV = M^e_{ee} X^e$,

$J = \int_V \rho (x_o^2 + y_o^2) dV = X^{eT} M^e_{ee} X^e$ - moment of inertia of a FE with respect to the origin of the moving reference system oxy;

$M^e_{\psi e} = \hat{r}^T + \tilde{M}^e_{ee} U^e$, $\hat{r} = \int_V \rho N^T \begin{bmatrix} 0 & -1 \\ 1 & 0 \end{bmatrix} \begin{pmatrix} X_o \\ y_o \end{pmatrix} dV = \tilde{M}^e_{ee} X$, $\tilde{M}^e_{ee} = \int_V \rho N^T \begin{bmatrix} 0 & -1 \\ 1 & 0 \end{bmatrix} N dV = -\tilde{M}^{eT}_{ee}$;

$M^e_{ee} = \int_V \rho N^T N dV = M^{eT}_{ee}$ - mass matrix of a FE;

$K^e_{ee} = \int_V B^T c^E B dV$ - stiffness matrix of a FE;

$W^e_r(\dot{\psi}, \dot{U}^e_e, U^e_e) = 2\begin{bmatrix} 0 & -1 \\ 1 & 0 \end{bmatrix} \tilde{m}\dot{U}\dot{\psi} + \tilde{m}(X^e + U^e)\dot{\psi}^2$;

$W^e_\psi(\dot{\psi}, \dot{U}^e_e, U^e_e) = -2(X^e + U^e)^T M^e_{ee} \dot{U}\dot{\psi}$;

$W^e_e(\dot{\psi}, \dot{U}^e_e, U^e_e) = 2\begin{bmatrix} 0 & -1 \\ 1 & 0 \end{bmatrix} \tilde{m}\dot{U}\dot{\psi} + \tilde{m}(X^e + U^e)\dot{\psi}^2$;

F^e_{ext} - vector of external forces acting upon a FE;

ΣF^e_{ext} - principal vector of FE nodal forces;

ΣM^e_{ext} - principal momentum of FE nodal forces with respect to the origin of the moving reference system.

A model presented by the matrix equation (6.38) possesses excessive d.o.f. because K and M are the matrices of an unconstrained structure. In order to eliminate the excessive d.o.f., a set of constraints can be introduced. An alternative approach for eliminating these d.o.f. is obtained considering the elastic displacements in modal coordinates. Representing the eigenfrequency vector as $(\omega_o^2, \omega_1^2, \omega_2^2)$ and an eigenform matrix as $[\Delta_o, \Delta_1, \Delta_2]$, we delete from consideration the zero eigenfrequencies ω_o^2 and the corresponding rigid body eigenforms Δ_o. Truncating the dynamic contributions of higher modes, we obtain the equation

$$\begin{bmatrix} M_{rr} & M_{r\psi} & \Delta_1 M_{re} & \Delta_2 M_{re} \\ M_{r\psi}^T & M_{\psi\psi} & \Delta_1 M_{\psi e} & \Delta_2 M_{\psi e} \\ \Delta_1^T M_{re}^T & \Delta_1^T M_{\psi e}^T & I & 0 \\ \Delta_2^T M_{re}^T & \Delta_2^T M_{\psi e}^T & 0 & 0 \end{bmatrix} \begin{pmatrix} \ddot{U} \\ \ddot{\psi} \\ \ddot{Z}_1 \\ \ddot{Z}_2 \end{pmatrix} + \begin{bmatrix} 0 & 0 & 0 & 0 \\ 0 & 0 & 0 & 0 \\ 0 & 0 & \mathrm{diag}(\omega_{1i}^2) & 0 \\ 0 & 0 & 0 & \mathrm{diag}(\omega_{2i}^2) \end{bmatrix} \begin{pmatrix} U \\ \psi \\ Z_1 \\ Z_2 \end{pmatrix} =$$

$$= \begin{pmatrix} W_r(\psi,\dot{U}_e,U_e) \\ W_\psi(\psi,\dot{U}_e,U_e) \\ \Delta_1^T W_e^e(\psi,\dot{U}_e,U_e) \\ \Delta_2^T W_e^e(\psi,\dot{U}_e,U_e) \end{pmatrix} + \begin{pmatrix} \Sigma F_{ext} \\ \Sigma M_{ext} \\ \Delta_1^T F_{ext} \\ \Delta_2^T F_{ext} \end{pmatrix} \qquad (6.39)$$

The obtained equation presents a full mathematical model of an elastic moving link of a VD. In many cases there is no need to take account for all the terms appearing in the equation. A reduction of (6.39) omitting the terms W_r, W_ψ, W_e containing $\dot{\psi}$ as factors is possible due to a negligible magnitude of the angular velocity. The terms connecting the elastic and rigid body displacement values can often be omitted, too. In such a case the mass matrix blocks take the form $M_{re}=0$, $M_{\psi e}=0$, $M_{\psi\psi}=J$, $M_{r\psi}^e=\begin{bmatrix}0 & -1\\ 1 & 0\end{bmatrix} r$.

The equation of motion of each VD link being (6.38) or (6.39), the mechanical contact between the links is described by employing unilateral or bilateral constraints

$$\begin{cases} P_N(\psi)\dot{U}_e \le d(\psi,\dot{U}_r) \\ P_T(\psi)\dot{U}_e = 0 \end{cases} .$$

The time laws of a VD motion are obtained by applying to the above equations the techniques of Chap.1-4.

6.4 DYNAMIC CHARACTERISTICS OF VIBRODRIVES

In order evaluate quantitatively the operation of VD, the dynamic characteristics are employed. The analysis of VD is carried out in two operation modes - a stationary motion and a step motion mode.

The stationary motion mode is obtained by applying a periodic excitation law (pulse series or harmonic) to an input link, the excitation frequency being in the vicinity of a mechanical resonance of an input link in order to obtain greater vibration amplitudes.

The step motion mode is obtained by applying to an input link separate pulses, pulse packages or several periods of a harmonic excitation law. In the latter case a transient vibration of VD links is of primary importance. It can have have a positive as well as a negative influence upon the operational characteristics of a VD.

The quantities evaluating operation parameters of a VD can be presented by averaged characteristics of motion, the construction features, maintenance features, etc. Nevertheless, here we present quantities evaluating the VD on the base of a mathematical model. They are obtained by means of a structural dynamic equation analysis of a VD.

The dynamic characteristics of a stationary motion mode are obtained considering the stationary motion law of a model. The formulas are presented for the point-contact interaction case and for a VD with a single d.o.f. of an output link. If an output link has more than one d.o.f., similar characteristics should be obtained for each displacement component of the output link. In the case of a continuous contact area of a VD, in the following formulas the surface integrals should be employed.

There are following dynamic characteristics of d VD in the stationary motion mode.

1. Mean velocity of an output link

$$\dot{\psi}_c = \frac{1}{T}\int_0^T \dot{\psi}\, dt ,$$

where ψ - displacement of an output link, T - input link vibration period.

2. Output velocity variation. Mean and root-mean-square (rms) ratios can be employed:

$$\delta\dot{\psi}_c = \frac{\Delta\psi}{\dot{\psi}_c}, \quad \delta\dot{\psi}_{ck} = \frac{1}{T}\int_0^T \left[1 - \frac{\dot{\psi}}{\dot{\psi}_c}\right]^2 dt .$$

The time interval for measuring a deviation $\Delta\psi$ can be taken equal to one vibration period. However, it isn't much sense to employ such a short time interval because usually $\Delta\psi$ is an infinitesimal of higher order in comparison with $\dot{\psi}_c$, and, as a result, $\delta\psi \approx 0$. As a rule, the time interval significantly exceeding the vibration period T is employed, and the obtained deviation $\Delta\dot{\psi}_c$ can be caused, e.g., by the irregularity of geometric parameters of a VD.

3. Mean torque in the case of an output link with a rotational d.o.f. :

$$M_{k.c} = \sum_i \frac{R_i}{T}\int_0^T \lambda_{Ti}\, dt ;$$

mean force in the case of a linearly moving output link

$$F_c = \sum_i \frac{1}{T}\int_0^T \lambda_{Ti}\, dt ,$$

where λ_{Ti} - tangential contact force at the i-th contact interaction point.

4. Mean normal interaction force between an input and output link (a prestressing force in a contact zone).

$$N_c = \sum_i \frac{1}{T}\int_0^T \lambda_{Ni}\, dt ,$$

where λ_{Ni} - normal contact interaction force at the i-th contact point.

5. Amount of work during one vibration period. In the case of an output link with a rotational d.o.f.

$$A_n = \int_0^T M_{k.c}\,\dot{\psi}\, dt .$$

In the case of a linearly moving output link in place of $M_{k.c}$ and $\dot{\psi}$ the values of F_c and of a linear velocity $\dot{u}$ should be substituted.

6. Amount of work A_T done by tangential interaction forces during one vibration period.

7. Efficiency

$$\eta = \frac{A_n}{A_n + A_T + A_{el} + A_{therm}} ,$$

where A_{el} - electrical losses and A_{therm} - thermal losses.

If a mathematical model of a VD is investigated, a mechanical efficiency value obtained by considering only mechanical work is often employed:

$$\eta = \frac{A_n}{A_n + A_T} .$$

In the step motion mode the following characteristics are employed (Fig.7.4):

$$l_1 = \psi_{max}, \quad l_2 = T_{max}, \quad l_3 = \left|\frac{\dot{\psi}_{max}}{\dot{\psi}_p}\right| ,$$

where ψ_{max} - maximum displacement of an output link; T_{max} - motion time of an output link in forward direction until the first stop; $\dot{\psi}_{max}$ - maximum velocity of an output link in forward direction; $\dot{\psi}_p$ - maximum velocity of an output link in backward direction caused by transient motions of VD links.

7. ANALYSIS AND SYNTHESIS OF VIBRODRIVES

In this chapter the dynamic analysis of vibrodrives (VD) is carried out employing the techniques presented in Chap.1-4 and the mathematical models presented in Chap.7.

The free and forced impact vibration of a rod-type vibroconverter (VC) is investigated employing the finite element model and phenomenological contact interaction models. The complex friction laws are presented as a superposition of the Coulomb, linear and cubic components. Employing the time-averaging and numerical integration techniques a step motion of vibration-controlled kinematic pairs (VCKP), free and forced motion of VD are investigated employing the lumped-mass as well as finite element mathematical models. An analysis of a VD with an internal impact interaction pair employing purely longitudinal vibration of a VC is carried out. VC shape synthesis problems are solved employing the optimal design techniques.

The techniques presented in Chap.5 enabled to obtain the optimal control laws and feedback circuit parameters in order to damp transient vibrations occurring due to the externally excited stepwise increments of longitudinal elastic deformation.

The following original results are presented in this chapter:

- the impact interaction of a discrete mechanical system approximating the continuous one is shown to be elastic, irrespectively of the restitution coefficient values in the vicinity of the contact point. It is reasonable to employ the rheological model of the dynamic contact interaction, if the stiffness coefficient of the model exceeds the static stiffness of the structure at the contact point less than to one order (10 times). Otherwise the impact vibration law doesn't depend upon the local contact condition, and it appears preferable to represent the problem employing unilateral constraints rather than by means of the suggested nonlinear repulsive contact force. The numerical examples show, that an extension of a generalized Newmark's numerical integration scheme in order to take account for unilateral constraints retain the asymptotic features of the original one. Analysis of free impact vibrations carried out on the reduced dynamic models compared with the results obtained employing the full model justify the validity of the dynamic

reduction approach . It is based upon the truncation of the dynamic contributions of higher modes of the linear part, simultaneously retaining their quasistatic contributions and the approximately evaluated dissipation forces (see Chap.1);

- analysis of longitudinal resonant impact-vibrations of a VC employing time-averaging techniques has shown that the solution considering two Fourier components time-averaged equations present satisfactory results only in the case of a two-mass elastic system. For obtaining reliable results when considering structural models, at least four Fourier components are to be taken on account;

- it has been shown that the motion of VCKP links can be controlled employing tangential vibrations in the contact zone. The values of the normal contact interaction forces are obtained ensuring the equal slopes of an output link velocity pulse. The amplitude-frequency characteristics (AFCH) of the input link vibration and the velocity-frequency characteristics of the output link in the stationary motion mode have been obtained, the duration of transient vibration being dependent upon a Q-factor value of a VC and upon the mass of an output link;

- a dynamic behavior of the finite element model of the VCKP with the magnetostrictive input link and two friction contact points has been investigated. Such an VCKP isn't sensitive to the modulation depth of the normal force and to the curve shape of a friction law;

- investigating the system of two elastically connected masses impacting upon each other under harmonic excitation law and moving upon a rough surface, the directive motion of a system as of a whole has been obtained. The direction of motion can be reversed by an appropriate adjustment of the Coulomb friction coefficient value;

- employing two-dimensional vibration paths of the contact points of a VD at stepwise and stationary motion modes the amplitude-frequency, velocity-frequency, motional force-output velocity, mechanical efficiency relations and the feasibility area of stationary motion laws have been obtained;

- asymmetric vibration cycles in the ring-type VC are excited by means of adjusting the geometric parameters of a bimorfic ring in order to obtain multiple eigenfrequencies. The

locations of asymmetrically vibrating points on the circumference of a ring are preconditioned by an excitation level of the corresponding modal vibration.

- asymmetric vibration cycles in rod-type VC are obtained by means of an optimal shape synthesis techniques in order to satisfy necessary eigenfrequency and eigenform relations. The shape forms for asymmetric vibration cycle concentrators and vibration cycle transformers have been obtained.

- a VC producing asymmetric vibration under harmonic excitation have been obtained by means of supplying the VC with an internal impact interaction pair;

- the programmed and closed-loop control laws have been obtained ensuring the damping of transient vibrations occurring due to the externally excited stepwise increments of a longitudinal elastic deformation of a VC ;

- investigating the models of VCKP controlled by a varying normal force, the complex friction laws ensuring the equal slopes of an output link velocity pulse have been obtained. In the case of a high normal force modulation frequency value a stationary motion mode has been obtained, the control of the velocity and acceleration values being possible by means of the width-modulated pulses of the normal force.

7.1 FREE AND FORCED VIBRATION OF SYSTEMS WITH NORMAL INTERACTION

The free impact vibration of a cantilever beam VC. Here we consider finite element models of several discretization levels, Fig.7.1. If the number of elements NEL=1 , the model presents a mass attached to a spring. By increasing the number of elements the number of d.o.f. increases and a structure approximating the dynamics of the VC with distributed parameters is obtained. In an undeformed state, the constraint coincides with the right-hand end of the VC. At the initial state the VC is compressed by the force F_n, and released at the time instant t=0. The time laws of the displacements of the model during the free impact vibration depend upon the discretization level as well as upon local contact conditions. The computed results are presented in terms of the following dimensionless quantities: displacement

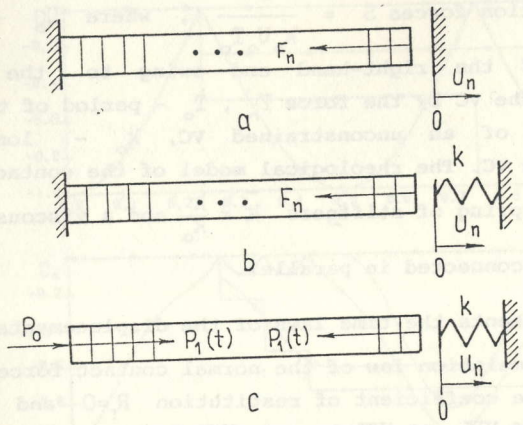

Fig.7.1 Finite element models of vibroconverters

of the right-hand end $\bar{U}_n = \frac{U_n}{U_o}$, time $\bar{t} = \frac{t}{t_o}$, impetus of normal contact interaction forces $\bar{S} = \frac{S}{k_o U_o T_o}$, where U_o - initial displacement of the right-hand end owing to the initial compression of the VC by the force F_n, T_o - period of the first vibration mode of an unconstrained VC, k_o - longitudinal stiffness of the VC. The rheological model of the contact pair is presented by a spring of stiffness $\bar{k} = \frac{k}{k_o}$ and a viscous damping element $\bar{c} = \frac{c}{kT_o}$ connected in parallel.

Fig.7.2 presents the time laws of the displacements $\bar{U}_n$ and the impetus accumulation law of the normal contact forces $\bar{S}$ for the values of the coefficient of restitution R_f=0 and R_f=1 at several values of NEL. At NEL=1 and NEL=2 the finite element model of the VC presents one- and two-mass elastic structures correspondingly. The internal damping is assumed to be very small. We investigate the influence of the coefficient of restitution R_f upon the dynamic behavior of the structure.

At R_f=0 the energy dissipation level is high, and the accumulated impetus of the contact forces is significantly lower than at R_f=1 . Obviously, the energy of the structure isn't conserved because of the perfectly plastic local impact condition of the point mass at the right-end of the model. The larger amounts of mass of the structure is concentrated at the contact point, the more energy is lost at each impact interaction, and the greater is the rate of the mechanical energy decrease (if NEL=1 , the energy equals to zero after the very first impact). By increasing the number of elements, i.e., by approaching the distributed parameter model of the VC, the motion law becomes less and less dependent upon the coefficient of restitution R_f . If R_f>0 , each impact presents a series of microimpacts (quasi-plastic impact,[122]). It follows that in general the impact of an elastic structure is always elastic, independently of the value of the restitution coefficient in the vicinity of the contact area.

The free impact vibration has been investigated, employing the rheological contact interaction models, Fig.7.1b. Fig.7.3

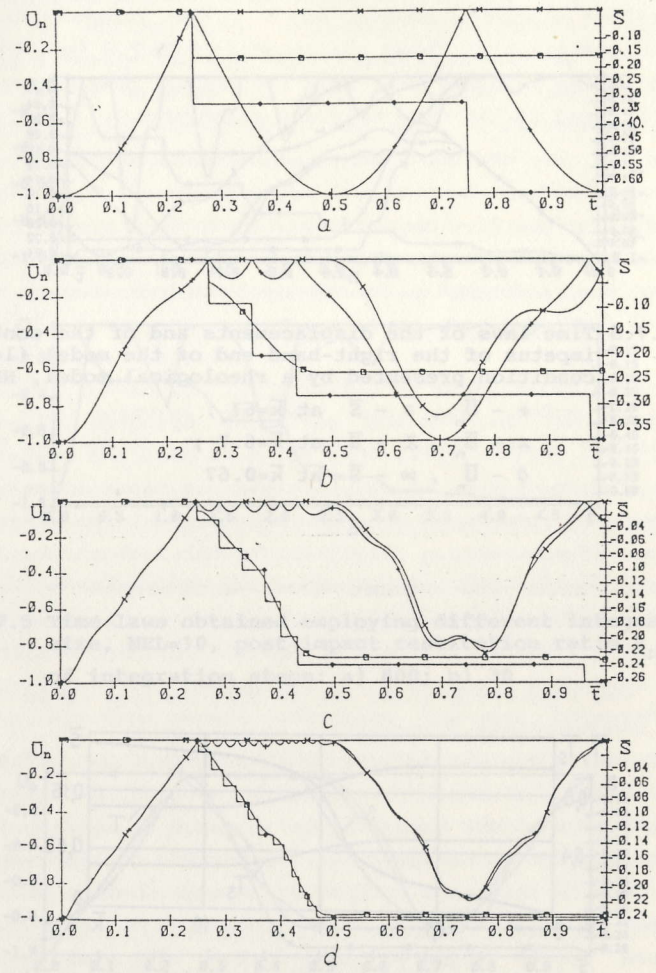

Fig.7.2 Time laws of the displacements and of the contact force impetus of the right-hand end of the model (absolutely rigid local contact condition)
+ - $\bar{U}_n$ at R_f=0, ◊ - $\bar{S}$ at R_f=0;
x - $\bar{U}_n$ at R_f=1, □ - $\bar{S}$ at R_f=1;
a)NEL=1; b)NEL=2; c)NEL=5; d)NEL=10

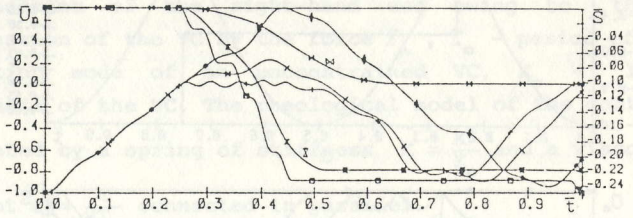

Fig.7.3 Time laws of the displacements and of the contact force impetus of the right-hand end of the model (local contact condition presented by a rheological model, NEL=5)

+ - $\bar{U}_n$, □ - $\bar{S}$ at $\bar{k}$=67 ;

x - $\bar{U}_n$, ⊠ - $\bar{S}$ at $\bar{k}$=6.7 ;

◊ - $\bar{U}_n$, ⋈ - $\bar{S}$ at $\bar{k}$=0.67

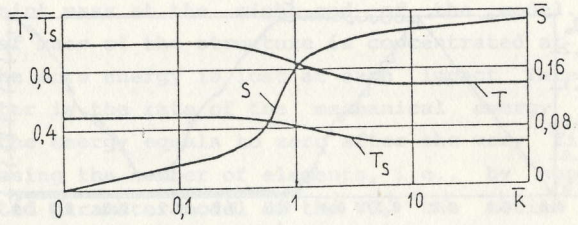

Fig.7.4 Free impact vibration characteristics related to the stiffness coefficient of the contact rheology, NEL=10: $\bar{T}$ - free impact vibration period; $\bar{T}_e$ - contact time during one vibration period; $\bar{S}$ - contact force impetus during one vibration period

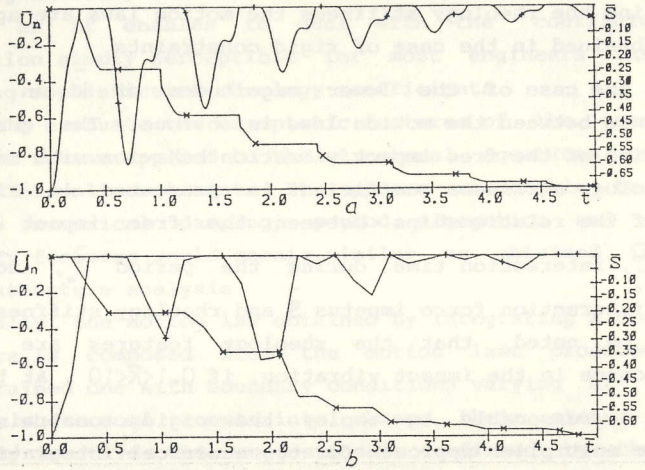

Fig.7.5 Time laws obtained employing different integration step size, NEL=10, post-impact restitution ratio R_f=0, number of integration steps: a) 800; b) 30

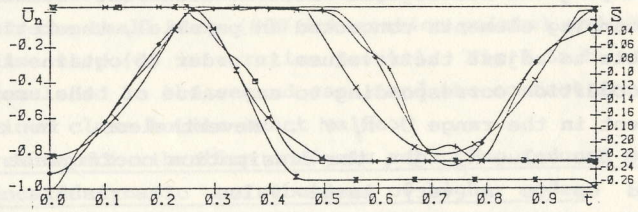

Fig.7.6 Time laws of the displacements and of the contact force impetus of the right-hand end of the model. Absolutely rigid local contact condition, number of elements NEL=10:

+ - $\bar{U}_n$, □ - $\bar{S}$ - full model, R_f=0 ;

x - $\bar{U}_n$, ⋈ - $\bar{S}$ - reduced model, single dynamic d.o.f;

◊ - $\bar{U}_n$, ⊠ - $\bar{S}$ - reduced model, two dynamic d.o.f

presents the time laws of the displacements and of the accumulated normal interaction force impetus at several values of the rheology stiffness coefficient $\bar{k}$. The comparison of the obtained results with those presented in Fig.7.2 implies that by increasing the rheology stiffness the motion laws are approaching those obtained in the case of rigid constraints.

In the case of the lower magnitudes of $\bar{k}$ an essential difference between the motion laws is obvious. The quantitative evaluation of the free impact vibration behavior with respect to the rheology stiffness coefficient is presented in Fig.7.4 by means of the relationships between the free impact vibration period $\bar{T}$, interaction time during the period $\bar{T}_e$, accumulated normal interaction force impetus $\bar{S}$ and rheology stiffness $\bar{K}$. It should be noted, that the rheology features are of great significance in the impact vibration, if $0.1<\bar{K}<10$. At the values $\bar{k}>10$ it is reasonable to employ the rigid constraint and a Lagrange multiplier approach for the numerical integration of the equations of motion (see Chap.3.3). In the latter case it isn't necessary to know the exact value of the rheology stiffness coefficient, because it has no influence upon the lower harmonic components of the resulting free motion law. On the contrary, if $\bar{k}<0.1$, the impact vibration law is very similar as in the case of the unconstrained structure.

Employing the rheological models with the stiffness and viscous damping elements connected in parallel, theoretically it is possible to adjust their values in order to obtain the local contact condition corresponding to any value of the restitution coefficient in the range $0< R_f <1$. Nevertheless, in order to represent the value $R_f \cong 0$, the dissipation coefficient is to be increased up to a very large value. It results in poor convergence when solving the nonlinear algebraic dynamic equilibrium equation at each time integration step. On the other hand, for each particular case of analysis it necessary to adjust the contact stiffness and damping coefficients individually, because from the very nature they are employed in order to obtain the motion laws adequate to those taking place in a real system rather than for representing some physical quantities. Therefore,

if it is possible to neglect the local elasticity of the contact area, it should be done. In this case the problem is to be represented the dynamic contact problem by the linear structural equation of motion with unilateral constraints rather by including directly the nonlinear terms representing the contact forces, as it enables to deal with the coefficients of restitution simply perceptible for most engineers instead of employing sophisticated rheology coefficients.

Let's evaluate the asymptotic features of the generalized Newmark's scheme applied to the structural equations of motion with unilateral constraints. It appears reasonable to expect, that the numerical damping, period elongation and numerical stability features would remain similar as obtained in purely linear structure analysis.

Really, the motion law obtained by integrating a constrained structure is composed from the motion laws produced by an unconstrained one with boundary conditions varying at the time instants where some constraints change their status becoming active or inactive. This suggestion is confirmed by the motion law analysis presented in Fig.7.2a,b , for which the exact solutions can be easily obtained. On the Fig.7.2a there is no amplitude decay, and the period elongation comprises $\approx 1\%$ at 50 time integration steps during the time interval $[0,T_o]$. In order to illustrate the unconditional numerical stability of the algorithm, the free impact vibration law was obtained for a two-element structure (NEL=2) during the time interval $\bar{t}=0-5$ at $R_f=0$ with the small step (800 integration points) and with a very large time step (30 integration points), Fig.7.5a,b. No errors are accumulated in the second case, and the contact force impetus is obtained close to its exact value.

Free impact vibration analysis employing reduced model with the truncated dynamic contributions of higher modes. In Fig.7.2 displacement time laws of the right-hand end and of the corresponding force impetus are presented, obtained by integrating the dynamic equations of the 10 element model at the impact restitution coefficient values $R_f=0$ and $R_f=1$. As was mentioned above, the value of the coefficient of restitution hasn't a great influence upon the vibro-impact motion law of an elastic structure.

Fig.7.6 presents the motion laws, obtained employing the reduced models, taking on account the dynamic contribution of the first mode only and of the first and second modes. It should be noticed, that the approximation by the reduced model with two dynamic d.o.f. presents the impact vibration behavior with the sufficient accuracy for practical purposes. The time laws in Fig.7.7 enable to analyze the influence of the dissipative contributions of the higher modes, assuming zero values during the integration step for the second and third generalized displacement time derivatives (relations (1.30) and (1.31) for obtaining the normal contact force). The discontinuous changes of the displacements correspond to the inertialess motion of the higher modal components,e.g.,discontinuities at the time instant of removing the prestressing force ($\bar{t}=0$), and at the time instant of impact ($\bar{t}=0.24$). Fig.7.7d presents the time laws of the impact vibration during the time interval $\bar{t}\in[0,5]$. The comparison between the amplitude fade rates implies, that the dissipation in the reduced models is higher than in the full ones.

Forced impact vibration of a VC prestressed against a rigid constraint by longitudinal force . A rod-type VC presented in Fig.7.1c is employed in VD for creating a varying normal interaction force. A VC unsupported rigidly in a frame is preferable in comparison with a cantilever one, because in the latter case great amounts of vibration energy are transferred through the rigid support to the frame. A VC of the length l is presented by a finite element model, the prestressing force being P_o, and a longitudinal harmonic excitation force is $P_1(t)=P_1\sin\omega t$. The computed results are presented employing the dimensionless quantities $\bar{t}=\frac{t}{l}(E/\rho)^{\frac{1}{2}}$, $\bar{U}=\frac{U}{l}$, $\dot{\bar{U}}=\dot{U}(\rho/E)^{\frac{1}{2}}$, $\bar{k}=\frac{k}{El}$, $\bar{P}=\frac{P}{EF}$, $\omega=\omega l(\rho/E)^{\frac{1}{2}}$, where E, ρ are the Young's modulus and density of material. The dimensionless impetus of normal contact interaction forces is obtained from the relation $\bar{S}=\frac{S}{EFl}(\rho/E)^{\frac{1}{2}}$. A vibration Q-factor of the VC is assumed to be Q=50.

Fig.7.8, 7.9 present the time laws of the right-hand end displacements of the VC obtained by means of the direct numerical

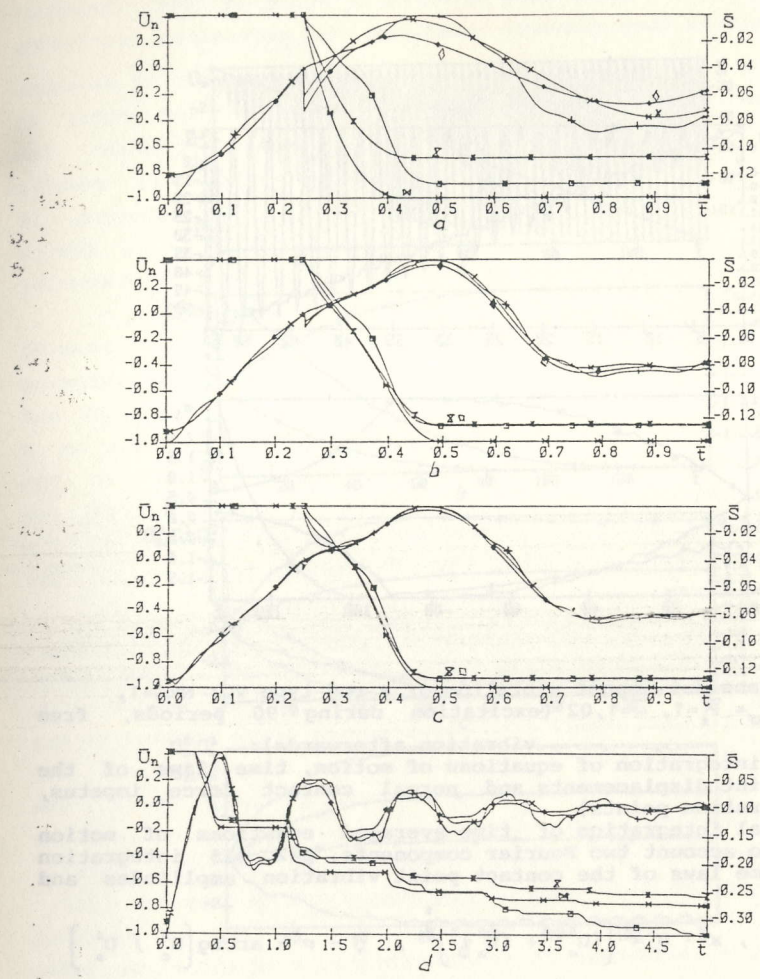

Fig.7.7 Time laws of the displacements and of the contact force impetus of the right-hand end of the model (local contact rheological model, NEL=5, k=0.33, c=0.8 :

+ - $\bar{U}_n$, □ - $\bar{S}$ - full model;

x - $\bar{U}_n$, ⊠ - $\bar{S}$ - reduced model, time derivatives $\ddot{z}^{(3)} = z^{(3)} = \ldots = 0$ λ obtained by the relation (1.43);

◊ - $\bar{U}_n$, ⋈ - $\bar{S}$ - reduced model, time derivatives $\ddot{z}^{(4)} = z^{(4)} = \ldots = 0$ λ obtained by the relation (1.44);

a) reduced model, single dynamic d.o.f; b) reduced model, two dynamic d.o.f; c) reduced model, three dynamic d.o.f; d) reduced model, two dynamic d.o.f, time interval $t\in[0,5]$

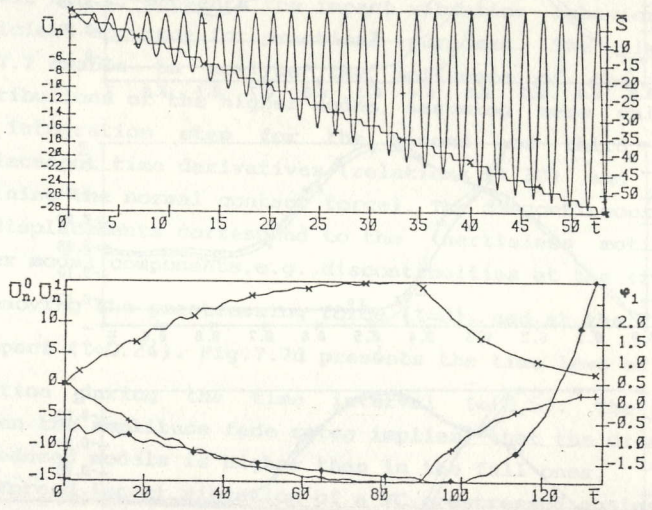

Fig.7.8 Transient impact vibration of a rod-type VC, NEL=1, $\bar{P}_o = \bar{P}_1 = 1$, $\bar{\omega} = 1{,}02$ (excitation during 90 periods, free vibration afterwards):

a) direct integration of equations of motion, time laws of the contact point displacements and normal contact force impetus, 2400 integration points)

b) numerical integration of time-averaged equations of motion taking into account two Fourier components, p=2, 75 integration points, time laws of the contact point vibration amplitudes and phases,

$$+ - U_c^o \quad , \quad x - U^1 = \left[(U_c^1)^2 + (U_s^1)^2 \right]^{\frac{1}{2}} \quad , \quad \Diamond - \varphi^1 = \operatorname{arctg}\left[U_c^1 \; / \; U_s^1 \right]$$

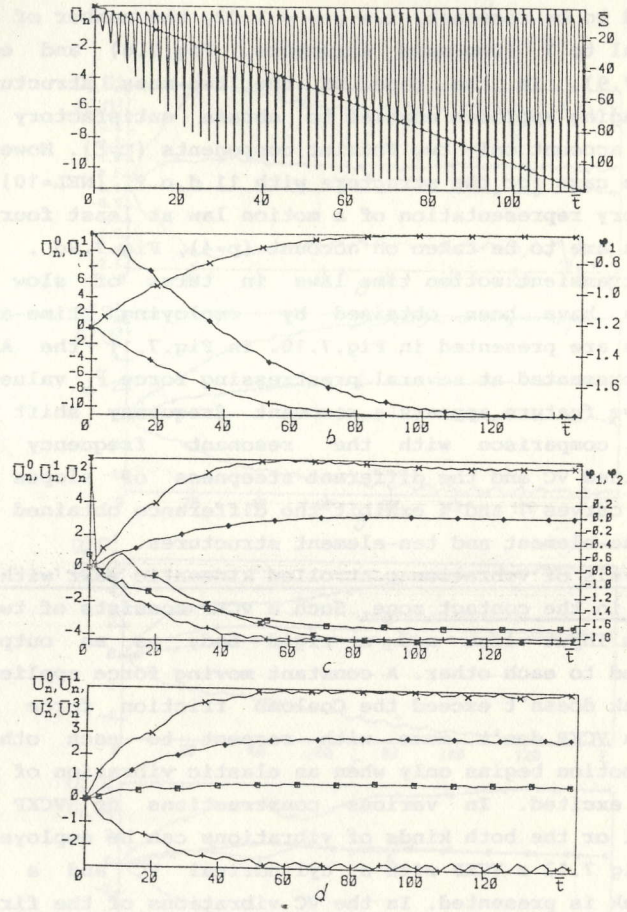

Fig.7.9 Transient impact vibration of the rod-type VC, NEL=10, $\bar{P}_o = \bar{P}_1 = 1$, $\bar{\omega} = 1.02$(90 excitation periods, free vibration afterwards):

a) direct integration of equations of motion, time laws of the contact point displacements and normal contact force impetus, 2400 integration points)

b) numerical integration of time-averaged equations of motion taking on account two Fourier components, p=2, 75 integration points, time laws of the contact point vibration amplitudes and phases, $+ - U_c^o$; $x - U^1$; $\Diamond - \varphi^1$;

c)three Fourier components, p=3, 75 integration points,
$+ - U_c^o$; $x - U^1$; $\Diamond - U^2$; $\square - \varphi^1$; $\bowtie - \varphi^2$;

d) four Fourier components, p=4, 75 integration points,
$+ - U_c^o$; $x - U^1$; $\Diamond - U^2$; $\square - U^3$

integration of the equations of motion, and the time laws of Fourier component amplitudes obtained by means of the numerical integration of time-averaged equations. The excitation frequency is assumed to be resonant, i.e., $\bar{\omega} = 1.02$, the number of elements being equal to 1 (two-mass structure, Fig.7.8) and equal to 10 (Fig.7.9). In the case of the two-mass structure the time-averaging approach enables to obtain satisfactory results taking on account only two Fourier components (p=2). However, it is not the case for the structure with 11 d.o.f. (NEL=10) for a satisfactory representation of a motion law at least four Fourier components are to be taken on account (p=4), Fig.7.9d .

The transient motion time laws in terms of slow varying amplitudes have been obtained by employing time-averaging techniques are presented in Fig.7.10. In Fig.7.11 the AFCH and PFCH are presented at several prestressing force P_o values. As a distinctive feature appears a resonant frequency shift to the right in comparison with the resonant frequency of an unconstrained VC and the different steepness of slopes of the AFCH. The curves 1 and 4 exhibit the difference obtained in the case of one-element and ten-element structures.

Analysis of vibration-controlled kinematic pair with normal vibration in the contact zone. Such a VCKP consists of two links: a VC as an input link and a rigid body as an output link prestressed to each other. A constant moving force applied to the output link doesn't exceed the Coulomb friction force and the links of a VCKP don't move with respect to each other. The relative motion begins only when an elastic vibration of an input link is excited. In various constructions of VCKP normal, tangential or the both kinds of vibrations can be employed [92].

In Fig 7.12 a VCKP with a cylindrical VC and a rotating output link is presented. In the VC vibrations of the first mode are excited, where the vibration normal to the contact surface prevail. The rotational rigid body motion of the VC is prevented by the vibro-isolating fixing at the upper circumference of the cylinder. If the stiffness of the fixing is considerably lower than the stiffness of the VC, the influence of the fixing upon the resonant frequency value and upon the vibration amplitude of the VC is insignificant. Therefore the problem can be presented as axisymmetric one employing the equations of motion

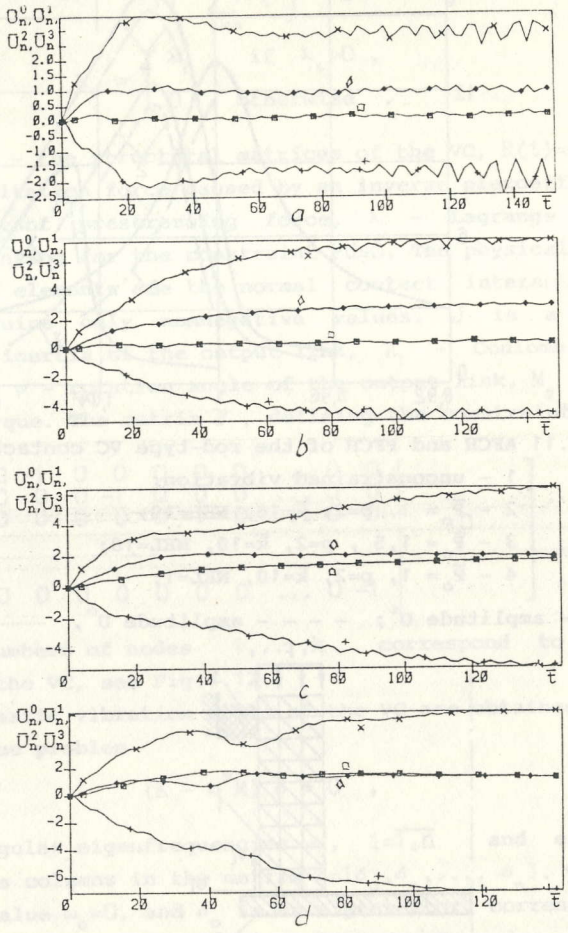

Fig.7.10 Transient impact vibration of the rod-type VC at several values of the excitation frequency , NEL=10, $\bar{P}_o = \bar{P}_1 = 1$, (numerical integration of time-averaged equations of motion taking on account four Fourier components, p=4, 75 integration points, time laws of the contact point vibration amplitudes

+ - U_c^o , x - U^1 , ◊ - U^2 , □ - U^3 ;

a) $\bar{\omega}$=0,99; b) $\bar{\omega}$=1,01 ; c) $\bar{\omega}$=1,03 ; d) $\bar{\omega}$=1,05

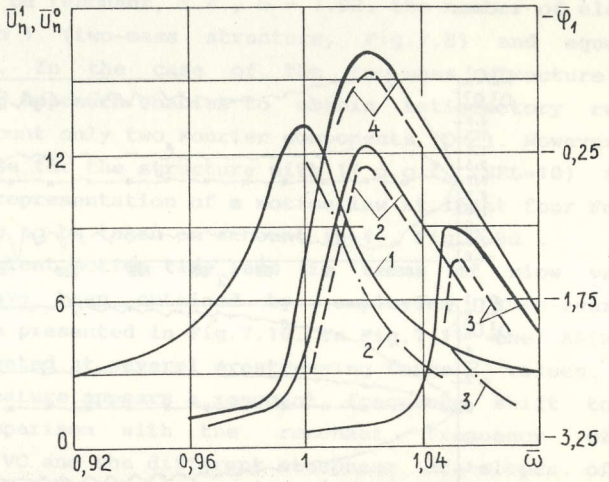

Fig.7.11 AFCH and PFCH of the rod-type VC contact point, P_1=1:
1 - unconstrained vibration;
2 - $\bar{P}_o$= 1, p=2, $\bar{k}$=10, NEL=10;
3 - $\bar{P}_o$= 1,5 , p=2, $\bar{k}$=10, NEL=10;
4 - $\bar{P}_o$= 1, p=2, $\bar{k}$=10, NEL=1;
—— - amplitude U^1; - - - - amplitude U^o, ... - phase φ^1

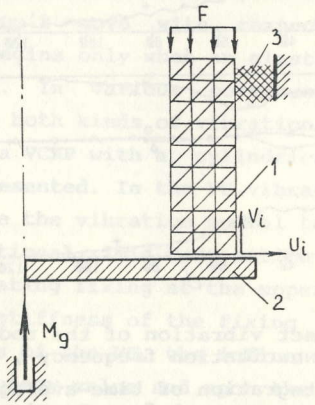

Fig.7.12 Finite element model of the vibration controlled kinematic pair:
1- Finite element model of an axisymmetric VC,
2- output link, 3- vibro-isolating fixing,
M_g - constant external torque, F- normal force

$$\begin{cases} M\ddot{U} + C\dot{U} + KU = -P^T\lambda + R(t) + F , \\ PU \le 0 , \\ J\ddot{\psi} = -k_f \left(\sum_{i=1}^{k} \lambda_i \right) \operatorname{sign} \dot{\psi} + M_g , \\ \lambda_i = \begin{cases} \lambda_i , & \text{if } \lambda_i > 0 , \\ 0 , & \text{otherwise} . \end{cases} \end{cases} \qquad (7.1)$$

where M,C,K - the structural matrices of the VC, R(t)=R(t+T) - periodic excitation force caused by an inverse piezoeffect in the VC, F - constant prestressing force, λ - Lagrange multiplier vector accounting for the constraint PU≤0. The physical sense of the vector λ elements are the normal contact interaction forces able to acquire only nonnegative values. J is a principal momentum of inertia of the output link, k_f - Coulomb friction coefficient, ψ - rotation angle of the output link, M_g - constant external torque. The matrix P , defining the constraint system is

$$P_{k\times n} = \left[\begin{array}{cccccccccc|c} 0 & -1 & 0 & 0 & 0 & 0 & 0 & \dots & 0 & 0 & \\ 0 & 0 & 0 & -1 & 0 & 0 & 0 & \dots & 0 & 0 & \\ 0 & 0 & 0 & 0 & 0 & -1 & 0 & \dots & 0 & 0 & 0 \\ & & & & \cdot & \cdot & \cdot & & & & \\ 0 & 0 & 0 & 0 & 0 & 0 & 0 & \dots & 0 & -1 & \end{array}\right] ,$$

where the numbers of nodes 1,...,k correspond to the lower surface of the VC, see Fig.7.12.

The elastic vibration modes of the VC are obtained by solving an eigenvalue problem

$$(K - \omega^2 M)\,\delta = 0 ,$$

yielding angular eigenfrequencies ω_i, $i=\overline{1,n}$ and eigenvectors presented as columns in the matrix $\Delta=[\delta_o,\delta_1,\dots,\delta_n]$. The eigenfrequency value ω_o=0, and δ_o is an eigenvector corresponding to the axial motion of the VC as a rigid body. In order to present the problem in modal coordinates, the substitution

$$U = \Delta\, Z .$$

is employed.

We present the vector of the squares of eigenfrequencies as $\begin{pmatrix}\omega_1^2\\ \omega_2^2\end{pmatrix}$, and the matrix of eigenvectors as $\Delta = [\Delta_1, \Delta_2]$, where the submatrix Δ_2 and the subvector ω_2^2 correspond to the truncated modes. Assume $\Delta_1 = [\delta_o, \delta_1]$, $\Delta_2 = [\delta_2, \ldots, \delta_n]$, $S_k = \Delta_2 \mathrm{diag}(1/\omega_2^2)\ \Delta_2^T$, $A = P\,S_k P^T$. Neglecting the dynamic contributions of the modes $\omega_2, \delta_2, \ldots, \omega_n, \delta_n$ and taking account for their remaining quasistatic compliances, we obtain the set of reduced equations of motion

$$\begin{cases} \ddot{z}_o + \delta_o^T P^T A^{-1} P \delta_o z_o + \delta_o^T P^T A^{-1} P \delta_1 z_1 = \delta_o^T (I - P^T A^{-1} P S_k)(R(t)+F), & (7.2.1)\\ \ddot{z}_1 + 2\omega_1 c_1 \dot{z}_1 + \omega_1^2 z_1 + \delta_1^T P^T A^{-1} P \delta_o z_o + \delta_1^T P^T A^{-1} P \delta_1 z_1 = & \\ \qquad = \delta_1^T (I - P^T A^{-1} P S_k)(R(t)+F), & (7.2.2)\\ J\ddot{\psi} = -k_f \left(\sum_{i=1}^{k} \lambda_i \right) \operatorname{sign} \dot{\psi} + M_g, & (7.2.3) \end{cases}$$

where $\lambda = A^{-1}(P\delta_o z_o + P\delta_1 z_1 + P S_k (R(t)+F))$.

The equations (7.2.1) and (7.2.2) present a nonlinear dynamic behavior of the VC as of the mechanical system with two d.o.f. They are independent from the equation (7.3.3) presenting the dynamics of a rotational motion of the output link. Making the corresponding notations and assuming the harmonic external excitation law, the equations (7.2.1) and (7.2.2) appear as

$$\begin{cases} \ddot{z}_o + k_{oo} z_o + k_{io} z_1 = f_o, & \\ \ddot{z}_1 + 2\omega_1 c_1 \dot{z}_1 + \omega_1^2 z_1 + k_{io} z_o + k_{11} z_1 = p \sin\omega t + f_1. & (7.3) \end{cases}$$

where k_{oo}, k_{io}, k_{11} are assumed to be zero at the time instants when the values of λ are negative. Fig.7.13a,b present the AFCH of the generalized displacement z_1 and of the relative contact time during a vibration period obtained by employing time-averaging techniques at the values of the dimensionless coefficients $\bar{k}_{oo} = -\bar{k}_{io} = \bar{k}_{11} = 2$, $\overline{2\omega_i c_i} = 0{,}02$, $\bar{f}_1 = 0$ and at several values of f_o. The dimensionless quantities are obtained from the relations

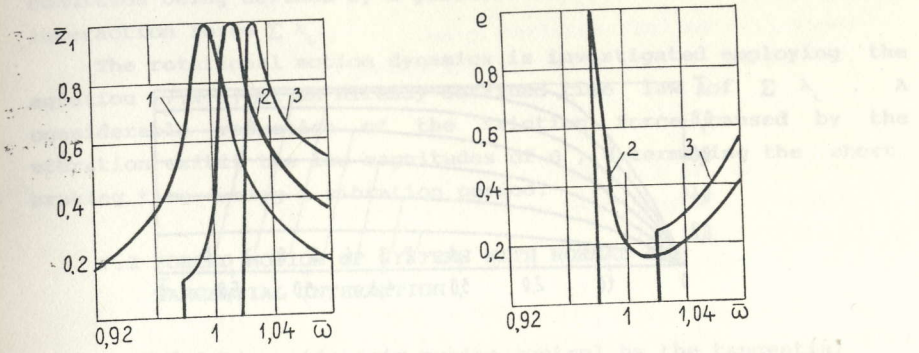

Fig.7.13 Dynamic characteristics of VCKP:
a- AFCH of the generalized displacement z_1;
b- relative contact time during the vibration period, $e = T_k/T$;
1- unconstrained vibration; 2- $f_o = 0.05$; 3- 2- $f_o = 0.1$;

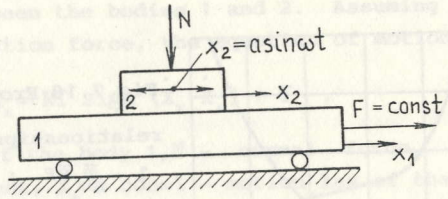

Fig.7.14 Vibrating link interacting with a massive output link:
1 - input link ; 2 - output link

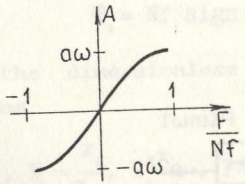

Fig.7.15 Output link velocity relationship against the moving force - critical friction force ratio $\bar{F}/\bar{N}f$

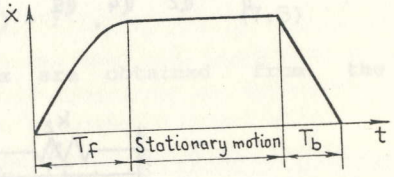

Fig.7.16 Velocity pulse of the VCKP output link

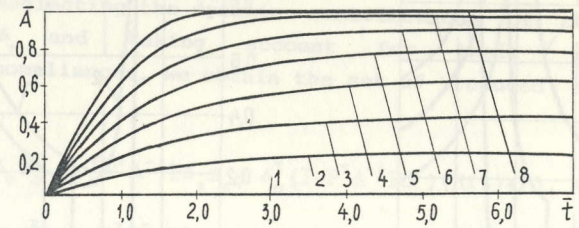

Fig.7.17 Time laws of establishing of the stationary value of the output link velocity

1 - $\bar{F}/\bar{N}f=0$, 2 - 0.143 , 3 - 0.286 , 4 - 0.428 , 5 - 0.571 , 6 - 0.714 , 7 - 0.857 , 8 - 1

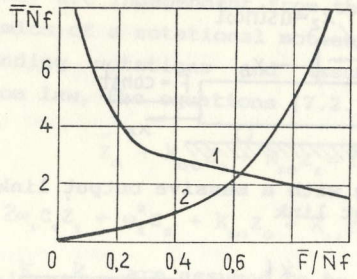

Fig.7.16 Front and back slope duratic relationships from the ratio $\bar{F}/\bar{N}f$:

1 - $\bar{T}_f\bar{N}f$; 2 - $\bar{T}_b\bar{N}f$

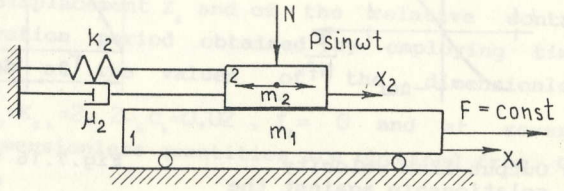

Fig.7.19 Elastic vibrating system interacting with a rigid output link; 1 - input link , 2 - output link

$\bar{\omega} = \frac{\omega}{\omega_1}$, $\bar{k} = \frac{k}{\omega_1^2}$, $\bar{t} = t\omega_1$, $\bar{f} = \frac{2\omega cf}{p\omega_1}$, $\overline{2\omega c} = \frac{2\omega c}{\sqrt{k}}$, the contact condition being defined by a positive value of the total normal interaction force $\Sigma \lambda_i$.

The rotational motion dynamics is investigated employing the equation (7.2.3) at an already obtained time law of $\Sigma \lambda_i$. A considerable reduction of the friction force caused by the vibration exibit the low magnitudes of e , determining the short braking time during a vibration period.

7.2 FORCED MOTION OF SYSTEMS WITH NORMAL AND TANGENTIAL INTERACTION

7.2.1 Kinematic pair motion control by the tangential vibration

Interaction of a vibrating link with a massive moving body . The simplest mechanical system presenting such an interaction is presented in Fig.7.14. Assume the time law of a vibrating body being harmonic $x_2=a\cos\omega t$. The massive body 1 moves rectilinearly under a constant external force F and friction forces in the interface between the bodies 1 and 2. Assuming the Coulomb tangential interaction force, the equation of motion is

$$m_1\ddot{x}_1 = Nf \operatorname{sign}(\dot{x}_2 - \dot{x}_1) + F \quad , \qquad (7.4)$$

where m_1 - mass of the body 1, N - normal force, f - Coulomb friction coefficient, $x_2=a\cos\omega t$ - motion law of the body 2, x_1 - displacement of the body 1.

We present the equation (7.4) in a dimensionless form

$$\ddot{\bar{x}}_1 = \bar{N}f \operatorname{sign}(\cos t - \dot{\bar{x}}_1) + \bar{F} \quad , \qquad (7.5)$$

where the dimensionless quantities are obtained from the relations

$$\bar{t} = \omega t,\ \bar{x} = \frac{x_1}{a},\ \dot{\bar{x}}_1 = a\omega,\ \bar{F} = \frac{F}{m_1\omega^2 a},\ \bar{N} = \frac{N}{m_1\omega^2 a} .$$

We'll investigate the motion laws at high vibration frequencies ω , i.e., when the values of the dimensionless forces

are considerably less than unity. Presenting the equation (7.5) as

$$\ddot{\bar{x}}_1 = \varepsilon \bar{N}f \operatorname{sign}(\cos t - \dot{\bar{x}}_1) + \varepsilon \bar{F} \quad , \qquad (7.6)$$

where ε – an infinitesimal quantity, we apply the averaging techniques. At the first approximation we search the solution as

$$\dot{\bar{x}}_1 = A \quad , \qquad (7.7)$$

where A is a function slow varying in time. Averaging the right-hand side of the equation (7.6) during the time interval $[0,2\pi]$, we obtain

$$\dot{A} = -\frac{2}{\pi} \bar{N}f \arcsin A + \bar{F} \quad . \qquad (7.8)$$

In order to determine the mean velocity $\dot{\bar{x}}_1$ of an output link in the continuous motion mode, we assume $\dot{A}=0$. The relation between the normal force $\bar{N}$, tangential force $\bar{F}$ and the mean velocity is obtained as

$$\frac{\bar{F}}{\bar{N}f} = -\frac{2}{\pi} \arcsin A \quad , \qquad (7.9)$$

where $-1 \le A \le 1$, (see also Fig.7.15). The relation (7.9) corresponds to the result obtained in [55]. From (7.9) we determine the amplitude value of the vibration with the frequency ω in order to ensure a stationary motion of the output link with the mean velocity A . At the same value of the normal and tangential force ratio, the mean velocity depends upon the vibration velocity amplitude $a\omega$. A stationary motion with the velocity greater than $a\omega$ isn't possible, therefore a tangential force $|\bar{F}|>|\bar{N}f|$ shouldn't be applied. Moreover, at such a magnitude of $\bar{F}$ the output link can't remain in a state of rest even when no vibration of an input link is excited.

An important dynamic characteristic of VCKP is the time interval from the beginning of vibration necessary to establish a stationary velocity value of an output link, and the braking time interval from the instant when vibration is cancelled. Of interest is the case, where the front and back slopes of the

velocity pulse are of equal duration, and this duration is as short as possible, Fig.7.16. In order to determine the duration of the front slope we employ the time-averaged equation for a transient motion as

$$\begin{cases} \dot{A} = \bar{F} - \frac{2}{\pi} \bar{N}f \arcsin A \ , & \text{if} \quad -1 \le A \le 1 \ , \\ \dot{A} = \bar{F} + \bar{N}f \ , & \text{if} \quad A \le -1 \ , \\ \dot{A} = \bar{F} - \bar{N}f \ , & \text{if} \quad A \le -1 \ . \end{cases} \qquad (7.10)$$

Integrating the equation (7.10) numerically at a number of values of $\bar{F}/\bar{N}f$, the time laws presented in Fig.7.17 are obtained, the front slope having a form of an exponent function. In order to determine the duration of the back slope the equation (7.5) is considered with no vibration of the output link:

$$\ddot{\bar{x}}_1 = -\bar{N}f \operatorname{sign} \dot{\bar{x}}_1 + \bar{F} \quad . \qquad (7.11)$$

The velocity of the output link decreases linearly, and the braking time from stationary velocity value v_o is obtained as

$$T_b = \frac{\bar{v}_o}{\bar{N}f - \bar{F}} \quad . \qquad (7.12)$$

Employing the relationships in Fig.7.17 for obtaining T_f and the relation (7.12) for obtaining T_b, in Fig.7.18 the relationships representing the durations of the front and back slopes are presented. The durations are equal, if $\bar{F}/\bar{N}f \approx 0.65$. The duration of each slope reduces, if the magnitude of the normal force $\bar{N}$ is increased. However, simultaneously increases the output velocity variation, as can be seen from the time laws obtained by a numerical integration of equations of motion and presented in Fig.7.19.

Interaction of resonant vibrating system with massive moving body. The model of the VCKP considered above is valid only when the input link vibration is ensured with a prescribed amplitude. In reality the vibration is usually obtained by employing the

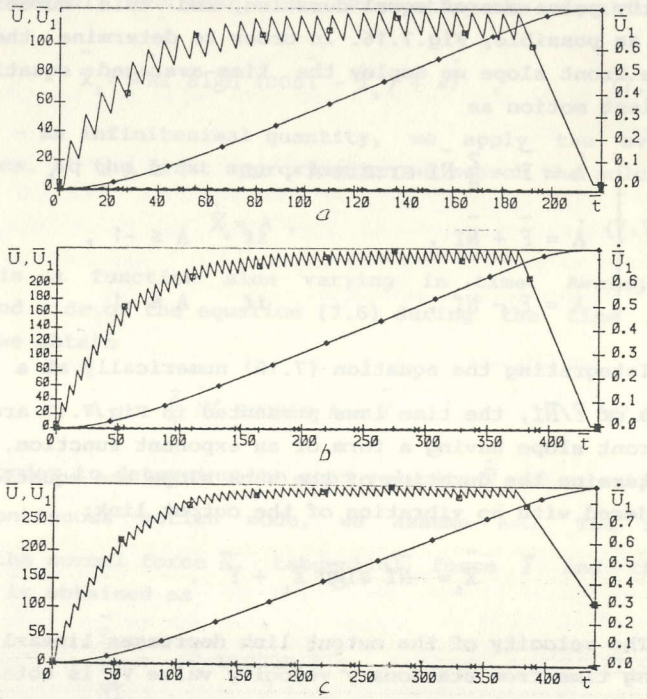

Fig.7.20 Time laws of displacements and velocities of the VCKP links obtained by the numerical integration

a) $\bar{N}f=0.05$, $\bar{F}=0.025$, b) $\bar{N}f=0.025$, $\bar{F}=0.0125$, c) $\bar{N}f=0.025$, $\bar{F}=0.01625$

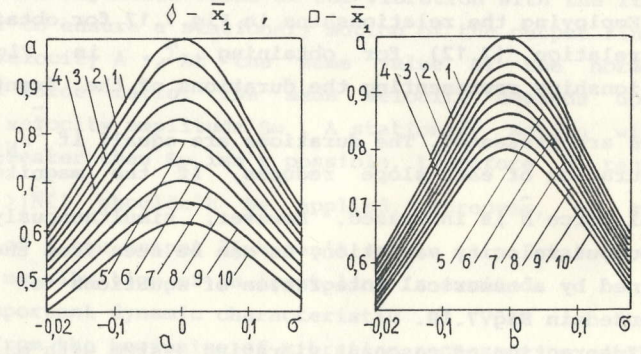

Fig.7.21 AFCH of the input link vibration at several values of the normal force:

a) $\bar{F}=0$ (no moving force);

b) $\bar{F}=0.65\bar{N}f$; 1 - $\bar{N}f=0$, 2 - 0.001 , 3 - 0.002 , 4 - 0.003 , 5 - 0.004 , 6 - 0.005 , 7 - 0.006 , 8 - 0.007 , 9 - 0.008 , 10 - 0.009

elastic resonant VC. The magnitude of their vibration amplitude at the same excitation level depends upon the contact interaction forces between the links of VCKP. Moreover, a time interval necessary for establishing a stationary vibration amplitude exceeds many times the vibration period.

The simplest model considering an input link as a resonant vibrator is presented in Fig.7.20. It differs from the one presented in Fig.7.14 because the input link contains the mass m_2, elastic spring and a dissipative element characterized by the coefficients k_2 and μ_2 correspondingly. The vibration is excited by the harmonic forcing law $P\sin\omega t$, the amplitude of the force being very small and the excitation frequency equal or close to the resonant frequency of the vibrator. A mechanical contact between the links and a friction law remain the same as in the case of the model in Fig.7.14. If the contact interaction forces are considerably less than the excitation force amplitude $|Nf|<<|P|$, the model in Fig.7.14 and the results obtained above can be employed. However, in the case of a resonant vibration, the equations of motion should be considered as

$$\begin{cases} m_2\ddot{x}_2+\mu_2\dot{x}_2+k_2x_2 = -Nf\ \mathrm{sign}\ (\dot{x}_2-\dot{x}_1)+P\sin\omega t\ , \\ m_1\ddot{x}_1 = Nf\ \mathrm{sign}\ (\dot{x}_2-\dot{x}_1)+F\ , \end{cases} \tag{7.13}$$

Employing dimensionless quantities, we obtain

$$\begin{cases} \ddot{\bar{x}}_2+\bar{\mu}\dot{\bar{x}}_2+\bar{x}_2 = -\bar{N}f\ \mathrm{sign}\ (\dot{\bar{x}}_2-\dot{\bar{x}}_1)+\bar{\mu}\sin\bar{\bar{\omega}}\bar{\bar{t}}\ , \\ \bar{m}\ \ddot{\bar{x}}_1 = \bar{N}f\ \mathrm{sign}\ (\dot{\bar{x}}_2-\dot{\bar{x}}_1)+\bar{F}\ , \end{cases} \tag{7.14}$$

where

$$\bar{\omega}=\omega(m_2/k_2)^{\frac{1}{2}},\quad \bar{t}=t(k_2/m_2)^{\frac{1}{2}},\quad \bar{\mu}=\mu(m_2k_2)^{-\frac{1}{2}},\quad \bar{N}f=\frac{Nf}{P}\bar{\mu}\ ,$$

$$\bar{F}=\frac{F}{P}\bar{\mu}\ ,\quad \bar{x}=\frac{x\mu_2}{P}(k_2/m_2)^{\frac{1}{2}},\quad \dot{\bar{x}}=\frac{\dot{x}\mu_2}{P}\ ,\quad \ddot{\bar{x}}=\frac{\ddot{x}\mu_2}{P}(m_2/k_2)^{\frac{1}{2}},\quad \bar{m}=\frac{m_1}{m_2}\ .$$

Assuming $\bar{\mu}$, $\bar{Nf}$, $\bar{F}$ to be of infinitesimal magnitudes, the quantities $\varepsilon\bar{\mu}$, $\varepsilon\bar{Nf}$, $\varepsilon\bar{F}$ are substituted into the system (7.14) and the time averaging techniques are employed.

We investigate the motion of the system in the vicinity of resonance ($\bar{\omega} \approx 1$). At the first approximation we search the solution as $\bar{X}_2 = a\cos(\bar{t}+\beta)$, $\dot{\bar{X}}_2 = -a\sin(\bar{t}+\beta)$, $\dot{\bar{X}}_1 = -A$, where a, β, A are assumed to be functions slow varying in time. The time-averaged equations for obtaining $a(\bar{t})$, $\beta(\bar{t})$, $A(\bar{t})$ are obtained as

$$\begin{cases} \dot{a} = -\frac{1}{2}\varepsilon\bar{\mu}a - \frac{2}{\pi}\varepsilon\bar{Nf}\left[1-\frac{A^2}{a^2}\right]^{\frac{1}{2}} - \frac{\varepsilon\bar{\mu}}{2}\sin[(1-\bar{\omega})\bar{t}+\beta], \\ a\dot{\beta} = -\frac{\varepsilon\bar{\mu}}{2}\cos[(1-\bar{\omega})\bar{t}+\beta], \\ \dot{A} = -\frac{2}{\pi}\varepsilon\bar{Nf}\arcsin\frac{A}{a} + \varepsilon\bar{F}. \end{cases} \qquad (7.15)$$

Stationary motion laws. In order to obtain dynamic characteristics of the stationary motion mode of the VCKP, the case $\dot{a}=0$, $\dot{A}=0$ is investigated. As the value of the dimensionless vibration frequency is close to unity, we denote

$$1-\bar{\omega} = \sigma, \quad \varepsilon\sigma\bar{t} + \beta = \gamma, \quad \dot{\beta} = \dot{\gamma} - \sigma\varepsilon. \qquad (7.16)$$

Substituting (7.16) into (7.15), after some manipulation an algebraic equation system is obtained as

$$\begin{cases} \frac{\bar{\mu}^2a^2}{4} + \frac{4(\bar{Nf})^2}{\pi^2}\left[1-\frac{A^2}{a^2}\right] + \frac{2\bar{\mu}a\bar{Nf}}{\pi^2}\left[1-\frac{A^2}{a^2}\right]^{\frac{1}{2}} + a^2\sigma^2 - \frac{\bar{\mu}^2}{4} = 0, \\ \frac{A}{a} = \sin\left[\frac{\pi\bar{F}}{2\bar{Nf}}\right], \end{cases} \qquad (7.17)$$

from which amplitude a and mean velocity A of the output link are to be expressed.

Having determined the values of a from the system (7.17) at

different values of σ, we obtain an AFCH. Families of AFCH obtained at $\bar{\mu}=0{,}03$ are presented in Fig.7.21, the mechanical Q-factor of an input link being equal to 33.3 . It should be noticed that the vibration amplitude increases due to the directive motion of the output link subjected to the tangential external force $\bar{F}$. Substituting the value $\sigma=0$ into the system (7.17), the relation between the peak values of the amplitudes and the forces $\bar{F}$ and $\bar{Nf}$ is obtained explicitly as

$$a = \frac{4\bar{Nf}}{\pi\bar{\mu}}\cos\left[\frac{\pi\bar{F}}{2\bar{Nf}}\right] + 1 . \qquad (7.18)$$

It follows from (7.18) , that the vibration of the input link is possible, if the condition

$$\bar{N}f \le \frac{\pi\bar{\mu}}{\cos\left[\frac{\pi\bar{F}}{2\bar{Nf}}\right]}, \qquad (7.19)$$

determining the maximum value of the normal force, is satisfied.

At the prescribed value of the amplitude a , the mean output velocity value is obtained from the second equation of (7.17).

Transient motion in VCKP, i.e., a process of establishing of stationary vibration amplitudes and output link velocity values, can be investigated by solving time-averaged equations (7.15), or by integrating numerically the equations of motion (7.14). Further we present the results obtained by numerical integration. Fig.7.22 presents the time laws of the VCKP being initially in a state of rest after applying a harmonic excitation to the input link. Fig.7.22 presents the transient vibration law of the free VC (i.e.,at $\bar{Nf}=0$, Fig.7.22a) and the transient motion of the output link at several values of the mass $\bar{m}$ (Fig.7.22b). It is necessary to consider the process of establishing of the mean value of the output link velocity $\dot{\bar{X}}_1$. If $\bar{m}>1$, the duration of the transient motion of the whole system is prolonged in comparison with the free VC. At lower values of $\bar{m}$ the transient motion duration decreases, however, it can't be shorter than the transient vibration of the free VC. On the other hand, the

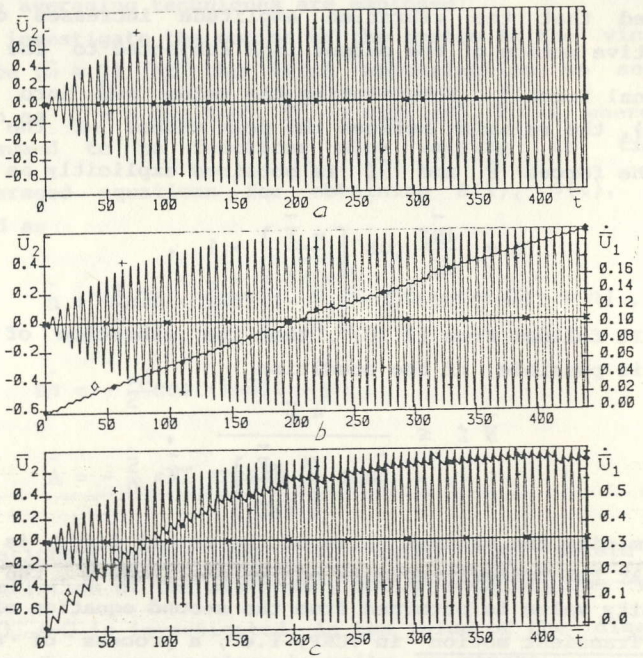

Fig.7.22 Transient vibration of the input link and the velocity of the output link at $\bar{\mu}$= 0.03 , $\bar{\omega}$=1 , $\bar{F}$=0.65$\bar{N}f$: a) $\bar{N}f$=$\bar{F}$=0 , b) $\bar{N}f$=0.009 , c) $\bar{N}f$=0.009

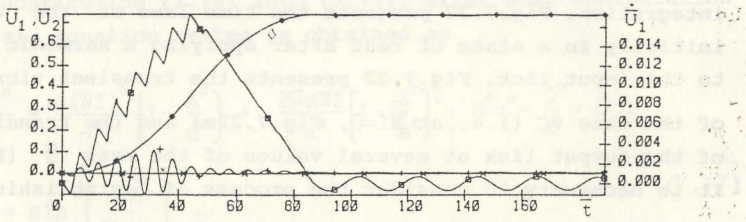

Fig.7.23 Time laws of the displacements and velocities of the VCKP links during the step-motion mode at $\bar{N}f$=0.009 , $\bar{F}$=$\bar{N}f$/2 , $\bar{m}$=10 , 5 excitation periods; 1 - $\bar{U}_1$, 2 - $\dot{\bar{U}}_1$, 3 - $\bar{U}_2$

stationary value of the vibration amplitude is obtained only after the stationary mean velocity value of the output link is established.

The above analysis enables to arrive at the following conclusions:

1. Increasing a normal force magnitude, the AFCH curve becomes more sloping. Nevertheless, the stationary input link vibration amplitude value establishes during the number of vibration periods approximately equal to the Q-factor of a VC irrespectively of the normal force magnitude.

2. The transient motion duration in a VCKP is determined by the duration of establishing the mean velocity of an output link, however, it can't be shorter than the transient vibration of the free VC.

Step-motion mode. A VCKP can be effectively used for obtaining precise small displacements of an output link, referred to as steps. During one step the input link performs one or several vibrational movements during which neither the vibration amplitude nor the output link velocity are established to their stationary values. After that the excitation is removed and the both links of a VCKP perform some transient motion until they come to a state of rest. As dynamic characteristics of such a motion the quantities T_{max}, ψ_{max}, $\dot{\psi}_{max}$, ψ_p, $\dot{\psi}_p$ introduced in Chap.6.4 are employed. Fig.7.23 presents the time laws of the output link step subjected to five external harmonic excitation waves of the resonant frequency $\bar{\omega}$ = 1 , the relation $\bar{F}=\frac{\bar{N}f}{2}$ being held. Keeping the constant ratio between the forces $\bar{F}$ and $\bar{N}f$, the relationships in Fig.7.24 present the dynamic characteristics of the step motion mode related to the magnitude of the normal force $\bar{N}f$. It appears reasonable to consider the value $\bar{N}f$=0,009 as optimal, because by the further increase of $\bar{N}f$ the step magnitude ψ_{max} decreases quickly, and, moreover, at the point the quantity $\dot{\psi}_p$ acquires its local minimum.

Finite element analysis of VCKP. Consider a VCKP as a magnetostrictive VC attached to a ferromagnetic plane, Fig.7.25. In the longitudinal direction force F is applied to the VC. The winding is connected to a high-frequency voltage source V_E,

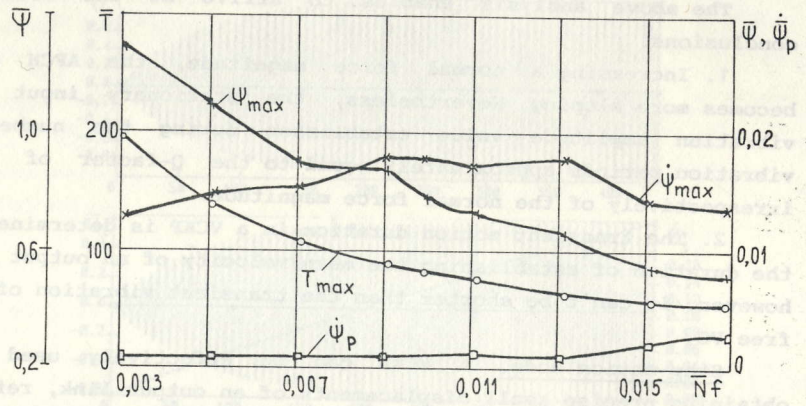

Fig.7.24 Relationships of the dynamic characteristics of the step-motion mode from the normal force

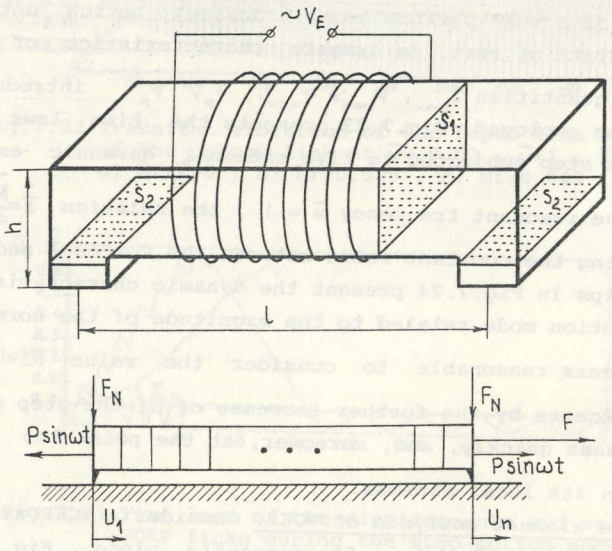

Fig.7.25 VCKP with the magnetostrictive VC: construction diagram and finite element model

creating in the winding the electric current $I(t)=I_c+ I_a\sin\omega t$. The constant component I_c creates the normal force attracting the VC to the surface, and the alternating component forces the VC to perform longitudinal vibrations and simultaneously ensures a varying normal force magnitude. If the alternating component $I_a=0$, the magnitude of the force F is assumed to be insufficient to overcome the static friction force. If $I_a\neq0$, the VC begins to slide in the direction of the force F because of the vibrations in the contact zone.

If the operating point of the VCKP is selected on the linear part of the magnetization curve of the material, the normal force attracting the VC to the surface is obtained by solving the magnetic circuit equation and is approximately obtained as

$$F_N=\left[\frac{\mu In}{\frac{lS_2}{S_1}+2h}\right]^2\frac{S_2}{2\mu_o}\ , \qquad (7.20)$$

where μ - magnetic permeability, n - number of loops of the winding, μ_o - magnetic constant.

In order to obtain the equivalent longitudinal force acting upon each end of the VC, we employ the analogy between the constitutive equations of piezoelectric and magnetostrictive materials [140]. Expanding thermodynamic functions of the magneto-polarized continua in the vicinity of an operating point B_o,H_o,M_o, four pairs of the isothermal magnetostrictive equations are obtained, one of which reads as

$$\begin{cases}\sigma = c^H\varepsilon - e_M H\\ M = \mu_o^{-1}e_M^T\varepsilon + \varkappa^\varepsilon H\ ,\end{cases} \qquad (7.21)$$

where B - magnetic induction, H - magnetic field strength, M - magnetization, c^H - stiffness tensor under constant magnetic field strength, $\varkappa^\varepsilon$ - magnetic susceptibility tensor under constant strain, e_M - magnetostrictive tensor. It is preferable in the equation (7.21) to employ magnetic induction B in place of magnetization M . Substituting $M = \mu_o^{-1}B - H$ into the system (7.21), we obtain

$$\begin{cases} \sigma = c^H \varepsilon - e_M H \\ B = e_M^T \varepsilon + \mu_o \mu^\varepsilon H \end{cases} \qquad (8.22)$$

where $\mu = 1+\varkappa$ - magnetic permeability of the material. The matrix equation of motion of the VCKP is

$$M\ddot{U} + C\dot{U} + KU = -\begin{bmatrix} F_N f\ \mathrm{sign}\dot{U}_1 \\ \vdots \\ F_N f\ \mathrm{sign}\dot{U}_n \end{bmatrix} + \begin{bmatrix} P_1 \\ \vdots \\ F-P_1 \end{bmatrix} + \begin{bmatrix} P \\ \vdots \\ -P \end{bmatrix} . \qquad (7.23)$$

The matrices M,C,K are obtained employing the relations of Chap.6.1, explicitly presented in [71], and the forces P_1, P caused by the constant and alternative components of the magnetic field strength H_c and H_a, are expressed as

$$P_1 = H_c S_1 e_{M11} , \quad P = H_a S_1 e_{M11} , \qquad (7.24)$$

where $$H_c = \frac{nI_c}{\left(\frac{2hS_1}{S_2} + 1\right)\mu_o} , \quad H_a = \frac{nI_a}{\left(\frac{2hS_1}{S_2} + 1\right)\mu_o} . \qquad (7.25)$$

The force P_1 can be neglected because it creates only a very small value of the longitudinal deformation.

For presenting the results we employ the following dimensionless quantities

$$\bar{\omega} = \omega(m/k)^{\frac{1}{2}}, \ \bar{t} = t(k/m)^{\frac{1}{2}}, \ \bar{\mu} = \mu(mk)^{-\frac{1}{2}}, \ \bar{N} = \frac{N}{P}\bar{\mu}, \ \bar{F} = \frac{F}{P}\bar{\mu},$$

$$\bar{U} = \frac{U\mu}{P}(k/m)^{\frac{1}{2}}, \ \dot{\bar{U}} = \frac{\dot{U}\mu}{P},$$

where $m = \frac{1}{3}\rho bhl$, $k = \frac{4c_{11}^H bh}{l}$, $\mu = \frac{1}{3}\nu bhl$, ρ and ν - density and damping factor of the VP.

The characteristics of a single step motion caused by a sine wave package excitation depend upon the normal force $\bar{F}_N$, moving force $\bar{F}$ and excitation frequency $\bar{\omega}$. It has been obtained that the

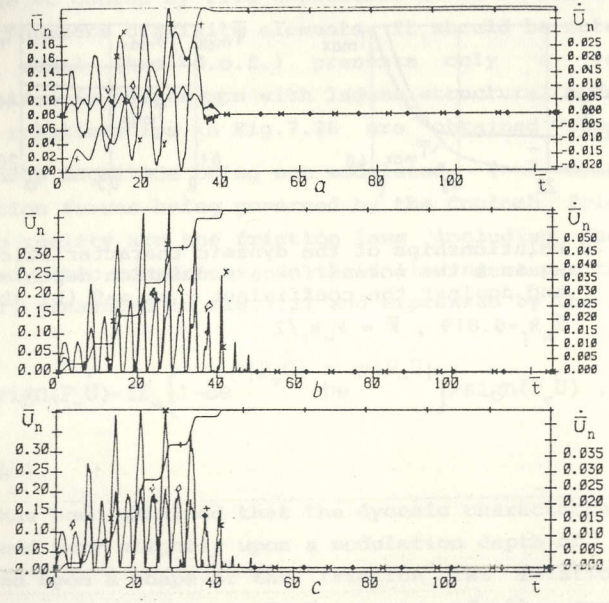

Fig.7.26 Time laws of the displacements and velocities of the right-hand end of the VC at $\bar{F}_N k_f = 0.019$, $\bar{F} = F_N k_f/2$, $\bar{\omega}=1$:
a) 1 element, b) 10 elements, c) 20 elements ;
+ - $\dot{U}_N$, x - $\dot{U}_N$, ◊ - $\frac{\dot{U}_1+\dot{U}_N}{2}$ (average rigid body velocity)

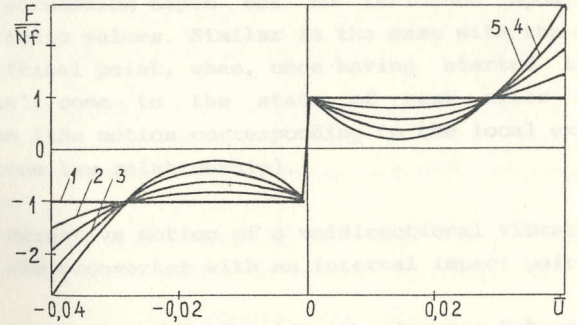

Fig.7.27 Family of friction law relationships
$1+\gamma\left[1-ae^{\beta\dot{U}}-be^{-\beta\dot{U}}\right]\mathrm{sign}\dot{U}$ at $a=\frac{3}{7}$, $b=\frac{4}{7}$, $\beta=10$:
1 - $\gamma = 0$, 2 - $\gamma = 20$, 3 - $\gamma = 40$, 4 - $\gamma = 60$, 5 - $\gamma = 80$

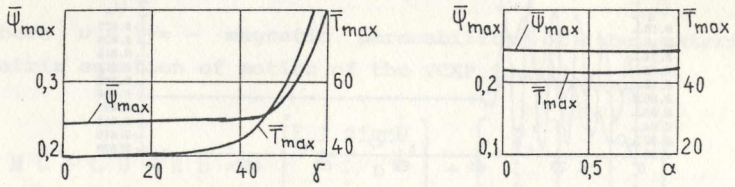

Fig.7.28 Relationships of the dynamic characteristics of the VCKP against the normal force modulation depth α at γ=40 (a) and against the coefficient γ at α=0 (b) at $\bar{F}_N k_f$=0.019 , $\bar{F} = F_N k_f/2$

optimal values are $\bar{\omega}$=1, $\bar{F}_N f$=0,019 , $\bar{F}=F_N f/2$. Fig.7.26 presents the time laws of the displacement and velocity of the right-hand end of the VC caused by five excitation waves $P=\mu\sin\omega t$ at several different numbers of finite elements. It should be noted that the simplest model (two d.o.f.) presents only a very rough approximation in comparison with larger structural models.

The relationships in Fig.7.26 are obtained assuming the normal force magnitude being not modulated, ($\bar{F}_N$=const), and the friction forces being governed by the Coulomb friction law. Closer to reality are the friction laws including the Coulomb, linear and cubic components. In the following we use the friction law family presented in Fig.7.27 and expressed by the relation

$$\bar{F}_T = -f\bar{F}_N \operatorname{sign}(P_T\dot{U}) - f\bar{F}_N\left[1-ae^{-\beta|P_T\dot{U}|}-be^{-\beta|P_T\dot{U}|}\right]\gamma\operatorname{sign}(P_T\dot{U}) , \quad (7.26)$$

where a+b=1.

It has been obtained that the dynamic characteristics of the VCKP depend very slightly upon a modulation depth of the normal force, and upon a shape of the friction law relationship. The modulation depth is expressed by means of the quantity α , expressing the ratio of the modulation amplitude to the mean value of the normal force. The quantity γ defines the local extreme values on the friction law curve shape. The corresponding relationships are presented in Fig.7.28. It should be noticed that the modulation depth has no influence upon the dynamic characteristic values. Similar is the case with the quantity γ up to the critical point, when, once having started to move, the VCKP doesn't come to the state of rest after removing the excitation (the motion corresponding to the local extreme zone of the friction law relationship).

7.2.2 Directive motion of a unidirectional vibration vibroconverter with an internal impact pair

Mathematical model. Consider the dynamic behavior of the VD in Fig.7.29a. It consists of the piezoelectric VC 1 and the rigid body of the mass m , prestressed to each other by means of a

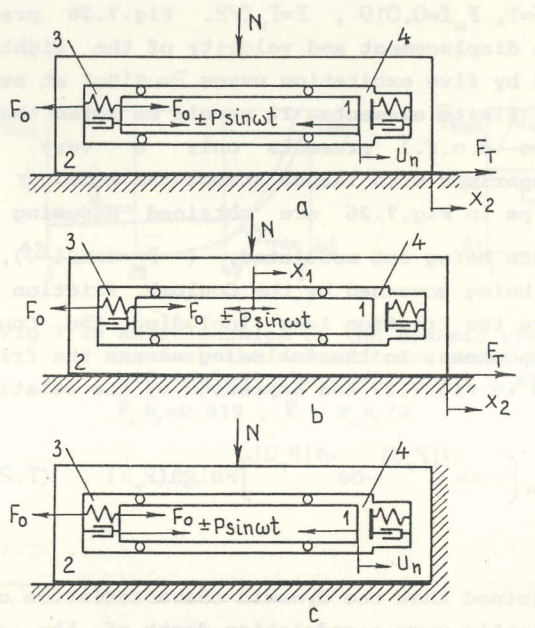

Fig.7.29
Vibroconverter with a nonlinear interaction point: 1-input link, 2-output link, 3-connecting element, 4- impact rheological model

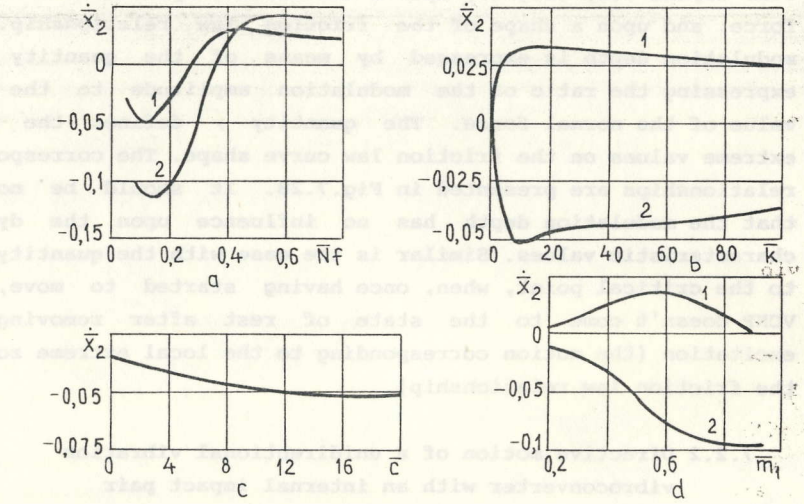

Fig.7.30 Mean velocity relationships:

a- 1- $\bar{m}_1=\bar{m}_2=0.5$; 2- $\bar{m}_1=0.8$; $\bar{m}_2=0.2$ at $\bar{k}=1000$, $\bar{c}=0.01\frac{k}{\omega}$;

b- 1 - $\bar{N}f=0.04$; 2 - $\bar{N}f=0.015$; at $\bar{c}=0.01\frac{k}{\omega}$, $\bar{m}_1=\bar{m}_2=0.5$;

c- $\bar{k}=1000$, $\bar{m}_1=\bar{m}_2=0.5$, $\bar{N}f=0.015$;

d- 1 - $\bar{N}f=0.04$; 2 - $\bar{N}f=0.015$; at $\bar{k}=10$, $\bar{c}=0.01\frac{k}{\omega}$

connecting element 3 of the stiffness k_1 and damping c_1. During the vibration of the VC, between its right-hand end and the body 2 the impact interaction takes place. For the mathematical representation of the impact interaction forces a phenomenological model is employed consisting of a spring and a dissipative element connected in parallel with the coefficients k and c correspondingly. Assume the value of the stiffness coefficient k_1 being considerably less than the longitudinal stiffness of the VC as well as the value of the coefficient k. Therefore it appears reasonable to assume that the influence of the connecting element upon the impact vibration is exhibited only as the action of the constant prestressing force F_o. The body 2 is in mechanical contact with the rough plane surface, and the tangential interaction force is assumed to be the Coulomb friction force obtained from the relation

$$F_T = -fN \operatorname{sign} \dot{x}_2 , \qquad (7.27)$$

where x_2 - rectilinear displacement of the body 2 along the axis Ox, f - Coulomb friction coefficient, and N - magnitude of the normal force holding down the body 2 to the surface. The input voltage $\pm P\sin\omega t$ applied to the electrodes of the VC creates the equivalent longitudinally acting harmonic excitation forces. The angular excitation frequency ω is selected in the vicinity of the eigenfrequency of the first longitudinal mode of the VC in order to obtain higher vibration amplitudes. As a result of the impact vibration of the VC 2, the friction force impetus during one vibration period isn't equal to zero, i.e., $\int_0^T F_T dt \neq 0$, and a directive rectilinear motion of the body 2 along the Ox axis is obtained, illustrating the principle of a VD employing purely longitudinal vibration and excited by a monoharmonic external forcing [47].

Taking on account that the values of the coefficients k_1 and c_1 are comparatively small, we present the equations of motion of the system in Fig.7.29 as

$$\begin{bmatrix} M & \\ & m \end{bmatrix}\begin{pmatrix} \ddot{U} \\ \ddot{X}_2 \end{pmatrix}+\begin{bmatrix} C & \\ & c \end{bmatrix}\begin{pmatrix} \dot{U} \\ \dot{X}_2 \end{pmatrix}+\begin{bmatrix} K & \\ & k \end{bmatrix}\begin{pmatrix} U \\ X_2 \end{pmatrix}=\begin{pmatrix} F_o \\ \vdots \\ 0 \\ -F_o \end{pmatrix}+\begin{pmatrix} P \\ \vdots \\ -P \\ 0 \end{pmatrix}\sin\omega t+\begin{pmatrix} 0 \\ \vdots \\ -F_N \\ F_N+F_T \end{pmatrix}, \quad (7.28)$$

where M, C, K - structural matrices of the finite element model, U - nodal displacement vector, F_T - friction force obtained from the relation (7.27), F_N - normal interaction force in the contact pair 4 expressed as

$$F_N = \begin{cases} (u_n-X_2)k+(\dot{u}_n-\dot{X}_2)c \text{ , if } u_n \geq X_2 \text{ и } F_N \geq 0 \text{ ,} \\ 0 \text{ , otherwise} \end{cases}$$

u_n being the last element of the vector U, corresponding to the displacement of the right-hand end of the finite element model of the VC.

In order to investigate the behavior of such a system, in place of (7.28) we consider two simplified models. The first one presented in Fig.7.29b reflects the directive motion feature of the two body system 1 and 2 connected by the spring 3 as of a whole. An external excitation here is applied by means of two harmonic forces. The impacts take place between the rigid bodies having the masses m_1 and m_2, their displacements being denoted through X_1 and X_2.

The second simplified model presented in Fig.7.29c reflects the behavior of the VC as of the resonant vibro-impact system. The difference from the model in Fig.7.29a is that the body 2 here is fixed, and in essence it coincides with the model in Fig.7.1c. It seems worth to notice that the impact vibration laws of the systems presented in Fig.7.29(a) and (c) differ very slightly because the velocity of the translational motion of the system as of a whole is considerably less than the vibrational velocity of the VC.

Transient motion laws are obtained by integrating numerically in time the equations of motion of the model presented in Fig.7.29b from zero initial values during the time interval 5-10T, where $T=\frac{2\pi}{\omega}$ - excitation period. Further the analysis is carried out keeping constant the following relations:

1) $m_1+m_2=$ const (total mass of the system);

2) $\omega = (k_1/m_1+k_1/m_2)^{\frac{1}{2}}$ (resonant frequency of the unconstrained vibration)

3) $c_1 = \left[(m_1+m_2)k_1\right]^{\frac{1}{2}}$ (Q-factor of the system is equal to 2),

and employing the dimensionless quantities $\bar{\dot{X}} = \frac{\dot{X}}{a\omega}$, $\bar{N}=\frac{N}{(m_1+m_2)g}$, $\bar{m}=\frac{m}{m_1+m_2}$, $\bar{k} = \frac{k}{K_1}$, $\bar{c} = \frac{c}{K_1}\omega$, where a demotes the mean peak-to-peak amplitude of the vibration, obtained from the formula

$a = \max\limits_{t\in(0,T)}(X_2-X_1) - \min\limits_{t\in(0,T)}(X_2-X_1)$, g - gravity constant.

It follows from the relationships presented in Fig.7.30a, that the directive motion of the system is possible in the forward as well as in the backward direction. The value $\bar{N}f$ at the point of reverse depends upon the remaining parameters of the system and is within the range $\bar{N}f=0,025 - 0,04$. Thus, a motion direction system can be reversed by adjusting an appropriate value of the critical friction force $\bar{N}f$.

The relationships of the velocities in the forward and backward directions (Fig.7.30b) point out that the value of the impact pair stiffness coefficient should exceed the stiffness of the connecting element at least to one order. Increasing the damping in the impact pair, increases the velocity of the body 2 (Fig.7.30c). In Fig.7.30d the relationships of the velocity upon the mass ratio of impacting bodies are presented. The values $\bar{N}f=0,015$ and $\bar{N}f=0,04$ were selected in order to obtain maximum velocity values in the forward and backward directions correspondingly. The shapes of the curves 1 and 2 differ severely from each other. The curve 1 (motion in forward direction) has the maximum value at $\bar{m}_1=0,6$, and the curve 2 (motion in backward direction) presents a monotonous decreasing relationship. The highest velocities in the both directions are obtained, if $\bar{m}_1=0,6-0,8$, that corresponds to the ratio $\frac{m_1}{m_2} = 1,5 - 4$.

Stationary vibration is investigated employing a model with the fixed output link, Fig.7.29b. The geometric parameters of the VC are length l=0.1m, width b=0.01m, thickness h=0.001m,

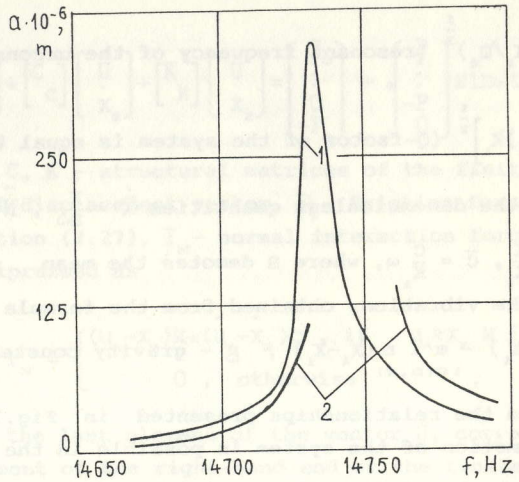

Fig.7.31 AFCH of the right-hand end of the VC at $k_1=5\times10^4$ N/m², $k=5\times10^6$ N/m², $c_1=c=0$, Q=2000, 6 Fourier components:
1 - F_o= 1N , 2 - F_o= 2N

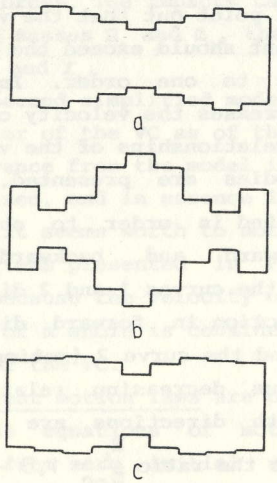

$\frac{\omega_2^2}{\omega_1^2}=6$, $\frac{\omega_3^2}{\omega_1^2}=12$

$\frac{\omega_2^2}{\omega_1^2}=2$, $\frac{\omega_0^2}{\omega_1^2}=7$

$\frac{\omega_2^2}{\omega_1^2}=5$, $\frac{\omega_3^2}{\omega_1^2}=10$

Fig.7.32 Shape forms of the rod-type VC, ensuring the prescribed ratios of the eigenfrequency values:

a) $\frac{\omega_2^2}{\omega_1^2}=6$, $\frac{\omega_3^2}{\omega_1^2}=12$; b) $\frac{\omega_2^2}{\omega_1^2}=2$, $\frac{\omega_3^2}{\omega_1^2}=7$; c) $\frac{\omega_2^2}{\omega_1^2}=5$, $\frac{\omega_3^2}{\omega_1^2}=10$

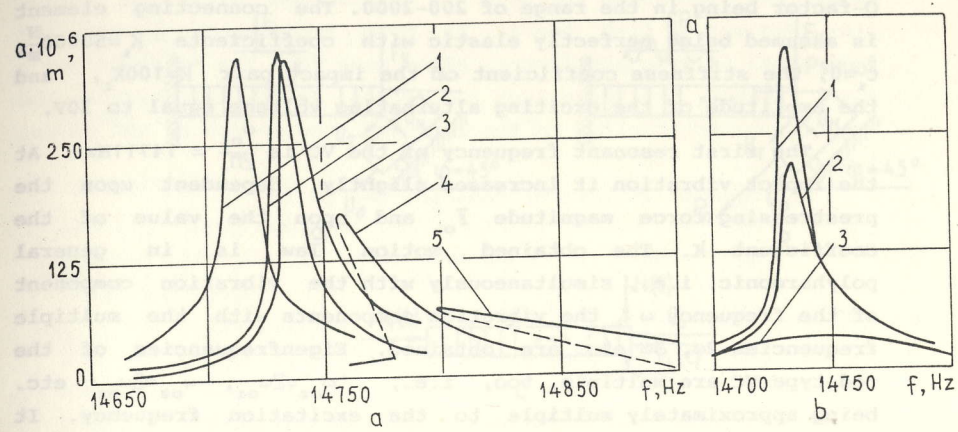

Fig.7.33 AFCH of the right-hand end of the VC (shape of the VC as in Fig.7.32b) at $k_1=5\times10^4$ N/m², $k=5\times10^6$ N/m², $c_1=c=0$, Q=2000, 6 Fourier components:

a- at Q=2000, c=0; 1- unconstrained vibration (linear);
2 - F_o= 1N ; 3 - F_o= 2N ; 4 - F_o= 3.5N ; 5 - F_o= 5N ;

b- at F_o= 1N; 1-Q=2000, c=0; 2 -Q-2000, c=5Ns/m; 3 -Q-200, c=0

material constants $c_{11}^E=0.6\times10^{11}\frac{N}{m^2}$, $\rho=7800\frac{kg}{m^3}$, $e_{31}=8.46$, the Q-factor being in the range of 200-2000. The connecting element is assumed being perfectly elastic with coefficients $k_1=50000\frac{N}{m}$, $c_1=0$, the stiffness coefficient of the impact pair $k=100k_1$, and the amplitude of the exciting alternating voltage equal to 30V.

The first resonant frequency of the VC is $\frac{\omega_{01}}{2\pi}$ = 14711Hz. At the impact vibration it increases slightly, dependent upon the prestressing force magnitude F_o and upon the value of the coefficient k. The obtained motion law is in general polyharmonic, i.e., simultaneously with the vibration component of the frequency ω, the vibration components with the multiple frequencies 2ω, 3ω etc. are obtained. Eigenfrequencies of the rod-type VC are multiple, too, i.e., $\omega_{02}=2\omega_{01}$, $\omega_{03}=3\omega_{01}$ etc. being approximately multiple to the excitation frequency. It appears as the main reason of an excessive excitation of the higher vibration components disturbing the expected motion law. Fig.7.31 presents the AFCH of the right-hand end vibration obtained employing the harmonic balance method taking on account the first six harmonic components. At the prestressing force value $F_o=2$ in the frequency range 14729-14749Hz stationary vibration laws don't exist.

In order to reduce the influence of the higher harmonic components it is necessary to employ the VC having no multiple eigenfrequencies. The eigenfrequency spectrum may be adjusted by means of the geometric shape (cross section) optimization employing the optimal design techniques [14].

In Fig.7.32 three shapes of the rod-type VC are presented with different ratios of the three first eigenfrequency values. The AFCH curves for the VC in Fig.7.32b are presented in Fig.7.33.

7.2.3 Free and forced motion of a vibrodrive.

Free motion of a vibrodrive with an elastic rod-type VC and a rigid output link is investigated by means of a model presented in Fig.7.34. In the initial state the input link is elastically compressed by longitudinal force F_x and is held down to the surface of the output link by the transverse force F_y. At the

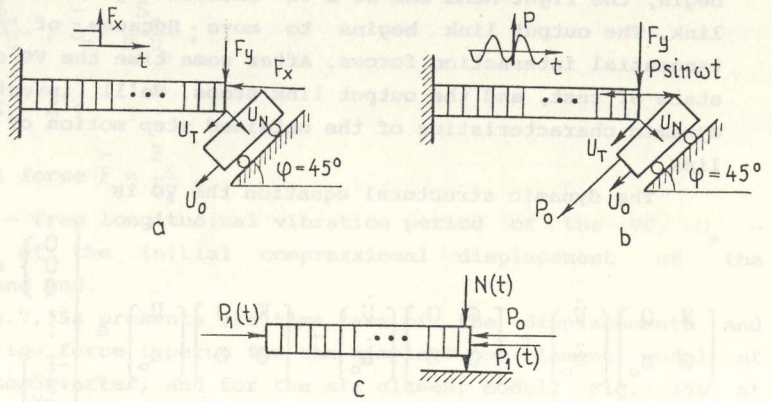

Fig.7.34 Finite element models of a vibrodrive

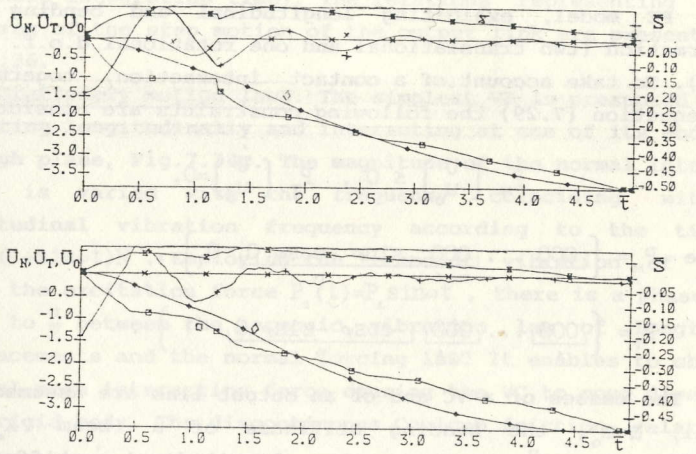

Fig.7.35 Time laws of the displacements and of the contact force impetus of the right-hand end of the vibroconverter at the free motion of a vibrodrive at $\bar{F}_y=0.075$, $m=m_o$, $k_e<<k_t$, f=0.5; a) NEL=1; b) NEL=6;

+ - $\bar{u}_N$; x - $\bar{u}_T$; ◊ - $\bar{u}_T$; □ - $\bar{S}_N$; X - $\bar{S}_T$

time instant t=0 the force F_x is removed, and free vibrations begin, the right-hand end of a VC interacting with the output link. The output link begins to move Because of normal and tangential interaction forces. After some time the VC comes to a state of rest, and the output link stops. We'll investigate the dynamic characteristics of the obtained step motion of the output link.

The dynamic structural equation the VD is

$$\begin{bmatrix} M & 0 \\ 0 & m_o \end{bmatrix}\begin{Bmatrix} \ddot{U} \\ \ddot{u}_o \end{Bmatrix} + \begin{bmatrix} C & 0 \\ 0 & 0 \end{bmatrix}\begin{Bmatrix} \dot{U} \\ \dot{u}_o \end{Bmatrix} + \begin{bmatrix} K & 0 \\ 0 & 0 \end{bmatrix}\begin{Bmatrix} U \\ u_o \end{Bmatrix} = \begin{Bmatrix} 0 \\ 0 \\ 0 \\ \vdots \\ -F_x \\ 0_y \\ 0 \end{Bmatrix}\begin{matrix} \\ \\ \\ \\ \}\,n \\ \\ \end{matrix}, \quad (7.29)$$

where M,C,K - structural matrices of the VC presented by a beam type FE model, exhibiting longitudinal and bending elastic deformation (two translational and one rotational d.o.f. at each node). To take account of a contact interaction, together with the equation (7.29) the following constraints are considered :

$$P_N \begin{Bmatrix} U \\ u_o \end{Bmatrix} \le 0 , \quad P_T \begin{Bmatrix} \dot{U} \\ \dot{u}_o \end{Bmatrix} = 0,$$

where $P_N = \left(\underbrace{000}_{i} \ldots \underbrace{000}_{n-i} \underbrace{\sin\varphi \ -\cos\varphi \ 0}_{n} \ 0 \right)$,

$$P_T = \left(\underbrace{000}_{i} \ldots \underbrace{000}_{n-i} \underbrace{-\cos\varphi \ -\sin\varphi \ 0}_{n} \ -1 \right) .$$

The masses of a VC and of an output link are assumed to be equal, $m=m_o$, the bending stiffness of a beam k_e being considerably less than the longitudinal stiffness k_l, i.e., $k_e << k_l$, and the Coulomb friction coefficient $k_f=0,5$. For representing the results the following dimensionless quantities will be employed:

- the displacements of the right-hand end of a VC and of an output link $\bar{u}_N = \frac{u_N}{u_p}$, $\bar{u}_T = \frac{u_T}{u_p}$, $\bar{u}_o = \frac{u_o}{u_p}$;

- the impetus of normal and tangential interaction forces

$$\bar{S}_N = \frac{S_N}{k_l u_p} , \quad \bar{S}_T = \frac{S_T}{k_l u_p} ;$$

- time $\bar{t} = \frac{t}{T}$;

- normal force $\bar{F}_y = \frac{F_y}{F_x}$,

where T - free longitudinal vibration period of the VC, u_p - modulus of the initial compressional displacement of the right-hand end.

Fig.7.35a presents the time laws of the displacements and interaction force impetus for the simplest one-element model of the vibroconverter, and for the six element model, Fig.7.35b at F_y=0,075 . By investigating the obtained time laws we find, that the integration scheme behaves itself stable, regardless of the comparatively large integration step (500 integration steps for the whole integration time). The relations representing dynamic features of the step motion of the output link are presented in Fig.7.36.

Stationary motion laws. The simplest VD is presented by a VC vibrating longitudinally and interacting at one of its ends with a rough plane, Fig.7.34c. The magnitude of the normal interaction force is varied with the frequency coinciding with the longitudinal vibration frequency according to the time law $N(t)=(1+\sin\omega t)N$. Employing the resonant vibration of the VC under the excitation force $P_1(t)=P_1\sin\omega t$, there is a phase shift equal to $\frac{\pi}{2}$ between the harmonic vibration law of longitudinal displacements and the normal forcing law. It enables to obtain an optimal mean interaction force causing the VC to move directively as a rigid body. The discontinuous Coulomb friction relationship $W_n = k_f N(t) \operatorname{sign} \dot{U}_n$ can be approximated as $W_n = \frac{2}{\pi} k_f N(t) \operatorname{arctg} \omega \dot{U}_n$, where $\dot{U}_n$ is the velocity of the right-hand (i.e., n-th)point of the VC. The dynamic behavior analysis of the 10 element structure of the VD is carried out by employing the time-averaging techniques taking on account two harmonic components (p=2). Fig.7.37 presents the AFCH of the contact point vibration (the amplitude of the first harmonic component $\bar{U}_n^1$) at several

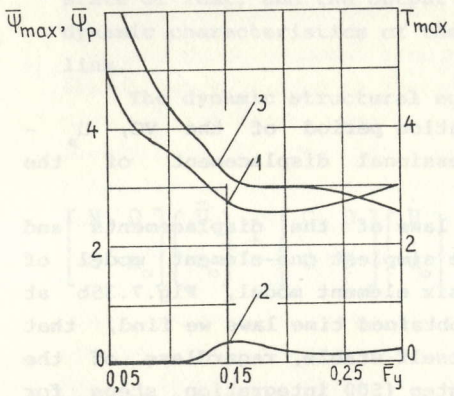

Fig.7.36 Free step-motion characteristics of a VD:
1 - ψ_{max}, 2 - ψ_p, 3 - T_{max}

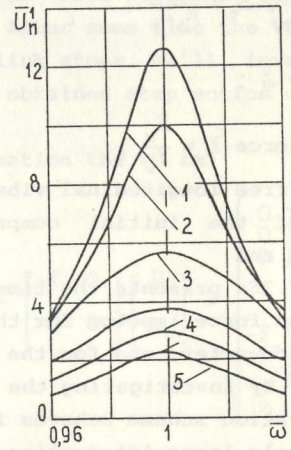

Fig.7.37 AFCH of the input link vibration:
1 - $\bar{N}$=0 (unconstrained vibration); 2 - $\bar{N}$=1 ;
3 - $\bar{N}$=3 ; 4 - $\bar{N}$=5 ;
5 - $\bar{N}$=7 ; 6 - $\bar{N}$=9

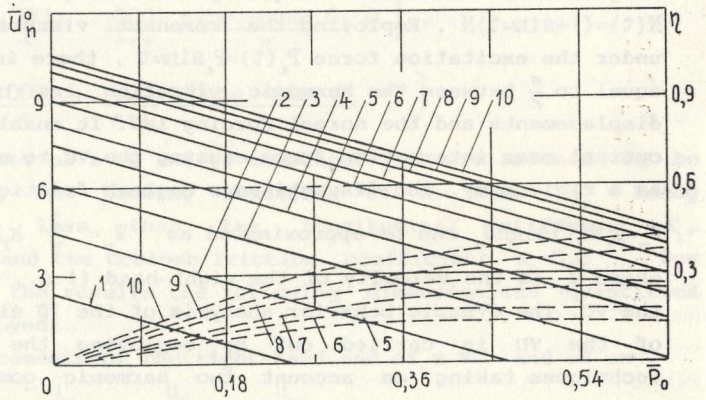

Fig.7.38 Relationships moving force - output link velocity (solid line) and the mechanical efficiency relationships against the moving force (dashed line):
1 - $\bar{N}$=1 ;2 - $\bar{N}$=2 ; 3 - $\bar{N}$=3 ; 4 - $\bar{N}$=4 ; 5 - $\bar{N}$=5 ;
6 - $\bar{N}$=6 ; 7 - $\bar{N}$=7 ;8 - $\bar{N}$=8 ; 9 - $\bar{N}$=9 ; 10 - $\bar{N}$=10

different values of the mean normal force. The resonant frequency of such a VD is the same as of the free VC at an arbitrary value of the normal force $\bar{N}$, however, vibration amplitudes depend considerably upon the magnitude of $\bar{N}$. Fig.7.38 presents the characteristic "moving force - velocity", where the magnitude of the moving force is assumed to be equal to the magnitude of the braking force $\bar{P}_o$ at the constant rigid body motion velocity of the VC (mean velocity value of the VC is equal to the zero harmonic component $\dot{\bar{U}}_o$ of the velocity). The mechanical efficiency of the VD is obtained as

$$\eta = \frac{A_n}{A_{exc}} , \qquad (7.30)$$

where A_n - useful work, A_{exc} - work done by excitation forces. The formula obtained employing the time-averaged equations reads as

$$\eta = \frac{2P_o U^o_{(i)}}{P_i (U^1_{s(i)} - U^1_{s(n)})} ,$$

where $U^o_{(i)}$ - zero harmonic component amplitude of the left-hand end of a VC, $U^1_{s(i)}, U^1_{s(n)}$ - first harmonic components of the left and right-hand ends correspondingly.

Another model of a VD presented in Fig.7.34b differs from the latter one by the external forcing pattern. In this case prestressing is ensured by means of the force F_y, and the equivalent harmonic excitation is applied to the right-hand end of the VC. The magnitude of the constant braking force P_o at the constant output link velocity value is considered as a moving force of the VD.

In order to represent the computed results in terms of dimensionless quantities, the longitudinal and transversional stiffness coefficients of the VC at the contact point are introduced (k_e and k_l correspondingly). The stiffness coefficient in the direction normal to the contact surface is equal to

$k_u = \frac{k_l k_e}{k_l \cos^2\varphi + k_e \sin^2\varphi}$. The stiffness and fluid friction coefficients of the contact rheology model in the normal and tangential directions are denoted through k_N, k_T, c_N, c_T . Computations have

been carried out employing the following numerical values :

$c^{D}_{11}=0.826\times10^{11}\frac{N}{m^2}$, $d_{a1}=113\times10^{-12}\frac{C}{N}$, $\varepsilon^{T}_{aa}=8.85\times10^{-9}\frac{F}{m}$, $k_{a1}=0,34$,

$k_U=1.22\times10^{4}\frac{N}{m}$, $k_N=k_T=1.7\times10^{6}\frac{N}{m}$, $c_N=c_T=0$, $\rho=5700\frac{kg}{m^3}$, $\varphi=\frac{\pi}{4}$.

Dependent on the values of the vibration frequency, prestressing force and some other parameters, the VC of the VD can operate in the in the main vibration mode (single impact during the excitation period) as well as employing complex vibration laws. For evaluating the vibration mode of a VC, the following quantities are introduced:

$$k_A=\sum_{i=1}^{e}|\bar{A}-A_i|/\bar{A}\;;\quad k_a=\sum_{i=1}^{e}|\bar{a}-a_i|/\bar{a}\;;$$

$$k_f=\sum_{i=1}^{e}|\bar{F}_{Nmax}-F_{Nmaxi}|/\bar{F}_{Nmax},$$

where $\bar{A}=\frac{1}{e-l}\sum_{i=l}^{e}A_i$; $\bar{a}=\frac{1}{e-l}\sum_{i=l}^{e}a_i$; $\bar{F}_{Nmax}=\frac{1}{e-l}\sum_{i=l}^{e}F_{Nmaxi}$;

e - total number of periods during the integration time, l - number of excitation periods necessary for obtaining the stationary vibration law ($l<e$ is assumed), A_i - maximum displacement value of the contact point during the i-th period, a_i - minimum displacement value of the contact point during the i-th period, F_{Nmaxi} - maximum value of the normal interaction force during the i-th period.

Employing these quantities enables to distinguish the parameter ranges determining the stability and existence region of the main vibration mode of a VC, requiring these values remain less than some constant value, e.g., $k_A,k_a,k_f<0,1$.

All the relationships presented below have been obtained in the main vibration mode region of the VD, employing the following dimensionless quantities: $\bar{F}_y=\frac{F_y}{k_u a_o}\cos\varphi$; $\bar{P}_o=\frac{P_o}{k_u a_o}$; $\dot{\bar{u}}_o=\frac{\dot{u}_o}{\omega_o a_o}$; $\bar{\omega}=\frac{\omega}{\omega_o}$; $\bar{a}=\frac{a}{a_o}$, where $a=\left(a_N^2+a_T^2\right)^{\frac{1}{2}}$, $a_o=\left(a_{No}^2+a_{To}^2\right)^{\frac{1}{2}}$; ω_o - angular eigenfrequency of the unconstrained VC, a_{No},a_{To} - resonant vibration amplitudes of the contact point of the unconstrained VC (at the frequency value ω_o) in the normal and tangential

directions correspondingly, a_N,a_T - contact point vibration amplitudes at the frequency ω; P_o - mean moving force.

Fig.7.39 presents the AFCH of the contact point of the input link at several prestressing force values assuming the output link being held-up (zero output link velocity, $\dot{u}_o=0$). The resonant frequency values increase slightly by increasing the prestressing force $\bar{F}_y$. The maximum vibration amplitude value remaining approximately the same, the left-hand slope of the AFCH curve becomes steeper by increasing the values of $\bar{F}_y$. The AFCH of the tangential vibration of the contact point are more complicated,and the positions of their peeks on the frequency axis don't coincide with the peeks of the normal vibration AFCH.

Fig.7.40 presents the existence region of the main vibration mode of the VC in the plane of parameters excitation frequency - prestressing force (the shaded region corresponds to the values $k_A,k_a,k_f>0.1$). Solid lines are the level curves of the moving force at the held-up output link (zero output link velocity). The maximum values of the moving force have been obtained at $13<\bar{F}_y<14$ and $1.08<\bar{\omega}<1.1$.

The mechanical efficiency η of the VD is obtained from the relation (7.30). Its value depends on several parameters, the velocity of the output link being among them. In Fig.7.40 for each pair of values $(\bar{F}_y,\bar{\omega})$ the maximum value of η obtainable by changing the velocity $\dot{\bar{u}}_o$ of the output link is considered. The dashed line presents the boundary of the region where the mechanical efficiency value exceeds 0.5 . The relationships of the mechanical efficiency and the moving force from the output link velocity are presented in Fig.7.41 by means of solid and dashed lines correspondingly. It is worth to notice that the maximum mechanical efficiency is obtained at the velocity values $\dot{\bar{u}}_o$ close to the maximum available. The maximum output velocities are obtained at comparatively small prestressing force values ($\bar{F}_y<10$) and exhibit tendency to increase by approaching the boundary of the main vibration mode existence region. In Fig.7.42 the parts of the curves drawn by dashed line don't belong to the main vibration mode.

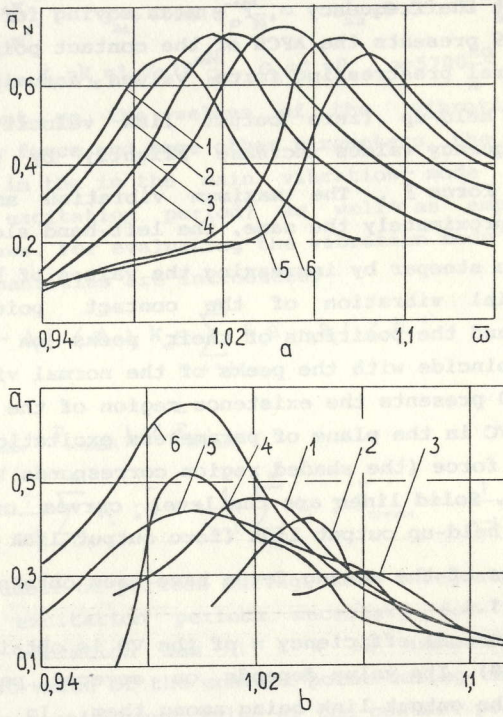

Fig.7.39 AFCH of the input link contact point vibration at $\dot{\bar{u}}_o=0$ in normal (a) and tangential (b) direction:
1- $\bar{F}_y=0$ (unconstrained harmonic vibrations);
2-$\bar{F}_y=3.37$; 3-$\bar{F}_y=6.73$; 4-$\bar{F}_y=10.1$; 5-$\bar{F}_y=13.5$; 6-$\bar{F}_y=16.8$

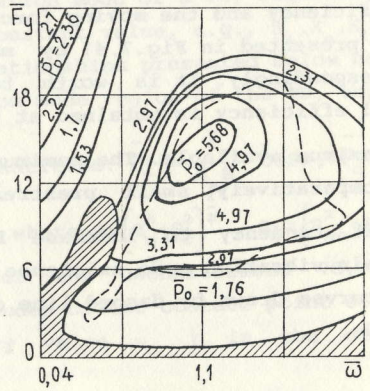

Fig.7.40 Existence area of the main vibration mode

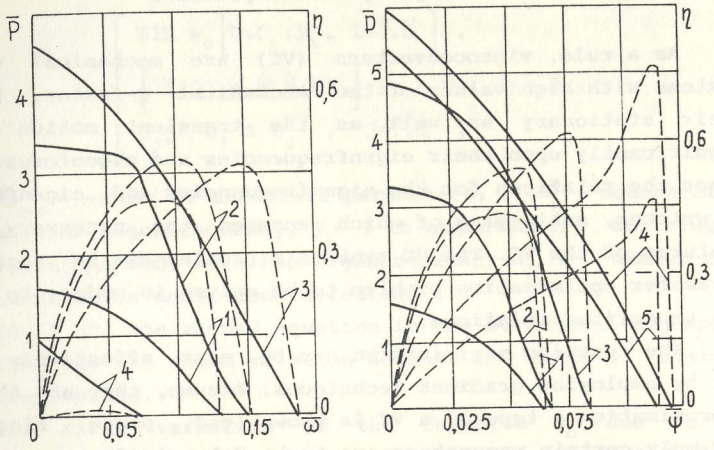

Fig.7.41 Relationships "moving force-output link velocity" (solid line) and the mechanical efficiency relationships against the moving force (dashed line) at $\bar{\omega}=1.03$ and $\bar{\omega}=1.12$:
1-$\bar{F}_y=3.37$; 2-$\bar{F}_y=6.73$; 3-$\bar{F}_y=10.1$; 4-$\bar{F}_y=13.5$; 5-$\bar{F}_y=16.8$

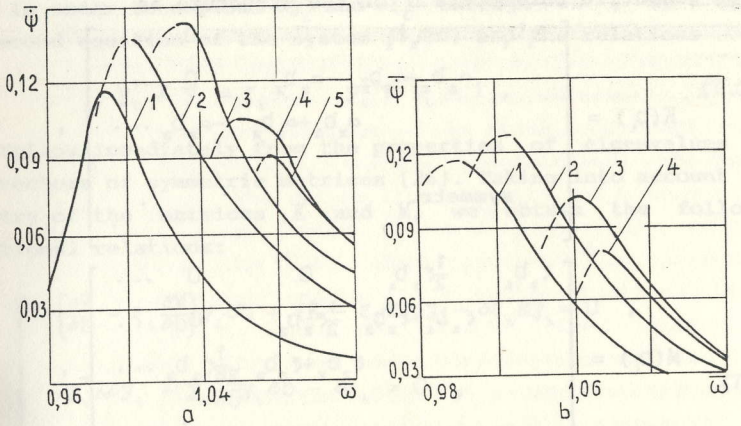

Fig.7.42 Excitation frequency-output link velocity relationships at the constant moving force at $\bar{P}_o=0.66$(a) and $\bar{P}_o=1.98$(b):
1-$\bar{F}_y=3.37$; 2-$\bar{F}_y=6.73$; 3-$\bar{F}_y=10.1$; 4-$\bar{F}_y=13.5$; 5-$\bar{F}_y=16.8$

7.3 SYNTHESIS OF ACTIVE LINKS OF VIBRODRIVES

7.3.1 Optimal shape synthesis problems

As a rule, vibroconverters (VC) are mechanical vibrating systems with high values of the mechanical Q-factor, therefore their stationary as well as the transient motion depends significantly upon their eigenfrequencies and eigenforms. In most cases the relations for the eigenfrequencies and eigenforms can be written, satisfying of which ensures the necessary dynamic features of the VC. The VC synthesis problem can be regarded as parameter optimization problem to be solved in order to satisfy the prescribed relations.

The function minimization can be most effectively carried out by employing gradient techniques. Assume, that at the first approximation a type of a VC is known (rod, plate, ring etc.), and only certain parameters are to be determined, e.g., the cross section of the rod, variable thickness of the plate, height and radiuses of the conical VC etc. In such a case finite element matrices of the VC can be presented as functions $K(b_i)$, $M(b_i)$ of the geometric parameters b_i of the structure as

$$K(b_i) = \begin{bmatrix} \alpha_1 b_1 & -\alpha_1 b_1 & 0 & 0 & \dots \\ & \alpha_1 b_1 + \alpha_2 b_2 & -\alpha_2 b_2 & 0 & \dots \\ & & \alpha_2 b_2 + \alpha_3 b_3 & -\alpha_3 b_3 & \dots \\ & & & \cdot & \\ & \text{symmetr.} & & & \cdot \end{bmatrix},$$

$$M(b_i) = \begin{bmatrix} \xi_1 b_1 & \frac{1}{2}\xi_1 b_1 & 0 & 0 & \dots \\ & \xi_1 b_1 + \xi_2 b_2 & \frac{1}{2}\xi_2 b_2 & 0 & \dots \\ & & \xi_2 b_2 + \xi_3 b_3 & \frac{1}{2}\xi_3 b_3 & \dots \\ & & & \cdot & \\ & \text{symmetr.} & & & \cdot \end{bmatrix},$$

where $\alpha_i = \frac{c^E_{11}}{l_i}$, $\xi_i = \frac{\rho l_i}{3}$, c^E_{11} – Young's modulus, ρ – material density, l_i – length of the i-th finite element.

In general, a penalty function ψ_o minimization problem is presented as

$$\begin{cases} \min \psi_o \left[b, \xi_i, y_i, \ i=\overline{1,h} \right], \\ \left[K(b) - \xi_i M(b) \right] y_i = 0, \ i=\overline{1,h}, \\ b_{j*} \le b_j \le b_j^*, \ j=\overline{1,m}, \end{cases} \tag{7.30}$$

where $b_{m\times 1}$ – vector of structure parameters, $\xi_i = \omega_i^2$ – square of the i-th angular eigenfrequency, y_i – i-th eigenvector, defining the i-th vibration mode with the eigenfrequency ω_i, h – number of the structural modes under consideration.

In (7.30) the second equation is the structural eigenproblem equation, and the third relation defines the range of admissible parameter values.

The first variation of the function ψ_o due to small variations of the structure parameters is presented as follows

$$\delta\psi_o = \sum_{i=1}^{h} \frac{\partial \psi_c}{\partial y_i} \delta y_i + \sum_{i=1}^{h} \frac{\partial \psi_c}{\partial \xi_i} \delta\xi_i + \frac{\partial \psi_o}{\partial b} \delta b . \tag{7.31}$$

In order to express δy_i and $\delta\xi_i$ through δb, we employ the second equation of the system (7.30) and the relations

$$y_i^T K y_i = \xi_i , \quad y_i^T M y_i = 1 , \tag{7.32}$$

that follow immediately from the properties of eigenvalues and eigenvectors of symmetric matrices [26]. Taking into account the symmetry of the matrices K and M, we obtain the following variational relations:

$$\begin{cases} \left[\frac{\partial K}{\partial b} - \xi_i \frac{\partial M}{\partial b} \right] y_i \delta b + (K - \xi_i M)\delta y_i - \delta\xi_i M y_i = 0 , \\ 2 y_i^T K \delta y_i + y_i^T \frac{\partial K}{\partial b} y_i \delta b - \delta\xi_i = 0 , \\ 2 y_i^T M \delta y_i + y_i^T \frac{\partial M}{\partial b} y_i \delta b = 0 . \end{cases} \tag{7.33}$$

From the second equation of the system (7.30) and from the relations (7.32), (7.33) we obtain

$$\delta y_i = A_i^{-1} B_i \delta b , \quad \delta\xi_i = C_i \delta b , \tag{7.34}$$

where $A_i = K - \xi_i M - 2M y_i y_i^T K$, $B_i = \left(\frac{\partial K}{\partial b} - \xi_i \frac{\partial M}{\partial b} - 2M\, y_i y_i^T \frac{\partial K}{\partial b} \right) y_i$,

$C_i = y_i^T \left(\frac{\partial K}{\partial b} - \xi_i \frac{\partial M}{\partial b} \right) y_i$.

Taking on account (7.34), the function variation defined by the relation (7.31) is presented as

$$\delta\psi_o = g_o\, \delta b \quad , \tag{7.35}$$

where $g_o = \sum_{i=1}^{h} \left[\frac{\partial \psi_c}{\partial y_i} A_i^{-1} B_i + \frac{\partial \psi_c}{\partial \xi_i} C_i \right] + \frac{\partial \psi_o}{\partial b}$ is the gradient vector of the function ψ_o in the space of the parameters b.

The minimization of the function ψ_o is carried out step-by-step employing the relations

$$b^{k+1} = b^k - \alpha\, g_o \quad , \quad k=0,1,2,\dots \quad , \tag{7.36}$$

where b^k, b^{k+1} - values of the structure parameters at the minimization steps k, k+1 correspondingly (b_o - the first approximation), α - coefficient determining the descent rate in the gradient direction. The coefficient α is selected in order to obtain a possibly high minimization rate and to avoid an oscillating behavior.

The inequalities of the system (7.30) are taken on account employing the relation

$$b_j^{k+1} = \begin{cases} b_j^{k+1} , & \text{if} \quad b_{j*} \le b_j^{k+1} \le b_j^{*} \\ b_{j*} , & \text{if} \quad b_j^{k+1} < b_{j*} \\ b_j^{*} , & \text{if} \quad b_j^{k+1} > b_j^{*} \end{cases} \quad , \tag{7.37}$$

If the constraint form is more complicated, the gradient projection techniques are to be employed [14].

Analysis of the cylindrical input link of a VD. The direct method to carry out optimization and synthesis leads through obtaining the relationships between eigenfrequencies, eigenforms and the parameters of the VC and selecting appropriate parameter values.

The dynamic model of the piezoelectric cylinder of radius r,

height H and wall thickness h is presented employing the theory of thin-wall shells. The radial, tangential and axial vibration modes are possible in such a VC. The response of the VC subjected to the harmonic excitation can be presented as a standing wave, the vibration of each point containing radial, tangential and axial displacement components. As a rule, the nodal points of each vibrational component don't coincide.

Further the results of the free and forced vibration analysis of the piezoelectric cylinder are presented. The following material constants of the piezoelectric ceramic $BaTiO_3$ are employed: $S^E_{11}=8.55\times10^{-12}m^2/N$; $S^E_{12}=2.61\times10^{-12}m^2/N$; $S^E_{66}=8.93\times10^{-12}m^2/N$; $e_{31}=-13.3C/m^2$; $k_{31}=0.208$; $\rho=5700kg/m^3$.

Fig.7.43 presents the relationships of the first four eigenfrequencies, corresponding to the modes possessing axial symmetry and the three-fold circumferential symmetry. At the height values less than 0.5r , two-dimensional analysis can be carried out in polar coordinates. Such relationships enable to obtain the parameter values ensuring desirable operational frequency, e.g., to keep it in the range of 20-100kHz (at higher frequencies too small vibration amplitudes are obtained, and at the lower frequencies the acoustic noise is produced. It has been obtained, that during the vibration corresponding to the third tangential mode, the tangential component of the standing wave amplitude approximately three times exceeds the radial component. In the case of the third radial mode the radial component of the standing wave amplitude approximately three times exceeds the tangential component. The output link velocity and a torque of a VD are usually predetermined by the tangential vibration amplitude, therefore the third tangential mode is preferable. However, often the corresponding eigenfrequencies are too high to obtain the necessary amplitude values (they exceed the eigenfrequencies of the radial modes 3 to 4 times, see Fig.7.43), and in the case of short cylinders H/r<0.5 the third radial mode is employed by means of introducing the metallic layer [71].

At H/r>0.5 the third tangential mode can be employed, because its eigenfrequency value reduces significantly when the height H increases. In Fig.7.44 the forced vibration amplitude relationships of the middle cross-section points of the cylinder are presented, corresponding to the line where the contact

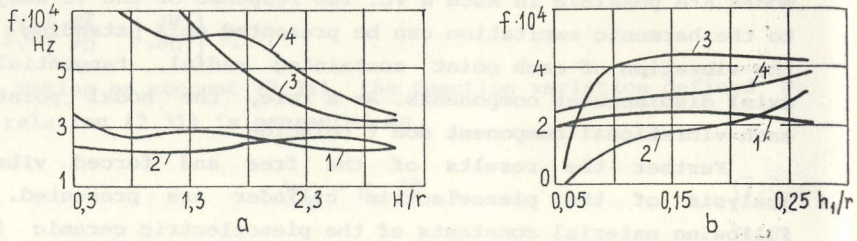

Fig.7.43 Eigenfrequency relationships of the cylindrical VC against the ratio H/r at $h_1/r=0.21$ (a) and against h_1/r at H/r=2.46 (b): 1- first axial mode, 2- third radial mode, 3 - second axial mode, 4 - third tangential mode

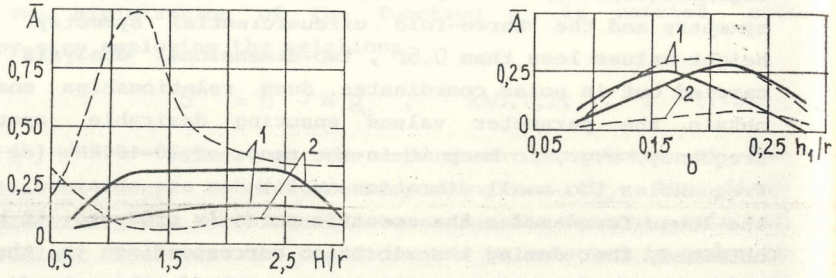

Fig.7.44 Forced vibration amplitude relationships against H/r at $h_1/r=0.21$ and from h_1/r at H/r=2.46 (b): 1-third tangential mode; 2-third radial mode; ——— - radial amplitude component; - - - - tangential amplitude component

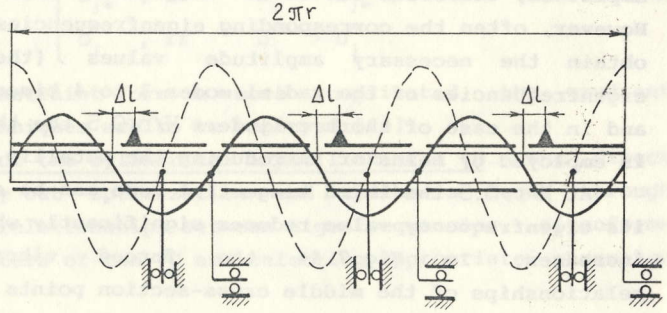

Fig.7.45 Wave-forms of the forced radial and tangential vibration, places of fixings and contact elements

elements of the VD are situated. The excitation frequencies are assumed to be equal to the eigenfrequencies of the corresponding modes. From the relationships in Fig.7.44a the optimal value of the ratio H/r=1 is obtained, enabling the most effective excitation of the tangential vibration. The optimal condition for exciting radial vibrations is obtained at H=(1.5 - 2)r, therefore preferable values lie in the range H=(1 - 1.5)r.

From the radial and tangential vibration amplitude component relationships it follows, that the maximum amplitude values are obtained at the cylinder wall thickness values h=0.2r, Fig.7.44b.

In order to select the points on the surface of the VC for the elements ensuring the mechanical contact between the input and output link, it is necessary to consider the positions of the nodal points of the radial and tangential vibration. Fig.7.45 presents the standing wave amplitude curve along the circumference of the short cylinder (H<<r) .The dashed line presents the tangential, and the solid line - the radial amplitude, the circumference of the cylinder being shown unrolled into a straight line.

The nodes of the radial and tangential waves don't coincide, being situated with the 1/4 wave length shift with respect to each other. Therefore there are no points in a state of rest, and only unidirectional supports can be applied in order to ensure the vibro-isolation of the VC from the environment. The elastic supports are also possible, however, they allow the rigid body motion of the VC and are undesirable when regarding precision of a VD.

The contact elements are situated in order to obtain their optimal vibration path. The angle of impact depends upon the distance Δl of the element from the radial component node and upon the ratio between the maximum amplitudes of the radial and tangential components. However, these quantities may be different due to the contact interaction between the input and output link of the VD, and a full model analysis of the VD should be carried out in order to obtain the optimal value of Δl .

7.3.2 Synthesis of asymmetric cycle vibroconverters

Exciting asymmetric vibration cycles in VC with the first eigenfrequency value being common multiple of other eigenfrequencies. The eigenfrequencies of all the longitudinal vibration modes of a rod type VC with the constant cross section have a common multiple being equal to the first mode eigenfrequency. By varying the length and the cross section inertia moment of a beam, it is possible to obtain the first two flexural mode eigenfrequencies to satisfy the relation $2\omega_1=\omega_2$. By varying the cross section inertia moment and the radius of a ring, similar relations can be obtained for ring-type VC.

For obtaining asymmetric vibration cycles at certain point of a VC, the eigenform values at these points must satisfy prescribed relations. E.g., the Fourier series expansion of the triangular pulse sequence of the height a reads as

$$f(t) = \frac{a}{\pi}\left(\sin\omega t + \frac{1}{2}\sin 2\omega t + \frac{1}{3}\sin 3\omega t + \ldots\right) .$$

In order to obtain the vibration law of a certain VC point approximating the triangular pulse sequence, harmonic component amplitudes of this point should be equal to $\frac{a}{\pi}$, $\frac{a}{2\pi}$,... correspondingly. It can be carried out by exciting in a VC the polyharmonic vibration with frequencies ω_1, $2\omega_1$,... and to adjust the forcing amplitudes in order to obtain the necessary vibration amplitude values. Having obtained the amplitudes of the harmonic forcing law components and applying them to a VC simultaneously, we obtain the desirable asymmetric vibration cycles. In order to obtain necessary patterns of the electric terminals of a VC, the techniques presented in Chap.5.3 can be employed. In the most general case, the prescribed vibration cycles can be obtained only at a single point of a VC. However, in symmetric VC (e.g., ring-type VC) there is a finite number of such points.

Exciting asymmetric vibration cycles in ring-type VC. Ring-type VC are widely employed as input links of VD. However, the asymmetric vibration cycle excitation in such VC meets certain difficulties, because none of their eigenfrequencies are common multiples of the remaining ones. However, ring type VC possessing two eigenfrequencies satisfying the relation $2\omega_1=\omega_2$ can be

employed in order to obtain the vibration law

$$f(t) = \frac{a}{\pi}\left(\sin\omega t \pm \frac{1}{2}\sin 2\omega t\right) .$$

Consider a bimorfic ring VC consisting of two rings: external piezoelectric ($BaTiO_3$) of the thickness h_1, and internal metallic (Al) of the thickness h_2, rigidly connected with each other. Electric terminals of the VC being properly partitioned, radial (flexural) as well as tangential modal vibrations can be excited [3,71]. Fig.7.46 presents the relationships of eigenfrequencies upon the thickness ratio of the external and internal rings, where r denotes the average radius of the VC, in this case assumed to be equal $r=19h_1$. Varying the thickness of only the passive (metallic) layer h_2, the necessary ratios between certain pairs of the eigenfrequencies can be obtained. At the value $\frac{h_2}{h_1}=0.5$ we obtain $\frac{\omega_2}{\omega_3} = 2$, at $\frac{h_2}{h_1}=1$ the value $\frac{\omega_3}{\omega_4}=2$ is obtained, etc.

Consider the asymmetrically vibrating points of the ring circumference obtained by applying a polyharmonic excitation. Assume the second and third modes to be excited in the VC by applying the excitation voltage as shown in Fig.7.47, the VC parameters satisfying the relations $h_1=2h_2$, $r=19h_1$. In [72] it has been shown that the relation between the tangential components of the amplitudes at the vibration frequencies ω_2, ω_3 is equal to $\frac{a_3}{a_2} = \frac{1}{1.4}$. However, the points of a vibrating ring always move in the radial as well as in the tangential directions, except the first, purely radial mode. Consider these components separately.

Fig.7.47 presents the tangential components of the second and third eigenforms of the VC (solid and dashed line correspondingly), the circumference of the ring being unrolled into a straight line. The triangles in Fig.7.47 mark the points, the vibration of which presents a two harmonic component approximation of asymmetric cycles. There are 4 such points along the circumference. The vibration of two of them approximate triangular pulses with the steep front slope, and the remaining two – triangular pulses with the steep back slope. The positions

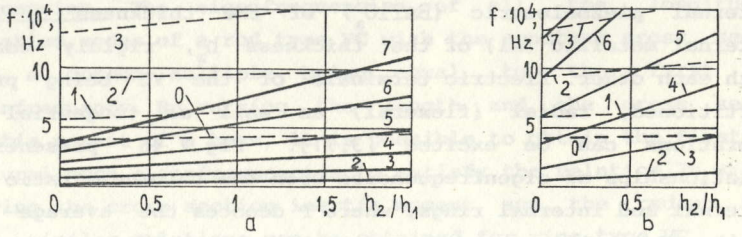

Fig.7.46 Eigenfrequency relationships of the bimorfic cylindrical VC at $h_1/r=0.055$ (a) and at $h_1/r=0.198$;

——— - radial mode eigenfrequencies;
- - - - tangential mode eigenfrequencies

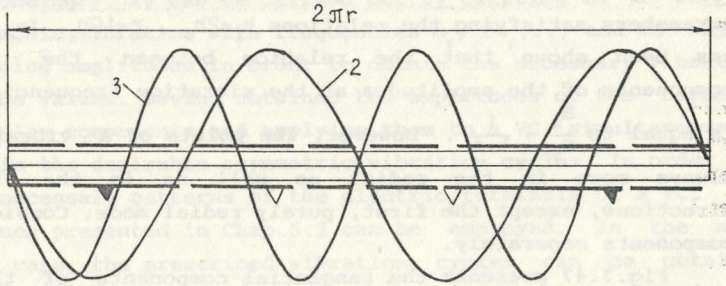

Fig.7.47 Wave-forms of the forced radial and tangential vibration at two-harmonic excitation of the second and third tangential modes, $\omega_3^2/\omega_2^2=2$;

- points performing asymmetric vibration cycles with the steep front slope, amplitude ratio $a_2/a_3=2:1$;
- points performing asymmetric vibration cycles with the steep back slope, amplitude ratio $a_2/a_3=2:-1$

of such points are determined by the ratio 2:1 or 2:-1 of the vibration amplitudes corresponding to the two modes.

It appears worth to notice, that the asymmetrically vibrating points on the ring circumference exist at an arbitrary ratio of the vibration amplitudes of the two modes. The amplitude ratio influents only the positions of such points on the ring circumference, so it is possible to situate such points symmetrically around the ring.

The above mentioned consideration remains valid for the radial components of the amplitudes, too. Similarly, 4 asymmetrically vibrating points are obtained, their positions being dependent upon the amplitudes of the two modal vibration components.

7.3.3 Synthesis of concentrators and pulse-transformers

Asymmetric vibration cycle concentrators employed for increasing the vibration amplitude of some points of a VC. In VD the concentrators of longitudinal and torsional vibrations are employed for adjusting a VC with load and increasing the output link velocity [56].

Usually concentrators are characterized by their amplitude amplification coefficient $k_a = \frac{\delta_n^1}{\delta_1^1}$, where δ_1^1, δ_n^1 - amplitudes of the first eigenform of the VC. Similarly the asymmetric vibration concentrators transform the asymmetric vibration of the input point into the same asymmetric vibration with the amplified amplitude. In order to do this it is necessary to ensure the same amplification coefficient value k for several modal components, i.e., $k = k^i = \frac{\delta_n^i}{\delta_1^i}$, $i=\overline{1,m}$, where δ_1^i, δ_n^i - amplitudes defined by the i-th vibration eigenform at the concentrator's input and output. The synthesis problem of such a concentrator can be presented as (7.30). E.g., in order to obtain a concentrator for amplifying two harmonic components, the target function ψ_o is presented as

$$\psi_o = \left(4 - \frac{\xi_2}{\xi_1}\right)^2 + \left(k + \frac{y_1^{(n)}}{y_1^{(1)}}\right)^2 + \left(k - \frac{y_2^{(n)}}{y_2^{(1)}}\right)^2 ,$$

its derivatives being

$$\frac{\partial\psi_o}{\partial y_1} = \left\{-2\frac{y_1^{(n)}}{(y_1^{(1)})^2}\left[k+\frac{y_1^{(n)}}{y_1^{(1)}}\right],\ 0,\ 0,\ldots,\ 0,\ \frac{2}{y_1^{(1)}}\left[k+\frac{y_1^{(n)}}{y_1^{(1)}}\right]\right\},$$

$$\frac{\partial\psi_o}{\partial y_2} = \left\{2\frac{y_2^{(n)}}{(y_2^{(1)})^2}\left[k-\frac{y_2^{(n)}}{y_2^{(1)}}\right],\ 0,\ 0,\ldots,\ 0,\ -\frac{2}{y_2^{(1)}}\left[k-\frac{y_2^{(n)}}{y_2^{(1)}}\right]\right\},$$

$$\frac{\partial\psi_o}{\partial\xi_1} = 2\frac{\xi_2}{\xi_1^2}\left[4-\frac{\xi_2}{\xi_1}\right],\quad \frac{\partial\psi_o}{\partial\xi_2} = -\frac{2}{\xi_1}\left[4-\frac{\xi_2}{\xi_1}\right].$$

In general, not only amplitude, but also a pulse shape can be transformed. Consider several Fourier expansions of pulse sequences, Fig.7.48. For transforming the pulses (a) into the pulses (b) (phase shift), the necessary relations for the amplitude amplification coefficients are $-k^1=k^2=\ =-k^3\ =\ldots=\ k$, where k - amplitude amplification coefficient.

Similarly, for transforming the pulses (c) into (d) the relations $k^1 = -\frac{1}{3}k^2 = \frac{1}{5}k^3 =\ldots=\ \frac{\pi}{2}k$ are to be satisfied. The varying cross-section of the rod-type VC ensuring the pulse transformation from (a) to (b) with the amplification coefficient k=-3 was obtained employing the optimal design techniques. Fig.7.49 presents the shapes of such concentrators for the first two (a) and three (b) Fourier components.

Transformation of the input forcing pulses into asymmetric pulse vibration. For obtaining the asymmetric pulse vibration of a VC, together with the prescribed ratios of the eigenfrequency values the necessary forcing law (in general polyharmonic) is to be applied. However, in the most practical cases it appears preferable to avoid the employment of several input excitation sources of different frequencies. Alternatively, the excitation can be applied as a sequence of shape pulses (symmetric or asymmetric).

Consider a forcing pulse transformation. Taking on account, that a VC operates in a resonant mode, each sine component of the input forcing law is transformed into a corresponding cosine component. If the forcing law is presented by the Fourier expansion

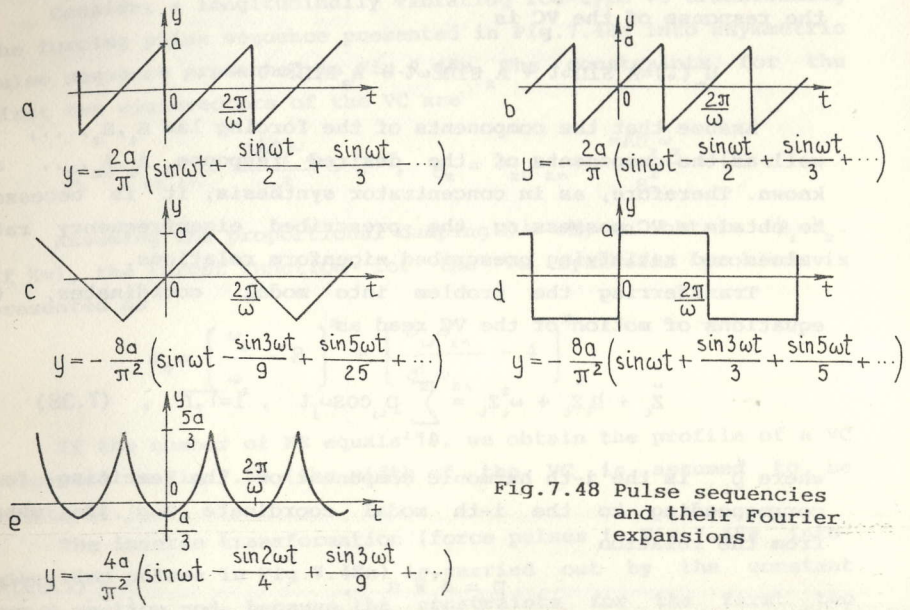

Fig.7.48 Pulse sequencies and their Fourier expansions

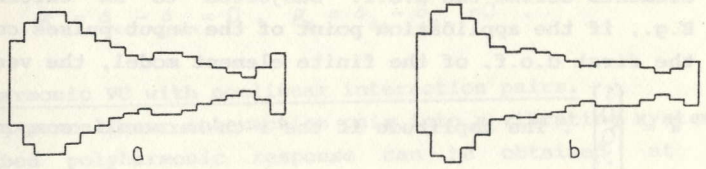

Fig.7.49 Shape-forms of the rod-type concentrators of the longitudinal asymmetric vibrations: a)k=3, h=2 ; b)k=3, h=3

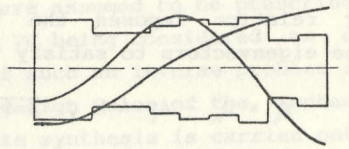

Fig.7.50 Shape-form of the rod-type VC converting voltage pulses into asymmetric cycle vibration, ω_1=26324.5Hz, ω_2=52603Hz

$$f(t)=a_1\cos\omega t + a_2\cos 2\omega t + a_3\cos 3\omega t + \dots \ ,$$

the response of the VC is

$$u_n(t)=A_1\sin\omega t + A_2\sin 2\omega t + A_3\sin 3\omega t + \dots \ .$$

Assume that the components of the forcing law $a_1, a_2, \dots,$ as well as the components of the desired response $A_1, A_2, \dots$ are known. Therefore, as in concentrator synthesis, it is necessary to obtain a VC possessing the prescribed eigenfrequency ratio values and satisfying prescribed eigenform relations.

Transferring the problem into modal coordinates, the equations of motion of the VC read as

$$\ddot{z}_i + h_i\dot{z}_i + \omega_i^2 z_i = \sum_{j=1}^{h} p_{ij}\cos\omega_j t \ , \ \overline{i=1,n} \ , \quad (7.38)$$

where p_{ij} is the j-th harmonic component of the exciting force corresponding to the i-th modal coordinate and is obtain from the relation

$$p_{ij} = \delta_i^T W a_j \ , \quad (7.39)\star$$

where W is a vector with elements equal to 0 or 1. The unity elements define the d.o.f. subjected to an external forcing. E.g., if the application point of the input pulses corresponds to the first d.o.f. of the finite element model, the vector reads as $W = \begin{pmatrix} 1 \\ 0 \\ 0 \\ \vdots \end{pmatrix}$. The amplitude if the i-th harmonic component of the output d.o.f. (e.g., n-th d.o.f.) is obtained as

$$u_n^i = \delta_{in}\frac{a_i}{h_i\omega_i}\delta_i^T W \ . \quad (7.40)$$

The latter relation imposes the requirement upon the components of the eigenvectors to satisfy the constraints

$$g_i = u_n^i - A_i = 0 \ , \ \overline{i=1,h} \ . \quad (7.41)$$

If a VC is excited employing electric voltage forcing, in the above relations in place of $\delta_i^T W$ the term $\delta_i^T T V$ should be

substituted, where V - vector depending upon the pattern of the electric terminals of a VC employed for exciting the i-th mode.

Consider a longitudinally vibrating rod-type VC transforming the forcing pulse sequence presented in Fig.7.48e into asymmetric pulse sequence presented in Fig.7.48a. The constraints for the first two eigenvectors of the VC are

$$g_1 = \delta_{11}\delta_{1n} - \frac{\pi A h_1 \omega_1}{2a^2} = 0 \ , \quad g_2 = \delta_{21}\delta_{2n} - \frac{\pi A h_2 \omega_2}{a^2} = 0 \ .$$

Assuming the proportional damping $C = \alpha M$, we obtain $h_1 = h_2$. If k=1, the target function for the VC synthesis problem is presented as

$$\psi_o = \left(\frac{\omega_2}{\omega_1} - 2\right)^2 + \left(\frac{\delta_{11}\delta_{1n}}{\delta_{21}\delta_{2n}} - 4\right)^2 \ .$$

If the number of FE equals 10, we obtain the profile of a VC presented in Fig.7.50 (the width of the VC is assumed to be constant).

The inverse transformation (force pulses in Fig.7.48a into vibration pulses in Fig.7.48e) is carried out by the constant cross section rod, because the constraints for the first two eigenvectors are

$$g_1 = \delta_{11} - \delta_{1n} = 0 \ , \quad g_2 = \delta_{21} - \delta_{2n} = 0 \ .$$

Polyharmonic VC with nonlinear interaction pairs.

Introducing a nonlinear interaction pair into a vibrating system, a prescribed polyharmonic response can be obtained at monoharmonic excitation, because the nonlinear interaction force can be interpreted as a polyharmonic excitation source.

The problem is solved employing the harmonic balance equations of the finite element model of a VC. The amplitude harmonic components are assumed to be prescribed, the geometric characteristics of a VC being considered as design parameters. The exact solution of such an inverse problem is hardly possible. However, assuming the high value of the mechanical Q-factor of the VC, an approximate synthesis is carried out as follows.

Assume the harmonic component frequencies of a prescribed motion law being close to the resonant frequencies of the VC.

Presenting the equations of motion of the system in modal coordinates of the unconstrained VC and taking on account, that the overwhelming contribution to the response of the VC is submitted by the modal components, the resonant frequencies of which are very close to the excitation frequencies, the constraints upon eigenfrequencies and eigenvectors can be obtained.

For the sake of simplicity we restrict ourselves with the case, when a nonlinear interaction takes place at a single d.o.f. of a VC, an external excitation law as well as a nonlinear function being known in advance. The structural equation of motion is presented as

$$M\ddot{U} + C\dot{U} + KU = R + R_s \sin\omega t + R_c \cos\omega t + \begin{bmatrix} 0 \\ \vdots \\ 0 \\ W(u_n, \dot{u}_n) \end{bmatrix}, \quad (7.42)$$

where M, C, K, U - structural matrices and the nodal displacement vector, R - constant external force, F_s, F_c - vectors of the sine and cosine amplitudes of the harmonic excitation force, $W(u_n, \dot{u}_n)$- function determining a nonlinear interaction force at the n-th d.o.f. of the VC.

The function W is assumed to be known as well as a source geometric shape of the VC and the matrices M, C, K. It is necessary to change the geometric parameters of the VC in order to ensure the necessary stationary response time law $u_n(t)$ to be equal to the desired periodic response $u^*(t)$ with the angular frequency ω .

The harmonic balance equations in modal coordinates of the linear part of the structure read as

$$\ddot{z}_i + h_i\dot{z}_i + \omega_{oi}^2 z_i = \delta_i^T R + \delta_i^T R_s \sin\omega t + \delta_i^T R_c \cos\omega t + \delta_{in}^T W(u_n, \dot{u}_n), \quad (7.43)$$
$$i=\overline{1,n} \ ,$$

where z_i - modal displacements of the finite element model of the VC , related to the displacements U as $U=\Delta Z$, h_i- damping coefficient of the i-th mode, and δ_{in} - n-th component of the i-th eigenvector δ_i.

The motion law $u_n(t)=u^*(t)$ being prescribed, the function

$W(u_n, \dot{u}_n)$ can be presented as a Fourier series expansion with the known coefficients as

$$W(u_n, \dot{u}_n) = \sum_{i=1}^{h} W_s^k \sin(k-1)\omega t + W_c^k \cos(k-1)\omega t \ . \quad (7.44)$$

The nonlinear vibration harmonic component frequencies being close to the resonant frequencies of the unsupported VC, the equation system (7.43) can be approximately presented as

$$\begin{cases} X_{2s} = \dfrac{-\left(\delta_i^T F_s + \delta_{in} W_s^2\right)\left(\omega^2 - \omega_{oi}^2\right) + \omega h_i \left(\delta_i^T F_c + \delta_{in} W_c^2\right)}{\left(\omega^2 - \omega_{oi}^2\right) + \omega^2 h_i} \ , \\ X_{2c} = \dfrac{-\left(\delta_i^T F_c + \delta_{in} W_c^2\right)\left(\omega^2 - \omega_{oi}^2\right) + \omega h_i \left(\delta_i^T F_s + \delta_{in} W_s^2\right)}{\left(\omega^2 - \omega_{oi}^2\right) + \omega^2 h_i} \ , \\ X_{i,s} = \dfrac{-\delta_{in} W_s^i \left(\omega^2 - \omega_{oi}^2\right) + \omega h_i \delta_{in} W_c^i}{\left(\omega^2 - \omega_{oi}^2\right) + \omega^2 h_i} \ , \quad i=\overline{3,h} \ , \\ X_{i,c} = \dfrac{-\delta_{in} W_c^i \left(\omega^2 - \omega_{oi}^2\right) + \omega h_i \delta_{in} W_s^i}{\left(\omega^2 - \omega_{oi}^2\right) + \omega^2 h_i} \ , \quad i=\overline{3,h} \ , \\ K U_c^1 = F + W_c^1 \ . \end{cases} \quad (7.45)$$

Finally, it is necessary to determine the geometric parameters of the VC, possessing the eigenfrequencies ω_{oi} and eigenvectors δ_i, and simultaneously satisfying the system (7.45).

Following the above presented method, we synthesize a VC producing the triangular asymmetric pulse sequence. As the source model of the VC the construction presented in Fig.7.29c is employed, requiring the right-hand end of the VC to produce vibrations similar to the triangular pulse sequence. In this case it isn't necessary to solve the full equation system (7.45), making use of the circumstance that the appropriate adjustment of the first two eigenfrequencies turns the corresponding equations of (7.45) into identities. Simultaneously the vibration law of the right-hand end of the VC presents the sequence of triangular pulses approximated by the first two Fourier components. Fig.7.51

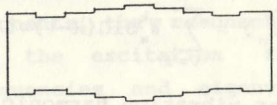

Fig.7.51 Shape-form of the rod-type VC performing asymmetric vibration cycles during the impact vibration, ω_2^2/ω_1^2 =3.94; f_1=14711Hz; f_2=29222Hz

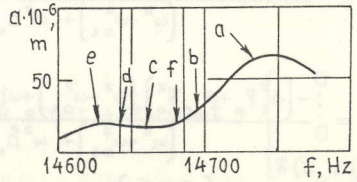

Fig.7.52 AFCH of the asymmetric vibration cycle VC at k_1=5.10⁴N/m, k=5.10⁵N/m, c_1=c=0, Q=200, F_o=1N
(in the shaded area the asymmetric vibration approximating a triangular pulse sequence takes place)

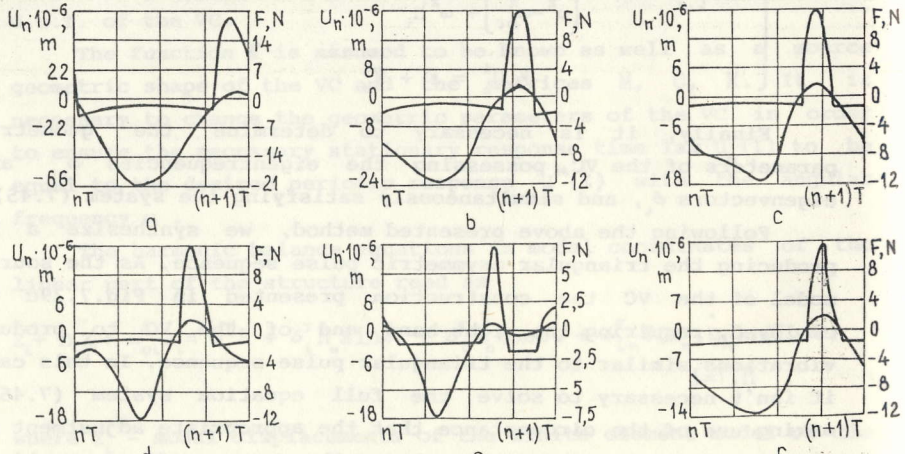

Fig.7.53 Time laws of the displacements of the right-hand end of the VC and of the normal impact interaction force at k_1=5.10⁴N/m, k=5.10⁵N/m, c_1=c=0, Q=200, F_o=1N ;
a- f = 14737Hz; b- f = 14687Hz; c- f = 14656Hz;
d- f = 14637Hz; e- f = 14625Hz; f- f = 14675Hz

presents the profile of a VC, the first two eigenfrequencies of which are equal to f_1=14711Hz and f_2=29222Hz.

In Fig.7.52 the AFCH of the right hand end of this VC is presented at the excitation voltage amplitude equal to 30V. The desired vibration law is obtained in the shaded area in Fig.7.52, the letters denoting the points, for which the vibrational displacement and nonlinear interaction force time laws are presented in Fig.7.53.

7.4 OPTIMAL CONTROL LAWS OF AN OUTPUT LINK

7.4.1 Aperiodic motion control of a piezoelectric vibroconverter

Consider the equations of motion of a VC as

$$\begin{cases} M\ddot{U} + C\dot{U} + KU + T\Phi = R, \\ T^{T}U - S\Phi = Q. \end{cases} \qquad (7.46)$$

where K , M , C , T , S - structural stiffness, mass, damping, electromechanical and capacity matrices of the VC, R - external nodal force vector, Q - nodal charge vector, Φ - nodal potential vector.

The solution of the system (7.46) isn't unique, because U and Φ , as well as Q are unknown. In order to obtain the unique solution, an additional information about the electric circuit parameters is necessary. Assuming an electric voltage value applied to the electric terminals of a VC known, we denote the corresponding part of the nodal potential vector as Φ_1, presenting the vector Φ as $\Phi=\begin{bmatrix}\Phi_1\\ \Phi_2\end{bmatrix}$, where Φ_2 - part of the nodal potential vector corresponding to the remaining nodes. Similarly, the nodal charge vector is presented as $Q=\begin{bmatrix}Q_1\\ Q_2\end{bmatrix}$. The subvector Q_2 corresponding to the nodes with no external electric voltage applied can be regarded as zero, because a VC has no free charge, i.e., $Q=\begin{bmatrix}Q_1\\ 0\end{bmatrix}$. Partitioning the matrices T and S into blocks corresponding to the partitioning of the nodal potentials and charges, after some manipulation the system (7.36) reads as

$$M\ddot{U} + C\dot{U} + K^{*}U = T^{*}\Phi_1 \ , \qquad (7.47)$$

where $K^{*} = K + T_2 S_{22}^{-1} T_2^{T}$, $T^{*} = -T_1 + T_2 S_{22}^{-1} S_{12}^{T}$.

Having obtained Φ_1 from (7.47) , the nodal charges are expressed as

$$Q_1 = S^{*}\Phi_1 - T^{*T}U \ , \qquad (7.48)$$

where $S^{*} = -S_{11} + S_{12} S_{22}^{-1} S_{12}^{T}$.

Presentation of the system (7.46) as (7.47), (7.48) enables to decompose the source problem. The displacements of the points of the VC with the prescribed voltages applied to the electric terminals are obtained by considering the equation (7.47) separately. The form of the equation enables to apply the techniques presented in Chap.5 for obtaining the optimal control laws of a VC.

Programmed control synthesis. Consider a rod-type VC , Fig.7.54a. The right-hand end moves due to the longitudinal deformation of the VC, the left-hand end being fixed rigidly. The lower electric terminal of the VC is grounded, and to the upper one, partitioned into m identical segments, electric voltages are applied. It is necessary to determine the control voltage laws $\Phi_i(t)$ ensuring the prescribed motion of the right-hand end of the VC.

Assume the prescribed motion being the movement from the position $u_n=0$ to $u_n=a$ within the prescribed time interval t_g, where u_n - the nodal displacement of the right-hand end. After the time instant $t=t_g$ the displacement value $u_n=a$ is to be ensured, i.e., vibration damping is to be performed. The control interval is assumed to be $[0,t_g]$. Consider the initial and the end states of the VC. At the initial state the zero displacement and velocity values $U(0)=0$, $\dot{U}(0)=0$ are assumed, and for obtaining the end state the static equilibrium equation

$$K^{*}U(t_g) = T^{*}\Phi(t_g) \ . \qquad (7.49)$$

is to be solved.

The components of the nodal potential vector

$$\Phi^{T}(t) = \left[\Phi_1(t), \Phi_2(t), \ldots, \Phi_m(t)\right]^{T}$$

at the end state must satisfy the equalities

$$\Phi_1(t_g) = \Phi_2(t_g) = \ldots = \Phi_m(t_g) = V_E \ ,$$

where the potential value V_E ensures the equality $u_n=a$ as a static equilibrium state. For obtaining V_E, the auxiliary problem

$$K^{*}\tilde{U} = T^{*}I \ . \qquad (7.50)$$

is to be solved, where $I = (1,1,\ldots,1)^{T}$. Having obtained $\tilde{u}_n$, the value of V_E follows as

$$V_E = \frac{a}{\tilde{u}_n} \ . \qquad (7.51)$$

Now the nodal displacement values at the end state can be presented by means of the vector b , employing the relation

$$b = \frac{a}{\tilde{u}_n}\tilde{U} \ . \qquad (7.52)$$

The time law of the movement during the time interval $[0,t_g]$ being expressed as (see Fig.7.54b)

$$s(t) = \frac{6}{t_g^5} t^5 - \frac{15}{t_g^4} t^4 + \frac{10}{t_g^3} t^3 \ , \qquad (7.53)$$

the target function to be minimized reads as

$$\psi = \int_0^{t_g} \left[\left(U - s(t)b\right)^{T}\left(U - s(t)b\right) + \left(\dot{U} - \dot{s}(t)b\right)^{T}\left(\dot{U} - \dot{s}(t)b\right)\right] dt \ , \qquad (7.54)$$

Employing the dynamic reduction by truncating higher mode dynamic contributions, the function ψ is presented in modal coordinates. The vector U is expressed through the lower modal displacements as $U=\Delta_1 Z$, where $\Delta_1 = \left[\delta_1, \delta_2, \ldots, \delta_h\right]$ of the dimension nxh is the matrix, containing the first h eigenvectors in its columns, n - number of d.o.f. of the finite element model of the VC. The expression of the target function is obtained as

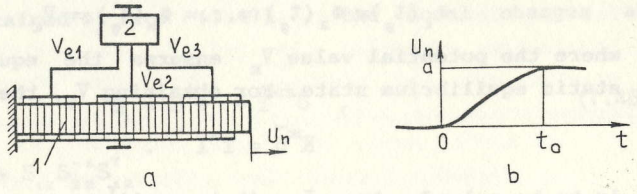

Fig.7.54 Programmed control of the aperiodic motion VC;
a- construction diagram, 1 - VC, 2 - voltage source;
b- prescribed time law of the end-point displacement

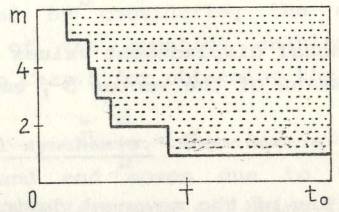

Fig.7.55 Satisfactory control area of the VC, m - number of control voltages

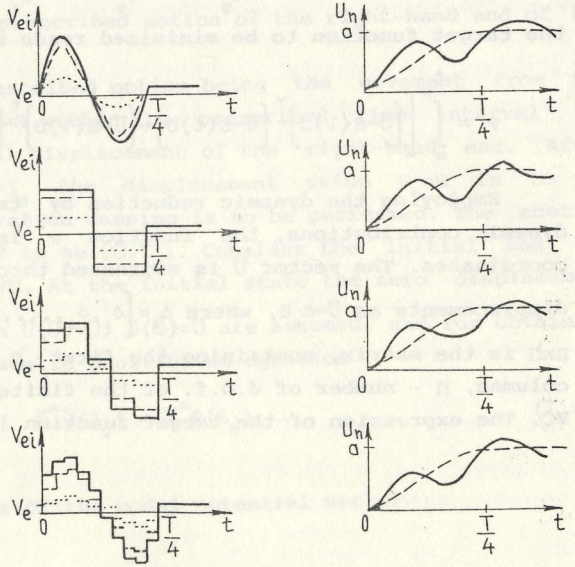

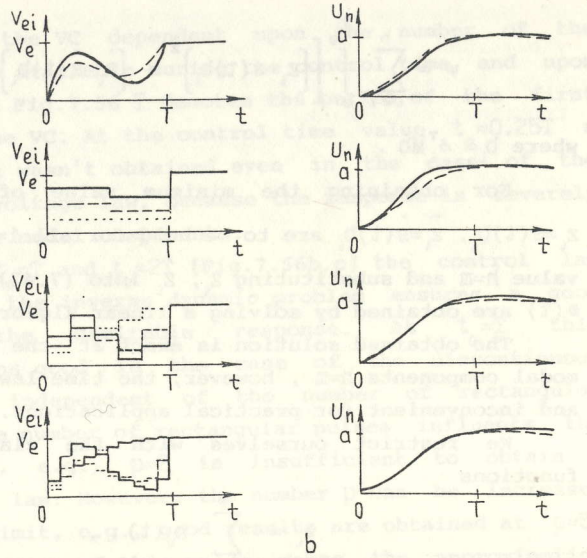

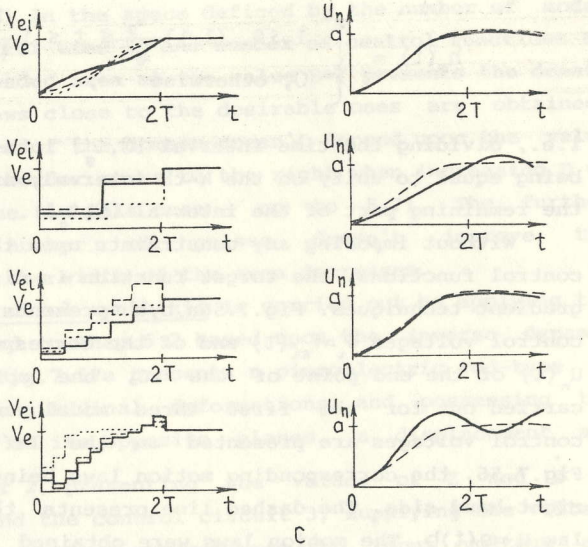

Fig.7.56 Time laws of the control voltages and the end-point displacement; ——— - V_{E1}; ----- - V_{E2}; ..... - V_{E3}

$$\psi = \sum_{i=1}^{h} \int_{0}^{t_g} \left[\left(z_i - s(t)b_i \right)^2 + \left(\dot{z}_i - \dot{s}(t)b_i \right)^2 \right] dt \ , \qquad (7.55)$$

where $b_i = \delta_i^T M b$.

For obtaining the minimum value of ψ the equalities $z_i = s(t)b_i$, $\dot{z}_i = \dot{s}(t)b_i$ are to be held for all $i=\overline{1,h}$. Selecting the value $h=m$ and substituting z_i, $\dot{z}_i$ into (7.47), the control laws $\Phi(t)$ are obtained by solving a linear algebraic equation system.

The obtained solution is exact at the selected number of modal components $h=m$, however, the time law $\Phi(t)$ can be complex and inconvenient for practical applications.

We restrict ourselves with the class of discontinuous functions

$$\Phi_i = \sum_{k=1}^{p} h_k(t) \ ,$$

where k-th element of the vector $h(t)$ is expressed as

$$h_k(t) = \begin{cases} 1, \text{if } (i-1)\dfrac{t_g}{p} \le t \le i\dfrac{t_g}{p} \ ; \\ 0, \text{ otherwise} \end{cases} ,$$

i.e., dividing the time interval $[0,t_g]$ into p equal parts, $h_k(t)$ being equal to unity on the k-th interval, and equal to zero on the remaining part of the interval $[0,t_g]$.

Without imposing any constraints upon the magnitudes of the control functions, the target function is minimized employing the gradient techniques. Fig.7.56a,b,c presents time laws of the control voltages $\Phi_i = V_{Ei}(t)$ and of the corresponding motion laws $u_n(t)$ of the end point of the VC, the optimal control being carried out for the first three modal components, $h=3$. The control voltages are presented on the left-hand side of the Fig.7.56, the corresponding motion laws being presented on the right-hand side. The dashed line presents the desirable motion law $u_n = s(t)b$. The motion laws were obtained employing the full dynamic finite element model (without truncation).

The presented relationships enable to treat the obtained

dynamic behavior of the VC dependent upon the number of the rectangular pulses p available during the control time and upon its duration t_g . In Fig.7.56 T denotes the period of the first vibration mode of the VC. At the control time value $t_g = 0.25T$ a satisfactory control wasn't obtained even in the case of the continuous control voltage law, because the response is severely influenced by higher modal components.

At the values $t_g = T$ and $t_g = 2T$ (Fig.7.56b,c) the control law obtained by solving the inverse dynamic problem ensures a good approximation of the desirable response. At $t_g = T$ this approximation remains good in the case of the discontinuous control functions, independent of the number of rectangular pulses. At $t_g = 2T$ the number of rectangular pulses influents the obtained motion law, e.g., $p=2$ is insufficient to obtain a satisfactory motion law. However, the number p can be increased up to the certain limit, e.g., good results are obtained at $p=5$, but the further increase of this value makes the approximation worse.

The above consideration allows to determine a region of satisfactory control in the space defined by the number of modal components p , control time t_g and number of control functions m. In Fig.7.55 the shaded area at the value $p=2$ presents the domain where the motion laws close to the desirable ones are obtained. The left-hand border of the domain doesn't depend upon the value p . The right-hand border moves to the right when increasing p up to the certain value (in this case - up to 5-7). The further increase of the number of pulses doesn't improve the approximation, and the width of the area decreases.

Closed-loop control synthesis is carried out be applying the techniques presented in Chap.5.2 based upon the inverse dynamic problem solution. Fig.7.57a presents a piezoelectric rod-type VC 1, subjected to longitudinal deformations and possessing the electric terminals on its opposite planes, a displacement and velocity transducer 2, presenting the values of z and $\dot{z}$ as electric signals and the control circuit 3, supplying the voltage to the electric terminals dependent upon the input voltage and upon the values z and $\dot{z}$. The VC 1 is a vibrating system with a high Q-factor value, and its motion between two stationary states

of deformation is accompanied by undesirable transient vibrations. The closed loop control circuit is to be obtained in order to ensure a prescribed speed of response and to damp transient vibrations.

Consider a VC of the length $l=0.085m$, thickness $h=0.0095m$ and width $b=0.012m$, material constants being $c^D_{11}=0.6\times10N/m^2$, $e_{31}=8.46C/m^2$, $\varepsilon^S_{33}=0.135\times10^{-7}F/m$, density $\rho=7000kg/m^3$ and assume zero material damping, i.e., vibration damping should be obtained purely by the control. The first longitudinal eigenfrequency of the cantilever VC equals $f_1=8646.36Hz$, vibration period being $T_1=f_1^{-1}$. Assume the desirable speed of response being equal to $0.5T_1$, and, consequently, from the relation (5.29) the values $\lambda=0.1T_1$, $\mu=2\lambda$ are obtained.

If only the displacement and velocity of the end point of the VC can be measured, the matrix Q reads as

$$Q_{1\times n}=(0,0,\ldots,0,1) \quad ,$$

where n- number of d.o.f. of the finite element model. Further we assume $G=0$, $\tilde{T}=T^+$, and the matrix $\tilde{R}$ being expressed as

$$\tilde{R} = R^+ + \alpha(I-R^+R)\begin{bmatrix}1\\1\\\vdots\\1\end{bmatrix} \quad ,$$

i.e., for obtaining the stability of the control system only the value of the parameter α is to be varied. The closed-loop matrices $\tilde{R}V\tilde{Q}$, $\tilde{R}S\tilde{Q}$ are obtained by the relations of the Chap.5.2.

In Fig.7.57b the transient motion laws of the end-point of the VC are presented at several values of α. The dashed line in Fig.7.57b presents the desirable motion law. The system is stable only at the values $\alpha>0.825$, the best approximation to the desirable motion law being obtained at $\alpha=0.825$.

In Fig.7.58a a control loop is presented in the case, when the electric terminals of the VC are partitioned into two identical segments, and in Fig.7.58b - the corresponding motion laws when the rectangular input pulse of the duration T_1 is applied, the dashed line presenting the desirable motion law.

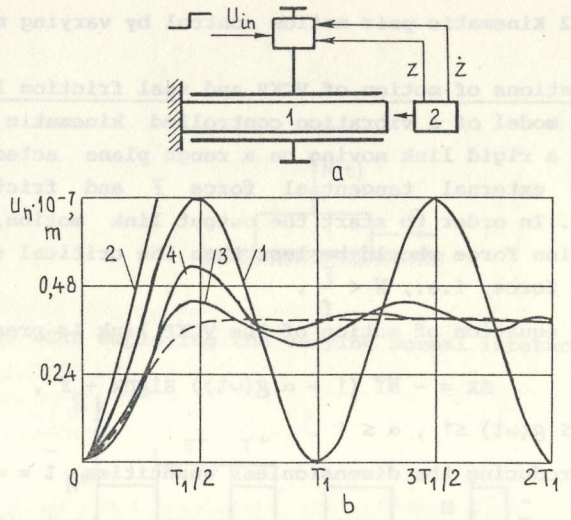

Fig.7.57 Closed-loop control system of the VC with a single control terminal; a) construction diagram; b) time laws of the right-hand end displacement of the VC: 1- without a feedback; 2 - $\alpha=0$; 3 - $\alpha=0.825$; 4 - $\alpha=1$, the dashed line presenting the prescribed motion law

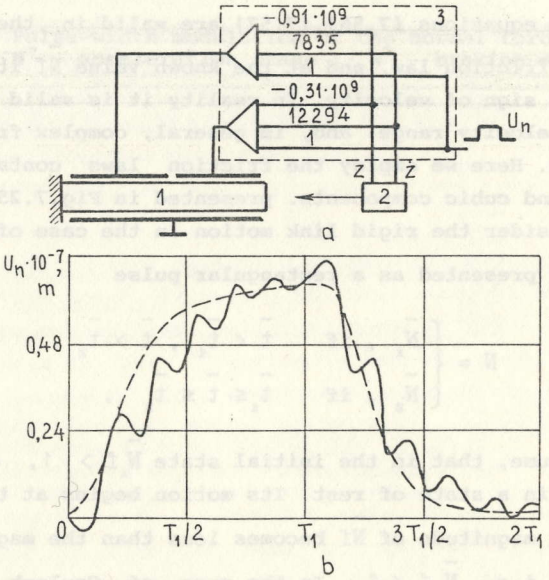

Fig.7.58 Closed-loop control system of the VC with two control terminals; a) construction diagram; b) time laws of the right-hand end displacement of the VC, the dashed line presenting the prescribed motion law

7.4.2 Kinematic pair motion control by varying normal force

Equations of motion of VCKP and real friction laws. The simplest model of a vibration controlled kinematic pair (VCKP) contains a rigid link moving on a rough plane acted upon by a constant external tangential force F and friction forces, Fig.7.59. In order to start the output link motion, the normal interaction force should be less than the critical value of the friction force, i.e., $N < \frac{F}{f}$.

The equation of motion of the VCKP link is presented as

$$m\ddot{x} = - Nf\,(1 + \alpha\, g(\omega t))\, \mathrm{sign}\dot{x} + F \,, \qquad (7.56)$$

where $-1 \le g(\omega t) \le 1$, $\alpha \le 1$.

Introducing the dimensionless quantities $\bar{t} = \omega t$, $\bar{Nf} = \frac{Nf}{F}$, $\dot{\bar{x}} = \dot{x}\frac{m\omega}{F}$, $\ddot{\bar{x}} = \ddot{x}\frac{m}{F}$, in place of (7.56) we obtain the equation

$$\ddot{\bar{x}} = - \bar{Nf}\,(1 + \alpha\, g(\bar{t}))\, \mathrm{sign}\dot{\bar{x}} + 1 \,. \qquad (7.57)$$

The equations (7.56),(7.57) are valid in the case of the Coulomb friction law, and at the known value $\bar{Nf}$ it depends only upon the sign of velocity. In reality it is valid only in a very narrow velocity range, and, in general, complex friction laws are employed. Here we employ the friction laws containing Coulomb, linear and cubic components. presented in Fig.7.25.

Consider the rigid link motion in the case of the time law $\bar{Nf}$ being presented as a rectangular pulse

$$N = \begin{cases} \bar{N}_1 \,, \text{ if } & \bar{t} < \bar{t}_1 \,,\ \bar{t} > \bar{t}_2 \,, \\ \bar{N}_2 \,, \text{ if } & \bar{t}_1 \le \bar{t} \le \bar{t}_2 \,. \end{cases}$$

Assume, that in the initial state $\bar{N}_1 f > 1$, and the rigid link is in a state of rest. Its motion begins at the time instant when the magnitude of $\bar{Nf}$ becomes less than the magnitude of the force $\bar{F}$, i.e., $\bar{N}_2 f < 1$. In the case of Coulomb friction, the velocity increases linearly

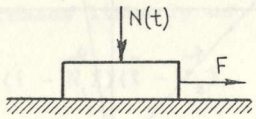

Fig.7.59 VCKP employing the varying normal interaction force

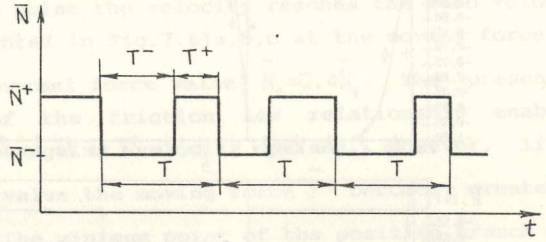

Fig.7.60 Pulse-width modulation of the normal force;
N^- - acceleration stage ; N^+ - braking stage

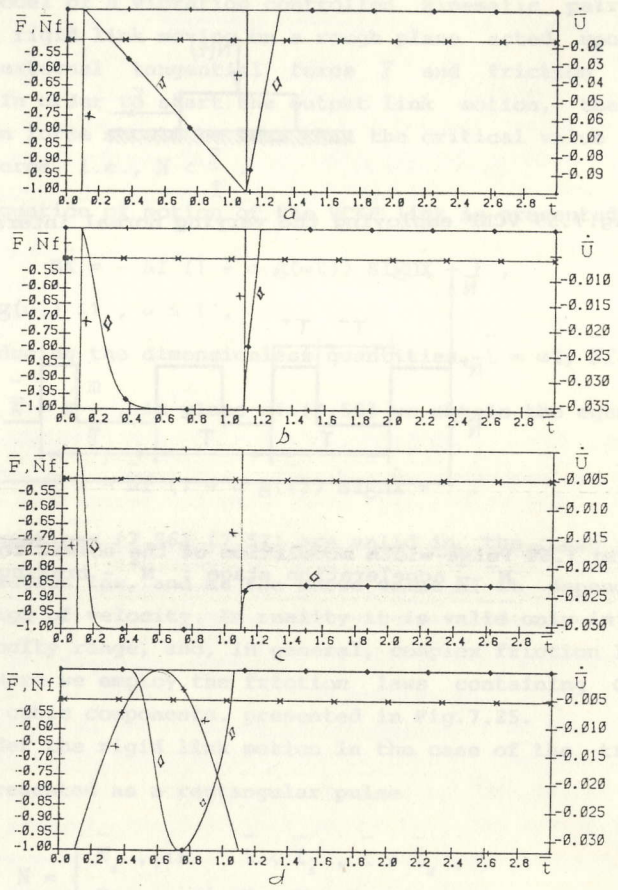

Fig.7.61 Time laws of the output link velocity at the rectangular pulse of the normal force at several friction law relationships: a) γ =0(Coulomb friction); b) γ =20 ; c) γ =80(non-stop motion); d) sine half-wave normal force pulse, γ =20 ;

+ - $\bar{N}f$; x - $\bar{F}$; ◊ - $\dot{\bar{x}}$

$$\dot{\bar{x}} = (1 - \bar{N}_2 f)(\bar{t} - \bar{t}_1) , \quad \bar{t}_1 < \bar{t} < \bar{t}_2 .$$

If at the time instant $\bar{t}_2$ the force $\bar{N}$ takes its initial value $\bar{N}_1$, the velocity decreases linearly as

$$\dot{\bar{x}} = (1 - \bar{N}_2 f)(\bar{t}_2 - \bar{t}_1) + (1 - \bar{N}_1 f)(\bar{t} - \bar{t}_2), \quad \bar{t} > \bar{t}_2 ,$$

until the zero value.

We investigate the form of velocity pulses at several friction laws, when during the time interval from $t=t_2$ until the next normal force pulse the velocity reaches the zero value. The results are presented in Fig.7.61a,b,c at the moving force value $\bar{F}=0.5\bar{N}_1 f$ and the normal force value $\bar{N}_2=0.4\bar{N}_1$. The presence of decreasing part of the friction law relationship enables to obtain nearly rectangular velocity pulses. However, if at a certain velocity value the moving force $\bar{F}$ becomes greater than the value of $\bar{N}f$ (the minimum point of the positive branch of the friction law relationship), the back front of the velocity pulse is never obtained, because the velocity doesn't reach the zero value after the end of the normal force pulse, Fig.7.61c. If the force pulse has the sine half-wave shape, at the friction force law with the coefficient values $a=\frac{3}{7}$, $b=\frac{4}{7}$, β=10 , γ=20 the normal force pulse and the velocity pulse end simultaneously, Fig.7.61d.

Mean velocity control employing pulse-width modulation of normal interaction force. If during the time interval between two force pulses the output link velocity doesn't reach the zero value, it operates in the continuous motion mode. Fig.7.60 presents the sequence of width-modulated pulses of the period $\bar{T}$, where $\bar{N}^+ f>1$, and $\bar{N}^- f<1$. Denote the velocity value at the beginning of the period through $\bar{v}_o$, at the time instant of the normal force change from $\bar{N}^-$ to $\bar{N}^+$ - through $\bar{v}^+$, and at the end of the period - through $\bar{v}_1$. In the case of Coulomb friction, the output link velocity during the time intervals $\bar{T}^-$ and $\bar{T}^+$ varies as follows:

$$\begin{cases} \dot{\bar{x}}^- = v_o^- + (1 - \bar{N}^- f)\bar{t} \\ \dot{\bar{x}}^+ = v^+ + (1 - \bar{N}^+ f)\bar{t} \end{cases} , \qquad (7.58)$$

We restrict ourselves with the continuous motion mode, i.e., when $\dot{\bar{x}}^+ > 0$, $\dot{\bar{x}}^- > 0$. In this case the relations

$$\begin{cases} v^+ = v_o^- + (1 - \bar{N}^- f)T^- , \\ v_1^- = v^+ + (1 - \bar{N}^+ f)T^+ \end{cases} , \qquad (7.59)$$

are valid, where $T = T^+ + T^-$.

The constant mean value of the velocity is obtained, if

$$v_1^- = v_o^- . \qquad (7.60)$$

Substituting (7.60) into (7.59) , we obtain

$$\frac{T^+}{T^-} = \frac{1 - N^- f}{N^+ f - 1} . \qquad (7.61)$$

It should be mentioned, that the relation (7.61) is valid for any value of v_o^- .

As a mean acceleration value the quantity

$$a = \frac{a_1^- - a_o^-}{T} \qquad (7.62)$$

is employed, defined as

$$a = \frac{(1 - \bar{N}^- f)T^- + (1 - \bar{N}^+ f)T^+}{T} . \qquad (7.63)$$

At the constant mean velocity value $v_o^- = v_1^-$, the variation of the velocity is obtained from the relation

$$\frac{v^+ - v_o^-}{v_o^-} = \frac{(1 - \bar{N}^- f)T^-}{v_o^-} . \qquad (7.64)$$

The above consideration leads to the conclusion, that the mean velocity of the VCKP can be controlled by means of the pulse width modulation, i.e.,by varying the ratio T^+/T^- at $T^+ + T^- = \text{const}$. The formulae (7.61),(7.63),(7.64) enable to determine the modulation depth according to the desirable values of the velocity and acceleration of the output link. Such a control method can be easily realized in a real-time and in closed-loop control systems.

CONCLUSION

The techniques for vibration analysis and motion control law synthesis of elastic structures with unilaterally constrained mechanical contact interaction points have been developed, systematically presented and applied to the dynamic analysis and synthesis problems of vibrodrives.

Considering the techniques, the following conclusions should be made.

1. The techniques for reducing the number of the dynamic degrees of freedom of elastic structures with nonlinearities based upon the truncation of dynamic contributions of higher modes have been developed. Such an approach enables to replace the dynamic equations of elastic structures with unilateral constraints upon the displacements and velocities by a low dimension equation of motion with a nonlinear term representing an elastic spring and dissipative element of unidirectional action.

2. The numerical integration schemes of linear dynamic equations have been extended in order to deal with nonlinear ones. For the direct numerical integration of equations of motion of the structures with unilateral constraints case oriented algorithms have been developed employing the Lagrangian multiplier approach and supposing the minimum work done by interaction forces for making corrections upon the velocities and accelerations at the time instant when the structure meets the constraint. The approach was applied to the structures with kinematic pairs interacting by normal, oblique impact and sliding friction forces. The ammount of computations can be reduced in the case of the structures with local zones of nonlinear interaction.

3. The analysis techniques of the resonant vibration of elastic mechanical structures with nonlinear contact interaction points with stationary or slow-varying amplitudes have been developed. For the stationary motion law analysis two alternative techniques have been employed: the solution of boundary value problem in time and the weighted residual approach, a special case of the latter being the harmonic balance method. Motion laws in terms of the slow varying amplitudes have been obtained by

means of the time averaging techniques. When integrating the averaged equations numerically, at each time station harmonic components are obtained by means of the Fourier transform. The application to the unilaterally constrained structures requires to transform equations of motion employing the higher mode dynamic contribution truncation techniques in order to obtain an equation system with a nonlinear term.

4. The programmed and closed-loop control synthesis methods have been developed employing the optimal control techniques, the inverse dynamic problem solution and the higher mode dynamic contribution truncation approach. The method can be applied to the motion control synthesis of structures with the feedback circuit consisting of logical elements. A linear closed-loop control with the displacement and velocity feedback is obtained by employing the inverse dynamic problem approach, the prescribed motion of a structure being expressed as a superposition of exponent functions. A structural motion control synthesis with the logical feedback circuit has been carried out by resolving the dynamic equations into modal components and employing a separate feedback for each of them. The excitation laws ensuring the prescribed resonant vibration patterns of the structure points are obtained by solving inverse dynamic and optimization problems.

5. The finite element models of piezoelectric vibroconverters (VC) have been obtained. Employing the variational formulation of thermopiezoelectricity the relations for obtaining matrices of piezoelectric continua finite elements have been derived, vibration energy dissipation models and the relations for taking account for vibroconverters as components of an electric circuit have been obtained.

6. A full model of a vibrodrive (VD) taking account for rigid body motions of the vibrating links has been obtained, the finite element models of each link being presented in truncated modal coordinates. The contact interaction models for point-interaction and travelling wave vibrodrives have been obtained employing a small displacement finite element model and phenomenological models of the interface between contacting links. The dynamic characteristics of vibrodrives have been formulated.

Considering applications, the following conclusions should be made.

7. The free and forced impact vibration of a rod-type VC has been investigated employing the finite element model and phenomenological models of a contact interaction. The following results have been obtained:

- the normal impact interaction of a discrete mechanical system approximating the continuous one has been shown to be elastic, irrespectively of the restitution coefficient values in the vicinity of the contact point;

-it is reasonable to employ the rheological model of the dynamic contact interaction, if the stiffness coefficient of the model exceeds the static stiffness of the structure at the contact point less than to one order (10 times). Otherwise the impact vibration law doesn't depend upon the local contact condition;

8. Considering a forced longitudinal impact vibration of a rod-type VC employed as an input link of a VD it has been obtained, that the solution of time-averaged equations considering two Fourier components presents satisfactory results only in the case of the two-mass elastic system. For obtaining reliable results when considering structural models, at least four Fourier components are to be taken on account.

9. Employing the time-averaging and numerical integration techniques a step motion of vibration-controlled kinematic pairs (VCKP) as well as free and forced motions of a VD have been investigated employing the lumped-mass and finite element models, complex friction laws being presented as a superposition of the Coulomb, linear and cubic components. It has been shown that the motion of the links of VCKP can be controlled employing a purely tangential vibration in a contact zone. The values of the normal contact interaction forces have been obtained, ensuring equal steepnesses of the slopes of an output link velocity pulse. The duration of transient vibration law has been shown being dependent upon a Q-factor value of a VC and upon the mass of an output link.

10. Investigating the motion upon a rough surface of a system of two elastically connected masses impacting upon each

other under the harmonic excitation law, the directive motion of a system as of a whole have been obtained. The direction of motion can be reversed by an appropriate adjustment of the Coulomb friction coefficient value. An analysis has been carried out and the dynamic characteristics of a VD employing this operation principle have been obtained. The shape forms of the rod-type VC and a frequency range of vibration laws containing a single impact during the excitation period have been determined.

11. The shape form synthesis problems have been solved employing the optimal design techniques. Special features of exciting asymmetric vibration cycles in ring-type VC have been pointed out and the locations of asymmetrically vibrating points on the circumference of the ring have been obtained. Placements of such points have been shown to be severely influenced by the excitation level of modal components.

12. Shape forms of asymmetric vibration cycle concentrators for two and three Fourier components and of a transformer of rectangular excitation pulse series into asymmetric triangular pulse series have been obtained.

13. By means of an inverse dynamic problem solution in modal coordinates a VC with the internal impact pair excited by a harmonic excitation law and producing a polyharmonic vibration law has been obtained. A shape form of a VC has been obtained ensuring an asymmetric triangular pulse series response.

14. Employing the developed techniques the optimal control laws and feedback circuit parameters have been obtained ensuring a damping of transient vibrations occurring due to the externally excited stepwise increments of longitudinal elastic deformation of a VC. The programmed and closed-loop control laws with the displacement and velocity feedback have been synthesized.

15. Investigating the models of the VCKP employing a varying normal force, the complex friction laws ensuring the equal slopes of an output link velocity pulse have been obtained. In some cases presence of a descending slope in a friction law relationship causes a non-stop motion of the output link after a normal force pulse. At a high normal force pulse frequency a stationary motion mode is obtained, the control of the velocity and acceleration values being possible by means of the width-modulated pulses of the normal force.

References

1. Argyris J.H.,Doltsinis J.St.,Knudson W.C.,Vaz L.E.,Willam K.J. Numerical Solution of Transient Nonlinear Problems, Comp.Meths.Appl.Mech.Engng.,17/18(1979),pp.341-409.

2. Bansevičius R.Barauskas R.,Giniotis V.,Ragulskis K. Control of Pitch Accuracy of Measuring Grids(Rasters),Vibration Engineering,1,N1-4(1987),pp.251-262.

3. Bansevičius R.,Barauskas R.,Kulvietis G.,Ragulskis K. Vibromotors for Precision Microrobots,English Edition,Ed.: E.Rivin,Hemisphere,1988,310p.

4. Barauskas R. Computation of Periodic Motion Regimes of Nonlinear Mechanical Systems,Vibration Engineering,2, (1988),pp.435-447.

5. Barauskas R.,Ragulskis K. Dynamic Modelling and Control of Active Elastic Mechanical Systems with Nonlinear Interaction. In:Dynamische Probleme-Modelierung und Wirklichkeit. Vortraege der Tagung am 4.-5.10.1990 in Hannover, Hannover,1990,pp.9-27.

6. Barauskas R.A.,Ragulskis K.M. Dynamics of Piezoelectric Vibromotors with Impact Interaction.-In: 13th International Conference on Machine Dynamics INTERDYNAMICS-81.Proceedings, Jadwisin near Warsaw,1981,pp.41-46.

7. Barauskas R.A.,Ragulskis K.M. Optimal Control Synthesis of Vibration Motion Converters.-In: 15th International Conference on Machines, INTERDYNAMICS-85.Proceedings, Frankfurt/Oder,GDR,1985,S-Reihe,N8. -Karl-Marx Stadt,1986,pp.23-30.

8. Bathe K.J., Wilson E.L., Numerical Methods in Finite Element Analysis,Prentice Hall, Englewood Cliffs,New Jersey, 1976,521p.

9. Bellman R. Dynamic Programming, Princeton University Press, Princeton, 1957.

10. Cheng J.,Kikutchi N. An Analysis of Metal Forming Processes Using Large Deformation Elastic-Plastic Formulations,Comp. Meths.Appl.Mech.Engng.,49(1985),pp.71-108.

11. Dokmeci M.C. Vibrations of Piezoelectric Crystals. -I.J.Engng.Sci.,18(3)(1980),pp.431-448.

12. Gill P.E., Murray W., Wright M.H. Practical Optimization, Academic Press, 1981.

13. Guyan R.J. Reduction of stiffness and mass matrices, J.A.I.A.A., 3(1965),p.380.

14. E.J.Haugh, J.S.Arrora. Applied Optimal Design. Mechanical and Structural Systems, Wiley, 1979.

15. Herrman L.R. Finite Element Analysis of Contact Problems, J.of Eng.Mech.Div.,104(5)(1978),pp.1043-1057.

16. Holland R.,EerNisse E.P. Design of Resonant Piezoelectric Devices,Cambridge:MIT Press,1969,-258p.

17. Hughes T.J.R.,Pister K.S.,Taylor R.L. Implicit-Explicit Finite Elements in Nonlinear Transient Analysis, Comp.Meths.Appl.Mech. Engng.,17/18(1979),pp.159-182.

18. Idelsohn S.R.,Cordona A. A Reduction Method for Nonlinear Structural Dynamic Analysis, Comp. Meths. Appl. Mech. Engng.,49(1985),pp.253-279.

19. Irons B.M. Structural eigenvalue problems: elimination of unwanted variables,J.A.I.A.A.,3(1965),p.961.

20. Kaczkowski Z. Magnetomechanical Coupling in Transducers. -Archives of Acoustics,6(4)(1981),pp.385-400.

21. Kagawa Y. A New Approach to Analysis and Design of Electro-mechanical Filters by Finite Element Technique,J.Acoust.Soc. Amer.,49(5)(1971),pp.1348-1356.

22. Kagawa Y.,Gladwell G.M.L. Finite Element Analysis of Flexure-Type Vibrators with Electrostrictive Transducers,IEEE Trans. on Sonics and Ultrasonics,SU-17(1)(1970),pp.41-50.

23. Kagawa Y.,Yamabuchi T. A Finite Element Approach to Electro-mechanical Problems with an Application to Energy Trapped and Surface-Wave Devices,IEEE Trans.on Sonics and Ultrasonics, SU-23(4)(1976),pp.263-272.

24. Kagawa Y.,Yamabuchi T. Finite Element Simulation of Two Dimensional Electromechanical Resonators,IEEE Trans.on Sonics and Ultrasonics,SU-21(4)(1974),pp.275-283.

25. Katona M.G.,Zienkiewitcz O.C. A Unified Set of Single Step Algorithms. Part 3: The Beta-m Method, the Generalization of the Newmarks Scheme, I.J.Numer.Meths.Engng.,21(1985),pp.1345-1359.

26. Lankaster P. Theory of Matrices, Academic Press, 1969.

27. Leung Y.T. An Accurate Method of Dynamic Substructuring with Simplified Computation, I.J. for Numerical Methods in Engng., 14(1979),pp.1241-1256.

28. Ling F.H. Numerische Berechnung periodisher Lösungen nichtlinearer Schwingungssysteme,ZAMM 62(1982),pp.T55-T58.

29. Masri S.F. et al. A Method for Reducing the Order of Nonlinear Mechanical System,J.of Appl.Mech.,51(1984),pp.391-398.

30. Nayfeh A.H. Introduction to Perturbation Techniques, Wiley, 1981.

31. Nashif A.D.,Johnes D.I.G., Henderson J.P. Vibration Damping, Wiley, 1985.

32. Nickel R.E. Nonlinear Dynamics by Mode Superposition, Comp.Meths.Appl.Mech.Engng.,7(1976),pp.107-129.

33. Nowacki J.P. Steady-State Problems of Thermopiezoelectricity. -J.of Thermal Stresses,5(1982),pp.183-194.

34. Ostaševičius V.,Ragulskis K.,Barauskas R.,Gaidys R. Optimization of Longitudinaly Oscillating Structures,Vibration Engineering,1(1-4)(1987),pp.25-32.

35. Parlett B.N. The Symmetric Eigenvalue Problem, Prentice Hall, Englewood Cliffs, 1980.

36. Peterson H. Application of the Finite Element Method in the Analysis of Contact Problems,Finite Elem.Nonlinear Mech., 2(1978),pp.845-862.

37. Ragulskis K.M. Vibromotors,The Shock and Vibration Digest, 12(2)(1980),pp.27-30.

38. Rosenblum G. Modal Synthesis: Generalisation of Mc'Neal's Methods.Theoretical basis,Comp.Meths.Appl.Mech.Engng., 48(1985),pp.139-154.

39. Sage A.P., White C.C.,III. Optimum Systems Control, Prentice Hall, Englewood Cliffs,New Jersey, 1977.

40. Shabana A.A. Transient Analysis of Flexible Multibody Systems.Part 1: Dynamics of Flexible Bodies,Comp.Meths. Appl.Mech.Engng.,54(1986),pp.75-91.

41. Tiersten H.F. Linear Piezoelectric Plate Vibration.Elements of the Linear Theory of Piezoelectricity and the Vibration of Piezoelectric Plates,Plenum Press,New York,1969,212p.

42. Wilson E.L. Numerical Methods for Dynamic Analysis, in Numerical Methods in Offshore Engineering,1977,pp.195-220.

43. Wood W.L. A Unified Set of Single Step Algorithms. Part 2: Theory,I.J.Numer.Meths.Engng.,20(1984),pp.2303-2309.

44. Zienkiewitcz O.C. The Finite Element Method, McGraw Hill, 1977,787p.

45. Zienkiewitcz O.C., Morgan K. Finite Elements and Approximation, Wiley, 1983.

46. Zienkiewitcz O.C.,Wood W.L.,Hine N.W.,Taylor R.L. A Unified Set of Single Step Algorithms. Part 1: General Formulation and Applications,I.J.Numer.Meths.Engng.,20(1984),pp.1529-1552.

47. Алексеенко В.И. Создание и исследование вибродвигателей с прямыми ударами: Автореф. дис. ... канд.тех.наук.-Каунас,1987.

48. Альберт А. Регрессия,псевдоинверсия и рекурентное оценивание. -М: Наука, 1977.-223с.

49. Андронов А.А., Витт А.А., Хайкин С.Э. Теория колебаний.-М.: Наука,1981.-568с.

50. Бабицкий В.И. Теория виброударных систем. -М.:Наука,1985.-320с.

51. Бабицкий В.И., Крупенин В.Л. Колебания в сильно нелинейных системах.-М.:Наука,1985.-320с.

52. Баничук Н.В. Оптимизация формы упругих тел.-М.:Наука,1982. -432с.

53. Бансявичюс Р.Ю.,Бараускас Р.А. Пьезоэлектрические преобразователи с переменным вектором поляризации и их применение // Применение пьезоактивных материалов в промышленности.Материалы краткосрочного семинара 20-21 мая 1988г.Ленинградский дом научно-технической пропаганды.-Л.,1988,с.16-19.

54. Бансявичюс Р.Ю.,Бараускас Р.А.,Гинетис В.П.,Рагульскис К.М. Управление погрешностью шага штриховых мер // Вибротехника. -1983.-N.3(47).-с.113-123.

55. Бансявичюс Р.Ю.,Курило Р.Э. Взаимодействие объекта конечных размеров с продольной бегущей высокочастотной волной. // Вибротехника.-1979.-N.4(28).-с.41-46.

56. Бансявичюс Р.Ю.,Рагульскис К.М. Вибродвигатели.-Вильнюс, Мокслас,1981.-193с.

57. Бараускас Р.А. Исследование динамики пьезокерамических входных звеньев вибродвигателей методом конечных элементов // Вибротехника.-1983.-N.3(43).-с.89-97.

58. Бараускас Р.А. Построение систем управления движением упругих механических систем на основе решения обратных задач динамики // Вибротехника.-1984.-N.3(51).-с.7-17.

59. Бараускас Р.А. Применение метода конечных элементов к расчету биморфных асимметричных пьезокерамических ведущих органов вибродвигателей в пространственной системе координат. // Вибротехника.-1983.-N.1(41).-с.7-15.

60. Бараускас Р.А. Прямое численное интегрирование уравнений динамики упругих механических систем с односторонними кинематическими ограничениями.I.Методы // Вибротехника.-1990. -N.3(64).-с.141-149.

61. Бараускас Р.А. Прямое численное интегрирование уравнений динамики упругих механических систем с односторонними кинематическими ограничениями.II.Расчет систем с парами прямого удара // Вибротехника.-1991.-N.66.-с.5-16.

62. Бараускас Р.А. Прямое численное интегрирование уравнений динамики упругих механических систем с односторонними кинематическими ограничениями.III.Расчет систем с парами трения и косого удара // Вибротехника.-1991.-N.67.

63. Бараускас Р.А. Расчет многопериодных и установившихся режимов вынужденных колебаний упругих механических систем с существенными нелинейностями // Вибротехника.-1991.-N.67.

64. Бараускас Р.А. Редукция динамических моделей упругих механических систем с односторонними кинематическими ограничениями // Вибротехника.-1991.-N.68.

65. Бараускас Р.А. Управление апериодическими движениями упругих механических систем.// Вибротехника.-1984.-N.4(52).

66. Бараускас Р.А. Численное моделирование динамического контакта упругих механических систем // Научные труды ВУЗов ЛитССР. Машиностроение.-Вильнюс,1989.-т.1.-с.26-41.

67. Бараускас Р.А. Численное определение периодических режимов движения нелинейных механических систем.// Вибротехника.-1986. -N.4(57).-с.41-52.

68. Бараускас Р.А.,Бяндорайтис К.К.,Рудгалвис Б.В. Нестационарные движения упругой системы с односторонними ограничениями.Метод численного расчета и его применения.-Научные труды ВУЗов ЛитССР. Машиностроение.-Вильнюс,1989.-т.1.-с.26-41.

69. Бараускас Р.А.,Кульветис Г.П. Пакет программ для формирования матриц жесткости, масс и демпфирования метода конечных элементов с возможностями модификации // Алгоритмы и программы(ВИНИТИ).- 1980.- N.2(34).-с.42.

70. Бараускас Р.А.,Кульветис Г.П. Подпрограммы и алгоритмы для проведения операций с разряженными матрицами // Алгоритмы и программы(ВИНИТИ).- 1980.- N.2(34).- с.31.

71. Бараускас Р.А.,Кульветис Г.П.,Рагульскис К.М. Расчет и проектирование вибродвигателей.-Л.:Машиностроение,1984.-99с.

72. Бараускас Р.А.,Лиманаускас Л.П. Исследование колебаний биморфной пезокерамической цилиндрической оболочки в двумерной системе координат // Вибротехника.-1981.-N.4(38).-с.93-101.

73. Бараускас Р.А.,Лиманаускас Л.П. Применение метода конечных элементов к расчету колебаний биморфных асимметричных пьезокерамических преобразователей // Вибротехника.-1981.-N.4(38).- с.85-92.

74. Бараускас Р.А.,Малишаускас М.А.,Мержвинскайте О.А.,Шведас Л.С.Расчет биморфных пьезокерамических элементов.// Вибротехника.-1983.-N.2(46).-с.118-127.

75. Бараускас Р.А.,Плёплис А.А.,Рагульскис К.М. Управление вынужденными резонансными колебаниями вибропреобразователей. // Вибротехника.-1987.-N.1(58).-с.14-19.

76. Бараускас Р.А.,Рагульскене В.Л.,Рагульскис К.М.. Динамика вибродвигателя, возбуждаемого отдельными импульсами // Вибротехника.-1983.-N.2(42).-с.141-149.

77. Бараускас Р.А.,Рагульскис К.М.. Динамика вибродвигателей кольцевого типа с ударным взаимодействием. // Вибротехника.-1983.-N.1(41).-с.61-68.

78. Бараускас Р.А.,Рагульскис К.М.,В.К.Рейникис. Управление апериодическими движениями пьезокерамического преобразователя. // Вибротехника.-1986.-N.2(55).-с.109-117.

79. Блехман И.И.,Джанелидзе Г.Ю.. Вибрационное перемещение.-М.:Наука,1964.-412с.

80. Блюмин С.Л.,Дарienко В.В. К построению алгоритмов управления движением линейных систем на основе решения обратных задач динамики // Изв.АНСССР.Техническая кибернетика.-1982.-N.1.-с.187-196.

81. Боли Б.,Уэйнер Дж..Теория температурных напряжений.-М.:Мир,1964.-517с.

82. Болотин В.В. Динамическая устойчивость упругих систем.-М.:Гостехиздат,1956.

83. Бондаренко А.,Карась И.И.,Улитко А.Ф. Методы определения характеристик диссипации при колебаниях пьезокерамических элементов конструкций // Прикладная механика.-1982.-т.XVIII,N.2.-с.105-108.

84. Борисейко В.А.,Улитко А.Ф. Осесимметричные колебания тонкой пьезокерамической сферической оболочки // Прикладная механика.-1974.- Т.X,N.10.- с.3-10.

85. Бутенин Н.В., Неймарк Ю.И., Фуфаев Н.А. Введение в теорию нелинейных колебаний.-М.:Наука,1976.-384с.

86. Бычков Ю.А.,Васильев Ю.В.. Расчет периодических режимов в нелинейных системах управления.-Л.:Энергоатомиздат,1988.-112с.

87. Вейц В.Л.,Коловский М.З.,Кочура А.Е. Динамика управляемых машинных агрегатов.-М.:Наука,1984.-351с.

88. Вибрации в технике:Справочник.В 6-ти т./Ред.совет: В.Н.Челомей(пред.)-М.:Машиностроение,1978- ,т.1.Колебания линейных систем/под ред.В.В.Болотина,1978.-352с.

89. Вибрации в технике:Справочник.В 6-ти т./Ред.совет: В.Н.Челомей(пред.)-М.:Машиностроение,1978- т.2 Колебания нелинейных механических систем/под ред.И.И.Блехмана,1979.-351с.

90. Вибрационные преобразователи движения / Р.Ю.Бансявичюс и др.-Л.:Машиностроение,1984.-64с.

91. Вульфсон И.И.,Коловский М.З. Нелинейные задачи динамики машин.-Л.:Машиностроение,1968.

92. Гайвянис А.К. Прецизионные приводы с разделенными силовыми и управляющими воздействиями: Автореф. дис. ... канд.тех.наук.-Каунас,1990.

93. Галлиулин А.С. Методы решения обратных задач динамики.-М.:Наука,1986.-224с.

94. Гасюнас Й.Й. Создание, исследование и внедрение вибродвигателей с асимметричными циклами колебаний. Автореф. дис. ... канд.тех.наук.-Каунас,1984.

95. Генкин М.Д.,Елезов В.Г.,Яблонский В.В. Методы управляемой виброзащиты машин.-М.:Наука,1985.-240с.

96. Гололобов В.И. Численный расчет пьезокерамических оболочек вращения // Прикладная механика.-1981.-т.XVII.-с.38-42.

97. ГОСТ 12370-80.Материалы пьезокерамические.Методы испытаний.-М.:Изд-во стандартов,1980.-30с.

98. Гребенников Е.А. Метод усреднения в прикладных задачах.-М.:Наука,1986.-256с.

99. Гринченко В.Т.,Карлаш В.Л.,Мелешко В.В.,Улитко А.Ф. Исследование планарных колебаний прямоугольных пезокерамических пластин // Прикладная механика.-1976.-т.XII,N.5.-с.71-78.

100. Джагупов Р.Г.,Ерофеев А.А. Пьезокерамические элементы в приборостроении и автоматике.-Л.:Машиностроение,1986.-256с.

101. Евстифеев Ю.А. Разработка математического и программного обеспечения анализа многопериодных объектов : Автореф. дис. ... канд.тех.наук.-1984.

102. Ерофеев А.А. Пезоэлектронные устройства автоматики.-Л.:Машиностроение,1982.-212с.

103. Закржевский М.В. Колебания существенно нелинейных механических систем.-Рига,Зинатне,1980.-189с.

104. Кажис Р.-И.Ю.,Мажейка Л.Ю. Исследование переходных процессов в плоских пьезоизлучателях методом конечных элементов // Дефектоскопия.-1986.-N.12.-с.3-11.

105. Калиткин Н.Н. Численные методы.-М.:Наука,1978.-512с.

106. Кильчевский Н.А. Динамическое контактное сжатие твердых тел.-Киев,Наукова Думка,1969,-246с.

107. Кобринский А.А., Кобринский А.Е. Двумерные виброударные системы.-М.:Наука,1981.-335с.

108. Кобринский А.Е., Кобринский А.А. Виброударные системы.-М.:Наука,1973.-592с.

109. Коловский М.З. Автоматическое управление виброзащитиными системами.-М.:Наука,1976.-320с.

110. Коловский М.З. Динамика машин.-М.:Машиностроение,1989.-263с.

111. Коловский М.З. Нелинейная теория виброзащитиных систем.-М.:Наука,1966.

112. Комков В. Теория оптимального управления демпфированием колебаний простых упругих систем.-М.:Мир,1975.-178с.

113. Крагельский И.В., Гитис Н.В. Фрикционные автоколебания.-М:Наука, 1987.- 183с.

114. Красовский Н.Н. Теория управления движением.- М.:Наука,1968.-476с.

115. Крутько П.Д. Обратные задачи динамики управляемых систем. Линейные модели.-М.:Наука,1987.-304с.

116. Курило Р.Э.,Рагульскене В.Л. Двумерные вибрационные приводы.-Вильнюс, Мокслас, 1986,-137с.

117. Лавендел Э.Э.. Прикладные методы расчета изделий из высокоэластичных материалов.-Рига,Зинатне,1980.-238с.

118. Лавендел Э.Э. Синтез оптимальных вибромашин. -Рига,Зинатне, 1970.-251с.

119. Лавриненко В.В.,Карташев И.А.,Вишневский В.С. Пьезоэлектрические двигатели.-М.:Энергия,1980.-112с.

120. Масилюнас В.Б.,Бараускас Р.А. Применение метода конечных элементов к расчету пьезокерамических преобразователей с геометрической нелинейностью // Вибротехника.-1983.-N.1(41).-с.129-136.

121. Моисеев Н.И. Асимптотические методы нелинейной механики. -М.:Наука,1969.-379с.

122. Нагаев Р.Ф. Механические процессы с повторными затухающими соударениями.-М.:Наука,1985.-200.

123. Нагаев Р.Ф. Периодические режимы вибрационного перемещения. -М.:Наука,1980.-256.

124. Ольхофф Н. Оптимальное проектирвание конструкций. Вопросы вибрации и потери устойчивости.-М.:Мир,1981.-278с.

125. Осташявичюс В.В.,Рагульскис К.М.,Бараускас Р.А. Проектирование конструкций, имеющих заданные частоты собственных колебаний.// Динамика и прочность машин.-вып.40.-с.82-86.

126. Осташявичюс В.В.,Рагульскис К.М.,Бараускас Р.А.,Гайдис Р.Д. Проектирование конструкций, совершающих продольные колебания.// Вибротехника.-1986.-N.1(54).-с.7-12.

127. Осташявичюс В.В.,Рудгалвис Б.В.,Рагульскене В.Л.,Бакшис Б.П. Контактные системы.-Л.:Машиностроение,1987.-279с.

128. Пановко Я.Г. Внутреннее трение при колебаниях упругих систем.-Киев,Наукова Думка,1976,-85с.

129. Петров Б.Н.,Крутько П.Д. Обратные задачи динамики управляемых систем.Линейные модели // Изв.АНСССР,Техническая кибернетика.-1980.-N.4.-с.147-156.

130. Понтрягин Л.С.,Болтянский В.Г.,Гамкрелидзе П.В.,Мищенко Е.Ф. Математическая теория оптимальных процессов.-М.:Наука,1983.-392с.

131. Попов Е.П. Теория нелинейных систем автоматического регулирования и управления.-М.:Наука,1988.-256с.

132. Постнов В.А.,Хархурим И.Я. Метод конечных элементов в расчете судовых конструкций.-Л.:Судостроение,1974.-342с.

133. Рагульскене В.Л. Виброударные системы. -Вильнюс:Мокслас, 1978.-319с.

134. Рагульскис К.М.,Бараускас Р.А.,Купчюнас Р.В. Динамические характеристики вибродвигателей // Инерционно-импульсные системы.Межвузовский тематический сборник научных трудов.-Челябинск,1983.-с.16-21.

135. Розин Л.А. МКЭ в применении к упругим системам.-М.: Стройиздат, 1978.-129с.

136. Седов Л.И. Методы подобия и размерности в механике. -М.:Наука,1987.-430с.

137. С.Скельбое. Временной стационарный анализ нелинейных электрических систем // ТИИЭР.-1982.-т.70,N.10.-с.89-119.

138. Сорокин Е.С. К теории внутреннего трения при колебаниях упругих систем.-М.:Росстройиздат,1960.-131с.

139. Троицкий В.А., Петухов Л.В. Оптимизация формы упругих тел. -М.:Наука,1982.-432с.

140. Ультразвук.Маленькая энциклопедия./под ред.И.П.Голямина. -М.:Советская энциклопедия,1979.-400с.

141. Уткин В.И. Скользящие режимы в задачах оптимизации и управления.-М.:Наука,1981.-367с.

142. Хаяси Т. Нелинейные колебания в физических системах.-М.: Мир,1968.-432с.

143. Черноусько Ф.Л., Акуленко Л.Д., Соколов Б.Н. Управление колебаниями.-М.:Наука,1980.-383с.

144. Черноусько Ф.Л., Баничук Н.В. Вариационные задачи механики и управления.-М.:Наука,1973.-238с.

145. Якубович В.А., Старжинский В.М. Параметрический резонанс в линейных системах.-М.:Наука,1987.

146. Яффе Б.,Кук У.,Яффе Г. Пьезоэлектрическая керамика.-М.:Мир, 1974.-156с.

147. А.с.N.461470 СССР Шаговый двигатель/ А.П.Лукошявичюс, К.М.Рагульскис,А.Ю.Славенас,Р.В.-К.Улозас.

148. А.с.по заявке N.2676963/18-25 от 17.10.1978 СССР Вибродвигатель/Л.-А.Л.Штацас,К.М.Рагульскис,Р.Ю.Бансявичюс, С.Ю.Гервицкас

149. А.с.по заявке N.2688949/18-10 от 23.11.1978 СССР Двигатель лентопротяжного механизма/С.Ю.Гервицкас,К.М.Рагульскис, Л.-А.Л.Штацас,Р.Э.Курило.

150. А.с.N.1053190 СССР H 01 L 41/08, H 02 N 11/00 Устройство для получения вращательного движения / Я.Ш.Флейтман,Р.А.Бараускас.-Опубл.07.11.83, Бюл.N.41.

151. А.с.N.1287735 СССР Вибродвигатель / К.М.Рагульскис, А.С.Любинас,Р.В.Купчюнас,Р.А.Бараускас.

152. А.с.по заявке N.2847170/18-25 СССР H 01 L 41/08 // H 02 N 11/00 Реверсивный вибропривод /Л.-А.Л.Штацас, К.М.Рагульскис,В.Л.Рагульскене,Р.А.Бараускас;Каунасский политехн.ин-т.

APPENDICES

APPENDIX 1. NUMERICAL INTEGRATION SCHEMES, THEIR PARAMETERS AND FEATURES

A1.1 ALGORITHM SSpj (O.Zienkiewitcz et.al. [46])

Algorithm SS22

1. $\tilde{U}_{t+\Delta t} = U_t + \dot{U}_t \theta_1 \Delta t$,
   $\dot{\tilde{U}}_{t+\Delta t} = \dot{U}_t$;

2. $\alpha_t^{(2)} = (M + \theta_1 \Delta t\, C + \frac{\Delta t^2}{2} \theta_2 K)^{-1} (\bar{R} - C\, \dot{\tilde{U}}_{t+\Delta t} - K\, \tilde{U}_{t+\Delta t})$;

3. $U_{t+\Delta t} = U_t + \Delta t\, \dot{U}_t + \alpha_t^{(2)} \frac{\Delta t^2}{2}$;
   $\dot{U}_{t+\Delta t} = \dot{U}_t + \alpha_t^{(2)} \Delta t$;

The matrix $E^{(2)}$ for the algorithm SS22 reads as

$$E^{(2)} = \begin{bmatrix} 1 & 1 & 1/2 \\ 0 & 1 & 1 \\ \omega_o^2 \Delta t^2 & 2h\Delta t + \omega_o^2 \Delta t^2 \theta_1 & 1 + 2h\Delta t \theta_1 + \omega_o^2 \Delta t^2 \theta_2 \end{bmatrix} \qquad (2.49)$$

Algorithm SS32

1. $\tilde{U}_{t+\Delta t} = U_t + \dot{U}_t \theta_1 \Delta t + \ddot{U}_t \Delta t^2$;
   $\dot{\tilde{U}}_{t+\Delta t} = \dot{U}_t + \ddot{U}_t \theta_1 \Delta t$;
   $\ddot{\tilde{U}}_{t+\Delta t} = \ddot{U}_t$;

2. $\alpha_t^{(3)} = (\theta_1 \Delta t M + \frac{\Delta t^2}{2} \theta_2 C + \frac{\Delta t^3}{6} \theta_3 K)^{-1} (\bar{R} - M \ddot{\tilde{U}}_{t+\Delta t} - C \dot{\tilde{U}}_{t+\Delta t} - K \tilde{U}_{t+\Delta t})$;

3. $U_{t+\Delta t} = U_t + \Delta t\, \dot{U}_t + \frac{\Delta t^2}{2} \ddot{U}_t + \alpha_t^{(3)} \frac{\Delta t^3}{6}$;
   $\dot{U}_{t+\Delta t} = \dot{U}_t + \Delta t\, \ddot{U}_t + \alpha_t^{(3)} \frac{\Delta t^2}{2}$;
   $\ddot{U}_{t+\Delta t} = \ddot{U}_t + \alpha_t^{(3)} \frac{\Delta t^2}{2}$;

The matrix $E^{(3)}$ for the algorithm SS32 reads as

$$E^{(3)} = \begin{bmatrix} 1 & 1 & 1/2 & 1/6 \\ 1 & 1 & 1 & 1/2 \\ 0 & 1 & 1 & 1 \\ \omega_o^2 \Delta t^2 & 2h\Delta t + \omega_o^2 \Delta t^2 \theta_1 & 1 + 2h\Delta t \theta_1 + \omega_o^2 \frac{\Delta t^2}{2} \theta_2 & \theta_1 + h\Delta t \theta_2 + \omega_o^2 \frac{\Delta t^2}{6} \theta_3 \end{bmatrix} .$$

Algorithmic features of the above presented schemes are summarized in Table A1.1, taken from [46].

A1.2 GENERALIZED NEWMARK'S SCHEME

(M.Katona ,O.Zienkiewitcz, [25])

For an undamped oscillator ($h = 0$) the error of the displacement $U_{t+\Delta t}$ at the time point $t+\Delta t$ is expressed as

$$\frac{1}{\Delta t^2}\left[C_0+ C_1\Delta t + C_2\Delta t^2+\ldots+ C_i\Delta t^i+\ldots\right],$$

where the values of the coefficients C_i are presented in Table A1.2 , taken from [25]. For the m-th order scheme at arbitrary parameter values $\beta_0,\ldots,\beta_{m-1}$ we obtain $C_0= C_1= C_2=\ldots= C_m= 0$. Therefore in the worst case the error doesn't exceed $\tau=O(\Delta t^{m-1})$. Selecting parameter values β_k ensuring the value $C_{m+1}= 0$, a higher accuracy order can be obtained. However, stability condition of the numerical scheme is to be regarded when selecting the β_k values.

In [25] it has been shown, that the necessary and sufficient conditions for the numerical scheme stability when applied to the undamped oscillator equation are as follows:

$$\begin{aligned}
&m = 2 : a_0> 0,\ a_1\geq 0,\ a_2\geq 0 ;\\
&m = 3 : a_0> 0,\ a_1,a_2,a_3\geq 0,\ a_1a_2- a_3a_0\geq 0 ;\\
&m = 4 : a_0> 0,\ a_1,a_2,a_3,a_4\geq 0,\ a_1a_2a_3- a_0a_3^2- a_4a_1^2\geq 0 ;
\end{aligned}\qquad (A1.1)$$

where the expressions of a_i through the parameters β_i are presented in Table A1.3.

From Table A1.3 , conditions (A1.1) and assuming $\lambda= \omega\Delta t = 0$ we obtain the necessary stability conditions as

$$\begin{aligned}
&m = 2 : \beta_1\geq 0.5 ;\\
&m = 3 : \beta_2\geq 0.5 ;\\
&m = 4 : \beta_3\geq 0.5 ,\ \beta_2- \beta_3\geq 0 .
\end{aligned}\qquad (A1.2)$$

A numerical scheme has no numerical damping, if the following equations are satisfied:

$$\begin{aligned}
&m = 2 : a_1= 0 ;\\
&m = 3 : a_1a_2- a_3a_0= 0 ,\ (a_2\geq 0) ;\\
&m = 4 : a_1a_2a_3- a_0a_3^2- a_4a_1^2\geq 0 ,\ (a_2^2- 4a_4a_0\geq 0) .
\end{aligned}\qquad (A1.3)$$

The values of the parameters β_k can be selected in order to submit some other features to a numerical scheme. E.g., for obtaining an unconditionally stable scheme, it is necessary to satisfy the conditions (A1.1) at $\omega\Delta t \rightarrow \infty$. At $m=2$ (traditional Newmark scheme) these conditions are as follows

$$\beta_0\geq \beta_1 ,\ \beta_1\geq 0.5 .$$

Table A1.4 presents the values of parameters β_k and the corresponding algorithmic features. The well-known Houbolt and Wilson schemes can be regarded as special cases of this algorithm family. The traditional form of the Houbolt scheme is a multistep one, and it can be identified with the generalized Newmark scheme after presenting as a single-step one. It can be carried out by writing the relation (2.60) for the time points $t-2\Delta t$, $t-\Delta t$, t, $t+\Delta t$ and eliminating from the obtained system the derivatives $\dot U$, $\ddot U$, $U^{(3)}$.

A1.3 FINITE ELEMENTS IN TIME DOMAIN (HERMITIAN INTERPOLATION)

(J.Argyris et al., [1])

A1.3.1 Hermitian functions

p = 0 (linear interpolation, 2p + 1 = 1)

$$\vartheta^0_{00}= 1 - \xi ,\quad \vartheta^0_{01}= \xi .$$

p = 1 (cubic interpolation, 2p + 1 = 3)

$$\vartheta^1_{00}= 1 - 3\xi^2+ 2\xi^3 ,\quad \vartheta^1_{01}= 3\xi^2- 2\xi^3 ,$$
$$\vartheta^1_{10}= (\xi - 2\xi^2+ \xi^3)\Delta t ,\quad \vartheta^1_{11}= (-\xi^2+ \xi^3)\Delta t .$$

p = 2 (fifth order interpolation, 2p + 1 = 5)

$$\vartheta^2_{00}= 1 - 10\xi^3+ 15\xi^4- 6\xi^5 ,\quad \vartheta^2_{01}= 10\xi^3- 15\xi^4+ 6\xi^5 ,$$

$$\vartheta^2_{10}= (\xi - 6\xi^3+ 8\xi^4- 3\xi^5)\Delta t ,\quad \vartheta^2_{11}= (-4\xi^3+ 7\xi^4- 3\xi^5)\Delta t ,$$

$$\vartheta^2_{20}= (\tfrac{1}{2}\xi^2- \tfrac{3}{2}\xi^3+ \tfrac{3}{4}\xi^4- \tfrac{1}{2}\xi^5)\Delta t^2 ,\quad \vartheta^2_{21}= (\tfrac{1}{2}\xi^3- \xi^4+ \tfrac{1}{2}\xi^5)\Delta t^2 .$$

A1.3.2 Numerical schemes

Linear scheme, $p = 0$

$$ {}_1B_1 X_1 = {}_1B_0 X_0 + P_1 , $$

$$ {}_1B_1^{11} = I + \alpha_1 \Delta t \, \bar{C} , \qquad {}_1B_0^{11} = I + \beta_1 \Delta t \, \bar{C} , $$

$$ {}_1B_1^{12} = \alpha_1 \Delta t \, \bar{K} , \qquad {}_1B_0^{12} = \beta_1 \Delta t \, \bar{K} , $$

$$ {}_1B_1^{21} = -\alpha_1 \Delta t \, I , \qquad {}_1B_0^{21} = -\beta_1 \Delta t \, I , $$

$$ {}_1B_1^{22} = I , \qquad {}_1B_0^{22} = I , $$

$$ P_1^1 = \alpha_1 \Delta t \, \bar{R}_1 - \beta_1 \Delta t \, \bar{R}_0 , \quad P_1^2 = 0 . $$

$$ {}_1B_1 = \begin{bmatrix} {}_1B_1^{11} & {}_1B_1^{12} \\ {}_1B_1^{21} & {}_1B_1^{22} \end{bmatrix} , \quad {}_1B_0 = \begin{bmatrix} {}_1B_0^{11} & {}_1B_0^{12} \\ {}_1B_0^{21} & {}_1B_0^{22} \end{bmatrix} , \quad P_1 = \begin{bmatrix} P_1^1 \\ P_2^1 \end{bmatrix} , $$

$$ \bar{K} = M^{-1}K , \quad \bar{C} = M^{-1}C , \quad \bar{R} = M^{-1}R , \quad \alpha_1 = \xi , \quad \beta_1 = \xi - 1 . $$

In the case of homogeneous equation, i.e. at $R \equiv 0$, substituting the relations

$$ \ddot{U}_0 = - \bar{C} \dot{U}_0 - \bar{K} U_0 , $$

$$ \ddot{U}_1 = - \bar{C} \dot{U}_1 - \bar{K} U_1 $$

into the above formulae, we obtain, that for the linear scheme the following equalities are satisfied:

$$ \dot{U}_1 = \dot{U}_0 + \Delta t(-\beta_1 \ddot{U}_0 + \alpha_1 \ddot{U}_1) , $$

$$ U_1 = U_0 + \Delta t \, \dot{U}_0 + \Delta t^2(-\alpha_1\beta_1 \ddot{U}_0 + \alpha_1^2 \ddot{U}_1) . $$

At the parameter value $\xi = \frac{1}{2}$ this scheme coincides with the traditional Newmark scheme with the parameter values $\gamma = \frac{1}{2}$, $\beta = \frac{1}{4}$. It possesses an unconditional stability at $\frac{1}{2} \le \xi \le 1$, and at $\xi > \frac{1}{2}$ exhibits a numerical damping.

Cubic scheme, $p = 1$

$$ {}_3B_1 X_1 = {}_3B_0 X_0 + P_3 , $$

$$ {}_3B_1^{11} = I + \alpha_1 \Delta t \, \bar{C} + \alpha_2 \Delta t^2 (\bar{C}^2 - \bar{K}) , \quad {}_3B_0^{11} = I + \beta_1 \Delta t \, \bar{C} + \beta_2 \Delta t^2 (\bar{C}^2 - \bar{K}) , $$

$$ {}_3B_1^{12} = \alpha_1 \Delta t \, \bar{K} + \alpha_2 \Delta t^2 \bar{C} \, \bar{K} , \quad {}_3B_0^{12} = \beta_1 \Delta t \, \bar{K} + \beta_2 \Delta t^2 \bar{C} \, \bar{K} , $$

$$ {}_3B_1^{21} = -\alpha_1 \Delta t \, I + \alpha_2 \Delta t^2 \bar{C} , \quad {}_3B_0^{21} = -\beta_1 \Delta t \, I - \beta_2 \Delta t^2 \bar{C} , $$

$$ {}_3B_1^{22} = I - \alpha_2 \Delta t^2 \bar{K} , \quad {}_3B_0^{22} = I - \beta_2 \Delta t^2 \bar{K} , $$

$$ P_3^1 = \left[(\alpha_1 - \alpha_2 + \beta_2) \Delta t \, I + \alpha_2 \Delta t^2 \bar{C} \right] R_1 + \left[(-\beta_1 + \alpha_2 - \beta_2) \Delta t \, I + \beta_2 \Delta t^2 \bar{C} \right] R_0 , $$

$$ P_3^2 = \Delta t^2 (\beta_2 R_1 - \alpha_2 R_0) , $$

$$ \alpha_1 = \frac{\xi + 1}{3} , \quad \alpha_2 = - \frac{\xi}{6} , \quad \beta_1 = \frac{\xi - 2}{3} , \quad \beta_2 = \frac{1 - \xi}{6} . $$

For the cubic scheme the following equalities are satisfied:

$$ \dot{U}_1 = \dot{U}_0 + \Delta t(-\beta_1 \ddot{U}_0 + \alpha_1 \ddot{U}_1 + \Delta t \, \beta_2 \overset{(3)}{U_c} - \Delta t \, \alpha_2 \overset{(3)}{U_1}) , $$

$$ U_1 = U_0 + \Delta t \dot{U}_0 + \Delta t^2 \left[(-\alpha_1\beta_1 + \beta_2) \ddot{U}_0 + (\alpha_1^2 - \alpha_2) \ddot{U}_1) + \Delta t \alpha_1 \beta_2 \overset{(3)}{U_c} - \Delta t \alpha_1 \alpha_2 \overset{(3)}{U_1} \right] . $$

The cubic algorithm family possesses high accuracy, and at the parameter values $\frac{1}{2} \le \xi \le 1$ the unconditionally stable numerical schemes are obtained.

Fifth order scheme, p = 1

$$ {}_5B_1 X_1 = {}_5B_0 X_0 + P_5 \ , $$

$$ {}_5B_1^{11} = I + \alpha_1 \Delta t\, \bar{C} + \alpha_2 \Delta t^2 (\bar{C}^2 - \bar{K}) + \alpha_3 \Delta t^3 (\bar{C} - \bar{C}\,\bar{K} - \bar{K}\,\bar{C}) \ , $$

$$ {}_5B_1^{12} = \alpha_1 \Delta t\, \bar{K} + \alpha_2 \Delta t^2 \bar{C}\,\bar{K} + \alpha_3 \Delta t^3 (\bar{C}\,\bar{K} - \bar{K}^2) \ , $$

$$ {}_5B_1^{21} = -\alpha_1 \Delta t\, I + \alpha_2 \Delta t^2 \bar{C} - \alpha_3 \Delta t^3 (\bar{C}^2 - \bar{K}) \ , $$

$$ {}_5B_1^{22} = I - \alpha_2 \Delta t^2 \bar{K} - \alpha_3 \Delta t^3 \bar{C}\,\bar{K} \ , $$

$$ {}_5B_0^{11} = I + \beta_1 \Delta t\, \bar{C} + \beta_2 \Delta t^2 (\bar{C}^2 - \bar{K}) + \beta_3 \Delta t^3 (\bar{C} - \bar{C}\,\bar{K} - \bar{K}\,\bar{C}) \ , $$

$$ {}_5B_0^{12} = \beta_1 \Delta t\, \bar{K} + \beta_2 \Delta t^2 \bar{C}\,\bar{K} + \beta_3 \Delta t^3 (\bar{C}\,\bar{K} - \bar{K}^2) \ , $$

$$ {}_5B_0^{21} = -\beta_1 \Delta t\, I - \beta_2 \Delta t^2 \bar{C} - \beta_3 \Delta t^3 (\bar{C}^2 - \bar{K}) \ , $$

$$ {}_5B_0^{22} = I - \beta_2 \Delta t^2 \bar{K} - \beta_3 \Delta t^3 \bar{C}\,\bar{K} \ , $$

$$ P_5^1 = \left[(\alpha_1 - \alpha_2 + \beta_2) \Delta t\, I + (\alpha_2 - \alpha_3 + \beta_3) \Delta t^2 \bar{C} + \alpha_3 \Delta t^3 (\bar{C}^2 - \bar{K}) \right] R_1 + $$

$$ + \left[(-\beta_1 + \alpha_2 - \beta_2) \Delta t\, I + (-\beta_2 + \alpha_3 + \beta_3) \Delta t^2 \bar{C} - \beta_3 \Delta t^3 (\bar{C}^2 - \bar{K}) \right] R_0 \ , $$

$$ P_5^2 = \left[(\beta_2 - \alpha_3 + \beta_3) \Delta t^2 I + \beta_3 \Delta t^3 \bar{C} \right] R_1 + \left[(-\alpha_2 + \alpha_3 - \beta_3) \Delta t^2 I + \alpha_3 \Delta t^3 \bar{C} \right] R_0 . $$

$$ \alpha_1 = \frac{\xi+2}{5} \ , \quad \alpha_2 = \frac{1+2\xi}{20} \ , \quad \alpha_3 = -\frac{\xi}{60} \ , \quad \beta_1 = \frac{\xi-3}{5} \ , \quad \beta_2 = \frac{2\xi-3}{20} \ , \quad \beta_3 = \frac{1-\xi}{60} \ . $$

For the fifth order scheme the following equalities are satisfied:

$$ \dot{U}_1 = \dot{U}_0 + \Delta t (-\beta_1 \ddot{U}_0 + \alpha_1 \ddot{U}_1 + \Delta t\, \beta_2 \overset{(3)}{U_c} - \Delta t\, \alpha_2 \overset{(3)}{U_1} - \Delta t^2 \beta_3 \overset{(4)}{U_c} + \Delta t^2 \alpha_3 \overset{(4)}{U_1}) \ , $$

$$ U_1 = U_0 + \Delta t \dot{U}_0 + \Delta t^2 \left[(-\alpha_1\beta_1 + \beta_2) \ddot{U}_0 + (\alpha_1^2 - \alpha_2) \ddot{U}_1 \right) + \Delta t (\alpha_1\beta_2 - \beta_3) \overset{(3)}{U_c} + $$

$$ + \Delta t (-\alpha_1\alpha_2 + \alpha_3) \overset{(3)}{U_1} - \alpha_1\beta_3 \Delta t^2 \overset{(4)}{U_c} + \alpha_1\alpha_3 \Delta t^2 \overset{(4)}{U_1} \Big] \ . $$

The schemes are unconditionally stable at the parameter values $\frac{1}{2} \le \xi \le 1$. They possess high accuracy, however, larger amounts of computational resource are necessary than in the case of the cubic ones.

Table A1.1

Method	Parameters	h = 0			h ≠ 0		
		Phase error	Amplitude error	Stability	Phase error	Amplitude error	Stability
SS22	θ_1, θ_2	$O(\Delta t^2)$	$O(\Delta t)$	$0.5 \le \theta_1 \le \theta_2$	$O(\Delta t)$	$O(\Delta t)$	$0.5 \le \theta_1 \le \theta_2$
	$\theta_1 = 0.5$	$O(\Delta t^2)$	$O(\Delta t^3)$	$0.5 \le \theta_2$	$O(\Delta t^2)$	$O(\Delta t^2)$	$0.5 \le \theta_2$
	$\theta_1 = 0.5$, $\theta_2 = 1/6$	$O(\Delta t^4)$	$O(t^4)$	$\omega_0 \Delta t^2 < 6$	$O(\Delta t^2)$	$O(t^2)$	$\omega_0 \Delta t^2 < 6$
SS32	$a = \theta_1 - 0.5$ $b = \theta_1 - \theta_2 - \frac{1}{6}$ $c = \theta_3 - \frac{3}{2}\theta_2 + \frac{1}{4}$	$O(\Delta t^2)$	$O(\Delta t^3)$	$a > 0$ $b \ge 0$ $0 \le c \le 3ab$	$O(\Delta t^2)$	$O(\Delta t^2)$	$12a^2 > 1$ $b \ge 0$ $0 \le c \le 3ab$
	$b = -\frac{1}{3}$	$O(\Delta t^4)$	$O(\Delta t^3)$	$a > 0$ $c \le -a$ $\omega_0 \Delta t^2 < 6\left\|\frac{a}{c}\right\|$	$O(\Delta t^3)$	$O(\Delta t^3)$	conditional stability
	$b = 1/3$ $a + c = 0$	$O(\Delta t^4)$	$O(\Delta t^3)$	$\omega_0 \Delta t^2 < 6$			
	$b = -\frac{1}{3}$ $a = c = 0$				$O(\Delta t^4)$	$O(\Delta t^4)$	unstable

Table A1.2

c_i	m = 2	m = 3	m = 4
c_3	$(1-2\beta_1)/2$	0	0
c_4	$(2-3\beta_0-3\beta_1)/6$	$(6\beta_2-6\beta_1-1)/12$	0
c_5	$(1-3\beta_0-\beta_1)/6$	$(7\beta_2-6\beta_1-90\beta_0-19)/360$	$(-\beta_3+3\beta_2-2\beta_1)/12$
c_6	$(47-210\beta_0-30\beta_1)/720$	$(150\beta_2-105\beta_1-90\beta_0-19)/360$	$(-30\beta_3+100\beta_2-60\beta_1-10\beta_0-1)/240$
c_7	-	-	$(-52\beta_3+190\beta_2-100\beta_1-40\beta_0-35)/480$

Table A1.3

a_j	m = 2	m = 3	m = 4
a_0	$4+\lambda^2(2\beta_0-2\beta_1)$	$4(2\beta_2-1)+\lambda^2(1+4\beta_0-6\beta_1)/3$	$8(\beta_2-\beta_3)+\lambda^4(2\beta_3-4\beta_1+2\beta_0)/3$
a_1	$\lambda^2(2\beta_1-1)$	$4+\lambda^2(6\beta_1-6\beta_2-1)/3$	$4(2\beta_3-1)+\beta^2(2-2\beta_3-6\beta_2+4\beta_1)/3$
a_2	λ^2	$\lambda^2(2\beta_2-1)$	$4+\lambda^2(6\beta_2-6\beta_3-2/3$
a_3	-	λ^2	$\lambda^2(2\beta_3-1)$
a_4	-	-	λ^2

Table A1.4

Method	β_0	β_1	β_2	stability condition	accuracy order	
m = 2, maximal accuracy	$\frac{1}{3}$	$\frac{1}{2}$	-	$\lambda^2 \le 6$	3	no numerical damping
m = 2. unconditional stability	$\frac{1}{2}$	$\frac{1}{2}$	-	$\lambda < \omega$	2	
m = 2, explicit scheme	0	$\frac{1}{2}$	-	$\lambda^2 \le 4$	2	
m = 3, maximal accuracy	$\frac{1}{4}$	$\frac{1}{3}$	$\frac{1}{2}$	$\lambda^2 \le 6$	4	
m = 3, unconditional stability	$\frac{3}{4}$	$\frac{2}{3}$	$\frac{1}{2}$	$\lambda < \omega$	2	
m = 3, explicit scheme	0	$\frac{1}{6}$	$\frac{1}{2}$	$\lambda^2 \le 4$	2	
m = 3, Wilson scheme	1.4^3	1.4^2	1.4	$\lambda < \omega$	2	numerical damping
m = 3, Houbolt scheme	6	$\frac{11}{3}$	2	$\lambda < \omega$	2	
m = 3, explicit scheme	0	2	$\frac{13}{6}$	$\lambda^2 \le 3.6$	3	

Table A.1.5

$M\ddot{U}+C\dot{U}+KU=R(t)$ linear system	$M\ddot{U}+C\dot{U}+KU=W(U,\dot{U})+R(t)$ nonlinear system
1. $q_k=\sum_{j=k}^{m} U_t^{(j)} \frac{\Delta t^{j-k}}{(j-k)!}$, $b_k=\beta_k \frac{\Delta t^m}{(m-k)!}$, $b_k^*=\frac{b_k}{b_o}$, $q_k^*=q_k-b_k q_o$, $k=\overline{0,m}$; 2. $A\Delta U_{t+\Delta t}=G_{t+\Delta t}$, where $A=b_2^*M+b_1^*C+b_0^*K$, $G_{t+\Delta t}=R_{t+\Delta t}-(Mq_2^*+Cq_2^*+Kq_0^*)$; 3. $U^{(k)}_{t+\Delta t}=q_k^*+b_k^*\Delta U_{t+\Delta t}$, $k=\overline{0,m}$.	2. $A\Delta U_{t+\Delta t}=G_{t+\Delta t}+W_{t+\Delta t}$, where $W_{t+\Delta t}=W(U_{t+\Delta t},\dot{U}_{t+\Delta t})$, nonlinear equation at each time step a) simple iteration $A\Delta U^{i+1}_{t+\Delta t}=G^i_{t+\Delta t}+W^i_{t+\Delta t}$, $i=1,2,\dots$ b) Newton-Raphson iteration $\tilde{A}^i_{t+\Delta t}\Delta U^{i+1}_{t+\Delta t}=G^i_{t+\Delta t}+W^i_{t+\Delta t}$, $i=1,2,\dots$ where $\tilde{A}^i_{t+\Delta t}=Mb_2^*+b_1^*(C-\frac{\partial W}{\partial \dot{U}}\Big|_i)+b_0^*(K-\frac{\partial W}{\partial U}\Big|_i)$, at $i=1$ - tangential linearization

$$\begin{bmatrix} M_{11} M_{12} \\ M_{21} M_{22} \end{bmatrix} \begin{bmatrix} \ddot{U}_1 \\ \ddot{U}_2 \end{bmatrix} + \begin{bmatrix} C_{11} C_{12} \\ C_{21} C_{22} \end{bmatrix} \begin{bmatrix} \dot{U}_1 \\ \dot{U}_2 \end{bmatrix} + \begin{bmatrix} K_{11} K_{12} \\ K_{21} K_{22} \end{bmatrix} \begin{bmatrix} U_1 \\ U_2 \end{bmatrix} = \begin{bmatrix} 0 \\ W_2 \end{bmatrix} + R(t) \quad , \quad W_2 = W_2(U_2, \dot{U}_2)$$

system with local nonlinearities

2. $(\tilde{A}^i_{22}-A_{21}A_{11}^{-1}A_{12})\Delta U_2^{i+1}= G_2^i - A_{21}A_{11}^{-1}G_1^i + W_2(U_2^i,\dot{U}_2^i)$,

where $\tilde{A}^i_{22}= A_{22}- b_1\frac{\partial W_2}{\partial \dot{U}_2}\Big|_{U_2,\dot{U}_2} -b_0\frac{\partial W_2}{\partial U_2}\Big|_{U_2,\dot{U}_2}$, $U_2\equiv U_{2,t+\Delta t}$, $G_2\equiv G_{2,t+\Delta t}$,

$\Delta U_1= -A_{11}^{-1}A_{12}\Delta U_2 + A_{11}^{-1}G_1$, $U_1\equiv U_{1,t+\Delta t}$, $G_1\equiv G_{1,t+\Delta t}$.

Table A1.6

$M\ddot{U}+C\dot{U}+KU=R(t)$, $P\,U \le d_0$, $P^{(k)}U = d_k$, $k=\overline{1,m}$	$\begin{bmatrix}M_{11}M_{12}\\M_{21}M_{22}\end{bmatrix}\begin{bmatrix}\ddot{U}_1\\\ddot{U}_2\end{bmatrix}+\begin{bmatrix}C_{11}C_{12}\\C_{21}C_{22}\end{bmatrix}\begin{bmatrix}\dot{U}_1\\\dot{U}_2\end{bmatrix}+\begin{bmatrix}K_{11}K_{12}\\K_{21}K_{22}\end{bmatrix}\begin{bmatrix}U_1\\U_2\end{bmatrix}=R(t)$, $P_2U_2 \le d_0$, $P_2^{(k)}U_2 = d_k$, $k=\overline{1,m}$
system with unilateral constraints on the displacements, and, when they are active, on the velocities	economization of the scheme taking on account local nonlinearities $P = [\,0\ P_2]$
2. $A\,\Delta U = G - P^T\lambda_0$, where $\lambda_0=(PA^{-1}P^T)^{-1}(PA^{-1}G-d_0)$; 3. $\overset{(k)}{U}{}_- = q_k^*+b_k^*\Delta U$, $\overset{(k)}{U} = \overset{(k)}{U}{}_- - M^{-1}P\,\lambda_k$, where $\lambda_k=(PM^{-1}P^T)^{-1}(P\overset{(k)}{U}-d_k)$, $k=\overline{1,m}$; normal interaction force impetus during one time step (t,t+Δt): $S=\frac{\Delta t}{2}(F_t+\lambda_{0,t+\Delta t})+\lambda_{1,t+\Delta t}$, normal contact interaction force at the time point t+Δt: $F=\lambda_{0,t+\Delta t}+\lambda_{2,t+\Delta t}$, iteration for determining active constraints , $\lambda\ge0, S\ge0, F\ge0$.	2. $\tilde{A}_{22}\Delta U_2 = \tilde{G}_2 - P_2^T\lambda_0$, where $\tilde{A}_{22}=A_{22}-A_{21}A_{11}^{-1}A_{12}$, $\tilde{G}_2=G_2-A_{21}A_{11}^{-1}G_1$, $\lambda_0=(P_2\tilde{A}_{22}^{-1}P_2^T)^{-1}(P_2\tilde{A}_{22}^{-1}\tilde{G}_2-d_0)$; 3. $\overset{(k)}{U}{}_- = q_k^*+b_k^*\Delta U$, где $\Delta U_1=-A_{11}^{-1}A_{12}\Delta U_2+A_{11}^{-1}G_1$; $\overset{(k)}{\Delta U}_2 = -\tilde{M}_{22}^{-1}P_2^T\lambda_k$, $\overset{(k)}{\Delta U}_1 = -M_{11}^{-1}M_{12}\overset{(k)}{\Delta U}_2$, where $\tilde{M}_{22}=M_{22}-M_{21}M_{11}^{-1}M_{12}$, $\lambda_k=(P_2\tilde{M}_{22}^{-1}P_2^T)^{-1}(P_2\overset{(k)}{U}_2-d_k)$; $\overset{(k)}{U} = \overset{(k)}{U}{}_- + \overset{(k)}{\Delta U}$, $k=\overline{1,m}$.

Table A1.7

$M\ddot{U}+C\dot{U}+KU=R(t)$, $P_N U \le d_0$, $P_N^{(k)}U = 0$, $P_T^{(k)}U = 0$, $k=\overline{1,m}$
nonlinear system with the constraints presenting the Coulomb friction interaction pairs
1. $q_k=\sum_{j=k}^{m}\overset{(j)}{U}_t\frac{\Delta t^{j-k}}{(j-k)!}$, $b_k=\beta_k\frac{\Delta t^m}{(m-k)!}$, $b_k^*=\frac{b_k}{b_0}$, $q_k^*=q_k-b_kq_0$, $k=\overline{0,m}$; 2. $A\Delta U_{t+\Delta t}=G_{t+\Delta t}-P^T\lambda_0$, where $A=b_2^*M+b_1^*C+b_0^*K$, $G_{t+\Delta t}=R_{t+\Delta t}-(Mq_2^*+Cq_2^*+Kq_0^*)$, 3. $U = q_0^*+b_0^*\Delta U$, $\overset{(k)}{U}{}_- = q_k^*+b_k^*\Delta U$, $\overset{(k)}{U} = \overset{(k)}{U}{}_- - M^{-1}\bar{P}^T\bar{\lambda}_k$, where $\lambda_0=(P_NA^{-1}P_N^T)^{-1}(P_NA^{-1}G-d_0)$; $\bar{\lambda}_k=(\bar{P}M^{-1}\bar{P}^T)^{-1}\bar{P}\overset{(k)}{U}$, $k=\overline{1,m}$; for sliding pairs $\lambda_{kj}=\bar{\lambda}_{kj}$, $\lvert\mu_{kj}\rvert=k_f\bar{\lambda}_{kj}$, $S_N=\frac{\Delta t}{2}(F_t+\lambda_{0,t+\Delta t})+\lambda_{1,t+\Delta t}$, $S_T=\mu_{1,t+\Delta t}$, $F_N=\lambda_{0,t+\Delta t}+\lambda_{2,t+\Delta t}$, $F_T=\mu_{2,t+\Delta t}$, iteration for determining active constraints, $\lambda_{0j}\ge0$, $S_{Nj}\ge0$, $F_{Nj}\ge0$, iteration for determining sliding pairs, $k_f\lvert S_{Nj}\rvert\le\lvert S_j\rvert$.

APPENDIX 2. METHOD FOR OBTAINING QUASISTATIC COMPLIANCE MATRIX IN THE CASE OF SINGULAR STIFFNESS MATRIX (G.Rozenblum, [38])

In the case of singular stiffness matrix the relation (1.19) can't be immediately applied. In order to find an expression for S_k without obtaining the higher structural modes, the following auxiliary differential equation is considered

$$M\ddot{U} + K\,U = F_0\cos\lambda t \ , \qquad (A2.1)$$

from which the limit value of the displacement vector U is obtained at $\lambda \to 0$. If the matrix K is singular, i.e., the structure possesses rigid body d.o.f., the vector of the squares of angular eigenfrequencies and the eigenvector matrix can be presented as $\omega^2=\begin{bmatrix}0_2\\ \omega_1^2\\ & \omega_2^2\end{bmatrix}$, $\Delta = [\,\Delta_0,\Delta_1,\Delta_2]$, where the index "0" corresponds to the rigid-body structural modes. Substituting the variables as (1.12), where the modal displacement vector Z appears as $Z=\begin{bmatrix}Z_0\\Z_1\\Z_2\end{bmatrix}$, the elastic component of the displacement vector U_e can be expressed as

$$U_e = \Delta_1Z_1+\Delta_2Z_2 = [\,\Delta_1\,\mathrm{diag}(1/\omega_1^2)\Delta_1^T + \Delta_2\,\mathrm{diag}(1/\omega_2^2)\Delta_2^T\,]\,F_0, \qquad (A2.2)$$

and the rigid-body component of the displacement vector - as

$$U_r = \Delta_0Z_0 \ , \qquad (A2.3)$$

where $U = U_r + U_e$. (A2.4)

Taking account for (A2.2), (A2.3), (A2.4), the equation (A2.1) can be presented as

$$M\ddot{U}_r + M\ddot{U}_e + K\,U = F_0\cos\lambda t \ . \qquad (A2.5)$$

Multiplying (A2.5) from the left-hand side by Δ_0^T and taking account upon the orthogonality condition $\Delta_0^TMU_e = \Delta_0^TKU_e = 0$, the expression of $\ddot{U}_r$ is obtained, substitution of which into the equation (A2.5) enables to obtain the equation

$$M\ddot{U}_e + K U_e = R F_o \cos\lambda t \quad , \qquad (A2.6)$$

where $R = I - M \Delta_o \Delta_o^T$.

Approaching the limit $\lambda \to 0$, the equation (A2.6) is obtained as

$$K U_e = R F_o \quad . \qquad (A2.7)$$

If the matrix K would be non-singular, the equations(A2.2) and (A2.7) would enable to obtain the relation (1.19). In the case of the singular stiffness matrix, a solution U_e of the equation (A2.7) isn't unique. Therefore we consider one of the admissible solutions $U_a = \begin{pmatrix} U_L \\ 0 \end{pmatrix}$, obtained from the equation

$$\begin{bmatrix} K_{LL} & K_{Lr} \\ K_{Lr}^T & K_{rr} \end{bmatrix} \begin{pmatrix} U_L \\ 0 \end{pmatrix} = R F_o \quad , \qquad (A2.8)$$

where the lower index "r" at the blocks of the matrix K corresponds to the number of rows and columns equal to the number of rigid body d.o.f. In general, it doesn't matter , what particular d.o.f. are "fixed" in the equation (A2.8), i.e., correspond to the blocks with the lower index "r", however, the block K_{LL} should be nonsingular. Denoting $G = \begin{bmatrix} K_{LL}^{-1} & 0 \\ 0 & 0 \end{bmatrix}$, the vector U_a is expressed as

$$U_a = G R F_o \quad . \qquad (A2.9)$$

The general solution U_e can be presented as

$$U_e = U_a + \Delta_o \xi \quad . \qquad (A2.10)$$

Multiplying (A2.10) from the left-hand side by $\Delta_o^T M$ and employing the orthogonality condition $\Delta_o^T M U_e = 0$, we obtain

$$\xi = - \Delta_o^T M G R F_o \quad . \qquad (A2.11)$$

Substituting (A2.11) and (A2.9) into (A2.10), we obtain

$$U_e = R^T G R F_o \quad . \qquad (A2.12)$$

Now from (A2.12)) and (A2.2) the compliance matrix is expressed as

$$S_k = R^T G R - \Delta_1 \mathrm{diag}({}^1/_{\omega_1^2}) \Delta_1^T \quad . \qquad (A2.13)$$

APPENDIX 3. RELATIONS FOR STATIONARY AND TRANSIENT MOTION ANALYSIS IN TERMS OF SLOW VARYING AMPLITUDES

A3.1 HARMONIC BALANCE METHOD

The harmonic balance method can be regarded as a special case of the weighted residual approach applied in Chap.4.2 to the system

$$M\ddot{U} + C\dot{U} + K U = W(U,\dot{U}) + R(t) \quad . \qquad (4.1)$$

The harmonic weight functions

$$N(t) = [\ I\ I\cos\omega t\ \ I\sin\omega t\ \ I\cos 2\omega t\ \ I\sin 2\omega t\ \ldots\ ]$$

$$\hat{N}(t) = [\ \hat{I}\ \hat{I}\cos\omega t\ \ \hat{I}\sin\omega t\ \ \hat{I}\cos 2\omega t\ \ \hat{I}\sin 2\omega t\ \ldots\ ] \qquad (A3.1)$$

are employed, where I- unity matrix of the dimension equal to the length of the vector U, $\hat{I}$- unity matrix of the dimension equal to the number of constraints (rows of the matrix P), and $T = \frac{2\pi}{\omega}$.

The generalized amplitude vector contains the amplitudes of Fourier components:

$$U_A = \left[\ U_c^1,\ U_c^2\ ,\ U_s^2\ ,\ U_c^3\ ,\ U_s^3\ ,\ \ldots\ \right]^T .$$

Displacements and forces are presented as truncated Fourier series as

$$U(t) = N(t)U_A = \sum_{k=1}^{p} U_c^k \cos(k-1)\omega t + U_s^k \sin(k-1)\omega t \ ,$$

$$R(t) = N(t)R_A = \sum_{k=1}^{p} R_c^k \cos(k-1)\omega t + R_s^k \sin(k-1)\omega t \ , \qquad (A3.2)$$

$$W(t) = N(t)W_A = \sum_{k=1}^{p} W_c^k \cos(k-1)\omega t + W_s^k \sin(k-1)\omega t \ .$$

The component amplitude vectors are denoted as

$$U^k = \begin{pmatrix} U_c^k \\ U_s^k \end{pmatrix} , \quad W^k = \begin{pmatrix} W_c^k \\ W_s^k \end{pmatrix} , \quad R^k = \begin{pmatrix} R_c^k \\ R_s^k \end{pmatrix} , \qquad k=\overline{1,p}. \qquad (A3.3)$$

As only stationary motions of the frequency ω are considered, the amplitude components are obtained as a result of

the Fourier transform

$$U^k = FT^k(U) \ , \quad W^k = FT^k(W) \ , \quad R^k = FT^k(R) \ .$$

Assume the nonlinear interaction taking place in local zones of the structure and present vectors and matrices in a block form

$$U = \begin{bmatrix} U_1 \\ U_2 \end{bmatrix} \ , \quad W = \begin{bmatrix} 0 \\ W_2(U_2, \dot{U}_2) \end{bmatrix} \ . \qquad (A3.4)$$

Denote through I_2 the unity matrix of the dimension $n_2 x n_2$, where n_2 is equal to the length of the vector U_2 . Matrices of the dimension nxn_2 containing the harmonic response amplitudes to unity harmonic excitations at the nonlinearity points denote through S^k , $k=\overline{1,p}$, where nxn - the dimension of the equation (4.1). Vectors P^k , $k=\overline{1,p}$ each of the length n contain the harmonic response amplitudes of the linear part of the structure to the external excitation $R(t)$.

The matrices S^k and vectors P^k are determined from the matrix equation

$$\begin{bmatrix} K - \omega_k^2 M & \omega_k C \\ -\omega_k C & K - \omega_k^2 M \end{bmatrix} \begin{bmatrix} S^k & P^k \end{bmatrix} = \left[\begin{array}{c|c} 0 & \\ I_2 & \\ 0 & R^k \\ I_2 & \end{array}\right] \ , \ k = \overline{1,p} \ . \qquad (A3.5)$$

where $\omega_k = (k-1)\omega$, and the zero submatrices on the right-hand side of the equation (A3.5) are of the dimension $n_1 x n_2$, where n_1 - length of the subvector U_1 .

Consider matrices S_2^k of the dimension $n_2 x n_2$ and vectors P_2^k of the length n_2, containing the rows of S^k and the elements of P^k , corresponding to the d.o.f. subjected to nonlinear interaction. Denoting

$$U_{A2} = \begin{bmatrix} U_2^1 \\ U_2^2 \\ \vdots \\ U_2^p \end{bmatrix} \ , \quad P_{A2} = \begin{bmatrix} P_2^1 \\ P_2^2 \\ \vdots \\ P_2^p \end{bmatrix} \ , \quad S_{A2} = \begin{bmatrix} S_2^1 & & 0 \\ & S_2^2 & \\ & & \ddots \\ 0 & & S_2^p \end{bmatrix} \ . \qquad (A3.6)$$

the equation (4.21)' reads as

$$U_{A2} = S_{A2} W_{A2}(U_2, \dot{U}_2) + P_{A2} \ . \qquad (A3.7)$$

From the equation (A3.7) immediately follows the simple iteration formula for obtaining the solution, however, very often it exhibits divergence.

The Newton-Raphson iteration scheme reads as follows:

$$(I - S_{A2} D)(U_{A2}^{i+1} - U_{A2}^{i}) = -U_{A2}^{i} + S_{A2} W_{A2}^{i} + P_{A2} \ , \qquad (A3.8)$$

where through D the derivative matrix $D = \dfrac{\partial W_{A2}}{\partial U_{A2}}$ is denoted.

Taking into account that the Fourier transform as well as differentiation are linear operations, their priority order can be exchanged:

$$\frac{\partial W_{A2}}{\partial U_{A2}} = \frac{\partial FT(W_2)}{\partial U_{A2}} = FT\left[\frac{\partial W_2}{\partial U_{A2}} \right] \ , \qquad (A3.9)$$

where through FT the Fourier transform is denoted, transforming a vector-column of time functions of the length n_2 into a vector of harmonic amplitude components of the length $2pn_2$. Expanding the relation (A3.9) we obtain

$$D = FT\left[\frac{\partial W_2}{\partial U_2} \frac{\partial U_2}{\partial U_{A2}} + \frac{\partial W_2}{\partial \dot{U}_2} \frac{\partial \dot{U}_2}{\partial U_{A2}} \right] \ , \qquad (A3.10)$$

where the derivatives $\dfrac{\partial U_2}{\partial U_{A2}}$, $\dfrac{\partial \dot{U}_2}{\partial U_{A2}}$ are expressed as

$$\frac{\partial U_2}{\partial U_{A2}} = \Big[\ \ldots \ , \ I_2 \cos(i-1)\omega t \ , \ I_2 \sin(i-1)\omega t \ , \ \ldots \ \Big]_{n2xp} \ ,$$

$$\frac{\partial \dot{U}_2}{\partial U_{A2}} = \Big[\ldots , -I_2(i-1)\omega \sin(i-1)\omega t, \ I_2(i-1)\omega \cos(i-1)\omega t, \ldots \Big]_{n2xp} \ .$$

Explicitly the derivative matrix is expressed as

$$D = \begin{bmatrix} \frac{\partial W^1_{2c}}{\partial U^1_{2c}} & \frac{\partial W^1_{2c}}{\partial U^1_{2s}} & \cdots & \frac{\partial W^1_{2c}}{\partial U^p_{2c}} & \frac{\partial W^1_{2c}}{\partial U^p_{2s}} \\ \frac{\partial W^1_{2s}}{\partial U^1_{2c}} & \frac{\partial W^1_{2s}}{\partial U^1_{2s}} & \cdots & \frac{\partial W^1_{2s}}{\partial U^p_{2c}} & \frac{\partial W^1_{2s}}{\partial U^p_{2s}} \\ \vdots & \vdots & & \vdots & \vdots \\ \frac{\partial W^p_{2c}}{\partial U^1_{2c}} & \frac{\partial W^p_{2c}}{\partial U^1_{2s}} & \cdots & \frac{\partial W^p_{2c}}{\partial U_{2c}} & \frac{\partial W^p_{2c}}{\partial U_{2s}} \\ \frac{\partial W^p_{2s}}{\partial U^1_{2c}} & \frac{\partial W^p_{2s}}{\partial U^1_{2s}} & \cdots & \frac{\partial W^p_{2s}}{\partial U^p_{2c}} & \frac{\partial W^p_{2s}}{\partial U^p_{2s}} \end{bmatrix} , \quad (A3.11)$$

where

$$\begin{bmatrix} \frac{\partial W^i_{2c}}{\partial U^j_{2s}} \\ \frac{\partial W^i_{2s}}{\partial U^j_{2s}} \end{bmatrix} = FT^i \left[\frac{\partial W_2}{\partial U_2} \sin(j-1)\omega t + \frac{\partial W_2}{\partial \dot{U}_2}(j-1)\omega \cos(j-1)\omega t \right] ,$$

(A3.12)

$$\begin{bmatrix} \frac{\partial W^i_{2c}}{\partial U^j_{2c}} \\ \frac{\partial W^i_{2s}}{\partial U^j_{2c}} \end{bmatrix} = FT^i \left[\frac{\partial W_2}{\partial U_2} \cos(j-1)\omega t - \frac{\partial W_2}{\partial \dot{U}_2}(j-1)\omega \sin(j-1)\omega t \right] ,$$

$$i,j = \overline{1,p} .$$

The dimension of the equation is reduced, taking into account that $U^1_s = W^1_s = 0$.

At each Newton-Raphson iteration it is necessary to solve a linear algebraic equation system of the dimension $(2p-1)n_2 \times (2p-1)n_2$ and to carry out $n_2 p$ times the discrete Fourier transform during the time interval $[0,T]$. Therefore the necessary ammount of the computational resource depends mainly upon the number of the nonlinearly interacted d.o.f. n_2, rather than upon the dimension n of the structure.

A3.2 NUMERICAL INTEGRATION OF TIME AVERAGED EQUATIONS. FORMULAE FOR OBTAINING DERIVATIVE MATRICES

$$\frac{\partial W_A}{\partial U_A} = \begin{bmatrix} \frac{\partial W^1_c}{\partial U^1_c} & \frac{\partial W^1_c}{\partial U^2_s} & \frac{\partial W^1_c}{\partial U^2_s} & \cdots & \frac{\partial W^1_c}{\partial U^p_c} & \frac{\partial W^1_c}{\partial U^p_s} \\ -\frac{\partial W^2_s}{\partial U^1_c} & -\frac{\partial W^2_s}{\partial U^2_s} & -\frac{\partial W^2_s}{\partial U^2_s} & \cdots & -\frac{\partial W^2_s}{\partial U^p_c} & -\frac{\partial W^2_s}{\partial U^p_s} \\ \frac{\partial W^2_c}{\partial U^1_c} & \frac{\partial W^2_c}{\partial U^2_s} & \frac{\partial W^2_c}{\partial U^2_s} & \cdots & \frac{\partial W^2_c}{\partial U^p_c} & \frac{\partial W^2_c}{\partial U^p_s} \\ \vdots & \vdots & \vdots & & \vdots & \vdots \\ -\frac{\partial W^p_s}{\partial U^1_c} & -\frac{\partial W^p_s}{\partial U^2_s} & -\frac{\partial W^p_s}{\partial U^2_s} & \cdots & -\frac{\partial W^p_s}{\partial U^p_c} & -\frac{\partial W^p_s}{\partial U^p_s} \\ \frac{\partial W^p_c}{\partial U^1_c} & \frac{\partial W^p_c}{\partial U^2_s} & \frac{\partial W^p_c}{\partial U^2_s} & \cdots & \frac{\partial W^p_c}{\partial U^p_c} & \frac{\partial W^p_c}{\partial U^p_s} \end{bmatrix} , \quad (A3.13)$$

where

$$\begin{bmatrix} \frac{\partial W^i_c}{\partial U^j_s} \\ \frac{\partial W^i_s}{\partial U^j_s} \end{bmatrix} = FT^i \left[\frac{\partial W}{\partial U} \sin(j-1)\omega t + \frac{\partial W}{\partial \dot{U}}(j-1)\omega \cos(j-1)\omega t \right] ,$$

(A3.14)

$$\begin{bmatrix} \frac{\partial W^i_c}{\partial U^j_c} \\ \frac{\partial W^i_s}{\partial U^j_c} \end{bmatrix} = FT^i \left[\frac{\partial W}{\partial U} \cos(j-1)\omega t - \frac{\partial W}{\partial \dot{U}}(j-1)\omega \sin(j-1)\omega t \right] ,$$

$$i,j = \overline{1,p} .$$

APPENDIX 4. METHOD FOR OBTAINING STABLE CLOSED-LOOP CONTROL SYSTEM

The expressions of feedback coefficients of the synthesized control law contain arbitrary constant matrices G and H (see the expressions (5.32), (5.37)). The arbitrariness of the matrices can be employed for ensuring the stability of the system, that, in general, isn't guaranteed by applying the synthesis method presented in Chap.5.2.2.

For obtaining a stability condition we employ the first Liapunov's theorem, presenting the equation (5.39) as a first order differential equation system in terms of the variables $S = \begin{pmatrix} U \\ \dot{U} \end{pmatrix}$ as

$$\dot{S} = \begin{bmatrix} 0 & I \\ -M^{-1}K & -M^{-1}C \end{bmatrix} S = B\,S \quad . \qquad (A4.1)$$

For the asymptotic stability of the system (5.42) a necessary and sufficient condition is that the real parts of the eigenvalues of the matrix $B_{2n\times 2n}$ would be negative. In the case of symmetric matrices K, C are symmetric, the sufficient stability condition is that the matrices K, C would be positive definite. However, the matrices can be symmetric only if $R = Q^T$, therefore we'll consider the general case.

We present B as a function of the components of the matrices G and H as $B = B(g_{ij}, h_{ij})$. In order to avoid cumbersome computations, further we restrict ourselves with the functional relation $B = B(g_{ij})$. An eigenvalue problem for the matrix B reads as follows:

$$\left[B - (\xi + i\eta) I \right] (a + ib) = 0 \quad , \qquad (A4.2)$$

where the scalar quantities ξ, η represent real and imaginary parts of an eigenvalue, and vectors a and b - real and imaginary parts of an eigenvector.

The problem (A4.2) has $2n$ solutions ξ_j, η_j, a_j, b_j, $j=\overline{1,2n}$. For the control system stability all the real parts of the eigenvalues ξ_j, $j=\overline{1,2n}$ should be negative. If an eigenvalue with the positive real part is present, the parameters g_{ij} should

be adjusted in order to make it negative. Taking on account that the relation between ξ and g_{ij} is nonlinear, we employ a gradient minimization techniques for obtaining the necessary values g_{ij}, defining the current increments Δg_{ij} direct proportional to the components of the gradient vector $(\frac{\partial \xi}{\partial g_{ij}}, i=\overline{1,n}, j=\overline{1,K})$.

For obtaining the partial derivatives $\frac{\partial \xi}{\partial g_{ij}}$ we employ the following relations. Together with the right-hand side eigenvalue problem (5.43) we consider the left-hand side problem

$$(\tilde{a} + i\tilde{b}) \left[B - (\xi + i\eta) I \right] = 0 \quad , \qquad (A4.3)$$

or, what is the same,

$$\left[B^T - (\xi + i\eta) I \right] (\tilde{a} + i\tilde{b})^T = 0 \quad ,$$

where the vectors $\tilde{a}$, $\tilde{b}$ represent the real and imaginary parts of the left-hand side row-vector, the eigenvalues $\xi+i\eta$ coinciding for the two problems.

Equating to zero the real and imaginary parts of the exact differentials of the left-hand sides of the equations (A4.2), (A4.3), we obtain

$$\begin{aligned}
&B\delta a - \xi\delta a + \eta\delta b - a\delta\xi + b\delta\eta + \frac{\partial(Ba)}{\partial g}\delta g = 0 \quad , \\
&B\delta b - \xi\delta b - \eta\delta a - b\delta\xi - a\delta\eta + \frac{\partial(Bb)}{\partial g}\delta g = 0 \quad , \\
&\delta\tilde{a}B - \xi\delta\tilde{a} + \eta\delta\tilde{b} - \tilde{a}\delta\xi + \tilde{b}\delta\eta + \frac{\partial(\tilde{a}B)}{\partial g}\delta g = 0 \quad , \\
&\delta\tilde{b}B - \xi\delta\tilde{b} - \eta\delta\tilde{a} - \tilde{b}\delta\xi - \tilde{a}\delta\eta + \frac{\partial(\tilde{b}B)}{\partial g}\delta g = 0 \quad ,
\end{aligned} \qquad (A4.4)$$

where the elements g_{ij} of the matrix G are presented as the vector $g = (g_{11}, g_{12}, \ldots, g_{1k}, \ldots, g_{nk})^T$. After some manipulation upon the system (A4.4), we obtain

$$\begin{cases} p\,\delta\xi + q\,\delta\eta + A\,\delta g = 0 , \\ -q\,\delta\xi + p\,\delta\eta + D\,\delta g = 0 , \end{cases} \qquad (A4.5)$$

where $p = \tilde{b}\tilde{b} - \tilde{a}\tilde{a}$, $q = \tilde{a}\tilde{b} + \tilde{b}\tilde{a}$, $A = \tilde{a}\dfrac{\partial(Ba)}{\partial g} - \tilde{b}\dfrac{\partial(Ba)}{\partial g}$,

$D = \tilde{b}\dfrac{\partial(Ba)}{\partial g} + \tilde{a}\dfrac{\partial(Bb)}{\partial g}$.

After eliminating $\delta\eta$ from the system (A4.5), we obtain the relationship between small variations of the elements of the matrix G and small variations of the real part of the eigenvalue as

$$\delta\xi = d\,\delta g , \qquad (A4.6)$$

where $d = \dfrac{1}{p^2 + q^2}(D\,q - A\,p)$ represents the gradient vector.

Assume $l_1, l_2, \ldots, l_t$ being the numbers of all eigenvalues possessing "dangerous" real parts, i.e., $\xi_{l_r} > -\varepsilon$, $r=\overline{1,t}$. The gradient vectors of the real parts is presented in the space of the parameters g_{ij} as

$$d_{l_r} = \left(\frac{\partial\xi_{l_r}}{\partial g_{11}} , \frac{\partial\xi_{l_r}}{\partial g_{12}} , \ldots , \frac{\partial\xi_{l_r}}{\partial g_{nk}} \right) .$$

It appears natural to expect, that a small increment $-\Delta g\ \mathrm{sign}\left(\dfrac{\partial\xi_{l_r}}{\partial g_{ij}}\right)$ of the parameter g_{ij} value enables to decrease the values of ξ_{l_r}, if all $\dfrac{\partial\xi_{l_r}}{\partial g_{ij}}$, $r=\overline{1,t}$ are of the same sign, i.e., if they are all positive or all negative.

For decreasing real parts of the "dangerous" eigenvalues until they become negative, the following algorithm can be employed.

Algorithm A4.1

1. Assume $g_{ij} = 0$, $i=\overline{1,n}$, $j=\overline{1,k}$.
2. Solve an eigenvalue problem
$$\left[B(g_{ij}) - (\xi + i\eta)\, I \right] (a + ib) = 0.$$
3. If all $\xi_{l_r} > -\varepsilon$, $r=\overline{1,2n}$, go to step 9, else go to step 4.
4. For all $\xi_{l_r} > -\varepsilon$, $r=\overline{1,t}$, obtain the vectors
$$d_{l_r} = \left(\frac{\partial\xi_{l_r}}{\partial g_{ij}} , i=\overline{1,n} , j=\overline{1,k} \right) .$$
5. Select the current element g_{ij} from the vector g .
6. If all $\dfrac{\partial\xi_{l_r}}{\partial g_{ij}}$, $r=\overline{1,t}$ are of the same sign, go to step 7, else go to step 8.
7. Assume $g_{ij} = g_{ij} - \Delta g\ \mathrm{sign}\left(\dfrac{\partial\xi_{l_r}}{\partial g_{ij}}\right)$, where Δg - some positive scalar quantity, and go to step 2.
8. If g_{ij} is the last element of the vector g , go to step 9, else go to step 5.
9. End.

If the application of the above presented algorithm wasn't successful, i.e., if the values of the parameters g_{ij} ensuring $\xi_{l_r} < 0$, $r = \overline{1,2n}$ haven't been obtained, the control system should be modified by selecting another values of the matrices R and (or) Q .

KAUNO TECHNOLOGIJOS UNIVERSITETAS

BARAUSKAS Rimantas

TAMPRIŲ KONSTRUKCIJŲ SU VIENPUSIAIS RYŠIAIS
DINAMINĖ ANALIZĖ IR SINTEZĖ

anglų kalba

Pasirašyta spausdinti 1992 06 24 SL Nr.344. Formatas 60x84/16.
Popierius spaudos.16,97 sąl.sp.l.18,25 apsk.sp.l.Tiražas 100egz.
Užsakymas 161.Leid.Nr.355.Kaina sutartinė.
Leidykla "Technologija", K.Donelaičio 73, 3006 Kaunas
Spausdino KTU, K.Donelaičio 73, 3006 Kaunas